2020

DEVELOPMENT OF ORGANOCATALYSTS FOR RING-OPENING POLYMERIZATION (ROP) OF LACTONES

Rukshika Shalani Hewawasam
University of Rhode Island, rukzmck@gmail.com

DEVELOPMENT OF ORGANOCATALYSTS FOR RING-OPENING POLYMERIZATION (ROP) OF LACTONES

BY

RUKSHIKA S HEWAWASAM

A DISSERTATION IN PARTIAL FULFILLMENT OF THE REQUIREMENTS FOR THE DEGREE OF DOCTOR OF PHILOSOPHY

IN

PHYSICAL ORGANIC CHEMISTRY

UNIVERSITY OF RHODE ISLAND

2020

DOCTOR OF PHILOSOPHY DISSERTATION

OF

RUKSHIKA S HEWAWASAM

APPROVED:

Dissertation Committee:

Major Professor Matthew Kiesewetter

Jiyeon Kim

Matthew Bertin

Bongsup Cho

Brenton Deboef

DEAN OF THE GRADUATE SCHOOL

UNIVERSITY OF RHODE ISLAND

2020

ABSTRACT

Organocatalysis for Ring-Opening Polymerization (ROP) has come a long way in recent developments to afford precisely tailored and highly adorned biodegradable polyesters. A remarkable milestone of the organocatalysts occurred in 2005 with the advent of dual H-bonding catalysts that produce superior reaction control and molecular weight distributions (M_w/M_n), which is ideal for material applications. However, these organocatalysts do not show the capability in faster reaction times which is limiting the feasibility for industrial implementation.

The polymerization of cyclic esters by (thio)urea/base cocatalyst has proved to be effective and controlled. One method of devising improved catalyst systems is through mechanistic investigations. It has shown that ROP can proceed via one of two mechanisms: Neutral H-bonding mechanism and (thio)imidate mediated mechanism. It has been found that (thio)imidate mechanism is preferred reaction conditions such as polar solvents, high temperature, high monomer concentration, presence of strong electron-withdrawing groups on the H-bond donor, and strong bases which resulted in effective ROP kinetics and precisely tailored polymers.

The synthetic addition of one or more (thio)urea H-bond donating arms to the parent (thio)urea has been shown to substantially increase the activity of (thio)urea H-bond donors. A series of conformationally flexible bis(thio)urea H-bond donors plus base cocatalyst were applied to understand the structure-function relationship of the multi H-

bonding (thio)ureas in the ring-opening polymerization of lactones. The rate of the ROP displays a strong dependence upon the length and identity of the tether, where a circa five methylene-unit long tether exhibits the fastest ROP of δ-valerolactone (VL) and ε-caprolactone (CL), which could be accelerating reaction rates from days to seconds, and remains active at low catalyst loadings under solvent-free conditions.

An extensive kinetic study was carried out with ROP of VL employing multi H-bonding urea catalysts in polar solvents. It has revealed that multiple urea moieties in the catalysts facilitate activation of several monomers, which resulted in higher-order kinetics in monomer; hence, higher initial rates in ROP reactions were observed. It is also found that the polymer architecture could be modified in copolymerization due to higher-order kinetics in VL with multi H-bonding urea catalysts in polar solvents.

For the first time, organocatalytic ring-opening polymerization (ROP) of thiono-macrolactones was conducted. The ROP of less strained (thiono)macrolactones showed entropic driving force for the reaction with minimal or negligible contribution from enthalpy for the ROP yet, retain the characteristics of living polymerization even at elevated temperatures. The copolymerization of thionomacrolactones and macrolactones showed altered material properties compared to its homopoly(thiono)lactones.

ACKNOWLEDGEMENT

Foremost, I would like to express my sincere gratitude to Prof. Matthew K. Kiesewetter for all his support, his patience, and immense wisdom. You have really made my time at the University of Rhode Island worth to learn life lessons more than just the degree. I would also like to thank my committee members for their support throughout this process.

I would like to thank my family and friends who have constantly encouraged me during this process, and thank you very much for tolerating my mood swings.

I would like to acknowledge my teammates, who brought joy and making the lab an enjoyable place. Thank you very much for making memories.

Thank you to the rest of the chemistry graduate community and the Department of Chemistry and Graduate school at the University of Rhode Island for all the support and resources.

-Rukshika S Hewawasam

PREFACE

This dissertation is written in Manuscript Format.

Chapter 1: A literature chapter links to the field of H-bonding organic catalysts used for the ring-opening polymerization of cyclic lactones. It is narrowly focused on the superlative organocatalysts for the reaction control and kinetics in ROP of selected strained and less strained cyclic lactones, and challenges still exist for the implementation of organocatalytic ROP at the industrial scale.

Chapter 2: A study that reveals the complicated interplay of reagents that give rise to catalysis through one of two mechanisms: *Neutral H-bonding mechanism* and *Imidate mediated mechanism* using Hammett principle. Kinetic studies with urea catalysts were performed by me. (*Macromolecules* **2018** 51 (8), 3203-3211)

Chapter 3: Structure-function relationship, by varying tether lengths of bis-(thio)urea catalysts, has been reported. The relationship between tether lengths of urea catalysts and its activity in the ROP of lactones was studied by me. (*Macromolecules*. **2019**, 52(23), 9232-9237).

Chapter 4: An extensive kinetic study was carried out with ROP of VL employing multi H-bonding urea catalysts in polar solvents, which revealed that higher-order kinetics in monomer using multi H-bonding urea catalysts. All the polymerization reactions and synthesis were carried out by me. This chapter includes unpublished data.

Chapter 5: For the first time, organocatalytic ring-opening polymerization (ROP) of thiono-macrolactones was studied. Solid, flexible, and porous crosslinked polymers with remarkable material properties were synthesized using poly(thionolactones). Thermodynamic and kinetic studies of (thiono)macrolactones were performed by me.

TABLE OF CONTENTS

LIST OF TABLES

LIST OF SCHEMES

LIST OF FIGURES

Figure page

MANUSCRIPT I

Formatted for publication in ACS macromolecules

Recent Efforts Focused on the Development of Organocatalysts for Ring-Opening Polymerization (ROP) of lactones

Rukshika S Hewawasam and Matthew K. Kiesewetter

Chemistry, University of Rhode Island, Kingston, RI, USA

Corresponding Author: Matthew Kiesewetter, Ph.D.

Chemistry

University of Rhode Island

140 Flagg Road

Kingston, RI, 02881, USA

Email address: mkiesewetter@uri.edu

ABSTRACT

Organocatalysis for ROP has come a long way with recent developments to afford precisely tailored biodegradable polyesters. The field of organocatalysts has developed for a broad monomer scope, easy use, and low cost. However, it is trapped on a laboratory-scale while struggling to get into the industrial level. In this chapter, we discuss the advanced uses of superlative organocatalysts systems for the ROP of selected strains and less strained lactones. This review focused on encouraging the polymer community to develop organocatalysts that are capable of resolving existing challenges.

INTRODUCTION

The petroleum-based polymers account for the consumption of ~7% worldwide fossil fuels.[1] It has been a general goal to develop sustainable polymers to mitigate the complications which occurred from petroleum-based polymers.[2,3] The class of polyesters turns out to be a promising alternative for synthetic plastics since it can be synthesized from renewable monomers.[1,3,4] Additionally biodegradability, biocompatibility and ability to mimic the characteristics of synthetic polymers are remarkable properties to use as a substitute.[3,5–10] Hence, polyesters are widely used as bulk commodity materials in a variety of applications including packaging[11,12], textile industry[13,14], biomedicine[15–17] and IT field.[18,19]

In general, the common pathways of extracting monomers from natural sources are 1) fermentation of carbohydrate substrates; (corn and sugar cane)[3,20], 2) chemical breakdown of lignocellulose substrates,[4,21] and 3) transesterification of glycerol in oilseed crops and algae.[4,20,22] Monomers that are obtainable from those natural sources are diacids, hydroxyl acids, diols, polyols, carbonates, epoxides, and cyclic lactones.[3,4,20,23] Among those monomers cyclic lactones are one of the most important precursors in the synthesis of polyesters. Most of the commercially available cyclic lactones are derived from natural sources and synthesized from enzymatic routes or platform chemicals through one or multistep synthesis.[4,24–26]

As the world's interest in the aliphatic polyesters emerges, the ring-opening polymerization (ROP) of cyclic lactones has received tremendous attention over the last

two decades[27–30]. The ring-opening polymerization is a type of chain-growth polymerization technique where the polymer chain propagates through the addition of cyclic monomers to an active chain end.[27,31,32] In this process, the initiator opens a cyclic monomer and forms an active center. Depending on the nature of this propagating active center, ROP mechanisms can be illustrated as; cationic, anionic, radical, and covalent.[33] The ROP stands out for end group fidelity, high stereoselectivity and regioselectivity, precise molecular weights and complex polymer architectures.[33–35] Thus, polyesters synthesized by ROP are chosen for tailor-made drug delivery systems.[4,5,36] Indeed, to obtain well-defined polymers, catalysis plays a significant role in ROP besides enhancing the rates.[31] Organometallic catalysts have been used widely in industry; however, metal residues in the final polymer can give detrimental effects on the applications such as biomedicine and microelectronics.[37,38] Hence, over the last decade understanding of organocatalytic ROP systems has increased and nurtured the need for precisely tailored polyesters.

Organocatalytic ROP has taken place with the aid of a vast variety of organocatalysts such as pyridine-based, N-heterocyclic carbenes (NHCs), guanidine, amidine, phosphazene bases, and thiourea/amine cocatalaysts.[31,33,38–41] Organocatalysts compared to organometallic catalysts are outstanding in its versatility, high selectivity, and the possibility of recovering the catalyst from the end product and easy purification of the final polymer.[37] Conceptually, these catalysts activate either monomer or active chain end or both together[31,33,42,43]. A dual catalyst system can activate both monomer and the chain end which enables the mitigation of side reactions and leads to narrow

molecular weight distribution (polydispersity index-PDI = M_w/M_n < 1.1).[31,38,44] A dual catalyst system can be a unimolecular or bimolecular catalyst system. However, it turned out that using bimolecular dual catalyst system resulted in extremely controlled polymerizations and predictable molecular weights (M_n).[31,33,38,44–46] The thiourea/base cocatalyst system is an effective bimolecular dual catalyst system which has high tunability, and stability over a wide range of reaction conditions[47–53]. It exhibits features of a "living" polymerization where no termination is present, which enables to gain controlled molecular weights and highly adorned and precisely tailored polymers.[27,31] However, in spite of the significant advantages of the organocatalyzed ROP from the viewpoint of material applications, the organocatalyzed ROP of cyclic esters has been insufficiently discussed when compared to the organometallic-catalyzed ROP. Thus, it is important to evaluate the organocatalysts available for the ROP of cyclic esters in order to develop the organocatalyzed polymerization as a new polymer synthetic methodology. Herein, it is narrowly focused on the superlative organocatalysts for the ROP of selected strained and less strained cyclic lactones (Figure 1.1).

Organocatalysts for the ROP of strained lactones

ROP of VL, CL, and LA

Organic acid catalysts. Different types of organic catalysts have been progressively developed to obtain higher molecular weights, higher selectivity, and higher rates for the ROP of lactones (Figure 1.2). The cationic ROP of VL, CL, and LA has been carried out with a wide range of organic acids. The polymerization is catalyzed via electrophilic

monomer activation (Scheme 1.1), where the carbonyl oxygen of the monomer get protonated by the acid catalyst and acts as the activated species which reacts readily with the initiator.[27] However, higher reactivity of the protonated monomer can be susceptible to side reactions, which leads to a broader M_w/M_n. The $HCl.Et_2O$ can be used to obtain controlled M_n for ROP of VL and CL with the range of M_w/M_n =1.10-1.49 in the presence of an alcohol initiator.[54] A milder acid, tartaric acid, has shown a higher activity towards the ROP of CL over lactic acid, fumaric acid, and citric acid resulting in M_w/M_n ~1.3 with 10 mol% of the catalyst.[55] The trifluoromethanesulfonic acid (HOTf) in the presence of a protic initiator has shown living ROP of CL and can be used to obtain isotactic L-PLA at room temperature.[56] However, it is proven that methanesulfonic acid (MSA) is active as HOTf for the ROP of CL while retaining narrow M_w/M_n.[57] Additionally, the catalytic activity of MSA can be enhanced by a tripodal hydrogen bonds network of methanesulfonic acid-thiophospheric triamide (MSA-TPTA) complex for the ROP of lactones in a living manner with narrow M_w/M_n (~1.1).[58] Trifluoromethanesulfonimide ($HNTf_2$) is another BrØnsted acid catalyst which can give living characteristics for the ROP of VL.[59] Diphenyl phosphate (DPP) is a commercially available, less toxic and a milder catalyst compared to $HNTf_2$ for the controlled ROP of VL and CL.[60] Further, a bulky chiral phosphoric acid, 1,10-binaphthyl-2,2'-diyl hydrogen phosphate (BNPH) was used for the ROP of VL and CL in bulk conditions at elevated temperature which could give living and controlled polymerization.[61] Though a wide range of acid catalysts has been used for the ROP of lactones, they still give low to moderate molecular weights and comparatively slow rates. Nevertheless, organic acids considered as the most straightforward class of

catalysts used for the ROP of cyclic lactones in terms of operational simplicity and accessibility.[31,56]

Phosphazene bases. Phosphazene base is another main category of organocatalysts for ROP (Figure 1.3). It has been found that 2-tert-butylimino-2-diethylamino-1,3-dimethylperhydro-1,3,2-diazaphosphorine (BEMP) is an active catalyst over *N′-tert-butyl-N,N,N′,N′,N″,N″*- hexamethylphosphorimidic triamide (P_1-*t*-Bu) for the ROP of VL and LA in the presence of an initiator which undergoes via chain end activation mechanism (Scheme 1.2). However, The ROP of CL with BEMP is sluggish even at elevated temperature with $M_w/M_n \sim 1.1$.[62] The ROP of *rac*-lactide catalyzed by BEMP yields a probability of 0.70 isotactic propagation (P_i) at room temperature.[62] A dimeric phosphazene base (P_2-*t*-Bu) has been used to obtain highly isotactic polymers (P_i =0.95*)* with *rac*-lactide at -75°C resulting in a minimum epimerization.[63] Recently, a study shows CTPB has a decent catalytic activity on ROP of *rac*-lactide at-75°C in terms of rates and isotacticity (P_i =0.93).[64]

Pyridine bases. Pyridine bases are widely used for the anionic ROP of LA due to its high nucleophilicity.[31] The commonly used pyridine bases are 4-(dimethylamino)pyridine (DMAP) and 4-pyrrolidinopyridine (PPY), whereas DMAP outstands in rates over PPY (Figure 1.4).[31,33,40] In the presence of either primary or secondary alcohol initiator, DMAP can be used to obtain isotactic L-PLA in both solution and melt conditions. Two plausible mechanisms have been proposed for DMAP catalyzed ROPs. Initially, it has been proposed, the monomer activation is taken place through a nucleophilic attack by DMAP on the monomer (Scheme 1.3, a).[65]

However, the chain-end activation mechanism is also supported by computational studies where it proves both pathways are energetically favorable. Thus, in the gas phase and polar aprotic solvents, the H-bonded pathway was proposed to be at a lower energy in the presence of an initiator (Scheme 1.3, b).[31] Even though, It is declared that controlled ROP of LA can be gained in the presence of a secondary alcohol initiator, the transesterification can be promoted on the PLA backbone specially at elevated temperatures due to the high activity and poor thermal stability of DMAP.[66] Additionally, DMAP catalyzed ROP of VL and CL were not reported; however, the ROP of LA with DMAP can be considered as sluggish compared to other organocatalysts.

***N*-Heterocyclic carbenes**. *N*-Heterocyclic carbenes (NHCs) are widely used as organocatalysts for the ROP of cyclic lactones (Figure 1.4). It is vastly recognized due to its facile synthesis, tunability of electronic, steric effects and the chemical reactivity.[67–69] Polymerization rates and selectivities depend on both nature of the carbene and lactone monomer. Besides, It is shown that less sterically hindered NHCs are active for the ROP of lactones than their sterically demanding analogues.[67,70–72] NHCs can act as nucleophiles; hence nucleophilic monomer activation mechanism was proposed. In addition, computational studies have suggested the H-bonding alcohol activation mechanism from NHCs is also preferable in the presence of an alcohol initiator.[39] Recently, it has been found that NHC can activate the alcohol through hydrogen bonding and promotes a nucleophilic attack on to the lactone monomer, that occurs during the polymerization of CL in the presence of methanol as the initiator

which is supported by density functional theory (DFT) calculations (Scheme 1.4 b).[73] In the absence of an alcohol initiator, the NHC is capable of forming controlled, high-molecular-weight cyclic polymers such as PLA, PCL, PVL and gradient block PVL-*co*-PCL through ROP, where NHC can acts as a catalyst/initiator via zwitterionic ring-opening polymerization (ZROP) (Scheme 1.4 c).[73–76] Thus, NHC catalysts are extensively studied for the ROP of both linear and cyclic esters. NHC catalysts outstand for LA polymerizations in terms of rates in seconds under low catalyst loadings (0.5 mol%). Additionally, in the presence of an alcohol initiator, it exhibits narrow M_w/M_n (<1.16) and remarkable end group fidelity.[39,67,69,77] Compared to NHC catalyzed ROP of LA, polymerization rates of VL and CL are much lower, and give broader M_w/M_n (1.16- 1.32).[33] Besides its higher catalytic activity, NHCs have been used in the stereoselective polymerization of *rac*-LA at low temperatures and for the formation of heterotactic polylactide from *meso*-lactide. Polymerization of *rac*-LA using sterically hindered, achiral Ph_2IMes catalyst can generate isotactic PLA (P_i =0.90) at -70°C. [78] Besides, the ROP of *rac*-LA using sterically hindered chiral $(CH(Me)Ph)_2$IMes catalyst also formed a highly isotactic PLA at low temperatures. It was suggested that stereo-control is originated from the steric congestion of the active site, rather than by the chirality of the catalyst. The mechanism for ROP of *rac*-LA using either achiral or chiral NHCs catalysts was proposed through the chain-end activation mechanism despite the presence of chiral groups close to the active site.

Unimolecular Bifunctional Catalysts. Another remarkable milestone of the organocatalysts occurred in 2005 with the introduction of Takemoto thiourea for the

ROP of LA (Figure 1.5). Takemoto thiourea acts as a unimolecular bifunctional catalyst which has H-bonding acceptor (thiourea) and H-bonding donor (tertiary amine) moieties. Lactide is activated by the thiourea moiety via H-bonding, and the initiator is activated by the tertiary amine via H-bonding (Scheme 1.5). This dual activation allowsfor a well-controlled polymerization with a living behavior. Despite its higher selectivity towards the monomer, slothful rates were observed.[44] Besides, Takemoto thiourea was not active towards the ROP of VL and CL. Takemoto thiourea catalyst shows modest stereoselectivities at room temperature for ROP of *rac*-LA.[79] Remarkably, it has shown that same activity for the ROP of LA with thiourea (**1-S**) and *N,N*- dimethylcyclohexylamine which proved the bifunctional nature of the catalyst is critical, yet activating units are not required in a single catalyst, it can be a bimolecular system.[44] This invention marked a key development on the mechanistic perception of organocatalysis.

Highly active, commercially available, a strong guanidine base 1,5,7-triazabicyclo [4.4.0]dec-5-ene (TBD) is a unimolecular bifunctional catalyst for the ROP for lactide (Scheme 1.5), which could increase the rate of polymerization to seconds with a minimum amount of catalyst loading in non-polar solvents. TBD is also able to polymerize VL and CL readily. Interestingly, polymerization of *rac*-lactide with TBD shows a slight isotactic enhancement with a P_i value of 0.58 compared to other organocatalysts at room temperature.[38] However, TBD can eventually transesterify the polymer backbone and can lead to poor end group fidelity and broad molecular weight distribution.[38,80] To mitigate the poor end group fidelity, an acyclic guanidine catalyst

has been designed as less basic than TBD. The ROP of LA with acyclic guanidine shows higher control and end group fidelity despite its low rates.[81] A guanidine base 7-Methyl-1,5,7-triazabicyclo[4.4.0]dec-5-ene (MTBD) and an amidine base 1,8-diazabicyclo[5.4.0]undec-7-ene (DBU) are substituted analogues for TBD which are active for the ROP of LA which provided a good selectivity and a narrow M_w/M_n (<1.1). However, the reaction rates are lower and require a higher catalyst loading than TBD. Yet, no significant differences were observed in the selectivity of stereochemistry for the polymerization of *rac*-LA between TBD, DBU, and MTBD.[38] Despite the activity of MTBD and DBU towards the ROP of LA, it is reported that those bases are not active for the ROP of VL and CL, but in the presence of **1-S**, MTBD and DBU can promote the ROP of VL and CL.[82] Amino-thiazoline is another unimolecular bifunctional catalyst which has been designed for the ROP of LA. This catalyst can give control polymers for the ROP *rac*-LA, though it is sluggish with compared to TBD.[83]

In 2013, Dixon and co-workers disclosed a novel class of unimolecular bifunctional Iminophosphorane (IPTU-1) catalyst, equipped with a H-bond donor and a BrØnsted base for the ROP of lactones. However, for the ROP of CL, an increasing discrepancy between the target molecular weight and M_n was observed as the $[M]_0/[I]_0$ increased.[84] Polymerization of *rac*-lactide catalyzed by chiral iminophosphorane catalyst (IPTU-2) gives slight isotactic enhancement (P_i =0.64) at room temperature.[84] Recently, the synthesis of bifunctional iminophosphorane thiourea/urea catalysts (IPTU-3 and IPU**)** has been reported for the ROP of *rac*-LA, which could afford controlled molecular weights, narrow M_w/M_n and well-defined end groups without any undesired side

reactions. The ROP of *rac*-LA catalyzed with IPU has shown a higher stereoselectivity (P_m = 0.80) under mild reaction conditions via chain-end control mechanism.[85] Besides, Chen and Bo-Zhu have newly designed a bifunctional chiral catalyst system incorporating three key elements (β-isocupreidine core, thiourea functionality, and chiral binaphthyl-amine (BINAM)) (β-ICD-TU-BINAM) into a single organic molecule, which is capable of furnishing ROP of *rac*-LA with supreme stereoselectivity factor (k_L/k_D)= 53 and *ee* = 91% at 50.6% monomer conversion.[86] The commercially available chiral version of Takemoto thiourea has been used to form semi-crystalline PLA via isoselective ROP of *rac*-LA. The polymerizations have been carried out at room temperature, and *rac*-LA conversion reached 85% after 238 hours giving expected molecular weight, narrow M_w/M_n and a P_m value of 0.87. Yet, epimerization of *rac*-LA to *meso*-LA was observed due to stereo errors during the ROP process.[87]

H-Bond Donors. Throughout the last decade, a wide range of H-bond donors were explored for the ROP of lactones. Some of the effective H-bond donors are 1) squaramide catalyst(SQA)[88],[89] 2) amides (A1)[90], 3) fluorinated alcohols (FA)[91], 4) sulfonamides (SA)[92] and 5) commercially available phenols (Figure 1.6)[93]. These H-bond donors were utilized with weaker tertiary amine bases for ROP of lactones. Hence, comparatively, these ROP reactions are time-consuming yet, well-controlled. As a remedy (thio)urea catalysts have been developed as H-bond donors with the combination of strong organic bases such as guanidine, amidine and phophazene bases.

(Thio)urea/base Cocatalysts. In the light of above advances of organocatalysts, (thio)urea/ base cocatalyst system was assembled to conduct highly selective ROP of

cyclic lactones, which resulted in precisely tailored polymers with high end group fidelity and narrow molecular weight distributions (M_w/M_n <1.1).[38] Despite the high selectivity, this catalyst system suffer from low rates for ROP.[46,94] In general, thiourea featuring aryl rings with strong electron-withdrawing substituent groups give faster rates, though it is dependent on the reaction conditions.[47] It is also proven that the high selectivity and activity of ROP of VL are proportional to the magnitude of binding constants of catalysts and the bases. However, when the binding is too strong between base and catalyst, a reduction of the reaction rates was observed. [94,95]

The synthetic addition of one and two thiourea moieties to **1-S** could increase the rates of the ROP of LA, VL, and CL in non-polar solvents without compromising the high selectivity.[46,96] Higher activity in **2-S** was explained by *activated thiourea* mechanism supported by computational studies (Figure 1.7). However, the **3-S** catalyst activity was rendered by intramolecular H-bonding network among the thiourea moieties. As a mitigation step of intramolecular H-bonding network, **3-O** was synthesized to have a free urea moiety to activate the monomer which could give remarkable enhanced rate without rendering the selectivity for ROP of VL and CL.[46] The **3-O**/MTBD cocatalyst system could give markable success over TBD for the ROP of CL and VL in terms of the rate and the selectivity.[51] This renaissance leads to conduct ROP with urea catalysts, which are better H-bond donors than its thiourea analogues in the presence of a base.[46,47,97] However, The **2-S** catalyst was effective for the ROP of LA than **1-S** and **3-O**.[96]

Recent studies show that the (thio)urea anion ((thio)imidate) which is corresponding to the deprotonation of H-bond donor by a metal hydride or an alkoxide or a strong amine or tetra-*n*-butylammonium hydroxide could give incredible rates and selectivity for the ROP of lactones.[49,50,52,97,98] It has been computationally and experimentally suggested that (thio)imidate structure can act similarly as TBD where H-bond donor and acceptor are in the same molecule.[49,50] Thiourea with metal alkoxides such as $NaOCH_3$ or $KOCH_3$ makes thioimidate salt and alcohol, which can act as a catalyst/initiator. Hence, for $[M]_0/[I]_0$= 200 ROP of LA, and 1-10 equiv. of thiourea to alcohol shows higher rates (minutes) and selectivity (M_w/M_n ~1.1) with lower amounts of thiourea. However, in the absence of excess thiourea, M_w/M_n was broadened to 1.55.[50] Compared to (thio)urea/alkoxide, (thio)urea/strong organic base shows promising results in reaction control. When (thio)urea mixed with a strong organic base, there can be an equilibrium between classical H-bond mediated ROP and (thio)imidate mediated ROP mechanisms. Hence, it is believed this equilibrium may help to gain reaction control compared to (thio)urea/alkoxide system.[47,51,52] In addition, it has been found that (thio)imidate mechanism is preferred reaction conditions such as polar solvents, high temperature, high monomer concentration, presence of strong electron-withdrawing groups on the H-bond donor and strong bases.[47,48,50,52,97,99,100] Moreover, It has shown that more imidate characteristics can attenuate ROP rates in the application of higher acidic (thio)urea, which resulted in the reduction of basicity of formed (thio)imidate structure.[47,99] A commercially available triclocarban (TCC) has been shown higher activity for the ROP of VL and CL in polar solvents which undergoes through imidate mediated mechanism.[52] Further, the conformational flexibility between (thio)urea moieties also

has an impact on rates. In reason studies, the **2-O5-O** catalyst has shown astonishing enhanced rates and selectivity for the ROP of VL and CL, due to the stability of the pseudo-7-membered cycle formation of the catalyst through intramolecular H-bonding even in non-polar solvents and under solvent free conditions, whereas **2-S5-O** catalyst shows higher rates for the ROP of LA.[97] Thiourea catalysts are more effective in the ROP of LA compared to urea catalysts which is contrary to what was observed for VL and CL, since the same structural analogues of thiourea and urea can have different ROP mechanisms. It was revealed that thiourea is more acidic than its identically substituted urea. Thus, it is more favored towards imidate mediated mechanism. A pair of urea and thiourea with an identical pK_a, can undergo the same mechanism during the ROP of LA, whereas the more polar urea, will become the more active H- bond donor while exhibiting higher rates. [97]

Thermal stability of Organocatalysts

The industrial implementation of organocatalyzed polymerizations is limited due to the requirements of high catalyst loading and poor thermal stability.[66] The standard temperature range for industrial polyester production is 150 °C- 300 °C.[101] Hence, organic acid and base mixtures have been advanced to mitigate the above-mentioned limitations due to its unique ability to form thermally stable complexes (Figure 1.8). One step forward to enhance the green features of organocatalyzed ROP is the use of solvent-less approaches. Hence ROP reactions were attempted under solvent-free conditions. Bulk ROP of LA has been conducted with the stoichiometric mixtures of creatinine + glycolic acid (CR:G) and creatinine + acetic acid (CR:A) at 110 °C and

130 °C. High polymers with a narrow dispersity were obtained, albeit the reactions take days to complete.[102] Recently, it was disclosed that DMAP with organic acids (DMAP.HX) could be used to suppress the reactivity of DMAP and overcome thermal instability. The dual activity of the DMAP.HX complex has been proposed through a cooperative activation mechanism (Scheme 1.7).[103,104] The mixture of DMAP and triflic acid (DMAP:HOTf) displays outstanding catalytic activity over the other tested DMAP.HX systems (X= Cl, OMs) at 130 °C for ROP of L-LA in a living manner.[105] However, at the elevated temperatures, inducement of the racemization reactions was significant. The ROP of VL and CL have attempted with DMAP and it shows meager rates in polymerization. The combining of DMAP with DMAP.HOTf in the presence of an alcohol initiator could increase the rates in the ROP of CL and VL, still, it can be considered as sluggish.[105] Following the same concept, in a recent study DMAP.Saccharin system has been used as a bifunctional catalyst system for the ROP of L-LA and VL. This system shows the adaptability at elevated temperatures (140 °C) with a good controlled polymerization (M_w/M_n = ~1.1) for low $[M]_0/[I]_0$. Albeit, only up to $[M]_0/[I]_0$= 120 molecular weights have attempted for the ROP of L-LA.[103] Further, pyridine base (2,2'-bispyridinium) - MSA ionic mixture was used for the ROP of CL at elevated temperature, which resulted in controlled polymerizations, although slight deviation of molecular weights than expected was observed for polymers which are $[M]_0/[I]_0$>100 indicating the occurrence of undesirable side reactions. [106] Additionally, MSA and TBD have been used to form either a eutectic or non-eutectic mixture to catalyze the ROP of CL under solvent-free conditions at low temperatures as 37 °C. Although, only low $[M]_0/[I]_0$ were attempted and M_w/M_n was broadened up to ~1.5

(Scheme 1.8).[107] However, It has been observed that (thio)urea catalysts are efficient under solvent-free conditions with a minimum amount of catalyst loadings for ROP of lactones while exhibiting excellent weight control from low M_n to high polymers.[53,97] Further, ROP of lactones can be carried out at elevated temperature (110 °C) using appropriate (thio)urea/base cocatalyst without observing any catalyst degradation.[48] As we believe, expansion of use and the development of new catalytic strategies will facilitate the path of organocatalysts toward the industrial applications.

Organocatalysts for the ROP of less-strained lactones

Organocatalytic ROP of macrolactones

Polyesters synthesized from the ROP of macrolactones have attracted much interest over the past few decades due to their mechanical and thermal properties.[8] ω-pentadecalactone (PDL), and ethylene brassylate (EB) are commonly used macrolactones which are obtainable from natural sources and are widely used in ROP to form polyesters with long aliphatic chains.[7,108] The polyesters made from PDL , have shown material properties similar to low-density polyethylene (LDPE) and have the potential to be used in biomedical applications.[7,8] The ROP of macrolactones has been carried out mainly by employing enzyme catalysts, metal catalysts, and organocatalysts.[6] However, only a handful of studies have been carried out for the organocatalytic ROP of macrolactones.

The ROPs of small lactones are known to be enthalpically driven ROPs resulting in the release of the angular and trans-annular strains. Hence, the polymerization reactions

show rapid rates at low or room temperatures.[27] However, the ROP of the macrolactones is stated as entropically driven ROPs, since the larger ring size causes a small/less ring-strain and leads to an entropic gain in the polymerization. According to Gibbs free energy equation, the entropy can be increased with the temperature; thus most of the ROPs of macrolactones are carried out at elevated temperatures.

Organocatalytic ROP of PDL and EB

Organic Acids. Only a few studies have been carried out on the organic acid-catalyzed ROP of marolactones. Dodecylbenzenesulfonic acid (DBSA), DPP, and HOTf are organic acids that have been used for the ROP of PDL in bulk conditions at elevated temperatures (80 ˚C) in the presence of an alcohol initiator.[109] The polymerization reactions catalyzed with DBSA and DPP have taken 24 hours to reach the full conversion and resulted in lower molecular weights than expected.[109] However, with HOTf, targeted molecular weights were achieved. Also, organic acid-catalyzed ROP of EB has been carried out with p-toluene sulfonicacid (PTSA), DPP, and DBSA. However, compared to DPP and DBSA, PTSA showed low molecular weight and a broad M_w/M_n.[108]

Phosphazene Bases. Phosphazene superbases have also been used in the ROP of macrolactones. The ROP of PDL has been carried out with P_2-*t*-Bu, P_4-*t*-Bu and P_4-*t*-Oct bases in the presence of an alcohol initiator in bulk and diluted conditions at 80 ˚C. Rapid rates of polymerization were observed with P_4-*t*-Bu and P_4-*t*-Oct with decent molecular weights ($M_n \leq 34000$ g mol-1) where P_2-*t*-Bu showed comparatively low

rates.[110] The ROP of PDL has also been carried out at room temperature under diluted conditions with P_4-*t*-Bu using an alcohol initiator which showed a high conversion with the expected molecular weight though the M_w/M_n was broad (M_w/M_n = 3.81).[110]

H-Bond donors. TBD has been used as the catalyst for the ROP of PDL in bulk and in solvent at 100 ˚C in the presence of an initiator ($M_n \leq 27100$, M_w/M_n = 1.3 - 2.1). [111,112] Similarly, TBD has also been used for the ROP of EB in bulk and in diluted conditions at 80 ˚C, but it took days to reach high conversions.[108] Other bases, 1,2,3-tricyclohexylguanidine (TCHG) and 1,2,3-triisopropylguanidine (TIPG) have also been tested on the ROP of EB though higher conversions were limited.[108] Additionally, The ROP of PDL has been studied with N-heterocyclic olefins (NHOs) using benzyl alcohol as the initiator in toluene at 110 ˚C which showed poor conversions and reaction rates.[113]

The H- bond mediated ROP of macrolactones has been carried out for PDL and EB in the presence of benzyl alcohol as the initiator. The reactions have been carried out in bulk conditions at 80 ˚C using TCC/BEMP co-catalyst system, which reached high conversions within few hours, resulting in expected molecular weight still, with broader M_w/M_n.[53] In general, it has been problematic to obtain narrow M_w/M_n due to the occurrence of transesterification side reactions, which is notable in the ROPs of macrolactones.

CONCLUSION

In this review, we describe the organocatalytic ROP of selected strained and less strained renewable monomers which are capable of synthesizing biodegradable and biocompatible polymers. The field of organocatalysts for the ROP of strained lactones has bloomed significantly in the past two decades, where advanced catalysts provide rapid and precision synthesis of high polymers, which can substitute petroleum-based polymers. Indeed, the higher activity, selectivity, diversity, cost-effectivity, and greener approach of the organocatalytic ROP give viability and advantageous impact in the polymerization field. Organocatalysts have provided new mechanistic insights and new approaches in synthesizing polymers using strained/less strained lactones while affording new types of materials. The organocatalytic ROP of thiono (macro)lactones can yield new families of materials; thus far, they are relatively understudied the polymer community and in the polymer industry.

Previously, BL, a less strained monomer, was considered a non-polymerizable yet a bioderived monomer. It was found that the organocatalytic ROP of BL requires extreme cold conditions, and only a handful of studies have been carried out. It is worth to disclose more active catalysts and mild reaction conditions for the ROP of BL, since poly(γ-butyrolactone) has been shown material properties which are much desired for biomaterials (in terms of degradability and mechanical properties) .[114]

The ROP of macrolactones has created pathways access to novel polymeric materials featuring long aliphatic polymer backbone. Though organometallic catalysts have been

used widely and performed a decent polymerization process of macrolactones, organocatalysts have become an efficient alternative. Most of the organocatalytic ROPs of macrolactones have been carried out at elevated temperatures, yet obtaining higher molecular, weights, and narrow distribution have become a challenge. Thus, developments in designing and synthesizing new effective organocatalytic systems are needed.

Despite the significant advances in the organocatalytic ROP of lactones, challenges still exist for the implementation of organocatalytic ROP at the industrial scale. Even if the industrial-scale polyester production is performed at high temperatures, most of the oraganocatalysts show low thermal stability, and in many cases, those catalysts get deactivated or degraded at high temperatures, which have been drawbacks in the industrial scale. However, organic acid-base mixtures and (thio)urea catalysts have been tested for ROP at elevated temperatures and reported thermal stability.[48] Nevertheless, only a few studies have been carried out for the use of organocatalysts in ROP at high temperature, and further developments are required to implement of organocatalysts in industry.

The polymers synthesized from LA are commercially important biodegradable and biocompatible polymers that have a wide range of applications. Thus, an adequate amount of studies has been carried out for synthesizing PLA with precise control of molecular weights and narrow M_w/M_n via organocatalytic ROP of L-LA or D-LA. Though, studies on PLAs with different degrees of tacticity are not sufficient to tackle the plausible applications of those polymers.

REFERENCES

1. Williams, C. K. & Hillmyer, M. A. Polymers from renewable resources: A perspective for a special issue of polymer reviews. *Polym. Rev.* **48**, 1–10 (2008).

2. US Department of Agriculture. US Biobased Products Market Potential and Projections Through 2025, OCE-2008-01. (2008).

3. Yao, K. & Tang, C. Controlled polymerization of next-generation renewable monomers and beyond. *Macromolecules* **46**, 1689–1712 (2013).

4. Zhang, X., Fevre, M., Jones, G. O. & Waymouth, R. M. Catalysis as an Enabling Science for Sustainable Polymers. *Chem. Rev.* **118**, 839–885 (2018).

5. Albertsson, A. C. & Varma, I. K. Recent developments in ring opening polymerization of lactones for biomedical applications. *Biomacromolecules* **4**, 1466–1486 (2003).

6. Wilson, J. A., Ates, Z., Pflughaupt, R. L., Dove, A. P. & Heise, A. Polymers from macrolactones: From pheromones to functional materials. *Progress in Polymer Science* vol. 91 29–50 (2019).

7. Wilson, J. A., Hopkins, S. A., Wright, P. M. & Dove, A. P. Synthesis and Postpolymerization Modification of One-Pot Pentadecalactone Block-like Copolymers. *Biomacromolecules* **16**, 3191–3200 (2015).

8. Wilson, J. A., Hopkins, S. A., Wright, P. M. & Dove, A. P. Synthesis of ω-

pentadecalactone copolymers with independently tunable thermal and degradation behavior. *Macromolecules* **48**, 950–958 (2015).

9. Pflughaupt, R. L., Hopkins, S. A., Wright, P. M. & Dove, A. P. Synthesis of poly(ω-pentadecalactone)-b-poly(acrylate) diblock copolymers via a combination of enzymatic ring-opening and RAFT polymerization techniques. *J. Polym. Sci. Part A Polym. Chem.* **54**, 3326–3335 (2016).

10. Wilson, J. A., Hopkins, S. A., Wright, P. M. & Dove, A. P. 'Immortal' ring-opening polymerization of ω-pentadecalactone by Mg(BHT)2(THF)2. *Polym. Chem.* **5**, 2691–2694 (2014).

11. Amass, W., Amass, A. & Tighe, B. A review of biodegradable polymers: Uses, current developments in the synthesis and characterization of biodegradable polyesters, blends of biodegradable polymers and recent advances in biodegradation studies. *Polym. Int.* **47**, 89–144 (1998).

12. Rabnawaz, M., Wyman, I., Auras, R. & Cheng, S. A roadmap towards green packaging: The current status and future outlook for polyesters in the packaging industry. *Green Chem.* **19**, 4737–4753 (2017).

13. Gupta, B., Revagade, N. & Hilborn, J. Poly(lactic acid) fiber: An overview. *Prog. Polym. Sci.* **32**, 455–482 (2007).

14. Cheng, X. W., Guan, J. P., Tang, R. C. & Liu, K. Q. Improvement of flame retardancy of poly(lactic acid) nonwoven fabric with a phosphorus- containing flame

retardant. *J. Ind. Text.* **46**, 914–928 (2016).

15. Vert, M. UA CNRS 500 - University of Rouen, LSM, INSA Rouen, BP OX, 76131 Mont-Saint-Aignan, France. BIORESORBABLE POLYMERS FOR TEMPORARY THERAPEUTIC APPLICATIONS M. VERT. **167**, (1989).

16. Leenslag, J. W., Pennings, A. J., Bos, R. R. M., Rozema, F. R. & Boering, G. Resorbable materials of poly(l-lactide). VII. In vivo and in vitro degradation. *Biomaterials* **8**, 311–314 (1987).

17. Kulkarni, R. K., Pani, K. C., Neuman, C. & Leonard, F. Polylactic Acid for Surgical Implants. *Arch. Surg.* **93**, 839–843 (1966).

18. Ree, M., Yoon, J. & Heo, K. Imprinting well-controlled closed-nanopores in spin-on polymeric dielectric thin films. *J. Mater. Chem.* **16**, 685–697 (2006).

19. Perepichka, I. I., Chen, X. & Bazuin, C. G. Nanopatterning of substrates by self-assembly in supramolecular block copolymer monolayer films. *Sci. China Chem.* **56**, 48–55 (2013).

20. Corma Canos, A., Iborra, S. & Velty, A. Chemical routes for the transformation of biomass into chemicals. *Chem. Rev.* **107**, 2411–2502 (2007).

21. Rose, M. & Palkovits, R. Cellulose-based sustainable polymers: State of the art and future trends. *Macromol. Rapid Commun.* **32**, 1299–1311 (2011).

22. Roesle, P. *et al.* Synthetic polyester from algae oil. *Angew. Chemie - Int. Ed.* **53**,

6800–6804 (2014).

23. Vilela, C. *et al.* The quest for sustainable polyesters-insights into the future. *Polym. Chem.* **5**, 3119–3141 (2014).

24. Tang, X. & Chen, E. Y. X. Toward Infinitely Recyclable Plastics Derived from Renewable Cyclic Esters. *Chem* **5**, 284–312 (2019).

25. Labet, M. & Thielemans, W. Synthesis of polycaprolactone: A review. *Chem. Soc. Rev.* **38**, 3484–3504 (2009).

26. Bhattacharyya, S. K. & Nandi, D. K. High Pressure Synthesis of Delta-Valerolactone and Adipic Acid. *Ind. Eng. Chem.* **51**, 143–146 (1959).

27. Dubois, P., Coulembier, O. & Raquez, J. *Handbook of Ring-Opening*.

28. Mecerreyes, D., Jérôme, R. & Dubois, P. Novel macromolecular architectures based on aliphatic polyesters: Relevance of the 'coordination-insertion' ring-opening polymerization. *Adv. Polym. Sci.* **147**, 2–59 (1999).

29. Polymerization, R. R. Radical Ring-Opening Polymerization. **39**, 265–276 (2001).

30. Sarazin, Y. & Carpentier, J. F. Discrete Cationic Complexes for Ring-Opening Polymerization Catalysis of Cyclic Esters and Epoxides. *Chem. Rev.* **115**, 3564–3614 (2015).

31. Kiesewetter, M. K., Shin, E. J., Hedrick, J. L. & Waymouth, R. M. Organocatalysis: Opportunities and challenges for polymer synthesis. *Macromolecules* **43**, 2093–2107 (2010).

32. goleman, daniel; boyatzis, Richard; Mckee, A. & Perdana. *済無No Title No Title*. *Journal of Chemical Information and Modeling* vol. 53 (2018).

33. Kamber, N. E. *et al.* Organocatalytic ring-opening polymerization. *Chem. Rev.* **107**, 5813–5840 (2007).

34. Guillaume, S. M., Kirillov, E., Sarazin, Y. & Carpentier, J. F. Beyond stereoselectivity, switchable catalysis: Some of the last frontier challenges in ring-opening polymerization of cyclic esters. *Chem. - A Eur. J.* **21**, 7988–8003 (2015).

35. Dechy-Cabaret, O., Martin-Vaca, B. & Bourissou, D. Controlled ring-opening polymerization of lactide and glycolide. *Chem. Rev.* **104**, 6147–6176 (2004).

36. Jérôme, C. & Lecomte, P. Recent advances in the synthesis of aliphatic polyesters by ring-opening polymerization. *Adv. Drug Deliv. Rev.* **60**, 1056–1076 (2008).

37. Mezzasalma, L., Dove, A. P. & Coulembier, O. Organocatalytic ring-opening polymerization of L-lactide in bulk: A long standing challenge. *Eur. Polym. J.* **95**, 628–634 (2017).

38. Lohmeijer, B. G. G. *et al.* Guanidine and amidine organocatalysts for ring-

opening polymerization of cyclic esters. *Macromolecules* **39**, 8574–8583 (2006).

39. Connor, E. F., Nyce, G. W., Myers, M., Möck, A. & Hedrick, J. L. First example of N-heterocyclic carbenes as catalysts for living polymerization: Organocatalytic ring-opening polymerization of cyclic esters. *J. Am. Chem. Soc.* **124**, 914–915 (2002).

40. Nederberg, F., Connor, E. F., Glausser, T. & Hedrick, J. L. Organocatalytic chain scission of poly(lactides): A general route to controlled molecular weight, functionality and macromolecular architecture. *Chem. Commun.* 2066–2067 (2001) doi:10.1039/b106125a.

41. Csihony, S. *et al.* Single-component catalyst/initiators for the organocatalytic ring-opening polymerization of lactide. *J. Am. Chem. Soc.* **127**, 9079–9084 (2005).

42. Dove, A. P. Organic catalysis for ring-opening polymerization. *ACS Macro Lett.* **1**, 1409–1412 (2012).

43. Winnacker, M. & Sag, J. Sustainable terpene-based polyamides: Via anionic polymerization of a pinene-derived lactam. *Chem. Commun.* **54**, 841–844 (2018).

44. Dove, A. P., Pratt, R. C., Lohmeijer, B. G. G., Waymouth, R. M. & Hedrick, J. L. Thiourea-based bifunctional organocatalysis: Supramolecular recognition for living polymerization. *J. Am. Chem. Soc.* **127**, 13798–13799 (2005).

45. Thomas, C., Peruch, F. & Bibal, B. Ring-opening polymerization of lactones using supramolecular organocatalysts under simple conditions. *RSC Adv.* **2**, 12851–

12856 (2012).

46. Fastnacht, K. V. *et al.* Bis- and Tris-Urea H-Bond Donors for Ring-Opening Polymerization: Unprecedented Activity and Control from an Organocatalyst. *ACS Macro Lett.* **5**, 982–986 (2016).

47. Pothupitiya, J. U., Hewawasam, R. S. & Kiesewetter, M. K. Urea and Thiourea H-Bond Donating Catalysts for Ring-Opening Polymerization: Mechanistic Insights via (Non)linear Free Energy Relationships. *Macromolecules* **51**, 3203–3211 (2018).

48. Coderre, D. N., Fastnacht, K. V., Wright, T. J., Dharmaratne, N. U. & Kiesewetter, M. K. H-Bonding Organocatalysts for Ring-Opening Polymerization at Elevated Temperatures. *Macromolecules* **51**, 10121–10126 (2018).

49. Lin, B. & Waymouth, R. M. Urea anions: Simple, fast, and selective catalysts for ring-opening polymerizations. *J. Am. Chem. Soc.* **139**, 1645–1652 (2017).

50. Zhang, X., Jones, G. O., Hedrick, J. L. & Waymouth, R. M. Fast and selective ring-opening polymerizations by alkoxides and thioureas. *Nat. Chem.* **8**, 1047–1053 (2016).

51. Dharmaratne, N. U., Pothupitiya, J. U. & Kiesewetter, M. K. The mechanistic duality of (thio)urea organocatalysts for ring-opening polymerization. *Org. Biomol. Chem.* **17**, 3305–3313 (2019).

52. Dharmaratne, N. U., Pothupitiya, J. U., Bannin, T. J., Kazakov, O. I. &

Kiesewetter, M. K. Triclocarban: Commercial Antibacterial and Highly Effective H-Bond Donating Catalyst for Ring-Opening Polymerization. *ACS Macro Lett.* **6**, 421–425 (2017).

53. Pothupitiya, J. U. *et al.* H-Bonding Organocatalysts for the Living, Solvent-Free Ring-Opening Polymerization of Lactones: Toward an All-Lactones, All-Conditions Approach. *Macromolecules* **50**, 8948–8954 (2017).

54. Shibasaki, Y., Sanada, H., Yokoi, M., Sanda, F. & Endo, T. Activated monomer cationic polymerization of lactones and the application to well-defined block copolymer synthesis with seven-membered cyclic carbonate. *Macromolecules* **33**, 4316–4320 (2000).

55. Casas, J., Persson, P. V., Iversen, T. & Córdova, A. Direct organocatalytic ring-opening polymerizations of lactones. *Adv. Synth. Catal.* **346**, 1087–1089 (2004).

56. Bourissou, D., Martin-Vaca, B., Dumitrescu, A., Graullier, M. & Lacombe, F. Controlled cationic polymerization of lactide. *Macromolecules* **38**, 9993–9998 (2005).

57. Gazeau-Bureau, S. *et al.* Organo-catalyzed ROP of ε-caprolactone: Methanesulfonic acid competes with trifluoromethanesulfonic acid. *Macromolecules* **41**, 3782–3784 (2008).

58. Li, X. *et al.* Tripodal hydrogen bond donor binding with sulfonic acid enables ring-opening polymerization. *Polym. Chem.* **7**, 1368–1374 (2016).

59. Kakuchi, R. *et al.* Controlled/living ring-opening polymerization of δ-valerolactone using triflylimide as an efficient cationic organocatalyst. *Macromolecules* **43**, 7090–7094 (2010).

60. Makiguchi, K., Satoh, T. & Kakuchi, T. Diphenyl phosphate as an efficient cationic organocatalyst for controlled/living ring-opening polymerization of δ-valerolactone and ε-caprolactone. *Macromolecules* **44**, 1999–2005 (2011).

61. Miao, Y. *et al.* Ring-opening polymerization of lactones using binaphthyl-diyl hydrogen phosphate as organocatalyst and resulting monosaccharide functionalization of polylactones. *J. Polym. Sci. Part A Polym. Chem.* **51**, 2279–2287 (2013).

62. Zhang, L. *et al.* Phosphazene bases: A new category of organocatalysts for the living ring-opening polymerization of cyclic esters. *Macromolecules* **40**, 4154–4158 (2007).

63. Zhang, L. *et al.* Organocatalytic stereoselective ring-opening polymerization of lactide with dimeric phosphazene bases. *J. Am. Chem. Soc.* **129**, 12610–12611 (2007).

64. Liu, S., Li, H., Zhao, N. & Li, Z. Stereoselective Ring-Opening Polymerization of rac-Lactide Using Organocatalytic Cyclic Trimeric Phosphazene Base. *ACS Macro Lett.* **7**, 624–628 (2018).

65. Nederberg, F., Connor, E. F., Möller, M., Glauser, T. & Hedrick, J. L. New paradigms for organic catalysts: The first organocatalytic living polymerization. *Angew. Chemie - Int. Ed.* **40**, 2712–2715 (2001).

66. Basterretxea, A., Jehanno, C., Mecerreyes, D. & Sardon, H. Dual Organocatalysts Based on Ionic Mixtures of Acids and Bases: A Step Toward High Temperature Polymerizations. *ACS Macro Lett.* **8**, 1055–1062 (2019).

67. Nyce, G. W. *et al.* In situ generation of carbenes: A general and versatile platform for organocatalytic living polymerization. *J. Am. Chem. Soc.* **125**, 3046–3056 (2003).

68. Naumann, S. & Dove, A. P. N-heterocyclic carbenes as organocatalysts for polymerizations: Trends and frontiers. *Polym. Chem.* **6**, 3185–3200 (2015).

69. Nyce, G. W., Lamboy, J. A., Connor, E. F., Waymouth, R. M. & Hedrick, J. L. Expanding the catalytic activity of nucleophilic N-heterocyclic carbenes for transesterification reactions. *Org. Lett.* **4**, 3587–3590 (2002).

70. Fèvre, M., Pinaud, J., Gnanou, Y., Vignolle, J. & Taton, D. N-Heterocyclic carbenes (NHCs) as organocatalysts and structural components in metal-free polymer synthesis. *Chem. Soc. Rev.* **42**, 2142–2172 (2013).

71. Enders, D., Niemeier, O. & Henseler, A. Organocatalysis by N-heterocyclic carbenes. *Chem. Rev.* **107**, 5606–5655 (2007).

72. Kamber, N. E., Jeong, W., Gonzalez, S., Hedrick, J. L. & Waymouth, R. M. N-heterocyclic carbenes for the organocatalytic ring-opening polymerization of E-caprolactone. *Macromolecules* **42**, 1634–1639 (2009).

73. Jones, G. O. *et al.* N-Heterocyclic carbene-catalyzed ring opening polymerization of ε-caprolactone with and without alcohol initiators: Insights from theory and experiment. *J. Phys. Chem. B* **119**, 5728–5737 (2015).

74. Culkin, D. A. *et al.* Zwitterionic polymerization of lactide to cyclic poly(lactide) by using N-heterocyclic carbene organocatalysts. *Angew. Chemie - Int. Ed.* **46**, 2627–2630 (2007).

75. Acharya, A. K. *et al.* Experimental and computational studies on the mechanism of zwitterionic ring-opening polymerization of δ-valerolactone with N-heterocyclic carbenes. *J. Phys. Chem. B* **118**, 6553–6560 (2014).

76. Shin, E. J. *et al.* Zwitterionic copolymerization: Synthesis of cyclic gradient copolymers. *Angew. Chemie - Int. Ed.* **50**, 6388–6391 (2011).

77. Dove, A. P. *et al.* N-Heterocyclic carbenes: Effective organic catalysts for living polymerization. *Polymer (Guildf).* **47**, 4018–4025 (2006).

78. Dove, A. P. *et al.* Stereoselective polymerization of rac- and meso-lactide catalyzed by sterically encumbered N-heterocyclic carbenes. *Chem. Commun.* 2881–2883 (2006) doi:10.1039/b601393g.

79. Pratt, R. C. *et al.* Exploration, optimization, and application of supramolecular thiourea-amine catalysts for the synthesis of lactide (co)polymers. *Macromolecules* **39**, 7863–7871 (2006).

80. Pratt, R. C., Lohmeijer, B. G. G., Long, D. A., Waymouth, R. M. & Hedrick, J. L. Triazabicyclodecene: A simple bifunctional organocatalyst for acyl transfer and ring-opening polymerization of cyclic esters. *J. Am. Chem. Soc.* **128**, 4556–4557 (2006).

81. Zhang, L. *et al.* Acyclic guanidines as organic catalysts for living polymerization of lactide. *Macromolecules* **43**, 1660–1664 (2010).

82. Lohmeijer, B. G. G. *et al.* Guanidine and amidine organocatalysts for ring-opening polymerization of cyclic esters. *Macromolecules* **39**, 8574–8583 (2006).

83. Becker, J. M. *et al.* Development of Amino-Oxazoline and Amino-Thiazoline Organic Catalysts for the Ring-Opening Polymerisation of Lactide. *Chem. - A Eur. J.* **16**, 6099–6105 (2010).

84. Goldys, A. M. & Dixon, D. J. Organocatalytic ring-opening polymerization of cyclic esters mediated by highly active bifunctional iminophosphorane catalysts. *Macromolecules* **47**, 1277–1284 (2014).

85. Lv, C. *et al.* Isoselective ring-opening polymerization and asymmetric kinetic resolution polymerization of: Rac -lactide catalyzed by bifunctional iminophosphorane-thiourea/urea catalysts. *New J. Chem.* **44**, 1648–1655 (2020).

86. Zhu, J. B. & Chen, E. Y. X. From meso-Lactide to Isotactic Polylactide: Epimerization by B/N Lewis Pairs and Kinetic Resolution by Organic Catalysts. *J. Am. Chem. Soc.* **137**, 12506–12509 (2015).

87. Orhan, B. *et al.* Isoselective Ring-Opening Polymerization of rac-Lactide from Chiral Takemoto's Organocatalysts: Elucidation of Stereocontrol. *ACS Macro Lett.* **7**, 1413–1419 (2018).

88. Liu, J. *et al.* Squaramide and amine binary H-bond organocatalysis in polymerizations of cyclic carbonates, lactones, and lactides. *Polym. Chem.* **8**, 7054–7068 (2017).

89. Liu, J. *et al.* A squaramide and tertiary amine: An excellent hydrogen-bonding pair organocatalyst for living polymerization. *Polym. Chem.* **6**, 3754–3757 (2015).

90. Koeller, S. *et al.* Ring-opening polymerization of L-lactide efficiently triggered by an amido-indole. X-ray structure of a complex between L-lactide and the hydrogen-bonding organocatalyst. *J. Am. Chem. Soc.* **131**, 15088–15089 (2009).

91. Coulembier, O. *et al.* Hydrogen-bonding catalysts based on fluorinated alcohol derivatives for living polymerization. *Angew. Chemie - Int. Ed.* **48**, 5170–5173 (2009).

92. Gmbh, E. D. & Technologies, C. cm 2 /Vs and an on/off ratio >10 6 , with negligible hysteresis, on standard silicon. *Polymer (Guildf).* **48**, 1973–1978 (2010).

93. Thomas, C. *et al.* Phenols and tertiary amines: An amazingly simple hydrogen-bonding organocatalytic system promoting ring opening polymerization. *Adv. Synth. Catal.* **353**, 1049–1054 (2011).

94. Thomas, C. & Bibal, B. Hydrogen-bonding organocatalysts for ring-opening

polymerization. *Green Chem.* **16**, 1687–1699 (2014).

95. Kazakov, O. I., Datta, P. P., Isajani, M., Kiesewetter, E. T. & Kiesewetter, M. K. Cooperative hydrogen-bond pairing in organocatalytic ring-opening polymerization. *Macromolecules* **47**, 7463–7468 (2014).

96. Spink, S. S., Kazakov, O. I., Kiesewetter, E. T. & Kiesewetter, M. K. Rate Accelerated Organocatalytic Ring-Opening Polymerization of l -Lactide via the Application of a Bis(thiourea) H-bond Donating Cocatalyst. *Macromolecules* **48**, 6127–6131 (2015).

97. Hewawasam, R. S. *et al.* Bisurea and Bisthiourea H-Bonding Organocatalysts for Ring-Opening Polymerization: Cues for the Catalyst Design. *Macromolecules* **52**, 9232–9237 (2019).

98. Jiang, Z., Zhao, J. & Zhang, G. Ionic Organocatalyst with a Urea Anion and Tetra- n-butyl Ammonium Cation for Rapid, Selective, and Versatile Ring-Opening Polymerization of Lactide. *ACS Macro Lett.* **8**, 759–765 (2019).

99. Lin, B. & Waymouth, R. M. Organic Ring-Opening Polymerization Catalysts: Reactivity Control by Balancing Acidity. *Macromolecules* **51**, 2932–2938 (2018).

100. Hewawasam, R. S. *et al.* Bisurea and Bisthiourea H-Bonding Organocatalysts for Ring-Opening Polymerization: Cues for the Catalyst Design. *Macromolecules* **52**, 9232–9237 (2019).

101. Lim, L. T., Auras, R. & Rubino, M. Processing technologies for poly(lactic acid). *Prog. Polym. Sci.* **33**, 820–852 (2008).

102. Li, H. *et al.* Controlled synthesis of polylactides using biogenic creatinine carboxylate initiators. *Biomacromolecules* **10**, 1311–1314 (2009).

103. Wei, F. *et al.* Food Sweetener Saccharin in Binary Organocatalyst for Bulk Ring-Opening Polymerization of Lactide. *Adv. Synth. Catal.* (2019) doi:10.1002/adsc.201801319.

104. Kadota, J. *et al.* Ring-opening polymerization of l-lactide catalyzed by an organocatalytic system combining acidic and basic sites. *Macromolecules* **43**, 8874–8879 (2010).

105. Kadota, J. *et al.* Controlled bulk polymerization of l-lactide and lactones by dual activation with organo-catalytic systems. *RSC Adv.* **4**, 14725–14732 (2014).

106. Gontard, G., Amgoune, A. & Bourissou, D. Ring-opening polymerization of ε-caprolactone catalyzed by ionic hydrogen bond activation with bis-pyridiniums. *J. Polym. Sci. Part A Polym. Chem.* **54**, 3253–3256 (2016).

107. García-Argüelles, S. *et al.* Near-to-eutectic mixtures as bifunctional catalysts in the low-temperature-ring-opening-polymerization of ε-caprolactone. *Green Chem.* **17**, 3632–3643 (2015).

108. Pascual, A., Sardon, H., Veloso, A., Ruipérez, F. & Mecerreyes, D.

Organocatalyzed synthesis of aliphatic polyesters from ethylene brassylate: A cheap and renewable macrolactone. *ACS Macro Lett.* **3**, 849–853 (2014).

109. Pascual, A., Leiza, J. R. & Mecerreyes, D. Acid catalyzed polymerization of macrolactones in bulk and aqueous miniemulsion: Ring opening vs. condensation. *Eur. Polym. J.* **49**, 1601–1609 (2013).

110. Ladelta, V., Bilalis, P., Gnanou, Y. & Hadjichristidis, N. Ring-opening polymerization of ω-pentadecalactone catalyzed by phosphazene superbases. *Polym. Chem.* **8**, 511–515 (2017).

111. Todd, R. *et al.* Poly(ω-pentadecalactone)- b -poly(l -lactide) block copolymers via organic-catalyzed ring opening polymerization and potential applications. *ACS Macro Lett.* **4**, 408–411 (2015).

112. Bouyahyi, M., Pepels, M. P. F., Heise, A. & Duchateau, R. ω-Pentandecalactone polymerization and ω-pentadecalactone/ Îμ -caprolactone copolymerization reactions using organic catalysts. *Macromolecules* **45**, 3356–3366 (2012).

113. Naumann, S., Thomas, A. W. & Dove, A. P. Highly Polarized Alkenes as Organocatalysts for the Polymerization of Lactones and Trimethylene Carbonate. *ACS Macro Lett.* **5**, 134–138 (2016).

114. Hong, M. & Chen, E. Y. X. Completely recyclable biopolymers with linear and cyclic topologies via ring-opening polymerization of γ-butyrolactone. *Nat. Chem.* **8**, 42–49 (2016).

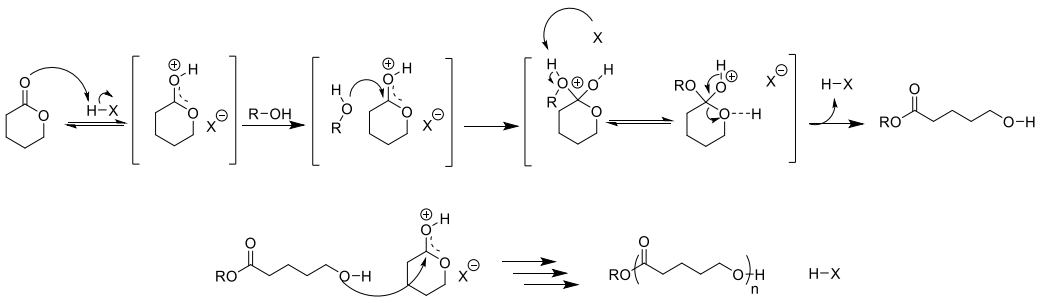

Scheme 1.1. Electrophilic Monomer Activation Mechanism for ROP

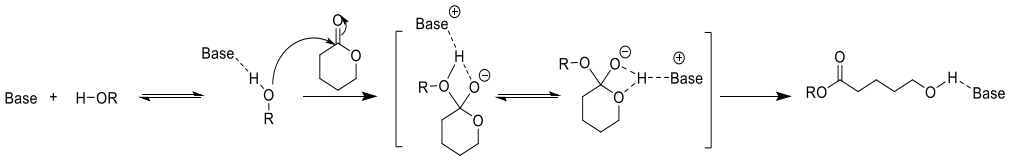

Scheme 1.2. Chain-End Activation Mechanism for ROP

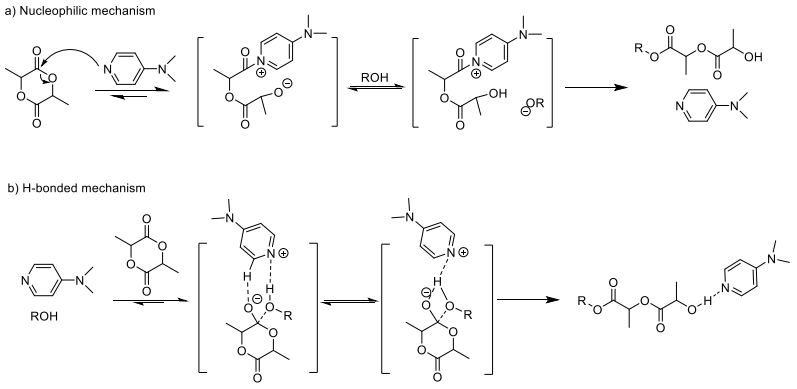

Scheme 1. 3. Proposed Mechanisms for ROP of Lactide with DMAP

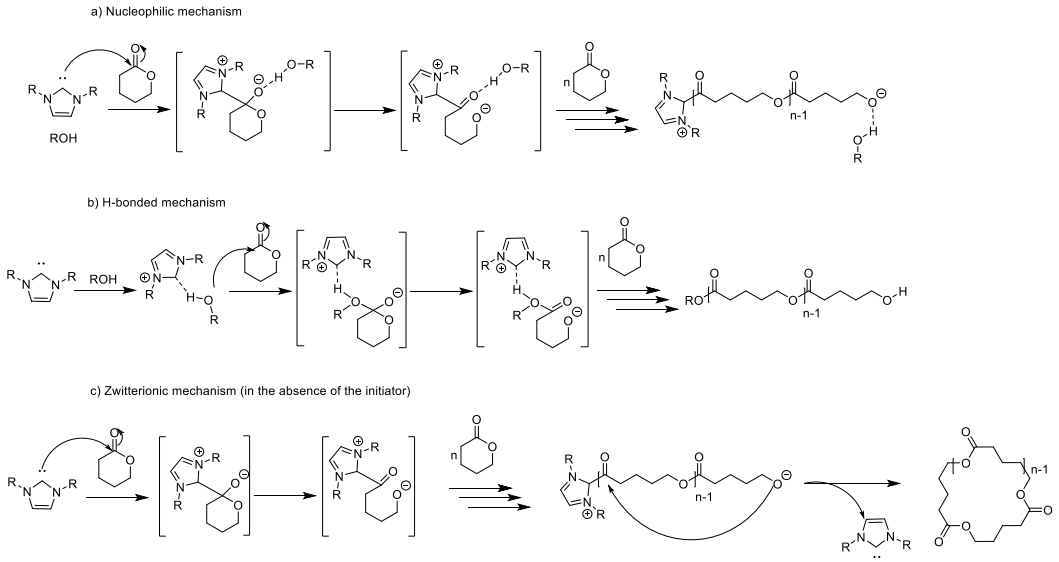

Scheme 1.4. Proposed Mechanisms for ROP of lactones with NHC

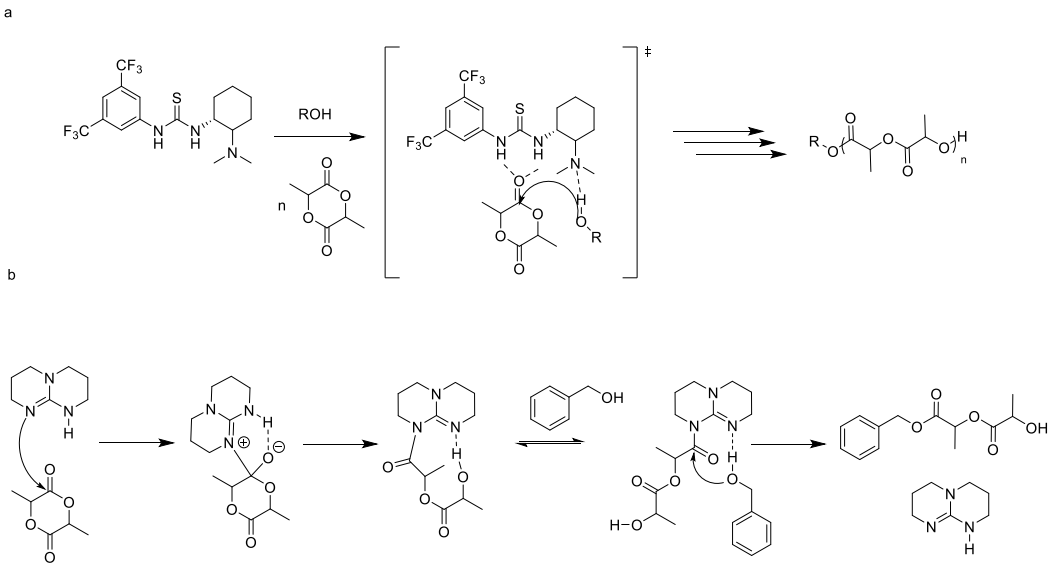

Scheme 1.5. Bifunctional activation of monomer and initiator/chain end by Takemoto thiourea (a) and by TBD (b)

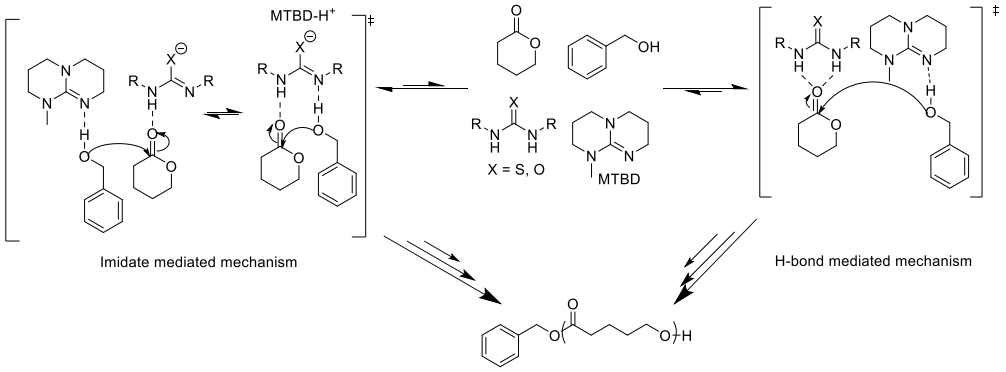

Scheme 1.6. Equilibrium between imidate mediated mechanism and H-bond mediated mechanism

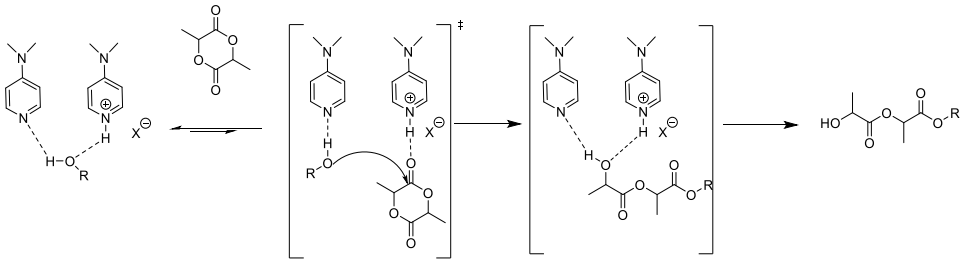

Scheme 1.7. DMAP/DMAP-HX catalyzed cooperative activation mechanism for the ROP of LA

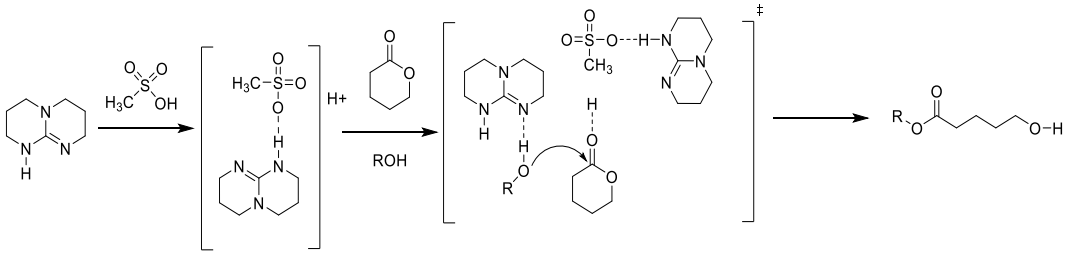

Scheme 1.8. non-eutectic mixture of TBD: MSA for the ROP of LA

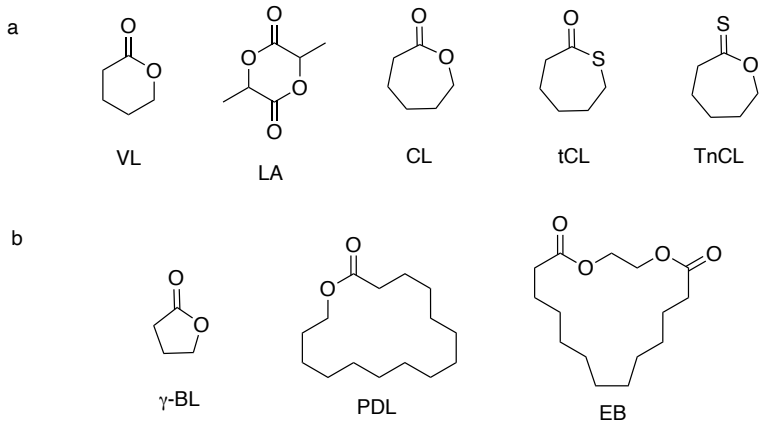

Figure 1.1. a) Some strained lactones b) Some less strained lactones used in organocatalytic ROP

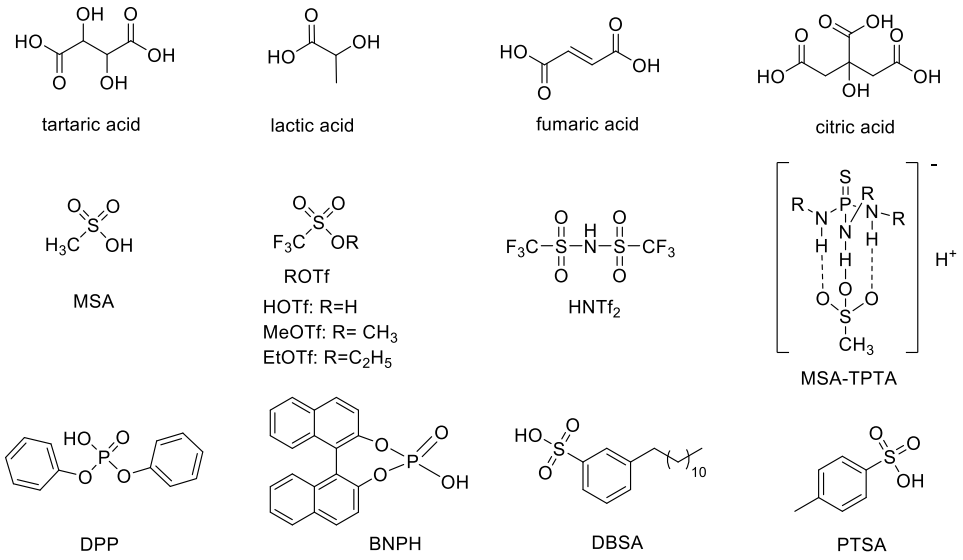

Figure 1.2. Organic acids as organocatalysts for ROP

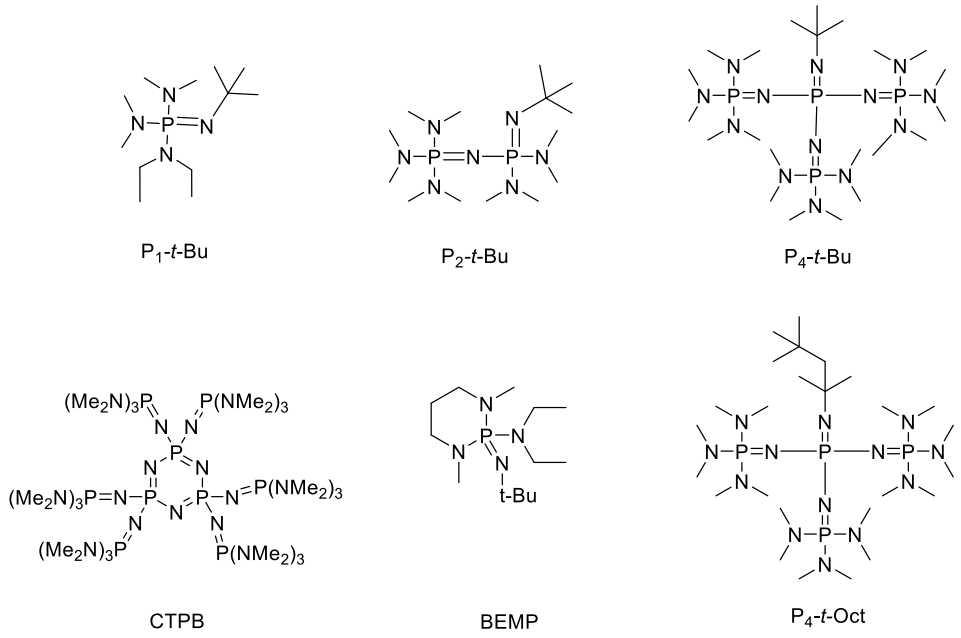

Figure 1.3. Phosphazene bases as organocatalysts for ROP

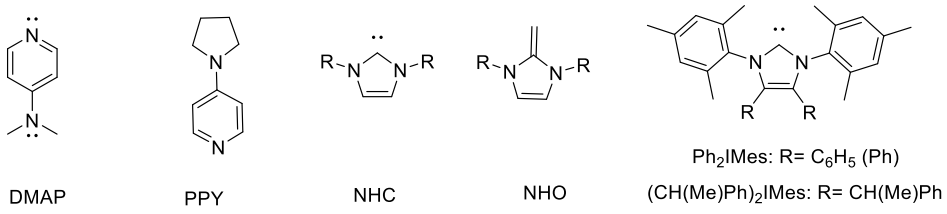

Figure 1.4. Pyridine bases and *N*-Heterocyclic carbenes and olefins for ROP

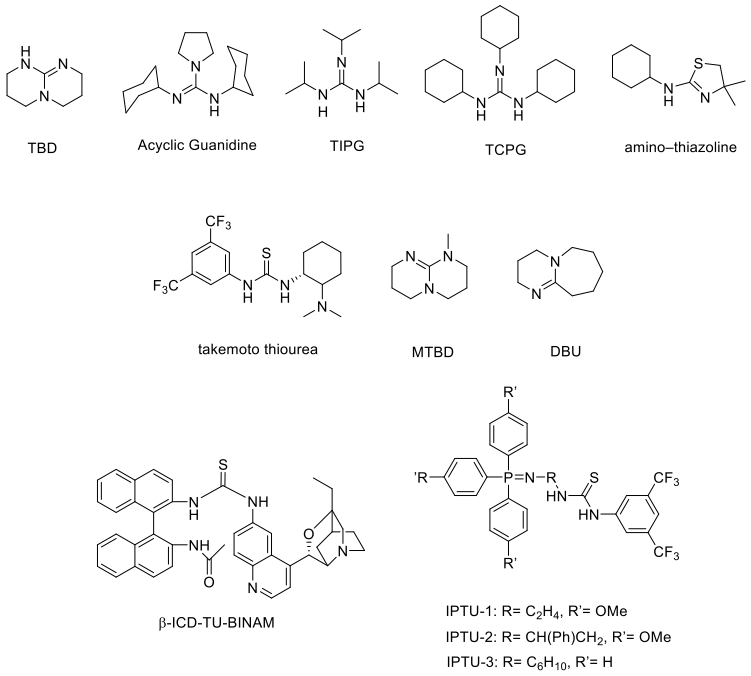

Figure 1.5. Unimolecular bifunctional catalysts for ROP

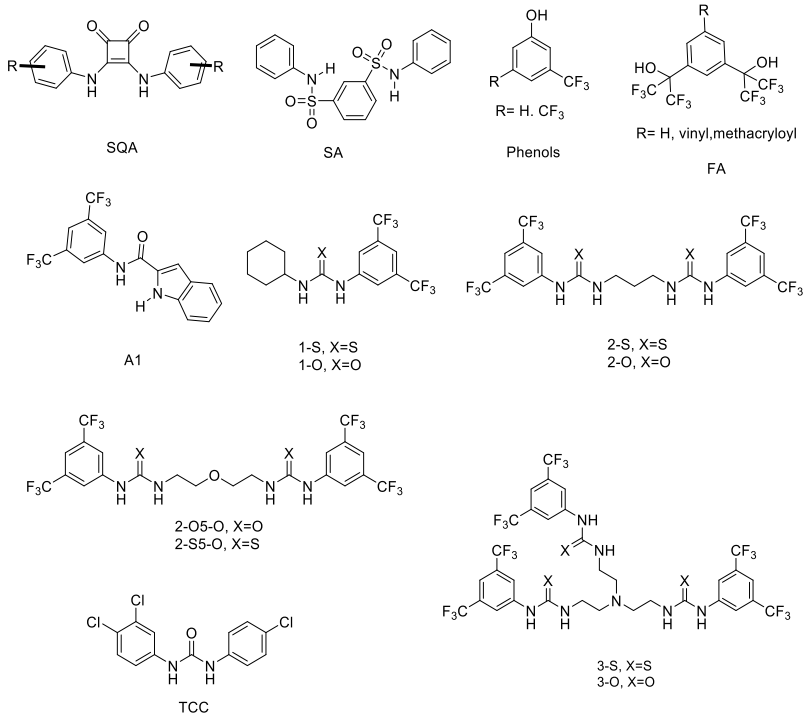

Figure 1.6. H-bond donor catalysts for ROP

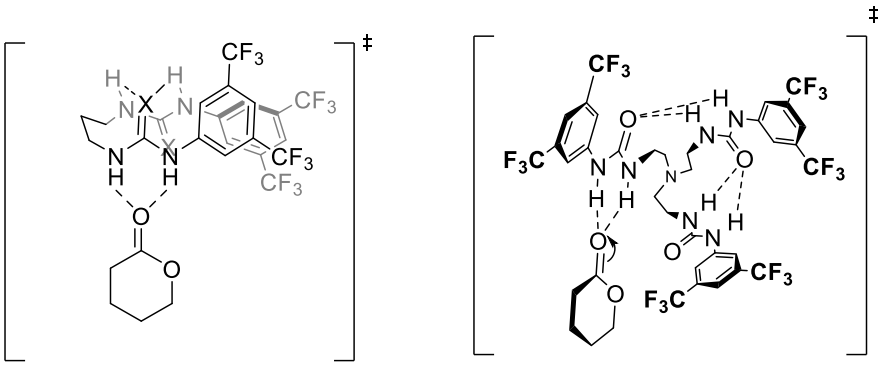

Figure 1.7. Proposed activated (thio)urea transition state for multi-donors

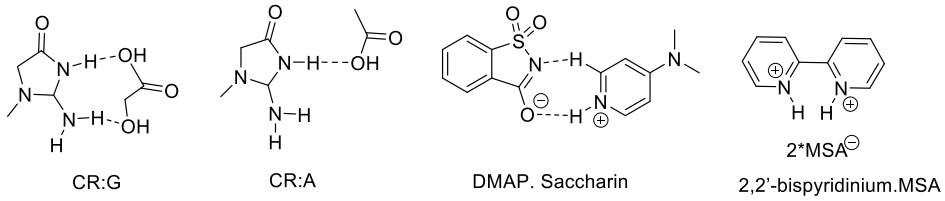

Figure 1.8. Organic acid base mixtures for ROP

MANUSCRIPT II

Published in ACS Macromolecules

Urea and Thiourea H-Bond Donating Catalysts for Ring-Opening Polymerization: Mechanistic Insights Via (Non)Linear Free Energy Relationships

Jinal U. Pothupitiya, Rukshika S. Hewawasam and Matthew K. Kiesewetter

Chemistry, University of Rhode Island, Kingston, RI, USA

Corresponding Author: Matthew Kiesewetter, Ph.D.

Chemistry

University of Rhode Island

140 Flagg Road

Kingston, RI, 02881, USA

Email address: mkiesewetter@uri.edu

ABSTRACT

Hammett-style free energy studies of (thio)urea/MTBD mediated ROP of δ-valerolactone reveal the complicated interplay of reagents that give rise to catalysis through one of two mechanisms. The operative mechanism depends most greatly on the solvent, where polar solvents favor a (thio)imidate mechanism and non-polar solvents favor a classic H-bond mediated ROP. Data suggest that the transition state is only adequately modeled with ground state thiourea-monomer interactions in the H-bonding pathway, and elusive urea/reagent ground state binding interactions may be irrelevant and, hence, not worth pursuing. However, neither relationship is robust enough to be predictive in the absence of other data. Isotope effects suggest that the base/alcohol binding event is directly observable in the ROP kinetics. New opportunities for catalysis emerge, and a reason for the observed mechanism change is proposed.

INTRODUCTION

For more than a decade, the remarkable selectivity of thiourea plus base cocatalysts for monomer (vs polymer) in the ring-opening polymerization (ROP) of lactones has been applied to the formation of highly-adorned and precisely tailored macromolecules.[1–3] In the last several years, this class of catalyst has received new attention from several research groups as efforts have been undertaken to increase the activity of these systems without sacrificing their high level of reaction control.[4–9] One method of devising improved catalysts structures is through mechanistic investigations. Thiourea/base cocatalysts are believed to operate through H-bond activation of monomer/polymer chain end, and this model has been widely corroborated with ^{1}H NMR titration experiments.[10–12] A newer model attributes the activity of a thiourea/base system to the nature of the binding between the cocatalysts.[13–16] The nascent class of urea/base cocatalysts complicates the picture by introducing yet another mechanism.[4–7] These urea/base cocatalysts have been proposed to form an imidate which functions as a discrete catalyst by dual H-bond activation of monomer and chain end; the epitome of this catalyst architecture is the 'hyperactive' urea imidates – formed by the treatment of urea with strong bases – which are incredibly active catalysts for ROP.[4] However, the imidate formed by the reaction of urea and organic base seems to exist along a continuum with a classic H-bond mediated ROP pathway, Scheme 2.1,[6,17] and developing a comprehensive mechanistic basis upon which new catalysts can be developed became a primary goal for our group. Studying urea and thiourea catalysts can be difficult because of the complicated and sensitive interplay of interactions that

give rise to catalysis. H-bonding catalysts are known to bind to monomer, base, each other and other species to a lesser extent (i.e. polymer).[11,14,16] Additionally, ureas and thioureas are susceptible to proton transfer to base cocatalyst which generates a new mechanism,[4,5] and we now have the new ability to conduct ROP in polar solvent.[6,17] 'Simple' structural modification of the H-bond donor catalyst modulates all of these interactions. Added to the difficulty in studying these systems is that ground state interactions (e.g. binding constants) are used to model catalytic interactions, which are only *presumed* to persist at the transition state. We believed that Hammett analysis would be uniquely suited to a big picture approach that is required to illuminate the many, dramatic changes that (thio)urea structure modification have upon ROP.

EXPERIMENTAL SECTION

General Considerations. All chemicals were purchased through Fisher Scientific and used as received unless stated otherwise. Benzene-d_6 and chloroform-*d* were purchased from Cambridge Isotope Laboratories, distilled from calcium hydride and stored under N_2. Acetone-d_6 was purchased from Cambridge Isotope Laboratories, distilled from calcium sulfate and stored under N_2. δ-valerolactone (VL) and benzyl alcohol were distilled under high vacuum from calcium hydride prior to use. Dry CH_2Cl_2 was obtained from an Innovative Technology solvent purification system. Aniline, and 3,5-dimethoxyphenyl isocyanate were purchased from Sigma Aldrich. Phenyl isothiocyanate and cyclohexyl amine, 4-nitrophenyl isocyanate, 3,5-bis(trifluoromethyl)phenyl isocyanate, 3,5-dichloromethylphenyl isocyanate were purchased from Acros Organics. 4-nitrophenyl isothiocyanate was purchased from Tokyo Chemical Industry. 4-chlorophenyl isothiocyanate, 4-fluorophenyl isothiocyanate, 4-methoxyphenyl isothiocyanate, 4-methylphenyl isothiocyanate, 4-chlorophenyl isocyanate, 4-fluorophenyl isocyanate, 4-methylphenyl isocyanate, 4-trifluoromethylphenyl isocyanate, 3,5-dimethyl isocyanate were purchased from Alfa Aesar. 4-(trifluoromethyl)phenyl isothiocyanate, 3,5-dichlorophenyl isothiocyanate, 3,5-dichlorophenyl isothiocyanate, 3,5-difluorophenyl isothiocyanate, 3,5-bis(trifluoromethyl)phenyl isothiocyanate, 3,5-dimethoxyphenyl isothiocyanate, 3,5-dimethylphenyl isothiocyanate were purchased from Oakwood Chemicals. All experiments were conducted in an MBRAUN or INERT stainless-steel glovebox or using a Schlenk line under nitrogen atmosphere with pre-dried (in an oven) glassware.

NMR experiments were performed on a Bruker Avance III 300 or 400 MHz spectrometer. Urea and thiourea H-bond donors were prepared by established methods.[12] Syntheses and characterization of ureas have been provided below. Gel Permeation Chromatography (GPC) was performed with an Agilent Infinity GPC system equipped with three Agilent PLGel columns 7.5 mm × 300 mm (5 μm, pore sizes: 10^3, 10^4, 50 Å) using dichloromethane eluent (HPLC grade) at 30 °C with a flow rate of 1 mL/min. M_n and M_w/M_n were obtained against polystyrene standards (500 g/mol-3150 kg/mol, Polymer Laboratories). The GPC samples were prepared at 1 mg/mL by dissolving polymer (cleaned by washing with methanol) in dichloromethane.

Mass spectrometry experiments were performed using a Thermo Electron (San Jose, CA, USA) LTQ Orbitrap XL mass spectrometer affixed with electrospray ionization (ESI) interface in a positive ion mode. Collected mass spectra was averaged for at least 50 scans. Tune conditions for infusion experiments (10 μL/min flow, sample concentration 5 μg/mL in 50/50 v/v water/ methanol) were as follows: ion spray voltage, 5000 V; capillary temperature, 275°C; sheath gas (N_2, arbitrary units), 11; auxiliary gas (N2, arbitrary units), 2; capillary voltage, 21 V; and tube lens, 90 V; multipole 00 offset, -4.25 V; lens 0 voltage, - 5.00; multipole 1 offset, - 8.50 V; Multipole RF Amplitude, 400 V; Ion trap's AGC target settings for Full MS was 3.0e4 and FT's 2.0e5 (with 3 and 2 averaged microscans, respectively). Prior to analysis, the instrument was calibrated for positive ions using Pierce LTQ ESI positive ion calibration solution (lot #PC197784).

An example of determining observed rate constant (k_{obs}) for ROP of VL. A 7 mL vial was charged with 4-nitrophenyl cyclohexylthiourea (13.9 mg, 0.049 mmol), VL (100 mg, 0.998 mmol) and benzene-d_6 (237 mg, 249.7 μL) and agitated to make a homogeneous solution. Another 7 mL vial was charged with MTBD (7.65 mg, 0.049 mmol), benzyl alcohol (1.08 mg, 0.009 mmol) and benzene-d_6 (237 mg, 249.7 μL) and shaken to mix. The contents of the second vial were transferred to the other by a Pasteur pipette, shaken to mix, and transferred to an NMR tube. Reaction progress was monitored using ^{1}H NMR. Observed rate constants (k_{obs}) were extracted from a first order evolution of [VL] versus time (min), where k_{obs} is:

$$\text{Rate} = -d[VL]/dt = k_{obs}[VL]$$

$$k_{obs} = k_p[cats][alcohol]$$

and

$$\ln([VL]_o/[VL]) = k_{obs}\, t$$

The (thio)urea plus base cocatalyzed ROP was previously shown to be first order in $[\text{thiourea + base}]_o$ as opposed to $[\text{thiourea}]_o[\text{base}]_o$.[14] Observed rate constants in the benzene-d_6 Hammett Plots are the average of at least 2 runs, and k_{obs} are given in min^{-1}. A tabulation of errors is given below (Tables 6.1 to 6.4).

Example binding study of a thiourea to VL. Stock solutions were prepared in benzene-d_6 of VL (500 mM) and phenyl cyclohexylthiourea (10 mM). To a NMR tube, 100 μL of the thiourea stock solution and varying amounts of VL stock solution were added,

and the final volume of solution was taken to 500 μL with benzene-d_6. The final concentrations of VL in the NMR tubes were varied between 400 mM ≥ $[VL]_o$ ≥ 0 mM, and the concentration of the thiourea was [phenyl cyclohexylthiourea] = 2 mM. ^{1}H NMR spectra (referenced to residual benzene-H) were acquired for each solution at 300 K, and the chemical shift of the *ortho*-protons of phenyl thiourea was determined. The binding was determined by a line fitting method,[30] and the values match those obtained by Lineweaver-Bruker method.[31] The errors on the binding constants were calculated by linear regression of the linear method, and a tabulation of errors is given in the Tables 6.1 and 6.4.

Example of binding study of a thiourea to MTBD. Stock solutions were prepared in benzene-d_6 of MTBD (500 mM) and phenyl cyclohexylthiourea (10 mM). To a NMR tube, 100 μL of the thiourea stock solution and varying amounts of MTBD stock solution were added, and the final volume was taken to 500 μL with benzene-d_6. The final concentrations of MTBD in the NMR tubes were varied between 400 mM ≥ [MTBD] ≥ 0 mM, and the concentration of the thiourea was [phenyl cyclohexylthiourea] = 2 mM. ^{1}H NMR spectra (referenced to residual benzene-H) were acquired for each solution at 300 K, and the chemical shift of the *ortho*-protons of phenyl thiourea was determined. The binding was determined by a line fitting method,[30] and the values match those obtained by Lineweaver-Bruker method.[31] The errors on the binding constants were calculated by linear regression of the linear method, and a tabulation of errors is given in Tables 6.3 and 6.4.

Example Isotopic Effect study. A 7 mL vial was charged with 4-(trifluoromethyl)phenyl cyclohexylthiourea (15.1 mg, 0.049 mmol), benzyl alcohol (1.08 mg, 0.009 mmol), VL (100 mg, 0.998 mmol) and C_6D_6 (249.7 μL) and agitated to make a homogeneous solution. Another 7 mL vial was charged with MTBD (7.6 mg, 0.049 mmol) and $CDCl_3$ (249.7 μL), and the contents of the second vial were transferred to the other by a Pasteur pipette followed by transfer of the reaction mixture into a NMR tube. The progress of reaction was monitored by ^{1}H NMR. This was repeated with varying portions of $CHCl_3$ in the chloroform portion of the solvent: 75 %, 67 %, 25% and 16.6%. The k_{obs} of each reaction were plot against the percentage of $CDCl_3$, and the line was extrapolated to obtain rate at 100 % $CHCl_3$ with which the k_H/k_D value was calculated. The errors on the k_H/k_D were calculated by linear regression of the k_{obs} vs %D line, and a tabulation of errors is given in Tables 6.1 to 6.4. ^{1}H NMR spectra of benzyl alcohol in these solvent mixtures indicates that the alcohol adopts the same isotopic ratio as the $CDCl_3/CHCl_3$ portion of the solvent, see Figure 2.11. The (thio)urea NHs also undergo H/D exchange and adopt the isotopic ratio of the chloroform feed. While we presume that the IE of the OD bond makes up the majority of the IE, we cannot rule out an IE from the D-bonding catalyst.

Synthesis of thiourea H-bond donors

1,3-diphenyl urea. A flame dried 25 ml Schlenk flask was charged with a stir bar, dichloromethane (20-25 mL), phenyl isocyanate (1 g, 8.39 mmol) and aniline (0.766 mL, 8.39 mmol). The solution was stirred overnight, and the solvent was removed under reduced pressure. Yield: 0.9231g, 62%. Characterization matches literature. [1]

4-chlorophenyl-3-phenyl urea. A flame dried 25 ml Schlenk flask was charged with a stir bar, dichloromethane (25 mL), 4-chlorophenyl isocyanate (1 g, 6.511 mmol) and aniline (0.59 mL, 6.51 mmol). The solution was stirred overnight, and the solvent was removed under reduced pressure. Yield: 1.12 g, 70%. Characterization matches literature.[2]

4-fluorophenyl-3-phenyl urea. A flame dried 25 ml Schlenk flask was charged with a stir bar, dichloromethane (25 mL), 4-fluorophenyl isocyanate (1 g, 7.29 mmol) and aniline (0.66 mL, 7.29 mmol). The solution was stirred overnight, and the solvent was removed under reduced pressure. Yield: 1.31 g, 78%. Characterization matches literature. [3]

4-nitrophenyl-3-phenyl urea. A flame dried 25 ml Schlenk flask was charged with a stir bar, dichloromethane (25 mL), 4-nitrophenyl isocyanate (1 g, 6.093 mmol) and aniline (0.567 mL, 6.093 mmol). The solution was stirred overnight, and the solvent was removed under reduced pressure. Yield: 1.33 g, 85%. Characterization matches literature.[4]

4-methylphenyl-3-phenyl urea. A flame dried 25 ml Schlenk flask was charged with a stir bar, dichloromethane (25 mL), 4-methylphenyl isocyanate (1 g, 7.51 mmol) and aniline (0.699 mL, 7.51 mmol). The solution was stirred overnight, and the solvent was removed under reduced pressure. Yield: 1.17 g 68%. Characterization matches literature.[5]

4-(trifluoromethyl)phenyl-3-phenyl urea. A flame dried 25 ml Schlenk flask was charged with a stir bar, dichloromethane (25 mL), 4-trifluoromethylphenyl isocyanate (0.786 g, 5.34 mmol) and aniline (0.29 mL, 0.98 mmol). The solution was stirred overnight, and the solvent was removed under reduced pressure. Yield: 0.67 g, 74%. NMR spectra given below. HRMS :*m/z* exp. = 281.0900 $(C_{14}H_{12}F_3N_2O+H)^+$, (calc. = 281.0896). ^{1}H NMR (400 MHz, Acetone-d_6) δ 8.22 (s, 1H), 8.12 (s, 1H), 7.66 – 7.48 (m, 9H), 7.39 – 7.22 (m, 9H), 7.07 – 6.94 (m, 2H).

3,5-dichlorophenyl-3-phenyl urea. A flame dried 25 ml Schlenk flask was charged with a stir bar, dichloromethane (25 mL), 3,5-dichlorophenyl isocyanate (1 g, 5.31 mmol) and aniline (0.724 mL, 5.31 mmol). The solution was stirred overnight, and the solvent was removed under reduced pressure. Yield: 1.32 g, 89%. NMR spectra given below. HRMS :*m/z* exp. = 281.0243 $(C_{13}H_{11}Cl_2N_2O+H)^+$, (calc. = 281.0245). ^{1}H NMR (400 MHz, Acetone-d_6) δ 8.40 (s, 1H), 8.22 (s, 1H), 7.69 – 7.45 (m, 8H), 7.31 (t, J = 7.8 Hz, 4H), 7.05 (dd, J = 15.6, 8.2 Hz, 3H).

3,5-bis(trifluoromethyl)phenyl-3-phenyl urea. A flame dried 25 ml Schlenk flask was charged with a stir bar, dichloromethane (25 mL), 3,5-bis(trifluoromethyl)phenyl isocyanate (1 g, 3.91 mmol) and aniline (0.35 mL, 3.91 mmol). The solution was stirred overnight, and the solvent was removed under reduced pressure. Yield: 1.31 g, 96%. NMR spectra given below. HRMS :*m/z* exp. = 349.0770 $(C_{15}H_{11}F_6N_2O+H)^+$, (calc. = 349.0774). ^{1}H NMR (400 MHz, Chloroform-*d*) δ 7.92 (s, 1H), 7.57 (s, 0H), 7.44 (t, J = 7.8 Hz, 1H), 7.39 – 7.34 (m, 1H), 7.26 (d, J = 7.5 Hz, 0H), 6.79 (s, 1H), 6.49 (s, 1H).

3,5-dimethoxyphenyl-3-phenyl urea. A flame dried 25 ml Schlenk flask was charged with a stir bar, dichloromethane (25 mL), 3,5-dimethoxyphenyl isocyanate (1 g, 5.58 mmol) and aniline (0.50 mL, 5.58 mmol). The solution was stirred overnight, and the solvent was removed under reduced pressure. Yield: 1.46 g, 97%. NMR spectra given below. HRMS :*m/z* exp. = 273.1234 $(C_{15}H_{17}N_2O_3+H)^+$, (calc. = 273.1239). ^{1}H NMR (300 MHz, Acetone-d_6) δ 8.03 (s, 0H), 7.55 (d, J = 8.0 Hz, 1H), 7.29 (t, J = 7.7 Hz, 1H), 6.99 (t, J = 7.5 Hz, 1H), 6.81 (d, J = 2.3 Hz, 1H), 6.29 – 6.03 (m, 1H).

3,5-dimethylphenyl-3-phenyl urea. A flame dried 25 ml Schlenk flask was charged with a stir bar, dichloromethane (25 mL), 3,5-dimethylphenyl isocyanate (1 g, 6.79 mmol) and aniline (0.62 mL, 6.79 mmol). The solution was stirred overnight, and the solvent was removed under reduced pressure. Yield: 1.08 g, 64%. NMR spectra given below. HRMS :*m/z* exp. = 241.1335 $(C_{15}H_{17}N_2O+H)^+$, (calc. = 241.1343) ^{1}H NMR (400 MHz, Acetone-d_6) δ 7.54 (d, J = 8.0 Hz, 4H), 7.28 (t, J = 7.8 Hz, 4H), 7.18 (s, 4H), 6.98 (t, J = 7.4 Hz, 2H), 6.65 (s, 2H).

Synthesis of thiourea H-bond donors

*1-cyclohexyl-3-phenylthiourea***.** A flame dried 25 ml Schlenk flask was charged with a stir bar, dichloromethane (10-15 mL), phenyl isothiocyanate (200 mg, 1.48 mmol) and cyclohexyl amine (168.87 µL, 1.48 mmol). The solution was stirred overnight, and the solvent was removed under reduced pressure. The crude solid was purified by

recrystallization in methanol. Yield: 242 mg, 70%. Characterization matches literature.[6,7]

1-cyclohexyl-3-(4-nitrophenyl)thiourea. A flame dried 25 ml Schlenk flask was charged with a stir bar, dichloromethane (10-15 mL), 4-nitrophenyl isothiocyanate (200 mg, 1.11 mmol) and cyclohexyl amine (125.8 μL, 1.11 mmol). The solution was stirred overnight, and the solvent was removed under reduced pressure. The resulting crude solid was purified by recrystallization in DCM. Yield: 285 mg, 92%. Characterization matches literature.[7,8]

1-(4-chlorophenyl)-3-cyclohexylthiourea. A flame dried 25 ml Schlenk flask was charged with a stir bar, dichloromethane (10-15 mL), 4-chlorophenyl isothiocyanate (200 mg, 1.18 mmol) and cyclohexyl amine (134.4 μL, 1.18 mmol). The solution was stirred overnight, and the solvent was removed under reduced pressure. The resulting crude solid was purified by recrystallization in DCM. Yield: 282 mg, 89%. Characterization matches literature.[7,9]

1-cyclohexyl-3-(4-fluorophenyl)thiourea. A flame dried 25 ml Schlenk flask was charged with a stir bar, dichloromethane (10-15 mL), 4-fluorophenyl isothiocyanate (200 mg, 1.31 mmol) and cyclohexyl amine (129.5 μL, 1.31 mmol). The solution was stirred overnight, and the solvent was removed under reduced pressure. The resulting crude solid was purified by recrystallization in DCM. Yield: 300 mg, 91%. Characterization matches literature.[7,10]

1-cyclohexyl-3-(4-methoxyphenyl)thiourea. A flame dried 25 ml Schlenk flask was charged with a stir bar, dichloromethane (10-15 mL), 4-methoxyphenyl isothiocyanate (200 mg, 1.21 mmol) and cyclohexyl amine (138.0 µL, 1.21 mmol). The solution was stirred overnight, and the solvent was removed under reduced pressure. The resulting crude solid was purified by recrystallization in methanol. Yield: 240 mg, 75%. Characterization matches literature.[9]

1-cyclohexyl-3-(p-tolyl)thiourea. A flame dried 25 ml Schlenk flask was charged with a stir bar, dichloromethane (10-15 mL), 4-methylphenyl isothiocyanate (200 mg, 1.34 mmol) and cyclohexyl amine (152.9 µL, 1.34 mmol). The solution was stirred overnight, and the solvent was removed under reduced pressure. The resulting crude solid was purified by recrystallization in methanol. Yield: 226 mg, 68%. Characterization matches literature.[9]

4-(trifluoromethyl)phenyl cyclohexyl thiourea. A flame dried 25 ml Schlenk flask was charged with a stir bar, dichloromethane (10-15 mL), 4-(trifluoromethyl)phenyl isothiocyanate (200 mg, 0.98 mmol) and cyclohexyl amine (112.2 µL, 0.98 mmol). The solution was stirred overnight, and the solvent was removed under reduced pressure. The resulting crude solid was purified by recrystallization in DCM. Yield: 266 mg, 90%. Characterization matches literature.[9,11]

1-cyclohexyl-3-(3,5-dichlorophenyl)thiourea. A flame dried 25 ml Schlenk flask was charged with a stir bar, dichloromethane (10-15 mL), 3,5-dichlorophenyl isothiocyanate (200 mg, 0.98 mmol) and cyclohexyl amine (111.7 µL, 0.98 mmol). The solution was

stirred overnight, and the solvent was removed under reduced pressure. The resulting crude solid was purified by recrystallization in DCM. Yield: 264 mg, 89%. NMR spectra given below. HRMS :*m/z* exp. = 303.0488 ($C_{13}H_{16}Cl_2N_2S + H)^+$, (calc. = 303.0484). ^1H NMR (400 MHz, Chloroform-*d*) δ 7.72 (s, 1H), 7.12 (d, *J* = 1.8 Hz, 2H), 5.93 (S, 1H), 4.23 (s, 1H), 2.09 (dt, *J* = 12.8, 3.5 Hz, 2H), 1.81 – 1.58 (m, 3H), 1.52 – 1.30 (m, 2H), 1.28 – 1.10 (m, 3H).

1-cyclohexyl-3-(3,5-difluorophenyl)thiourea. A flame dried 25 ml Schlenk flask was charged with a stir bar, dichloromethane (10-15 mL), 3,5-difluorophenyl isothiocyanate (200 mg, 1.17 mmol) and cyclohexyl amine (133.2 µL, 1.17 mmol). The solution was stirred overnight, and the solvent was removed under reduced pressure. The resulting crude solid was purified by recrystallization in DCM. Yield: 269 mg, 85%. NMR spectra given below. HRMS :*m/z* exp. = 271.1078 ($C_{13}H_{16}F_2N_2S + H)^+$, (calc. = 271.1075). ^1H NMR (400 MHz, Chloroform-*d*) δ 7.95 (s, 1H), 6.78 – 6.67 (m, 3H), 6.04 (s, 1H), 4.25 (s, 1H), 2.08 (dt, *J* = 12.3, 4.0 Hz, 2H), 1.67 (ddt, *J* = 29.0, 12.9, 3.9 Hz, 3H), 1.48 – 1.34 (m, 2H), 1.18 (tdq, *J* = 15.5, 8.4, 4.3, 3.9 Hz, 3H).

1-(3,5-bis(trifluoromethyl)phenyl)-3-cyclohexylthiourea. A flame dried 25 ml Schlenk flask was charged with a stir bar, dichloromethane (10-15 mL), 3,5-bis(trifluoromethyl)phenyl isothiocyanate (200 mg, 0.74 mmol) and cyclohexyl amine (84 µL, 0.74 mmol). The solution was stirred overnight, and the solvent was removed under reduced pressure. The resulting crude solid was purified by recrystallization in DCM. Yield 216 mg, 79%. Characterization matches literature.[9],[12]

1-cyclohexyl-3-(3,5-dimethoxyphenyl)thiourea. A flame dried 25 ml Schlenk flask was charged with a stir bar, dichloromethane (10-15 mL), 3,5-dimethoxyphenyl isothiocyanate (200 mg, 1.02 mmol) and cyclohexyl amine (116.8 µL, 1.02 mmol). The solution was stirred overnight, and the solvent was removed under reduced pressure. The resulting crude solid was purified by recrystallization in methanol. Yield: 219 mg, 73%. NMR spectra given below. HRMS :*m/z* exp. = 295.1485 $(C_{15}H_{22}N_2O_2S + H)^+$, (calc. = 295.1475). ^{1}H NMR (400 MHz, Chloroform-*d*) δ 7.47 (s, 1H), 6.36 (t, *J* = 2.2 Hz, 1H), 6.30 (d, *J* = 2.2 Hz, 2H), 6.13 (s, 1H), 4.28 (s, 1H), 3.78 (s, 6H), 3.78 (s, 6H), 2.06 (dt, *J* = 12.5, 4.0 Hz, 3H), 1.73 – 1.58 (m, 3H), 1.49 – 1.31 (m, 2H), 1.15 (qd, *J* = 11.8, 11.4, 3.3 Hz, 3H).

1-cyclohexyl-3-(3,5-dimethylphenyl)thiourea. A flame dried 25 ml Schlenk flask was charged with a stir bar, dichloromethane (10-15 mL), 3,5-dimethylphenyl isothiocyanate (200 mg, 1.22 mmol) and cyclohexyl amine (139.7 µL, 1.22 mmol). The solution was stirred overnight, and the solvent was removed under reduced pressure. The resulting crude solid was purified by recrystallization in methanol. Yield: 251 mg, 78%. NMR spectra given below. HRMS :*m/z* exp. = 263.1579 $(C_{15}H_{22}N_2S+ H)^+$, (calc. = 263.1576). ^{1}H NMR (400 MHz, Chloroform-*d*) δ 7.69 (s, 1H), 6.90 (s, 1H), 6.78 (d, *J* = 1.6 Hz, 2H), 5.94 (s, 1H), 4.26 (s, 1H), 2.31 (s, 6H), 2.04 (dq, *J* = 12.4, 3.8 Hz, 2H), 1.70-1.54 (m, 3H), 1.46-1.32 (m, 2H), 1.25 – 1.00 (m, 3H).

RESULTS AND DISCUSSION

Thioureas in Non-polar Solvent. Cyclohexyl aryl thioureas with variable aryl substitution display Hammett behavior in the rate of polymerization they exhibit for the thiourea/MTBD (0.049 mmol, 0.099 M each) (MTBD = 7-methyl-1,5,7-triazabicyclo-[4.4.0]dec-5-ene, Scheme 2.1) cocatalyzed ROP of δ-valerolactone (VL) (2 M) from benzyl alcohol (0.02 M) in benzene-d_6. A series of thiourea H-bond donors were synthesized with systematic variation at the *m*- and *p*- positions (see Experimental Section), Scheme 2.1, and the observed rate constants (k_{obs} in min^{-1}) they exhibit in the ROP of VL were measured by ^{1}H NMR from the first order evolution of [VL]. These ROP have previously been shown to be first order in [monomer], [benzyl alcohol]$_o$ and [catalysts]$_o$.[10,13,14] The plots of log k_{obs} versus σ_m or σ_p are linear, Figure 2.1, which suggest that changing the electronics of the aryl ring is felt at the H-bond donating thiourea moiety. The rates exhibited by the *m*-X-S series (σ_m = 1.9) are more sensitive to a change in group, X, than the *p*-X-S series (σ_p = 0.9), and this may be attributed to the two functional groups per H-bond donor in the former. The extent of reaction control, as measured by M_w/M_n, is similar across both series: *p*-NO_2-S, M_w/M_n = 1.041; *m*-CF_3-S, M_w/M_n = 1.048; H-S, M_w/M_n = 1.050 (90% conversion for all). ^{1}H NMR titration experiments between X-S and MTBD (discussed below) suggest that all X-S undergo *H-bonding* to the base cocatalyst in benzene-d_6 (vs deprotonation)[6,14], and that the Hammett (k_{obs}) behavior is due to modulation of the H-bond acidity in the transition state occurring in a *H-bond mediated ROP*, Scheme 2.1. Previous, truncated, Hammett studies on thiourea H-bond donors for ROP have observed a similar effect,[11] and

Hammett correlations on catalysts (versus substrate), while not classic, are well-documented.[18,19]

The strength of thiourea binding to monomer, K_{VL}, and base, K_{MTBD}, have both been suggested to be indicative of the reaction rate, but while these values can reasonably be predicted by σ, they have low correlation to observed rate constant, k_{obs}. Both *m*-X-S and *p*-X-S exhibit a good Hammett correlation to the thiourea/VL binding constant, K_{VL}. Thiourea H-bond donors have previously been shown via ^{1}H NMR titration to bind to monomer, and this binding has been used as a model for the catalytic mechanism for thiourea-mediated ROP and to account for the high selectivity exhibited by thioureas for monomer vs polymer. The binding constants of the thioureas to VL, K_{VL}, were measured in benzene-d_6 using established methods, see experimental section, and these values display Hammett behavior, especially for those H-bond donors with electron withdrawing groups σ>0), Figure 2.2. These plots suggest that the electron withdrawing groups (EWGs) and electron donating groups (EDGs) groups directly affect the monomer binding ability of the thiourea. The log k_{obs} vs log K_{VL} plots (for both *m*- and *p*-) show a weak correlation (Figure 2.25), suggesting that the binding of monomer to thiourea can *reasonably* predict catalytic activity (i.e. k_{obs}), and that, while ground state thiourea-monomer interactions provide *an approximate model* of the transition state, these models should be applied with caution.

The binding constant of the H-bond donors to MTBD, K_{MTBD}, show Hammett behavior, yet the magnitude of K_{MTBD} is only weakly correlated to k_{obs}. The binding constant of each H-bond donor to MTBD, K_{MTBD}, was measured in benzene-d_6 by ^{1}H NMR

titration, see experimental section, and these values show good Hammett correlations, Figure 2.3. These data reinforce the K_{VL} observations that EWG/EDG modulation directly influences H-bond acidity of the thiourea. The possibility of a coincidental relationship should not be discounted as a stronger H-bond acid would be expected to bind to all H-bond acceptors more strongly. However, the influence of changing σ on K_{MTBD} is stronger than upon K_{VL} ($\rho_{MTBD} > \rho_{VL}$), and the relationship is more robust (better fit for K_{MTBD}). This highlights a difficulty of catalyst modification, as thiourea binding to base – which is known to be inhibitory to catalysis[13,14] – will outpace increased binding to monomer. Our group has previously proposed that the activity of a cocatalyst system in the H-bond mediated ROP of lactones arises from the cooperative interruption of the thiourea•base adduct by initiator/chain-end and monomer.[14] Indeed, plots of log k_{obs} vs log K_{MTBD} (Figures 2.25 and 2.26) show weak correlation but suggest that the binding of thiourea to MTBD *influences* the rate exhibited by these cocatalysts and may exhibit a maximum rate. These observations suggest that the binding of thiourea to cocatalyst and monomer are important measures of catalyst efficacy and *adequately* describe catalytic (transition state) interactions. In this case, the cocatalyst binding constants could influence rate by forming the thiourea•base adduct which has previously been suggested by our group to be important to catalysis (i.e. $k_{obs} = k_p[\text{initiator}]_o[\text{thiourea+base}]_o$). [13,14]

Isotope effects (IEs) of propagating alcohol H/D substitution on ROP rate were conducted and suggest 1) that ground state binding is an adequate model for the transition state of the H-bonding mechanism, and 2) that rate dependencies of some

reagents in the ROP rate equations may arise from binding events prior to enchainment. The k_H/k_D of ROP were measured for the thiourea/MTBD cocatalyzed (0.099 M each) ROP of VL (0.99 mmol, 2 M) from benzyl alcohol (0.02 M) in a mixture of $C_6D_6/CDCl_3/CHCl_3$ (50% benzene, 50% chloroform), where the H/D ratio in the chloroform blends is adopted by the benzyl alcohol, see experimental section. The *m*-X-S H-bond donors exhibit very small (k_H/k_D~1), normal IEs that do not vary with σ_m, and the *p*-X-S with EWG exhibit the same trend, Figure 2.4. For the thioureas with EDGs in the *p*-X-S series, the IEs are inverse. The small magnitude of the IEs, particularly the inverse IEs, suggests that we are observing equilibrium isotope effects rather than small KIEs.[18,20] An inverse, primary KIE is impossible for an elementary reaction.[22] D-bonds have been observed to be stronger than H-bonds which implicates the MTBD/alcohol binding event as the source of the inverse IE.[23] This implies that the first order dependence upon $[initiator]_o$ in the H-bond mediated ROP is due to an equilibrium step prior to the enchainment event that shifts towards MTBD•alcohol + thiourea•VL adducts upon D for H substitution.[14] We presume that the inverse IEs are observed only for EDG-bearing thioureas because thiourea/MTBD binding for these compounds is comparably small (see Figure 2.3, lower). This renders apparent any minute change in alcohol/MTBD binding which occurs upon H/D substitution. In this interpretation, the rate dependencies of the ROP, which is first order in $[base + thiourea]_o$, $[alcohol]_o$ and [monomer],[10,13,14] could arise from the assembly of the reagents prior to the enchainment step, reinforcing the concept of thiourea/base catalysts functioning as an entropy trap.[21] We should note that the energy surface of this ROP is very shallow, and binding events occur with a similar energy to enchainment.[21] Hence,

the observed effects should also be consistent with an enchainment rate determining step exhibiting a very small KIE characteristic of a reactant-like transition state with a mostly intact OH/OD bond. Further study will be necessary to elucidate these suggestions, but we believe this is the first evidence for these systems of a binding event being directly measurable in the ROP kinetics. The touchstone analysis of thiourea/base mediated ROP (using *m*-CF_3-S/MTBD for the ROP of VL) predicted that reagent/catalyst binding events would be evident in ROP kinetics, and the Arrhenius analysis in that publication shows an entropy of activation consistent with a bimolecular reaction.[10] If the present suggestions prove to be true, they imply new opportunities for catalyst development based on isotopic substitution. *Thioureas in Polar, H-bonding Solvent*. Hammett analysis of thiourea/MTBD mediated ROP of VL in acetone-d_6 provides detailed mechanistic insight of two competing ROP mechanisms. Thiourea/base mediated ROP is traditionally run in non-polar solvent, but recent advances have favored the application of polar solvent.[4,17] Particularly, the development of thiourea anions allowed for the rapid ROP of lactones in polar solvent, and these reactions were proposed to proceed through a thioimidate mechanism, Scheme 2.1.[5] Hammett analysis is an ideal tool to probe the dueling mechanisms available to thiourea/base cocatalyzed ROP in polar solvent. Binding constants of either MTBD or VL to the thioureas are too small in acetone-d_6 to be accurately measured by ^{1}H NMR due to the competitive binding with solvent, so our Hammett analysis is limited to rate.

For thioureas with EDGs and weak EWGs in acetone-d_6, an H-bonding mechanism of ROP is favored, but thioureas with strong EWGs operate via a thioimidate mechanism. In the Hammett plot of log k_{obs} vs σ (acetone-d_6), both *m*-X-S and *p*-X-S exhibit a nonlinear plot with a maximum at σ ~0.2, Figure 2.5. The thioureas with substituents of σ ≤ ~0.2 show a positive ρ value and those with σ ≥ ~0.2 possess a negative ρ value. ^{1}H NMR spectra of the various thioureas plus one equivalent MTBD (0.099 M each) in acetone-d_6 reinforce a mechanism change at σ ~0.2. The NMR spectra of the positive ρ range indicate H-bonding (a downfield shift of the thiourea cyclohexyl methine resonance vs free thiourea) where the stronger EWGs presumably facilitate stronger H-bond activation of substrate (and faster rates) just as in benzene. The NMR spectra of thioureas with and without MTBD in the negative ρ range indicate thioimidate formation (an upfield shift, cyclohexyl methine). One explanation for this change is that the less-acidic thioureas (smaller σ) generate more basic anions which yield faster rates. This explanation is consistent with the initial reports of (thio)imidate mediated ROP.[4,5,17] We infer that the thioimidate mechanism appears to 'turn on' at σ ~ 0.2 because the pK_a of MTBD (pK_a (DMSO) MTBD-H^+ ~ 14-16)[24,25] may be the same as that of a thiourea at that σ value (e.g. pK_a (DMSO) *m*-CF_3-S = 13.2 < pKa *m*-Cl-S, presumably)[26]. The pK_a MTBD-H^+ in DMSO is not known, but is expected to be between that of DBU (DBU = 1,8-diazabicyclo[5.4.0]undec-7-ene, pK_a DBU-H^+ = 13.9) and BEMP (BEMP = 2-*tert*-butylimino-2-diethylamino-1,3-dimethylperhydro-1,3,2-diazaphosphorine, pK_a BEMP-H^+ = 16.5).[24,25] However, we prefer to view the mechanism as a continuum (vs an 'on/off' phenomenon) where the gradual change in acidity of the thioureas is the presumed source of the V-shaped Hammett plots[20] (Figure

2.5) as the mechanism gradually shifts from H-bonding to thioimidate with increasing σ. Treating *p*-CF_3-S with 0.5 equivalent MTBD in acetone-d_6 results in one set of ^{1}H NMR resonances for *p*-CF_3-S, which indicates that proton transfer is dynamic on the NMR timescale. This suggests that quantitative proton transfer is not required to effect thioimidate mediated ROP. In a continuum point of view, the reduction of basicity of thiourea anions (with increasing σ) is outpacing the formation of a higher [thioimidate] (Scheme 2.1) past σ~0.2. However, in the case of strong base cocatalysts (e.g. KH or potassium *tert*-butoxide) where proton transfer is 'irreversible', an on/off mechanism seems irrefutable.[4,5]

We would like to propose an alternative explanation for the V-shaped Hammett plots (Figure 2.5) that is reminiscent of a more classic Hammett-based argument that attributes the portions of the Hammett plots with negative ρ to the formation of positive charge during the transition state. In an imidate mechanism, the 'formation of positive charge' is tantamount to the thioimidate becoming 'less negative' and could arise from the donation of electron density from the thioimidate to the alcohol that is resisted by the stronger EWGs. This Hammett-based explanation seems inconsistent with the thioimidate acting as both H-bond donor and acceptor, as dual activation would not be expected to dramatically change the charge at the thioimidate at the transition state. This implicates the base-H^+ as the H-bond donor (activating monomer) during ROP in an imidate mechanism. These roles are similar to those proposed in the DBU/benzoic acid mediated ROP of lactide.[27] Ultimately, the two points of view are complementary and may be identical; a more acidic thiourea with strong EWGs will produce a weaker base

thioimidate (acid/base argument) and the strong EWGs will resist H-bond accepting (Hammett argument). The change in mechanism is not associated with a substantial change in alcohol k_H/k_D (versus Figure 2.4, benzene): *m*-CF_3-S, k_H/k_D = 1.6; *p*-NO_2-S, k_H/k_D = 1.5 (acetone-d_6:$CDCl_3$/$CHCl_3$, 50:50). While both mechanisms have been suggested previously,[4,5,17] we believe this the most systematic and controlled observation of the mechanism shift; with a V-shaped Hammett plot, a mechanism continuum becomes difficult to refute.

Ureas in Polar and Non-polar Solvent. The urea/MTBD cocatalyzed ROP of VL from benzyl alcohol undergoes ROP via solvent-determined H-bonding (benzene-d_6) or imidate (acetone-d_6) mechanisms. The Hammett plots of log k_{obs} (both *m*- and *p*-) show positive slopes in acetone-d_6 and benzene-d_6, Figure 2.6. Any number of equilibria (e.g. binding to VL or cocatalyst, proton transfer to form imidate, etc.) which are superimposed on the observed rate constant will result in a linear Hammett plot except in the case of a change in mechanism (i.e. X-S in acetone, Figure 2.5).[20,28] The positive slopes of the Hammett plots suggest that negative charge is building during the transition states and are consistent with either mechanism but arise through different phenomena. ^{1}H NMR spectra of *m*-CH_3-O or *m*-CF_3-O with and without MTBD indicate H-bonding (downfield shift with MTBD) in benzene-d_6 and imidate (upfield shift with MTBD) in acetone-d_6 (Figure 2.14). *In the H-bonding path*, higher σ values would be associated with stronger H-bonding to monomer in the transition state. This explanation is identical to that for the thiourea mediated ROP in C_6D_6 (Figure 2.1).

We propose that the simplest explanation of the positive, linear slopes of the σ_m or σ_p vs log k_{obs} plots (Figure 2.6, acetone-*d*$_6$) is the formation of more imidate character (higher [imidate]) with stronger EWGs. This explanation assumes that the imidate is in equilibrium with the neutral urea in acetone-*d*$_6$, just as proposed for thioureas in acetone-*d*$_6$. Indeed, a reversible imidate formation would be expected to result in a more controlled ROP (versus all imidate) as the imidate ion pair reverts to a relatively-inert H-bond donor/acceptor pair, as appears to be the case.[4,6] In a purely imidate mechanism, which occurs upon the treatment of urea H-bond donors with strong bases (e.g. KH), published studies have shown the opposite effect where more EWGs (CF_3 groups) on the urea resulted in slower ROP (an implied negative ρ).[4] For the published study, the slower rates were attributed to a reduced basicity of the imidate with increase number of CF_3 groups which was suggested to reduce H-bond accepting ability. This observation is analogous to the negative ρ portion of Figure 2.5, the treatment of *thioureas* with MTBD in acetone-*d*$_6$. Because ureas are less acidic than thioureas,[29] we propose that the data in Figure 2.6 (acetone-*d*$_6$) is analogous to the low ρ portion of Figure 2.5. That is, the ureas are not acidic enough to become fully deprotonated and result in a change in mechanism. We predict that ROP rate in Figure 2.6 may eventually reach a maximum value if extended to higher sigma. This appears to be the only explanation that is consistent with, 1) the published report,[4] 2) the ^{1}H NMR studies of urea with and without MTBD, 3) the Hammett behavior in Figure 2.6, and 4) a unified mechanism for both urea and thiourea cocatalysts. Controllably modulating the position of the H-bonding vs imidate equilibrium – or possibly developing true on/off abilities – could yield impressive control in the ROP

Kinetic isotope studies on observed rate constant for the *m*-X-O/MTBD catalyzed ROP of VL show a later transition state versus the thiourea cocatalyzed ROPs. The H/D substitution studies were performed by conducting the ROPs in $CDCl_3/CHCl_3$ blends which are adopted by the benzyl alcohol, see experimental section. The KIEs range from $k_H/k_D = 4.5$ for electron donating methyl- to $k_H/k_D = 2.09$ for electron withdrawing CF_3, Figure 2.7. The larger IEs versus thioureas (Figure 2.4) suggests that the present values are indeed *kinetic* isotope effects. It is possible that the large KIEs (vs thioureas) represent a change in mechanism, but this would not be consistent with ^{1}H NMR spectra of ureas in nonpolar solvent in the presence and absence of MTBD which indicate an H-bonding mechanism. Further, the KIEs measured in chloroform solvent match those performed in benzene/chloroform blends, which suggests that the H-bond mediated mechanism dominates in chloroform. Rather, the larger KIEs suggest a later transition state characterized by more equal sharing of the H/D in an H-bond mediated ROP. These results also suggest that catalyst/reagent interactions are not very similar to those at the transition state. Hence, the community might not be too concerned with the inaccessibility of urea/reagent binding constants as they may not be as meaningful as thiourea/reagent binding constants. Under the present conditions, stronger EWGs are associated with lower KIEs, which suggests that the more active catalysts feature a transition state closer to the reagents. If electronic changes to H-bond donating catalyst (urea) result in a KIE at the H-bond donating substrate (alcohol), the urea-dependent KIE reinforces the complicated interplay of the (thio)urea/base cocatalysts acting as a single system. When the KIE experiment is repeated in acetone/chloroform (50:50)

solvent mixtures (which is associated with imidate formation), the KIE for the *m*-MeO-O/MTBD cocatalyzed ROP of VL drops to $k_H/k_D = 2.02$.

CONCLUSION

Linear and nonlinear free energy studies of (thio)urea/MTBD mediated ROP of VL reveal the complicated interplay of reagents that give rise to catalysis through one of two mechanisms. Which mechanism is operative depends most greatly on the solvent, where polar solvents favor a (thio)imidate mechanism and non-polar solvents favor a classic H-bond mediated ROP. For thiourea H-bond donors in acetone, the mechanism is observed to change from H-bonding for thioureas with weak EWG (and EDGs) to a thioimidate mechanism for strong EWGs. The change in mechanism may occur when resistance to increased electron donation from thioimidate to alcohol caused by strong EWGs ($\rho<0$) outweighs increased [imidate] ($\rho>0$), which would occur in the regime that [imidate] is not a function of σ. We predict that the enhanced control of (thio)urea/base cocatalyzed ROP versus other highly active systems may be shown to arise from this mechanistic duality, and advanced, switchable catalysts may further improve selectivity. Despite the large amount of information that has been discovered about these catalysts over that last decade, hints at new opportunities emerge through the present studies. Particularly, the isotope studies tease at new catalysts and provide evidence of binding events in the rate determining step.

REFERENCES

(1) McKinlay, C. J.; Waymouth, R. M.; Wender, P. A. Cell-Penetrating, Guanidinium-Rich Oligophosphoesters: Effective and Versatile Molecular Transporters for Drug and Probe Delivery. *J. Am. Chem. Soc.* **2016**, *138* (10), 3510–3517.

(2) Geihe, E. I.; Cooley, C. B.; Simon, J. R.; Kiesewetter, M. K.; Edward, J. a; Hickerson, R. P.; Kaspar, R. L.; Hedrick, J. L.; Waymouth, R. M.; Wender, P. a. Designed Guanidinium-Rich Amphipathic Oligocarbonate Molecular Transporters Complex, Deliver and Release siRNA in Cells. *Proc. Natl. Acad. Sci. U. S. A.* **2012**, *109* (33), 13171–13176.

(3) Cooley, C. B.; Trantow, B. M.; Nederberg, F.; Kiesewetter, M. K.; Hedrick, J. L.; Waymouth, R. M.; Wender, P. A. Oligocarbonate Molecular Transporters : Oligomerization Based Syntheses and Cell Penetrating Studies. *J. Am. Chem. Soc.* **2009**, *131*, 16401–16403.

(4) Lin, B.; Waymouth, R. M. Urea Anions: Simple, Fast, and Selective Catalysts for Ring-Opening Polymerizations. *J. Am. Chem. Soc.* **2017**, *139*, 1645–1652.

(5) Zhang, X.; Jones, G. O.; Hedrick, J. L.; Waymouth, R. M. Fast and Selective Ring-Opening Polymerizations by Alkoxides and Thioureas. *Nat. Chem.* **2016**, *8*, 1047–1053.

(6) Dharmaratne, N. U.; Pothupitiya, J. U.; Bannin, T. J.; Kazakov, O. I.; Kiesewetter, M. K. Triclocarban: Commercial Antibacterial and Highly Effective H-

Bond Donating Catalyst for Ring-Opening Polymerization. *ACS Macro Lett.* **2017**, *6* (4), 421–425.

(7) Fastnacht, K. V.; Spink, S. S.; Dharmaratne, N. U.; Pothupitiya, J. U.; Datta, P. P.; Kiesewetter, E. T.; Kiesewetter, M. K. Bis- and Tris-Urea H-Bond Donors for Ring-Opening Polymerization: Unprecedented Activity and Control from an Organocatalyst. *ACS Macro Lett.* **2016**, *5* (8), 982–986.

(8) Xu, S.; Sun, H.; Liu, J.; Xu, J.; Pan, X.; Dong, H.; Liu, Y.; Li, Z.; Guo, K. Internal Lewis Pair Enhanced H-Bond Donor: Boronate-Urea and Tertiary Amine Co-Catalysis in Ring-Opening Polymerization. *Polym. Chem.* **2016**, *7* (44), 6843–6853.

(9) He, X.; Ji, Y.; Jin, Y.; Kan, S.; Xia, H.; Chen, J.; Liang, B.; Wu, H.; Guo, K.; Li, Z. Bifunctional Imidodiphosphoric Acid-Catalyzed Controlled/living Ring-Opening Polymerization of Trimethylene Carbonate Resulting Block, Dihydroxy Telechelic, and Star-Shaped Polycarbonates. *J. Polym. Sci. Part A Polym. Chem.* **2014**, *52* (7), 1009–1019.

(10) Lohmeijer, B. G. G.; Pratt, R. C.; Leibfarth, F.; Logan, J. W.; Long, D. A.; Dove, A. P.; Nederberg, F.; Choi, J.; Wade, C.; Waymouth, R. M.; et al. Guanidine and Amidine Organocatalysts for Ring-Opening Polymerization of Cyclic Esters. *Macromolecules* **2006**, *39* (25), 8574–8583.

(11) Pratt, R. C.; Lohmeijer, B. G. G.; Long, D. a.; Lundberg, P. N. P.; Dove, A. P.; Li, H.; Wade, C. G.; Waymouth, R. M.; Hedrick, J. L. Exploration, Optimization, and

Application of Supramolecular Thiourea−Amine Catalysts for the Synthesis of Lactide (Co)polymers. *Macromolecules* **2006**, *39* (23), 7863–7871.

(12) Dove, A. P.; Pratt, R. C.; Lohmeijer, B. G. G.; Waymouth, R. M.; Hedrick, J. L. Thiourea-Based Bifunctional Organocatalysis: Supramolecular Recognition for Living Polymerization. *J. Am. Chem. Soc.* **2005**, *127* (40), 13798–13799.

(13) Kazakov, O. I.; Kiesewetter, M. K. Cocatalyst Binding Effects in Organocatalytic Ring-Opening Polymerization of L -Lactide. *Macromolecules* **2015**, *48* (17), 6121–6126.

(14) Kazakov, O. I.; Datta, P. P.; Isajani, M.; Kiesewetter, E. T.; Kiesewetter, M. K. Cooperative Hydrogen-Bond Pairing in Organocatalytic Ring-Opening Polymerization. *Macromolecules* **2014**, *47* (21), 7463–7468.

(15) Koeller, S.; Kadota, J.; Peruch, F.; Deffieux, A.; Pinaud, N.; Pianet, I.; Massip, S.; Léger, J.-M.; Desvergne, J.-P.; Bibal, B. (Thio)Amidoindoles and (Thio)amidobenzimidazoles: An Investigation of Their Hydrogen-Bonding and Organocatalytic Properties in the Ring-Opening Polymerization of Lactide. *Chem. Eur. J.* **2010**, *16* (14), 4196–4205.

(16) Thomas, C.; Bibal, B. Hydrogen-Bonding Organocatalysts for Ring-Opening Polymerization. *Green Chem.* **2014**, *16* (4), 1687.

(17) Pothupitiya, J. U.; Dharmaratne, N. U.; Jouaneh, T. M. M.; Fastnacht, K. V.; Coderre, D. N.; Kiesewetter, M. K. H-Bonding Organocatalysts for the Living, Solvent-

Free Ring-Opening Polymerization of Lactones: Toward an All-Lactones, All-Conditions Approach. *Macromolecules* **2017**, *50*, 8948–8954.

(18) Palucki, M.; Finney, N. S.; Pospisil, P. J.; Güler, M. L.; Ishida, T.; Jacobsen, E. N. The Mechanistic Basis for Electronic Effects on Enantioselectivity in the (salen)Mn(III)-Catalyzed Epoxidation Reaction. *J. Am. Chem. Soc.* **1998**, *120* (5), 948–954.

(19) Zuend, S. J.; Jacobsen, E. N. Mechanism of Amido-Thiourea Catalyzed Enantioselective Imine Hydrocyanation: Transition State Stabilization via Multiple Non-Covalent Interactions. *J. Am. Chem. Soc.* **2009**, *131* (42), 15358–15374.

(20) Ansyln, E. V.; Dougherty, D. A. Experiments Related to Thermodynamics and Kinetics. In *Modern Physical Organic Chemistry*; University Science Books: United States, 6AD; pp 421–488.

(21) Datta, P. P.; Pothupitiya, J. U.; Kiesewetter, E. T.; Kiesewetter, M. K. Coupled Equilibria in H-Bond Donating Ring-Opening Polymerization: The Effective Catalyst-Determined Shift of a Polymerization Equilibrium. *Eur. Polym. J.* **2017**, *95*, 671–677.

(22) Churchill, D. G.; Janak, K. E.; Wittenberg, J. S.; Parkin, G. Normal and Inverse Primary Kinetic Deuterium Isotope Effects for C-H Bond Reductive Elimination and Oxidative Addition Reactions of Molybdenocene and Tungstenocene Complexes: Evidence for Benzene ??-Complex Intermediates. *J. Am. Chem. Soc.* **2003**, *125* (5), 1403–1420.

(23) Rao, C. N. R. Effect of Deuteration on Hydrogen Bonds. *J. Chem. Soc. Faraday Trans. 1 Phys. Chem. Condens. Phases* **1975**, *71*, 980.

(24) Kaljurand, I.; Kütt, A.; Sooväli, L.; Rodima, T.; Mäemets, V.; Leito, I.; Koppel, I. A. Extension of the Self-Consistent Spectrophotometric Basicity Scale in Acetonitrile to a Full Span of 28 pKa Units: Unification of Different Basicity Scales. *J. Org. Chem.* **2005**, *70* (3), 1019–1028.

(25) Schwesinger, R.; Schlempep, H.; Hasenfratz, C.; Willaredt, J.; Dambacher, T.; Breuer, T.; Ottaway, C.; Fletschinger, M.; Boele, J.; Fritz, H.; et al. Extremely Strong, Uncharged Auxiliary Bases; Monomeric and Polymer-Supported Polyaminophosphazenes (P2- P5). *Liebigs Ann.* **1996**, 1055–1081.

(26) Blain, M.; Yau, H.; Jean-Gérard, L.; Auvergne, R.; Benazet, D.; Schreiner, P. R.; Caillol, S.; Andrioletti, B. Urea- and Thiourea-Catalyzed Aminolysis of Carbonates. *ChemSusChem* **2016**, *9* (16), 2269–2272.

(27) Coady, D. J.; Fukushima, K.; Horn, H. W.; Rice, J. E.; Hedrick, J. L. Catalytic Insights into Acid/base Conjugates: Highly Selective Bifunctional Catalysts for the Ring-Opening Polymerization of Lactide. *Chem. Commun.* **2011**, *47* (47), 3105–3107.

(28) Espenson, J. H. *Chemical Kinetics and Reaction Mechanism*, 2nd ed.; McGraw-Hill Book Co: New York, 2002.

(29) Bordwell, F. G.; Algrim, D. J.; Harrelson, J. A. The Relative Ease of Removing a Proton, a Hydrogen Atom, or an Electron from Carboxamides versus

Thiocarboxamides. *J. Am. Chem. Soc.* **1988**, *110* (17), 5903–5904.

(30) Horman, I.; Dreux, B. Estimation of Association Constants of Bimolecular Organic Complexes. *Anal. Chem.* **1983**, *55*, 1219–1221.

(31) Deranleau, D. A. Theory of the Measurement of Weak Molecular Complexes. I. General Considerations. *J. Am. Chem. Soc.* **1969**, *91* (15), 4044–4049.

meta-substituted diphenyl urea						
	K_H/K_D	**Standard Error for (K_H/K_D)**	**k_{obs} (C_6D_6) (min^{-1})**	**Standard Error for k_{obs} (C_6D_6) (min^{-1})**	**k_{obs} (acetone-d_6) (min^{-1})**	**Standard Error for k_{obs} (acetone-d_6) (min^{-1})**
CF_3	2.09	0.0014	0.1538	0.005	0.2201	0.005
Cl	2.31	0.0018	0.0688	0.0016	0.2147	0.006
OMe	3.12	0.0004	0.016	0.0003	0.0529	0.002
H	-	-	0.0116	0.0002	0.0385	0.001
Me	4.5	8.90E-05	0.0079	0.0001	0.021	0.001

Table 2.1. Tabulation of Errors for *meta*-substituted diphenyl urea.

para-substituted diphenyl urea				
	k_{obs} (C_6D_6) (min^{-1})	**Standard Error for k_{obs} (C_6D_6) (min^{-1})**	**k_{obs} (acetone-d_6) (min^{-1})**	**Standard Error for k_{obs} (acetone-d_6) (min^{-1})**
CF_3	0.0346	0.0006	0.1599	0.0076
Cl	0.0221	0.0006	0.1127	0.0065
F	0.0225	9.00E-05	0.057	0.0026
H	0.0116	0.0002	0.0385	0.0014
NO_2	0.1608	0.0016	0.1353	0.0057
Me	0.0073	1.70E-05	0.0266	0.0009

Table 2.2. Tabulation of Errors for *para*-substituted diphenyl urea.

meta-substituted cyclohexyl thiourea										
	K_{eq} to VL	**Standard Error of K_{eq}**	**K_{eq} to MTBD**	**Standard Error for K_{eq}**	**K_H/K_D**	**Standard Error for (K_H/K_D)**	**k_{obs} (C_6D_6) / min^{-1}**	**Standard Error for k_{obs} (C_6D_6)**	**k_{obs} (acetone-d_6) / min^{-1}**	**Standard Error for k_{obs} (acetone-d_6) / min^{-1}**
CF_3	41	0.3	1500	100	1.0977	0.0001	0.0119	0.0070	0.0023	0.00003
Cl	6.8	0.5	533	8	0.9716	0.0005	0.0073	0.0014	0.0024	0.0002
F	7.2	0.6	319	15	1.0293	0.0003	0.0100	0.0003	0.0024	0.0002
OMe	1.8	0.1	40.2	2.4	1.1811	0.0003	0.0022	0.0001	0.0039	0.0001
H	1.2	0.04	58.5	3.6	1.2188	0.0001	0.0017	0.0001	0.0032	0.0001
Me	1.6	0.04	21.8	1.0	1.0514	0.00003	0.0011	0.00004	0.0023	0.0001

Table 2.3. Tabulation of Errors for *meta*-substituted cyclohexyl thiourea.

para-substituted cyclohexyl thiourea										
	K_{eq} to VL	**Standard Error of K_{eq}**	**K_{eq} to MTBD**	**Standard Error for K_{eq}**	**K_H/K_D**	**Standard Error for (K_H/K_D)**	**k_{obs} (C_6D_6) / min^{-1}**	**Standard Error for k_{obs} (C_6D_6) / min^{-1}**	**k_{obs} (acetone-d_6) / min^{-1}**	**Standard Error for k_{obs} (acetone-d_6) / min^{-1}**
NO_2	7.8	0.04	803	8	1.264	0.0003	0.0088	0.0007	0.0012	0.00001
CF_3	5.3	0.98	461	76	1.118	0.00003	0.0063	0.0006	0.0038	0.0001
Cl	3.5	0.07	79	4	1.245	0.0002	0.0041	0.0001	0.0055	0.0001
F	1.6	0.08	94	2	1.146	0.0001	0.0036	0.0001	0.0041	0.0002
H	1.2	0.04	58	4	1.219	0.0001	0.0017	0.0001	0.0032	0.0001
Me	1.6	0.08	57	4	0.951	0.0001	0.0018	0.00002	0.0038	0.0001
OMe	1.6	0.13	72	11	0.827	0.00004	0.0009	0.00001	0.0023	0.0001

Table 2.4. Tabulation of Errors for *para*-substituted cyclohexyl thiourea

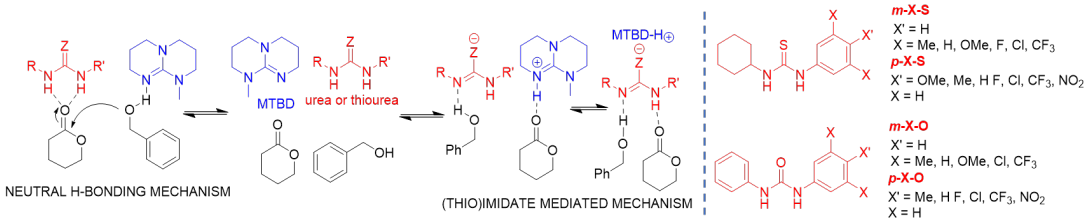

Scheme 2.1. The two mechanisms for (thio)urea plus base cocatalyzed ROP are proposed to exist along a continuum of reactivity from imidate- to H-bond-mediated ROP.

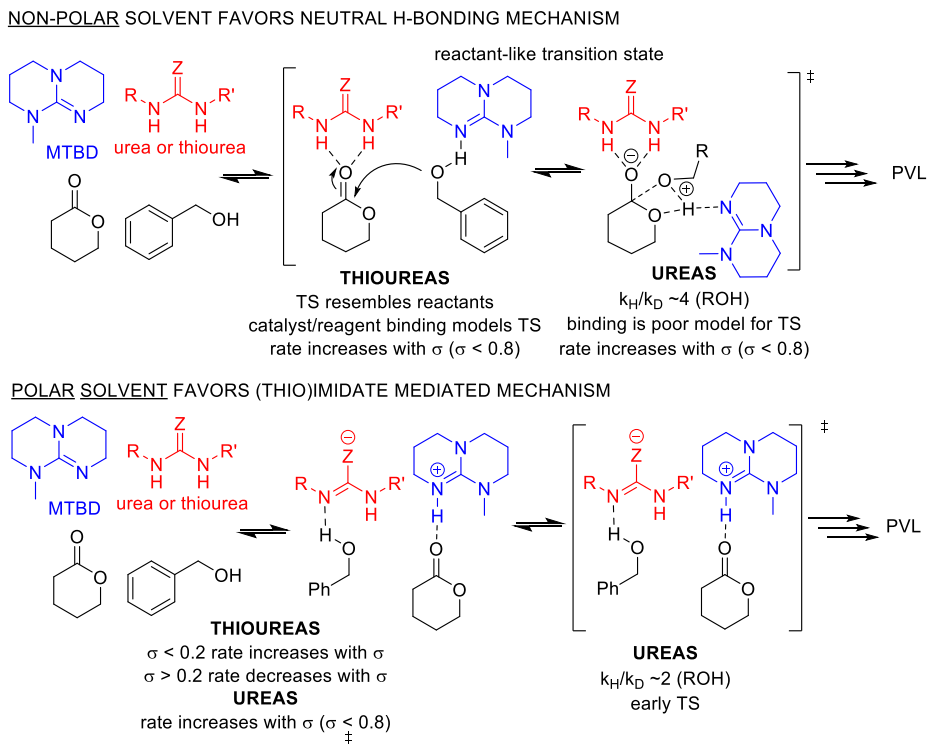

Scheme 2.2. Summary of the observations and competing mechanisms discussed in this study.

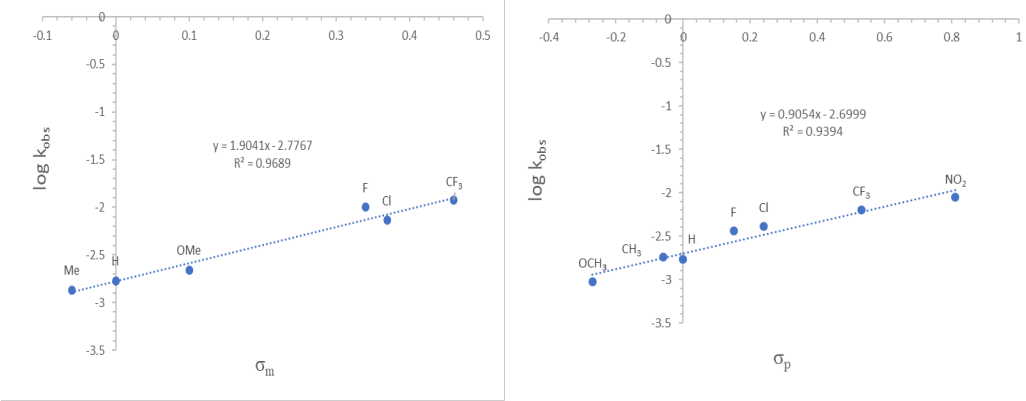

Figure 2.1. (left) Hammett plot (log k_{obs}) for the *m*-X-S/MTBD (0.099 M each) cocatalyzed ROP of VL (0.99 mmol, 2 M) from benzyl alcohol (0.02 M) in benzene-d_6. (right) Hammett plot (log k_{obs}) for the *p*-X-S/MTBD (0.099 M each) cocatalyzed ROP of VL (0.99 mmol, 2 M) from benzyl alcohol (0.02 M) in benzene-d_6. The log (k_{obs}/k_H) Hammett plots are in Figure 2.8.

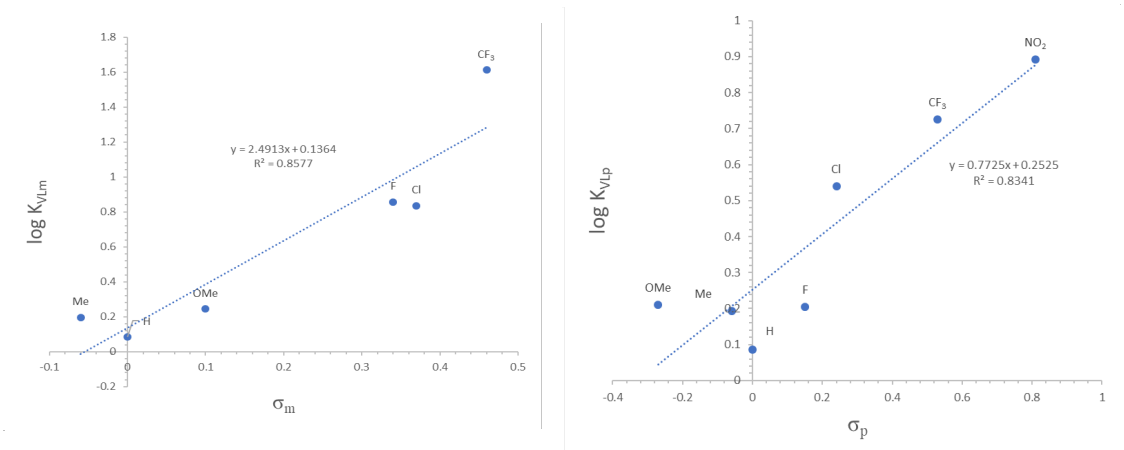

Figure 2.2. (left) Hammett plot of the binding constant of *m*-X-S to VL, K_{VLm}, in benzene-d_6. (right) Hammett plot of the binding constant of *p*-X-S to VL, K_{VLp}, in benzene-d_6. The log ($K_{VL}/k_{VL,H}$) Hammett plots are in Figure 2.9.

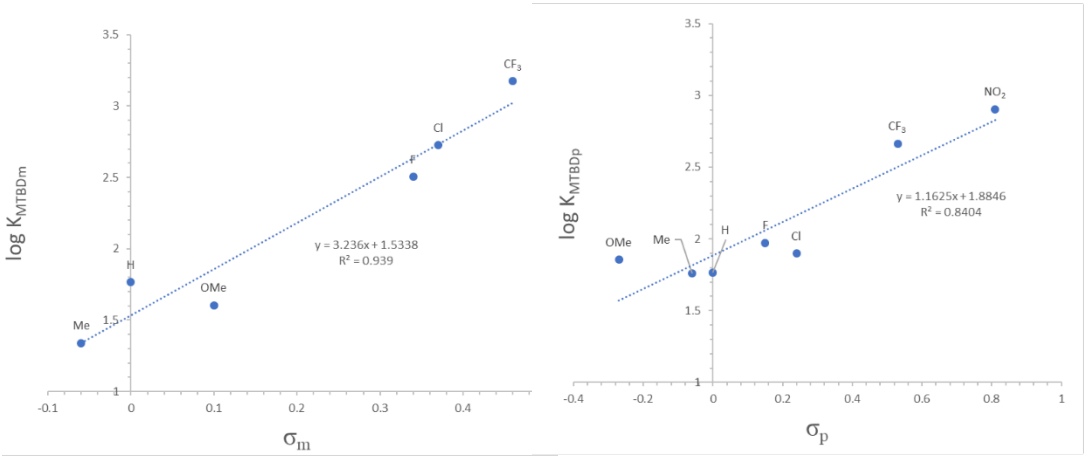

Figure 2.3. (left) Hammett plot of the binding constant, K_{MTBDm}, of *m*-X-S to MTBD in benzene-d_6. (right) Hammett plot of the binding constant, K_{MTBDp}, of *p*-X-S to MTBD in benzene-d_6. The log ($K_{MTBD}/k_{MTBD,H}$) Hammett plots are in Figure 2.10.

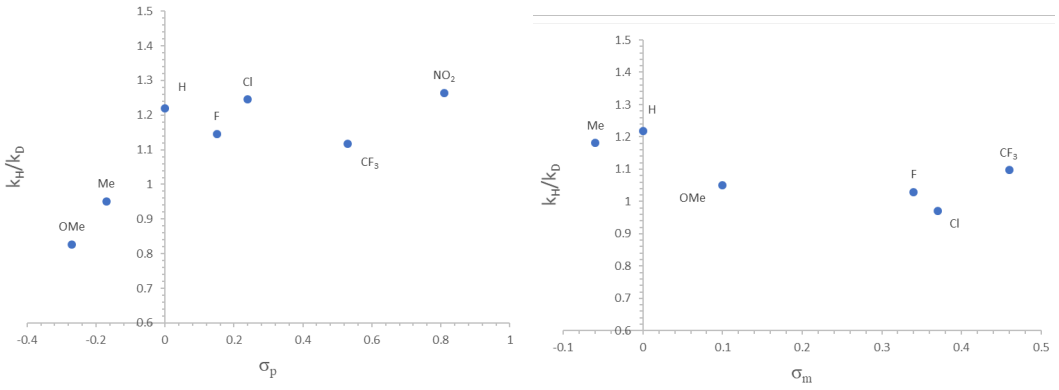

Figure 2.4. Plots of k_H/k_D vs σ_p and σ_m. Reaction conditions: VL (0.998 mmol, 2.00 M); X-O/MTBD (0.1 M each); benzyl alcohol (0.02 M) in $C_6D_6/CDCl_3/CHCl_3$ (varying $CDCl_3/CHCl_3$ ratio). The k_H and k_D were extracted from plots of k_{obs} vs %D in the chloroform feed.

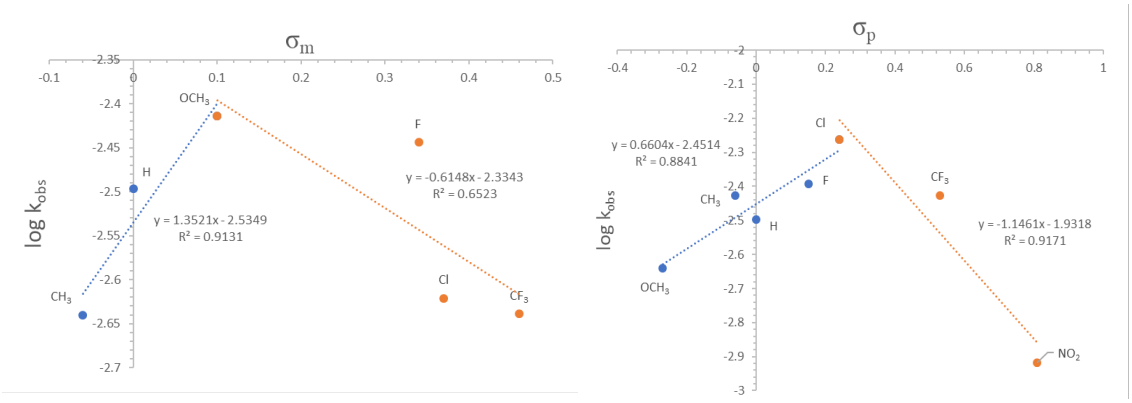

Figure 2.5. (left) Hammett plot of log k_{obs} of *m*-X-S in acetone-d_6. (right) Hammett plot of log k_{obs} of *p*-X-S in acetone-d_6. Conditions: VL (0.99 mmol, 2 M); X-S/MTBD (0.099 M each); benzyl alcohol (0.02 M) in acetone-d_6. The log (k_{obs}/k_H) Hammett plots are in Figure 2.12.

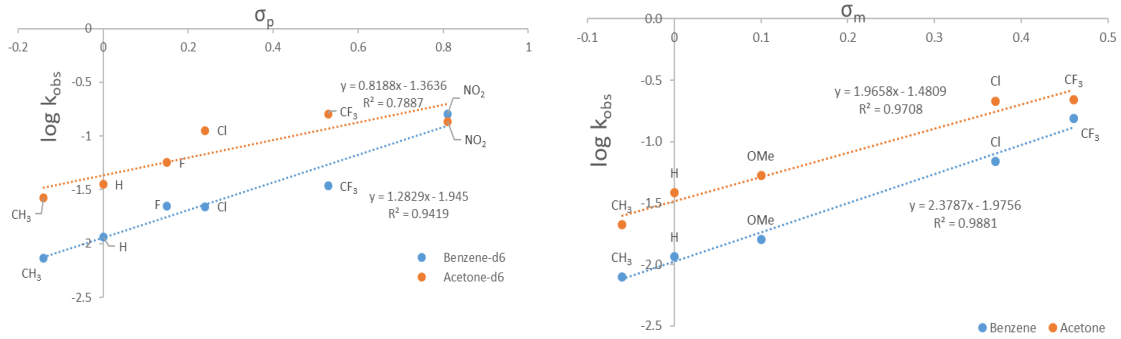

Figure 2.6. Hammett plots of k_{obs} for the ROP of VL (0.998 mmol, 2 M) from benzyl alcohol (0.02 M) in acetone-d_6 and benzene-d_6 by (left) *p*-X-O/MTBD (0.1 M each); and (right) *m*-X-O/MTBD (0.1 M each). The log (k_{obs}/k_H) Hammett plots are in Figure 2.13.

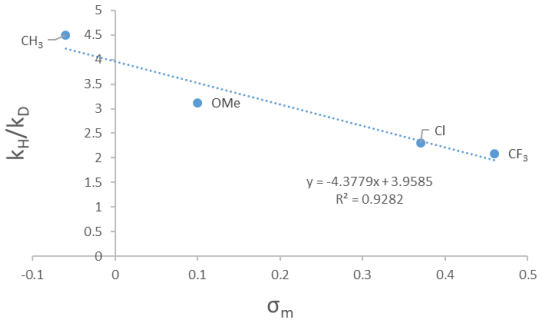

Figure 2.7. Plot of k_H/k_D vs σ_m. Reaction conditions: VL (0.998 mmol, 2.00 M); *m*-X-O/MTBD (0.1 M each); benzyl alcohol (0.02 M) in $CDCl_3/CHCl_3$. The k_H and k_D were extracted from plots of k_{obs} vs %D in the chloroform feed.

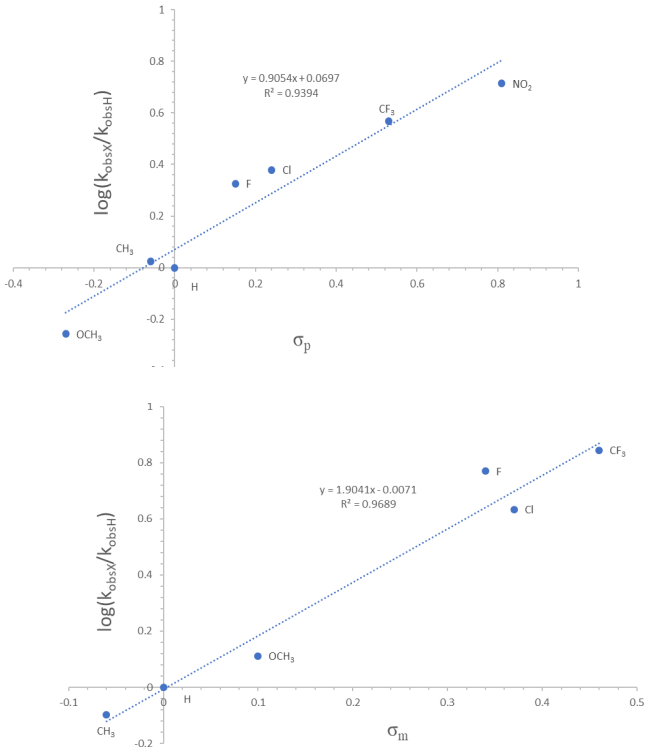

Figure 2.8. (upper) Hammett plot of the rate constant of *m*-X-S in the ROP of VL, $\log(k_X/k_H)$, in benzene-d_6. (lower) Hammett plot of the rate constant of *p*-X-S in the ROP of VL, $\log(k_X/k_H)$, in benzene-d_6. Conditions: X-S/MTBD (0.099 M each), VL (0.99 mmol, 2 M) benzyl alcohol (0.02 M) in benzene-d_6.

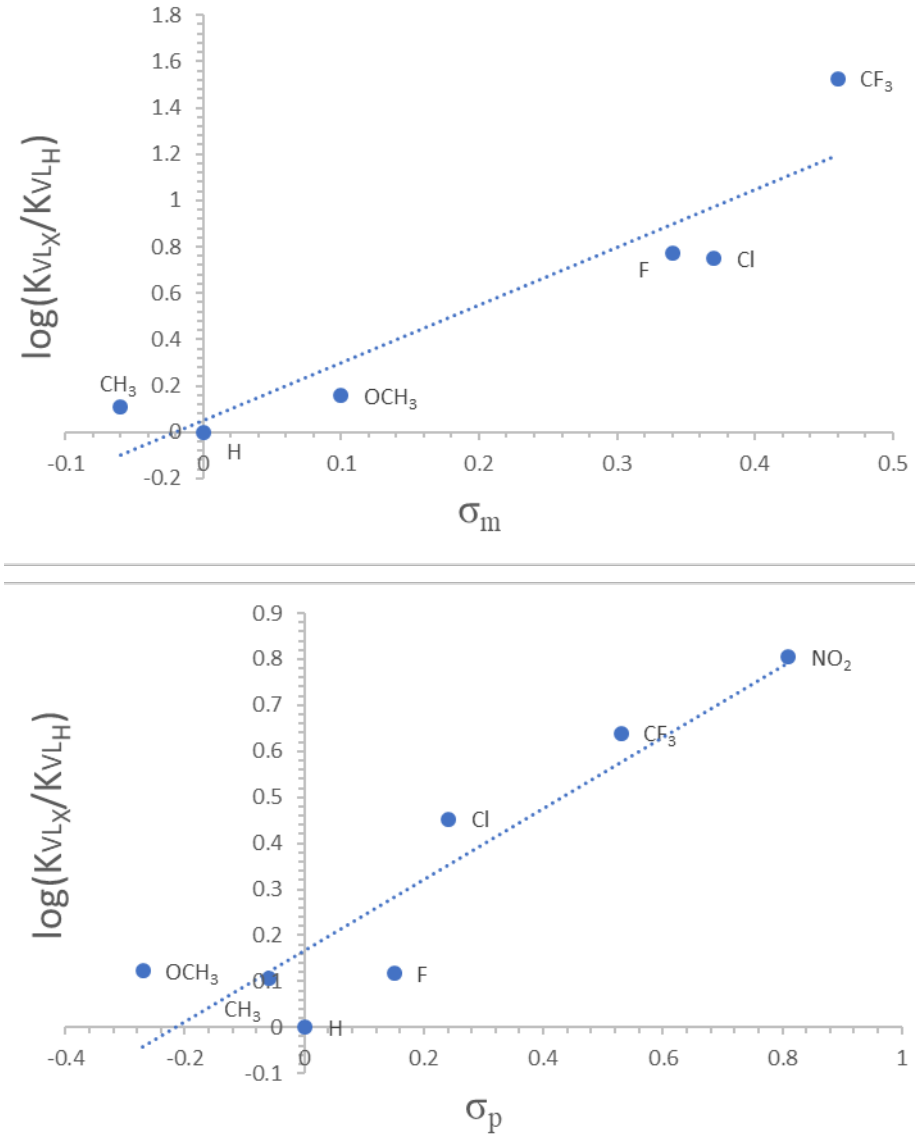

Figure 2.9. (upper) Hammett plot of the binding constant of *m*-X-S to VL, log(K_{VLx}/ K_{VLH}), in benzene-d_6. (lower) Hammett plot of the binding constant of *p*-X-S to VL, log(K_{VLx}/ K_{VLH}), in benzene-d_6.

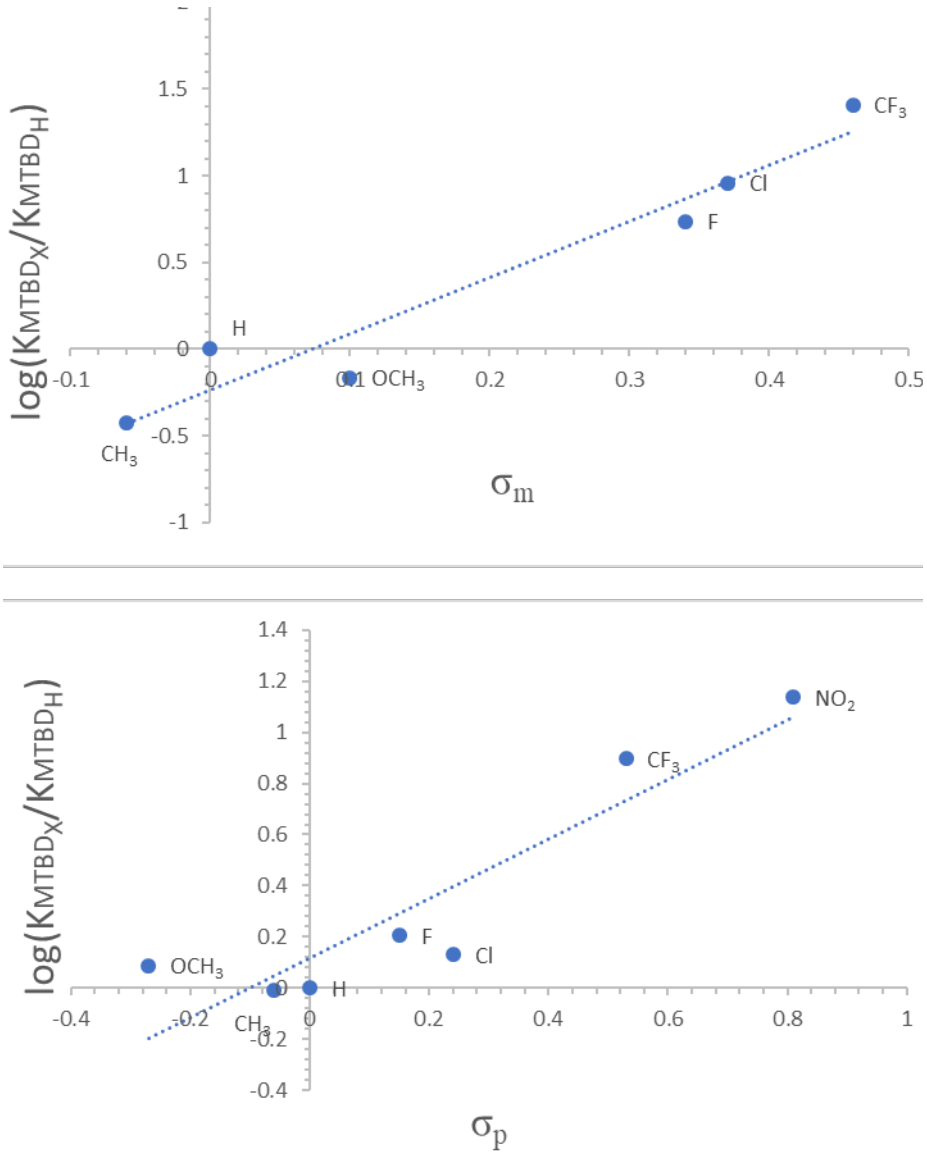

Figure 2.10. (upper) Hammett plot of the binding constant of *m*-X-S to MTBD, $\log(K_{MTBDx}/K_{MTBDH})$, in benzene-$d_6$. (lower)Hammett plot of the binding constant of *p*-X-S to MTBD, $\log(K_{MTBDx}/K_{MTBDH})$, in benzene-$d_6$.

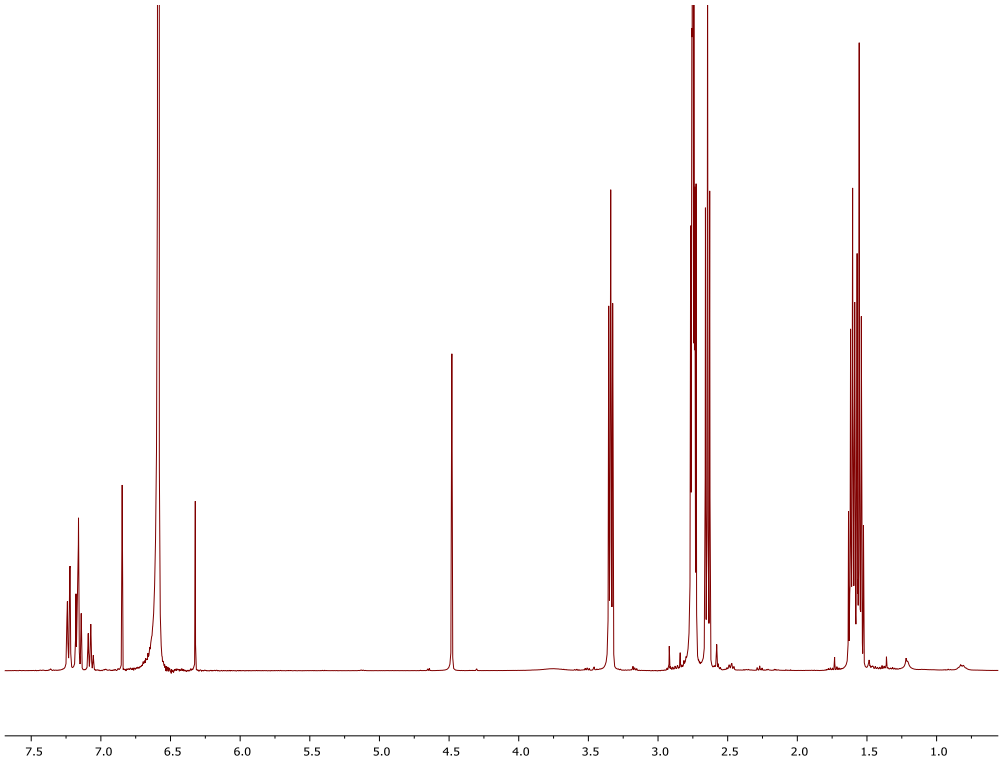

Figure 2.11. ^{1}H NMR (400 MHz) benzyl alcohol (1.08 mg, 0.009 mmol), MTBD (7.65 mg, 0.049 mmol), benzene-d_6 (249.7 µL), $CDCl_3$ (124.8 µL) and $CHCl_3$ (124.8 µL). The ratio of the OH resonance (3.75 ppm): benzylic CH_2 (4.5 ppm) is 1:2, suggesting that the isotopic ratio of the solvent matches the alcohol chain end.

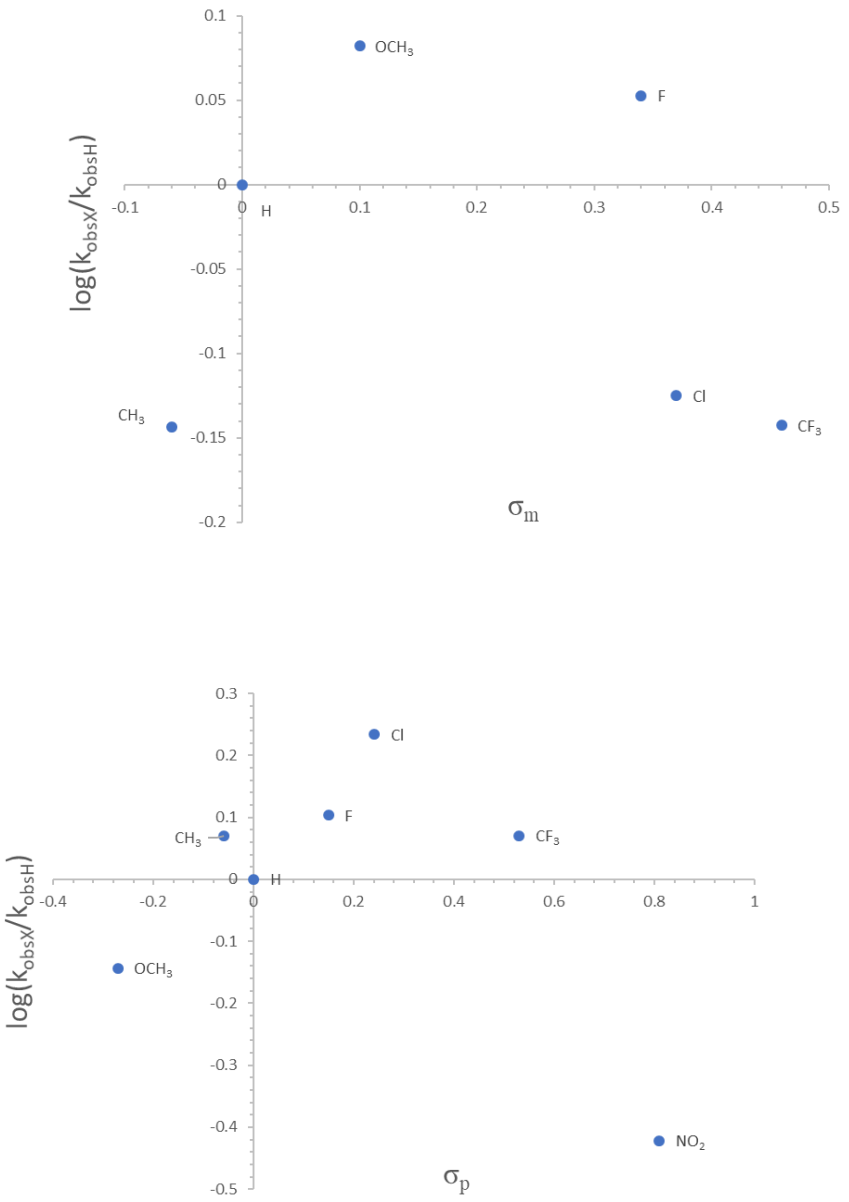

Figure 2.12. (upper) Hammett plot of log (k_{obs}/k_H) of *m*-X-S in acetone-d_6. (lower) Hammett plot of log (k_{obs}/k_H) of *p*-X-S in acetone-d_6. Conditions: VL (0.99 mmol, 2 M); X-S/MTBD (0.099 M each); benzyl alcohol (0.02 M) in acetone-d_6.

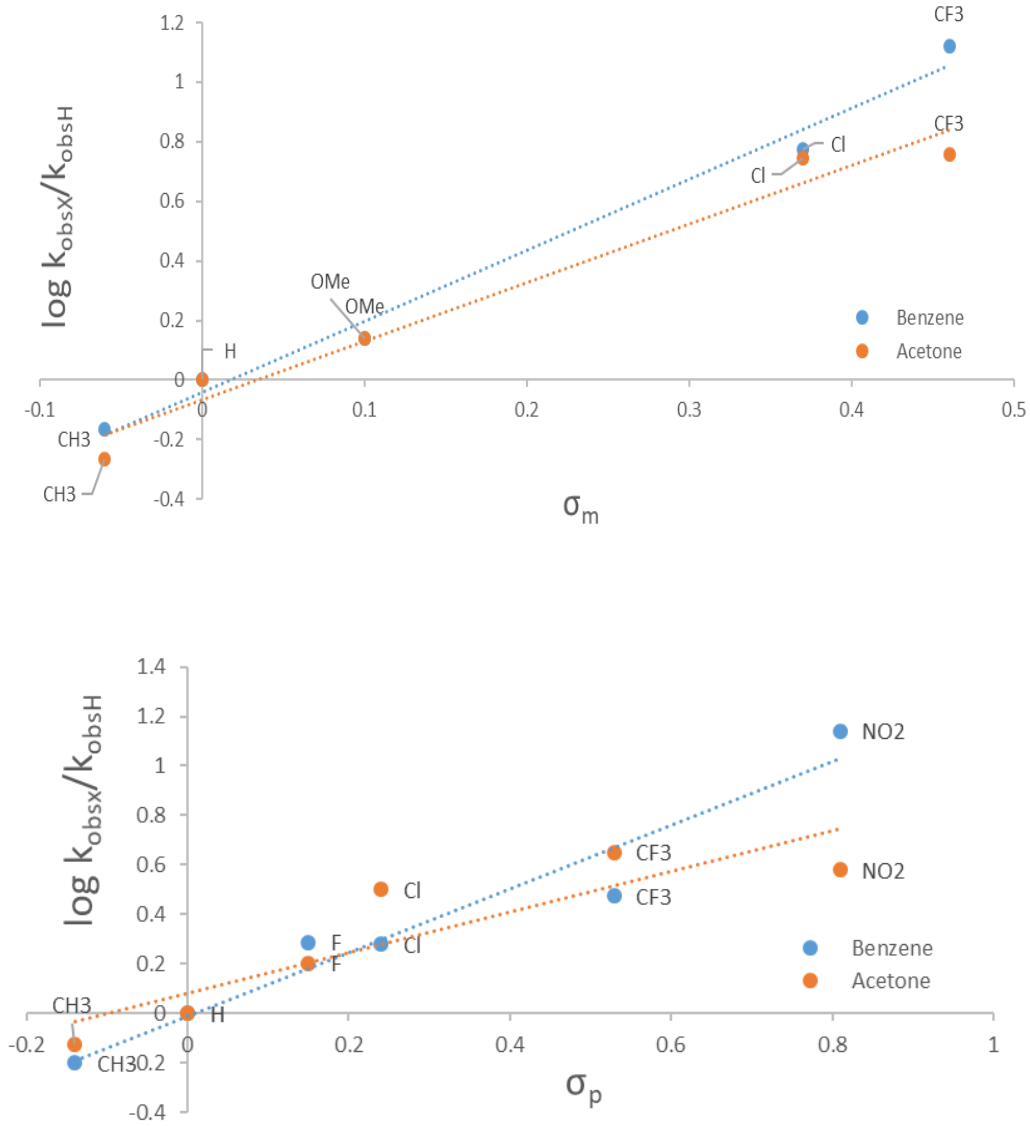

Figure 2.13. Hammett plots of log (k_{obs}/k_H) for the ROP of VL (0.998 mmol, 2 M) from benzyl alcohol (0.02 M) in acetone-d_6 and benzene-d_6 by (upper) *m*-X-O/MTBD (0.1 M each); and (lower) *p*-X-O/MTBD (0.1 M each).

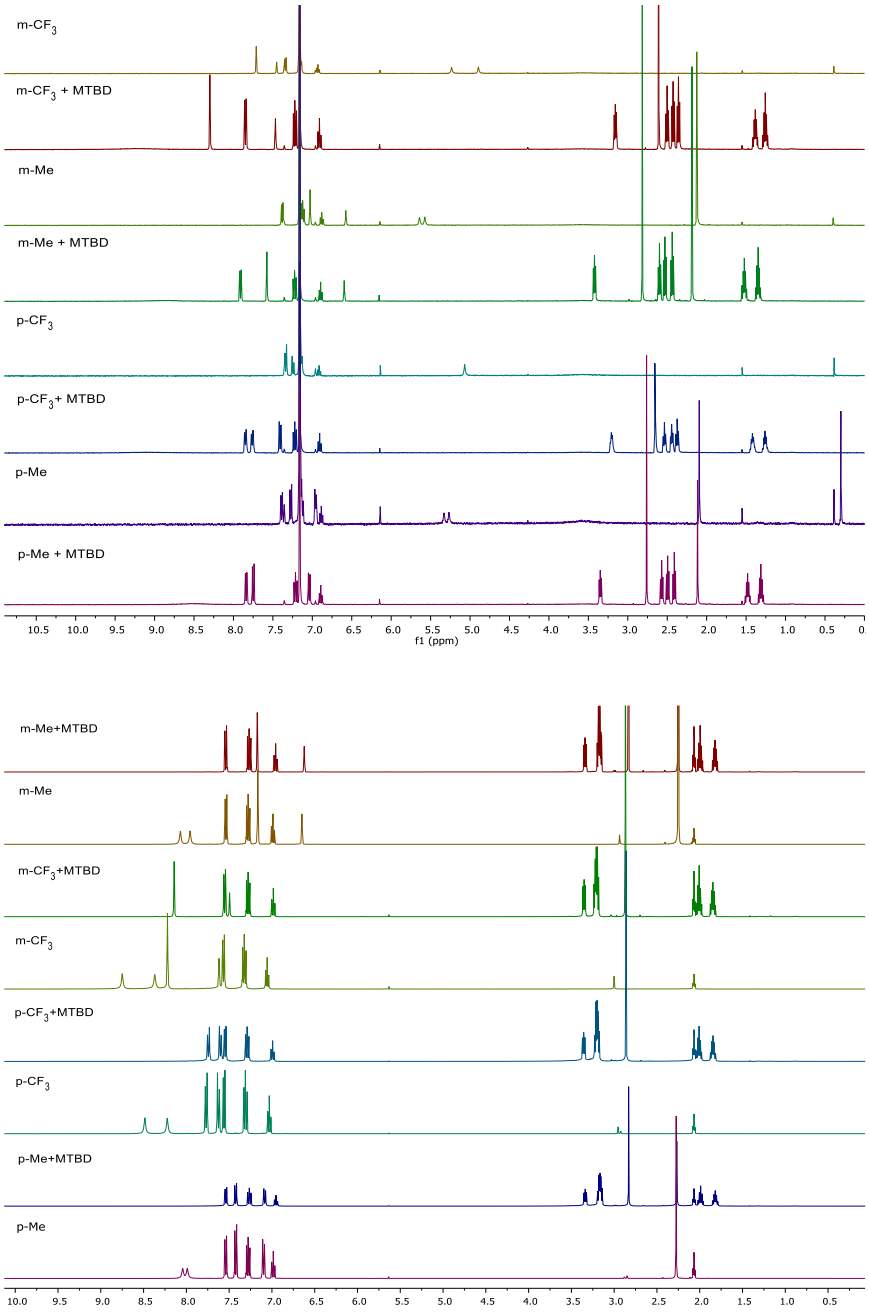

Figure 2.14. (upper) ^{1}H NMR (acetone-d_6, 400 MHz) spectra of select urea H-bond donors in the presence and absence of MTBD (0.098 M each) (referenced to residual acetone-H). (lower) ^{1}H NMR (C_6D_6, 400 MHz) spectra of select urea H-bond donors in the presence and absence of MTBD (0.0049 M each) (referenced to residual benzene-H).

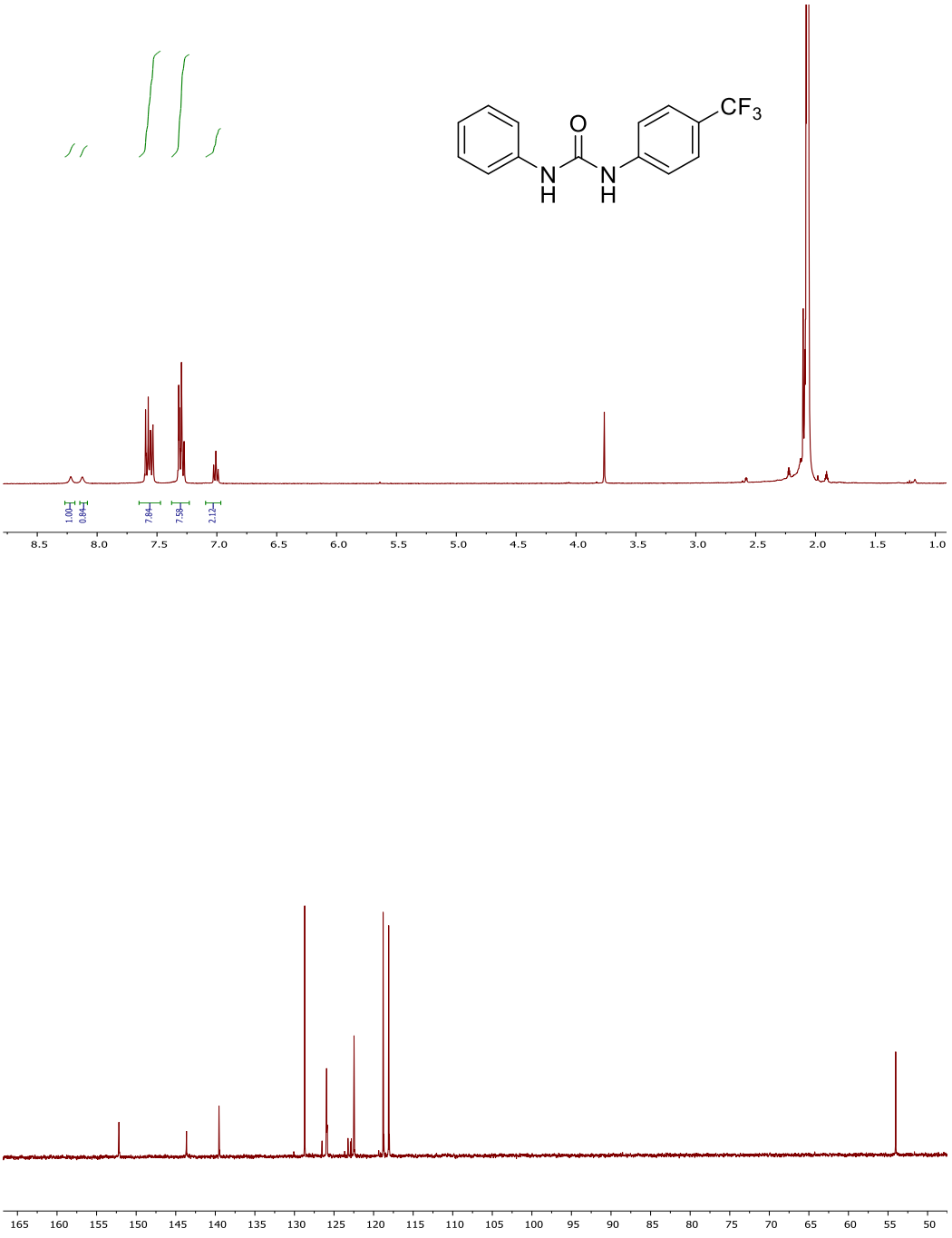

Figure 2.15. (Upper) ^{1}H NMR (acetone-d_6, 400 MHz) spectrum of 4-(trifluoromethyl)phenyl-3-phenyl urea (Lower) ^{13}C NMR (acetone-d_6, 100 MHz) spectrum of 4-(trifluoromethyl)phenyl-3-phenyl urea

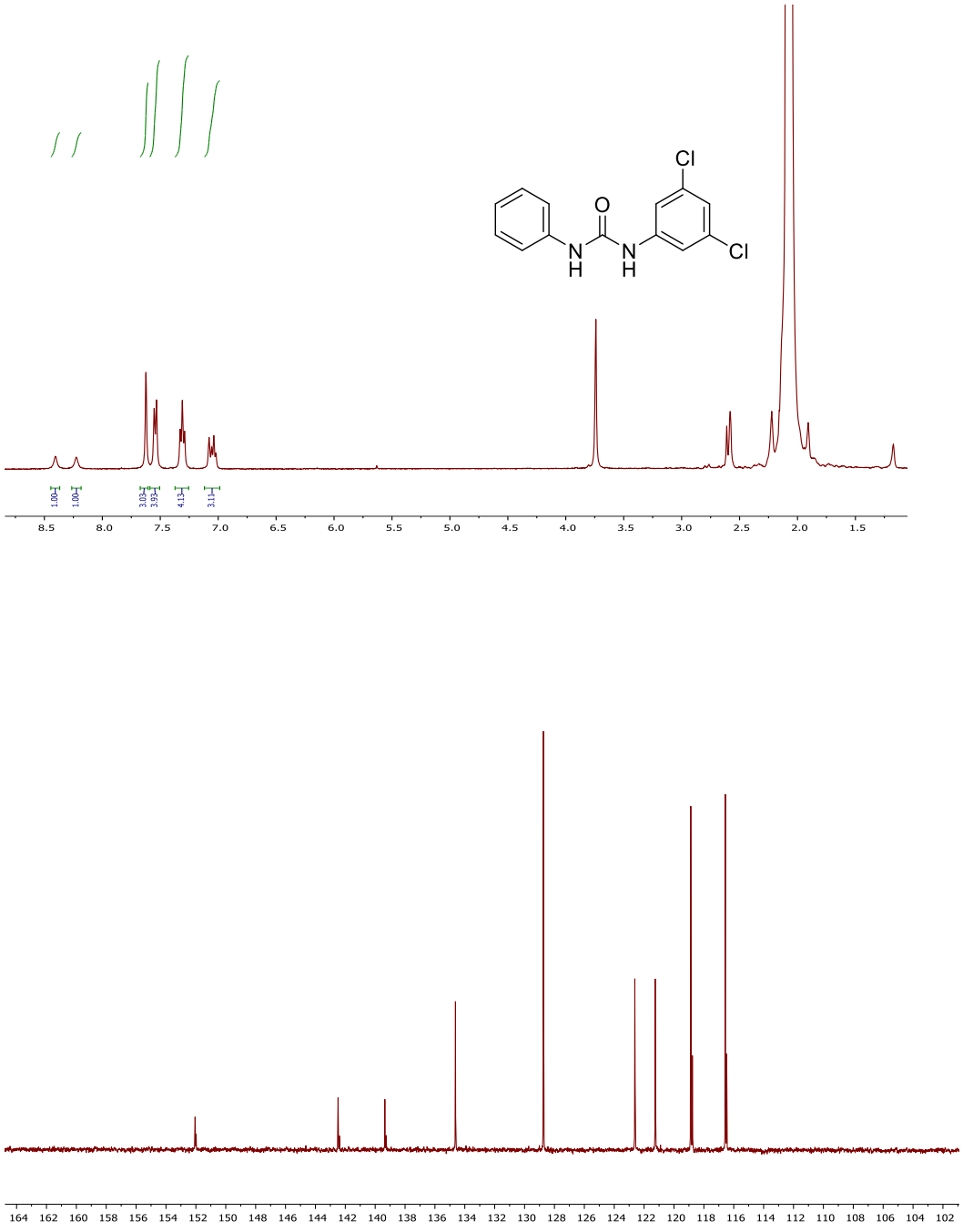

Figure 2.16. (Upper) ^{1}H NMR (acetone-d_6, 400 MHz) spectrum of 3,5-dichlorophenyl-phenyl urea (Lower) ^{13}C NMR (acetone-d_6, 100 MHz) spectrum of 3,5-dichlorophenyl-phenyl urea.

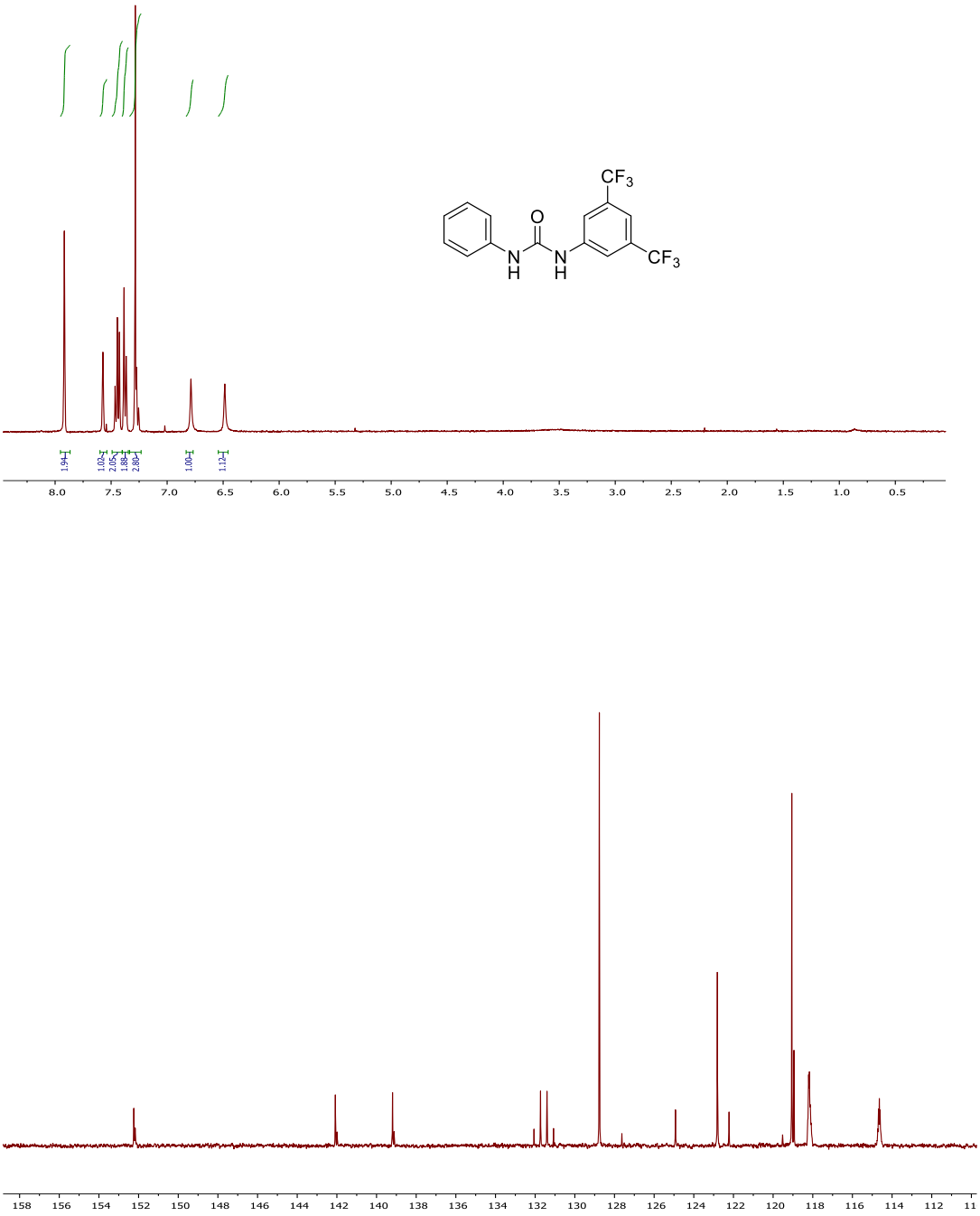

Figure 2.17. (Upper) ^{1}H NMR ($CDCl_3$, 400 MHz) spectrum of 3,5-bis(trifluoromethyl)phenyl-3-phenyl urea (Lower) ^{13}C NMR (acetone-d_6, 100 MHz) spectrum of 3,5-bis(trifluoromethyl)phenyl-3-phenyl urea.

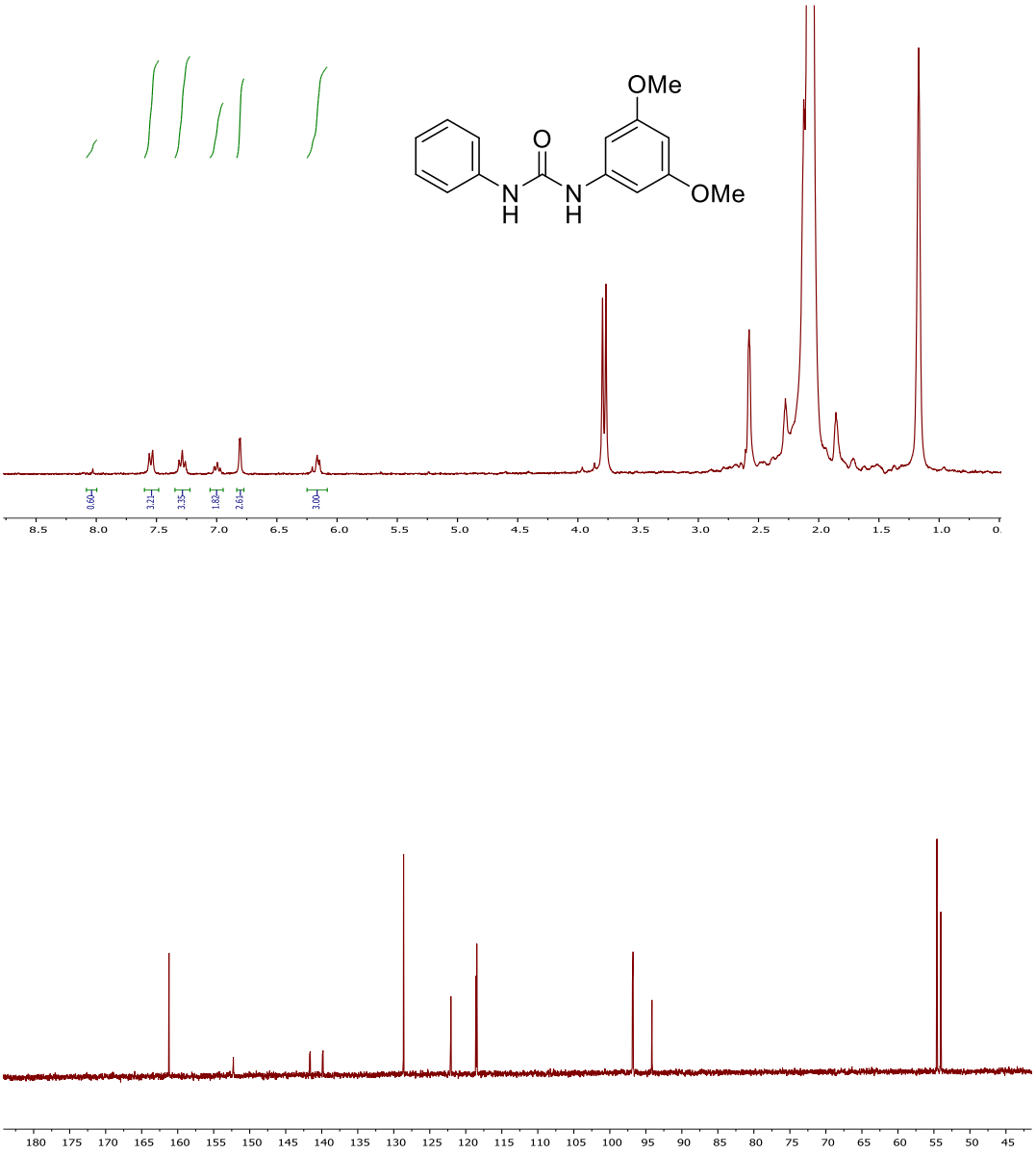

Figure 2.18. (Upper) ^{1}H NMR (acetone-d_6, 400 MHz) spectrum of 3,5-dimethoxyphenyl-3-phenyl urea (Lower) ^{13}C NMR (acetone-d_6, 100 MHz) spectrum of 3,5-dimethoxyphenyl-3-phenyl urea.

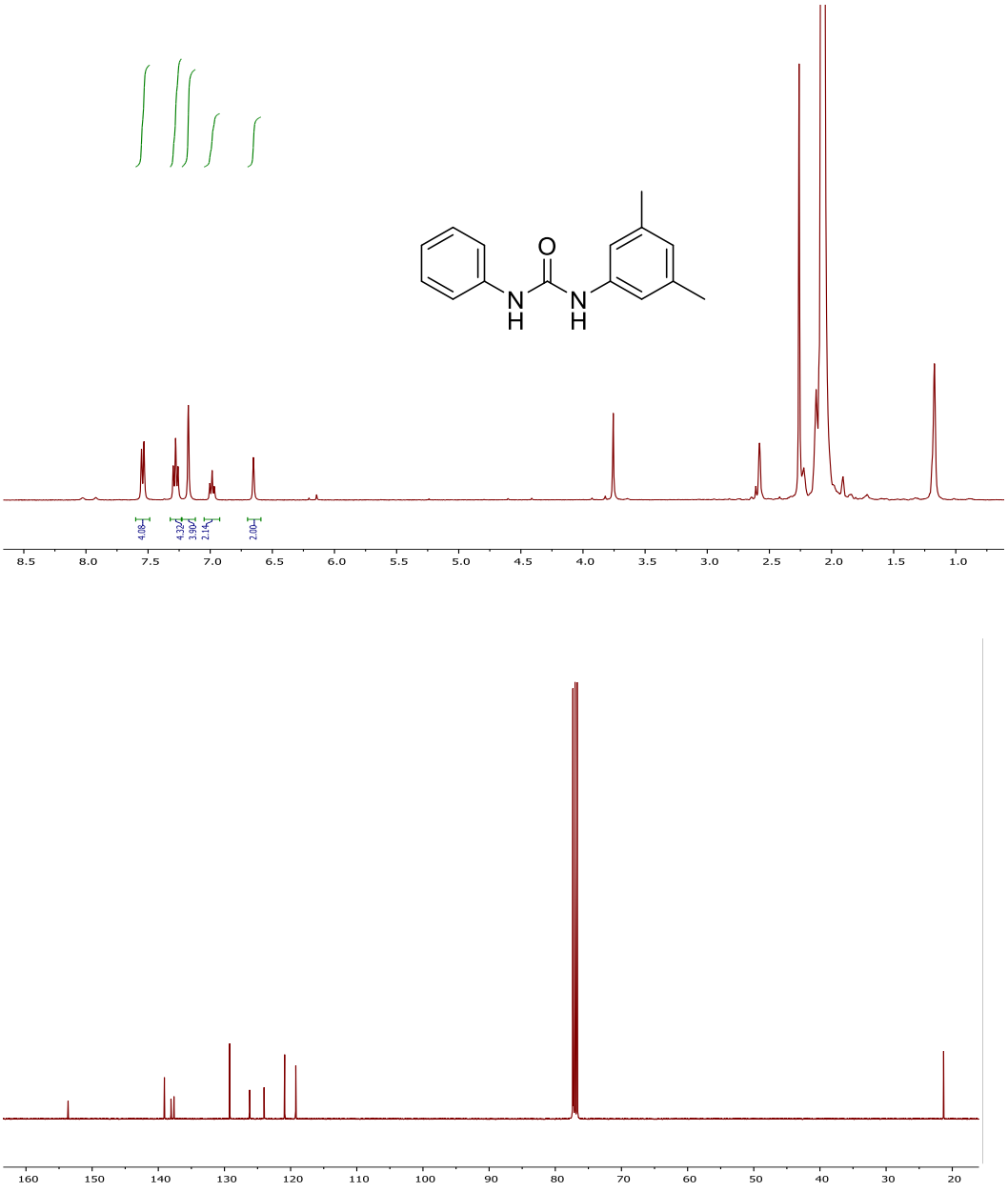

Figure 2.19. (Upper) ^{1}H NMR (acetone-d_6, 400 MHz) spectrum of 3,5-dimethylphenyl-3-phenyl urea (Lower) ^{13}C NMR ($CDCl_3$, 100 MHz) spectrum of 3,5-dimethylphenyl-3-phenyl urea.

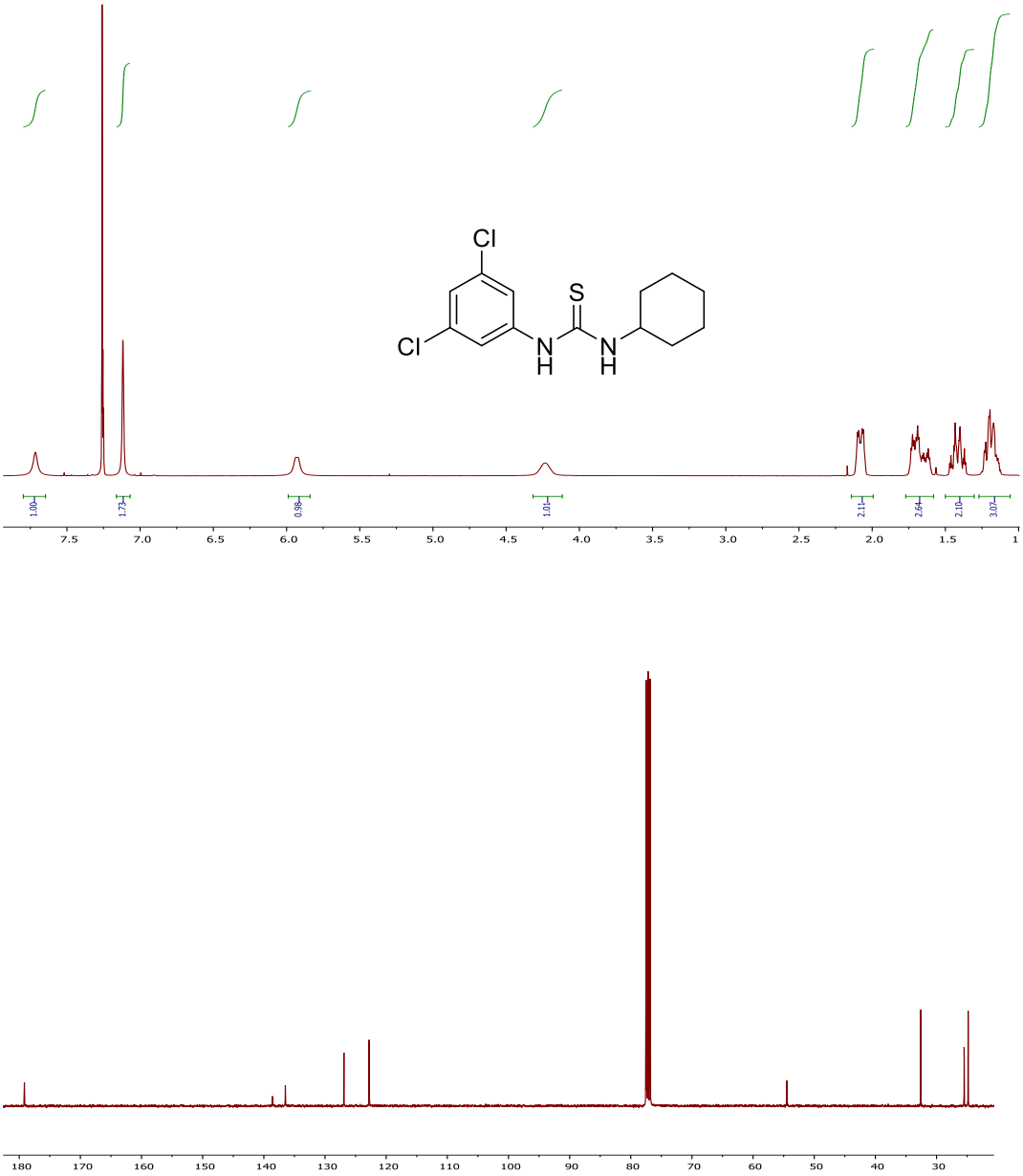

Figure 2.20. (Upper) ^{1}H NMR ($CDCl_3$, 400 MHz) spectrum of 3,5-dimethylphenyl cyclohexyl thiourea. (Lower) ^{13}C NMR ($CDCl_3$, 100 MHz) spectrum of 1-cyclohexyl-3-(3,5-dichlorophenyl)thiourea.

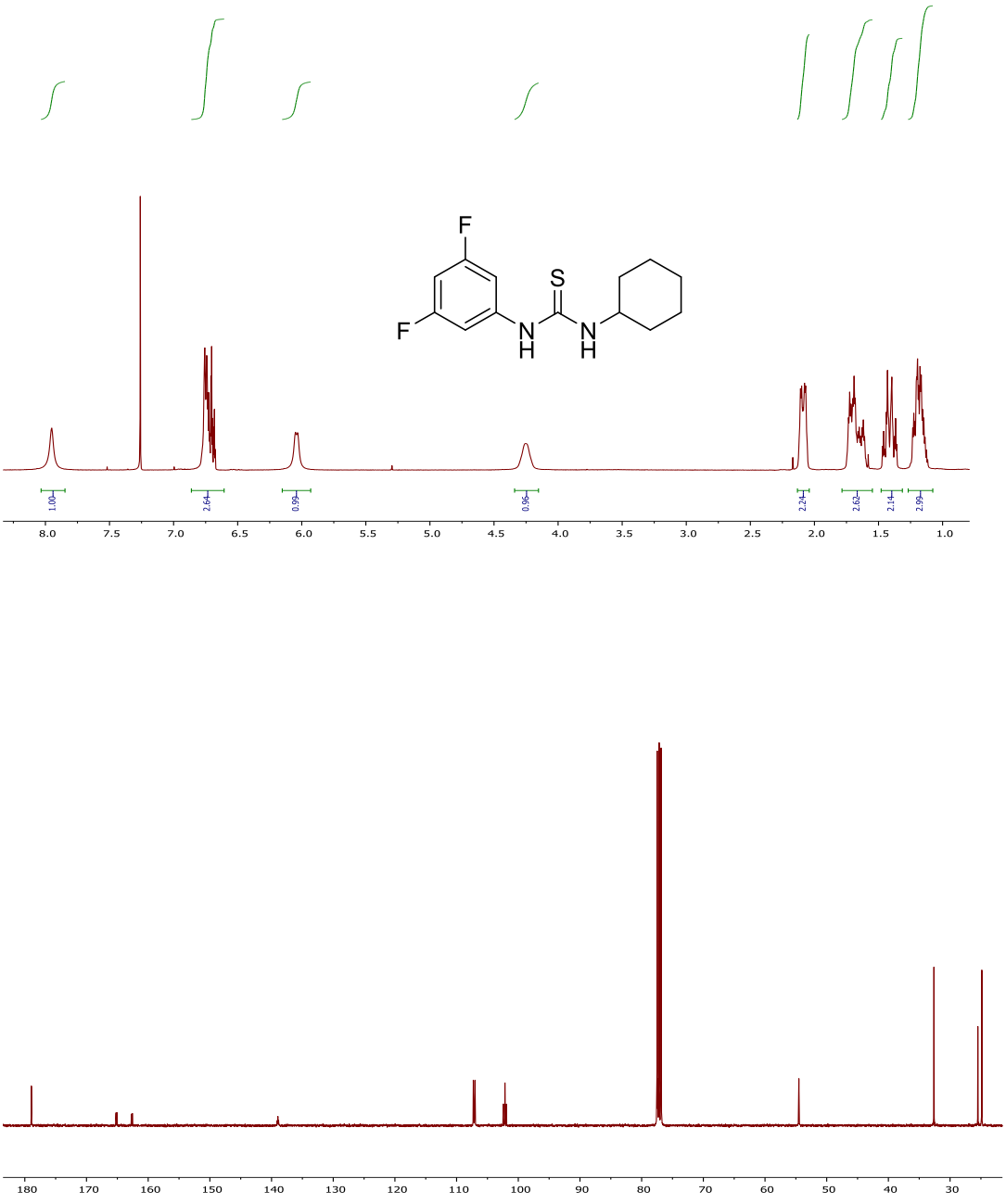

Figure 2.21. (Upper) ^{1}H NMR ($CDCl_3$, 400 MHz) spectrum of 3,5-difluorophenyl cyclohexyl thiourea. (Lower) ^{13}C NMR ($CDCl_3$, 100 MHz) spectrum of 1-cyclohexyl-3-(3,5-difluorophenyl)thiourea.

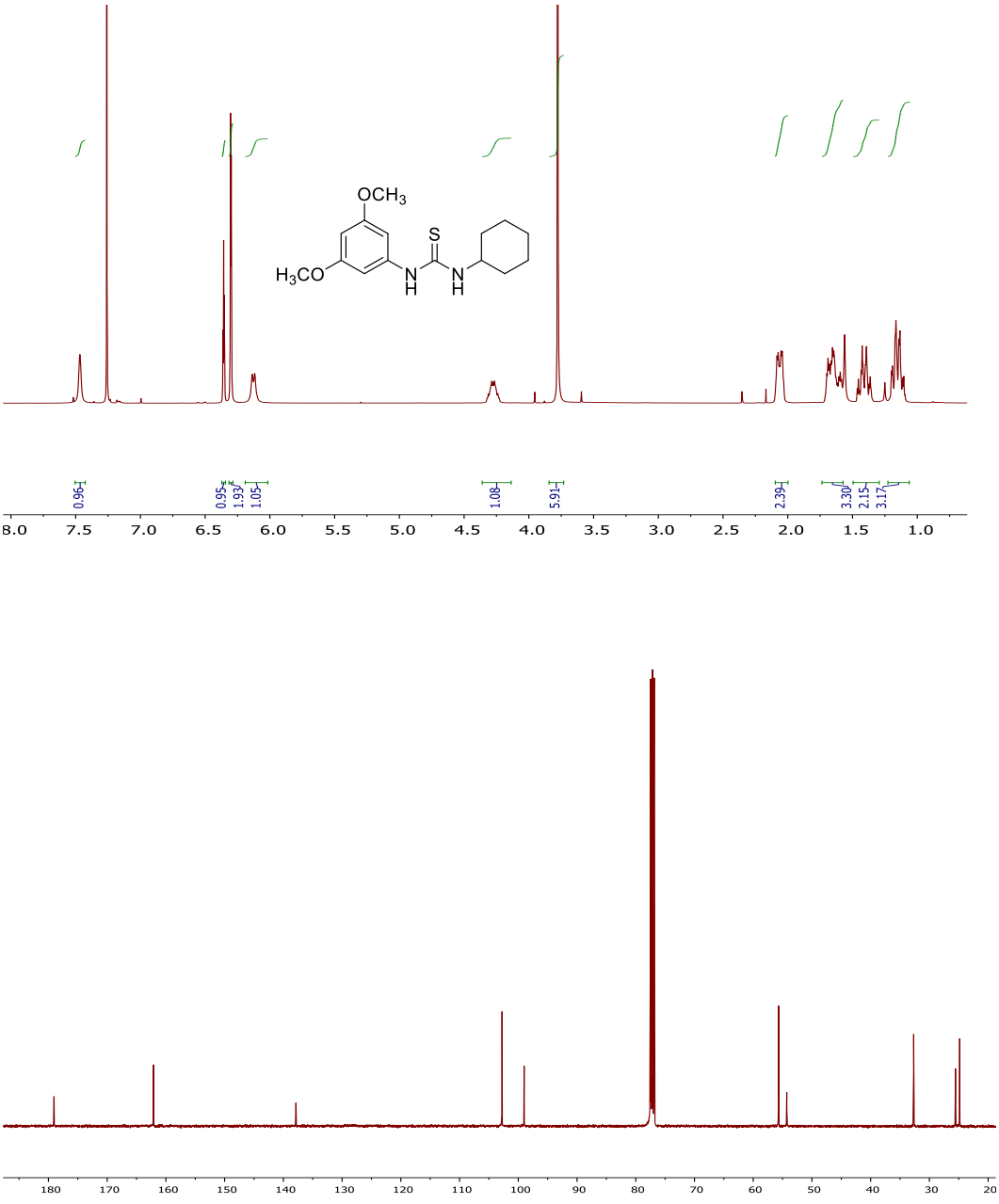

Figure 2.22. (Upper) ^{1}H NMR ($CDCl_3$, 400 MHz) spectrum of 3,5-dimethoxylphenyl cyclohexyl thiourea. (Lower) ^{13}C NMR ($CDCl_3$, 100 MHz) spectrum of 1-cyclohexyl-3-(3,5-dimethoxyphenyl)thiourea.

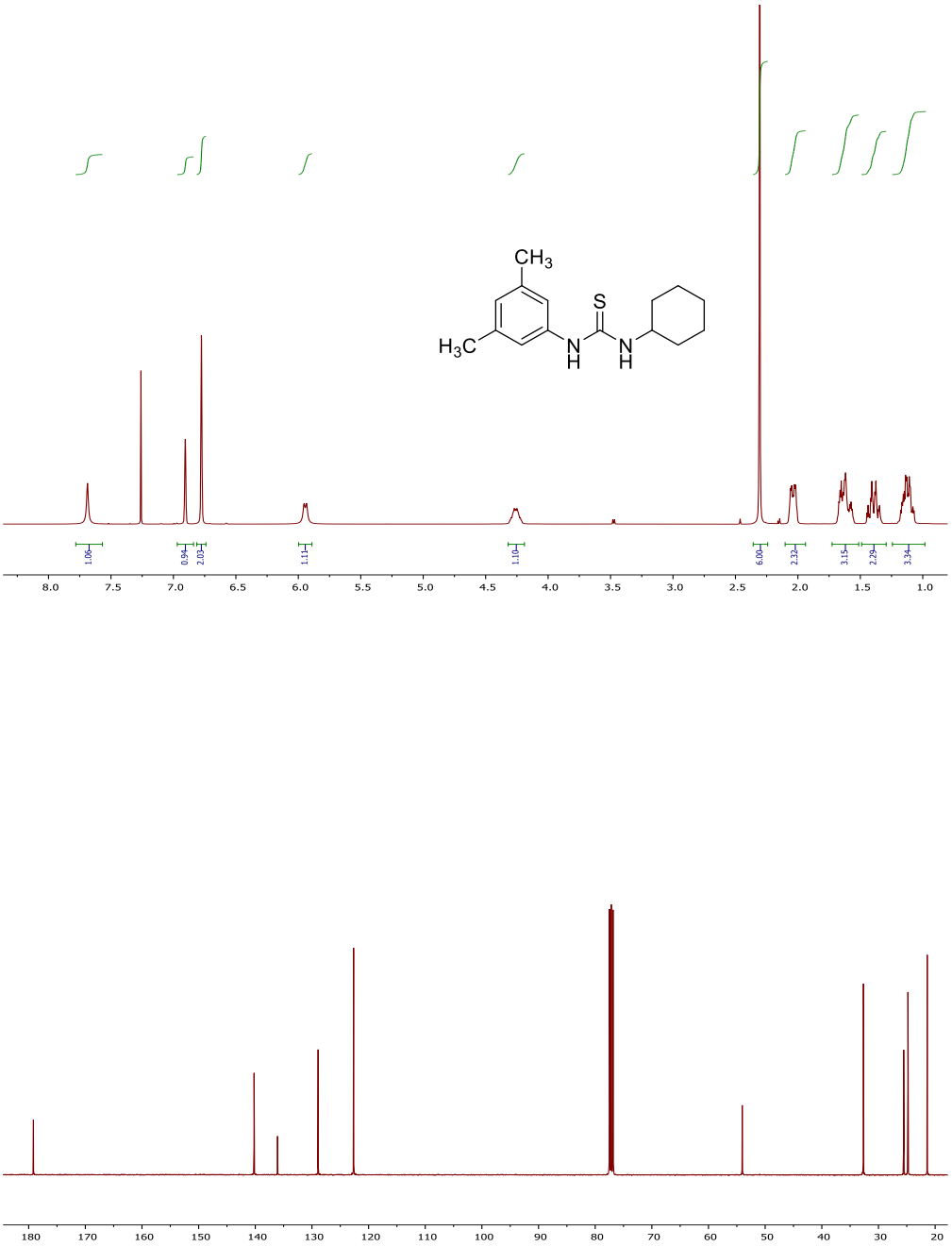

Figure 2.23. (Upper) ^{1}H NMR ($CDCl_3$, 400 MHz) spectrum of 3,5-dimethylphenyl cyclohexyl thiourea. (Lower) ^{13}C NMR ($CDCl_3$, 100 MHz) spectrum of 1-cyclohexyl-3-(3,5-dimethylphenyl)thiourea.

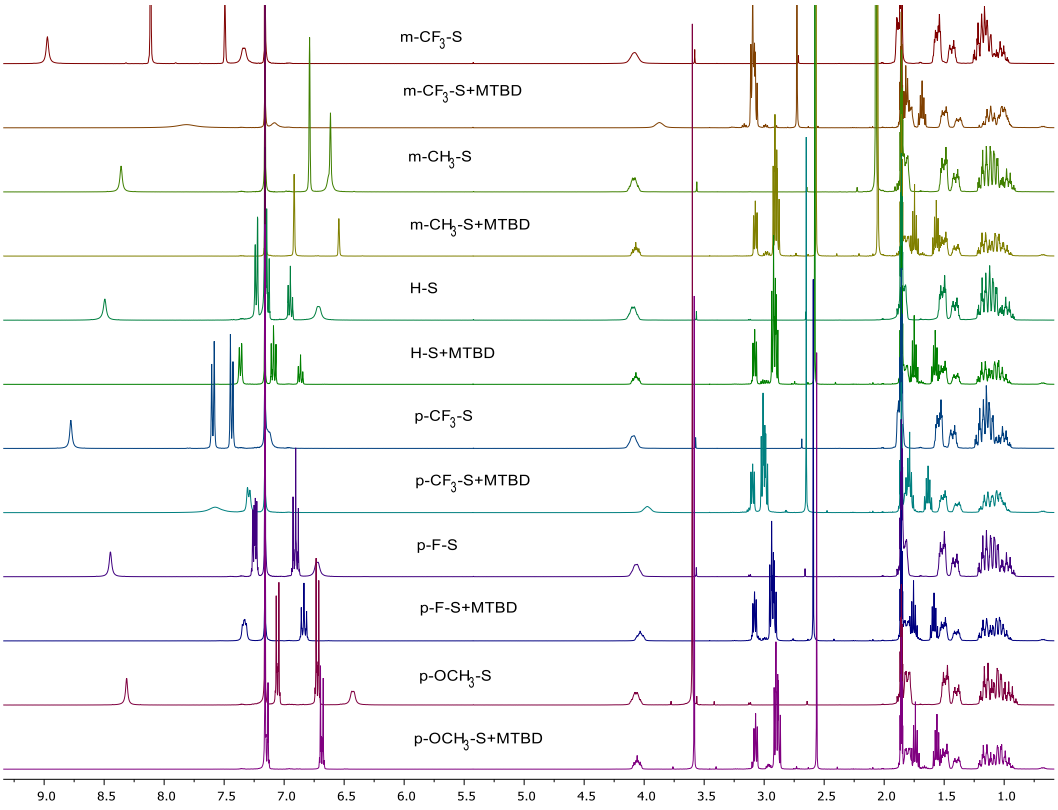

Figure 2.24. ^{1}H NMR spectra (acetone-d_6, 400 MHz) of select thiourea H-bond donors in the presence and absence of MTBD (0.099 M each) (referenced to C_6H_6 internal standard). Cyclohexyl methine ~4.1 ppm indicates thioimidate formation (upfield shift).

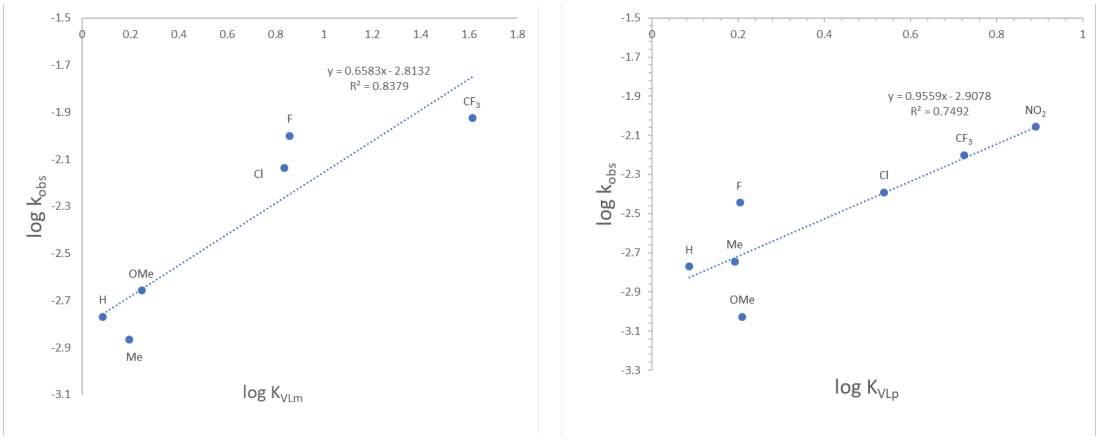

Figure 2.25. Plots of log k_{obs} vs log K_{VL} for *m*-X-S (left) and *p*-X-S (right). Note that axes do not extend to the origin.

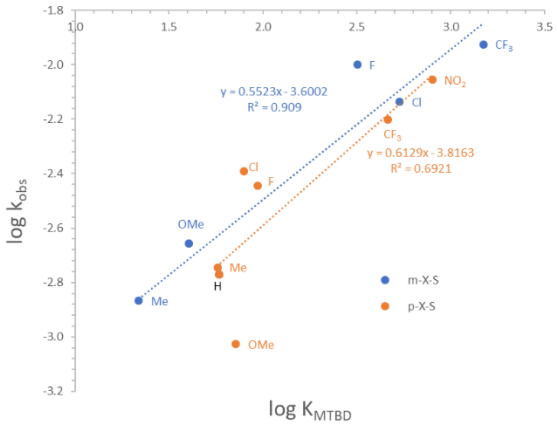

Figure 2.26. Plots of log k_{obs} vs log K_{MTBDm} and K_{MTBDp}. Note that the axes do not extend to the origin.

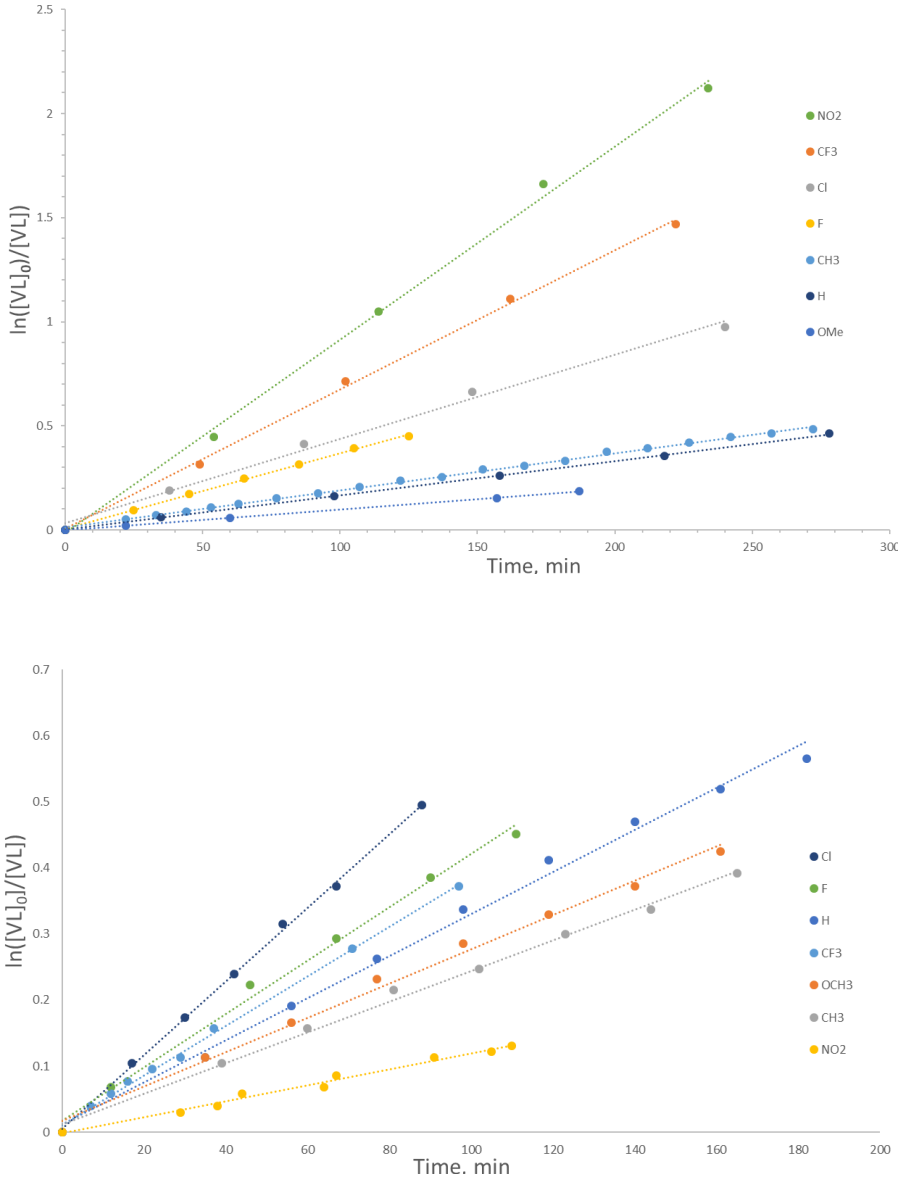

Figure 2.27. Plot of ln([VL]$_0$/[[VL]) vs time for *p*-X-S in benzene-d_6 (upper) and acetone-d_6 (lower). Note: only a selected run of many runs for each catalyst is included; the k_{obs} values in the Hammett plots represent the average of at least 2 runs.

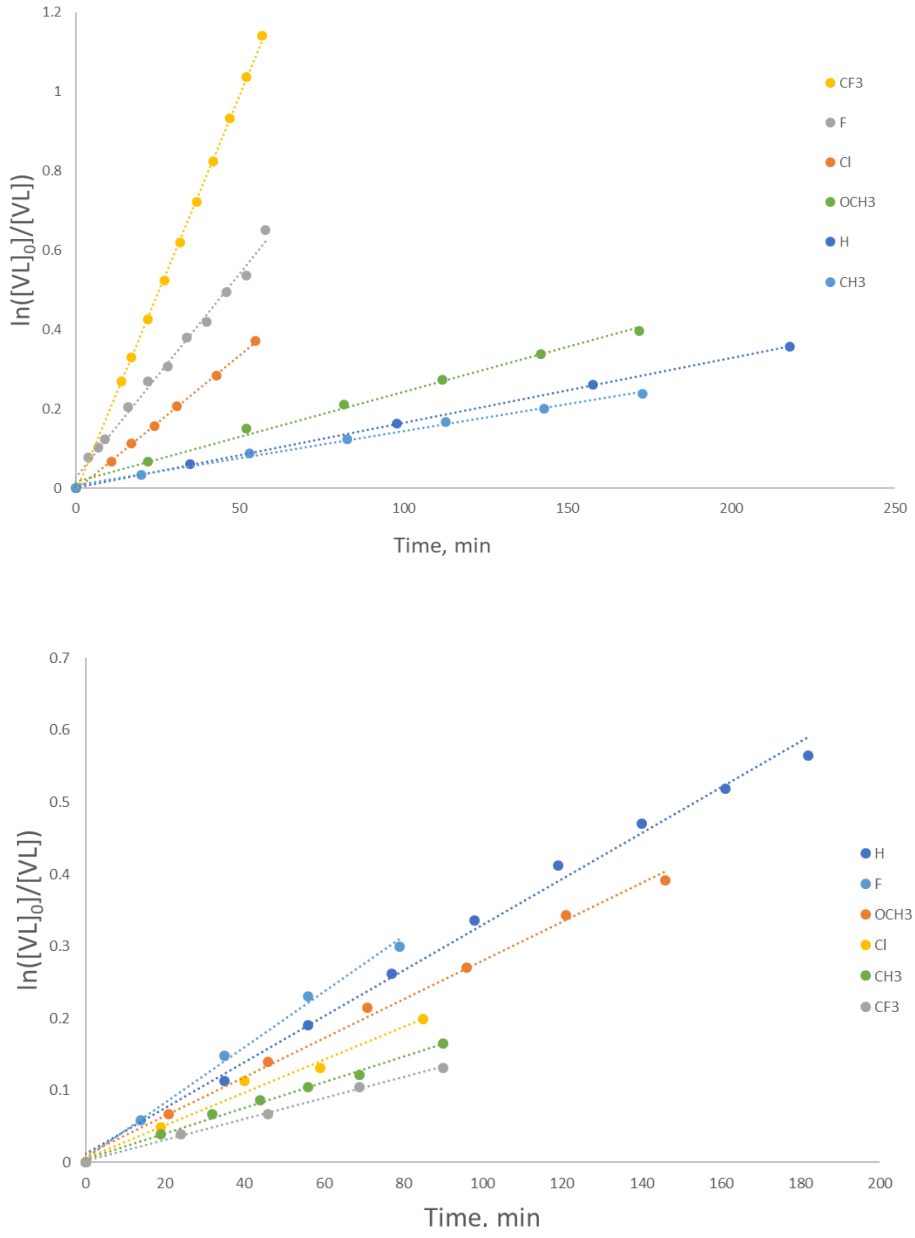

Figure 2.28. Plot of ln([VL]$_0$/[[VL]) vs time for *m*-X-S in benzene-d_6 (upper) and acetone-d_6 (lower). Note: only a selected run of many runs for each catalyst is included; the k_{obs} values in the Hammett plots represent the average of at least 2 runs.

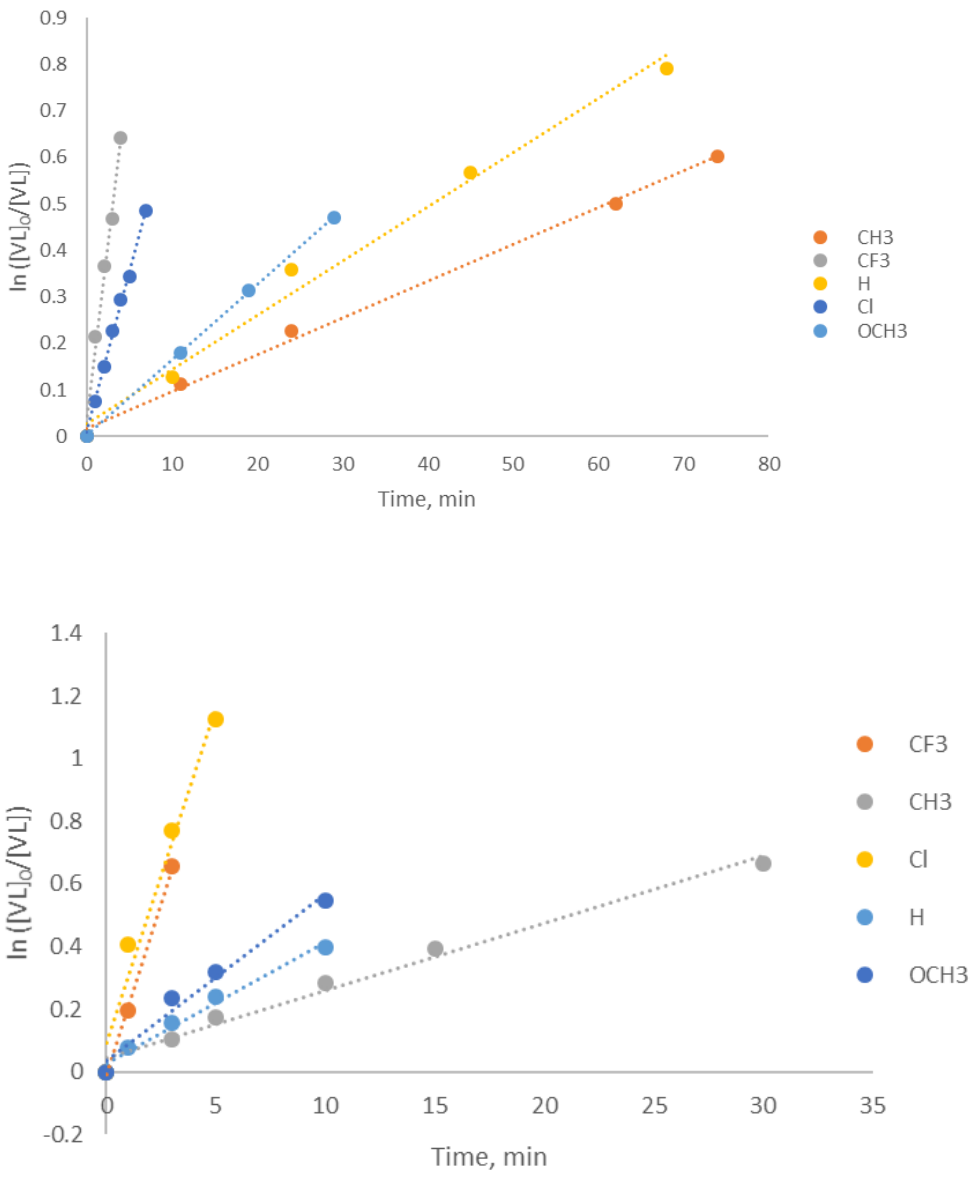

Figure 2.29. Plot of ln([VL]$_0$/[[VL]) Vs time for *m*-X-O in benzene-d_6 (upper) and acetone-d_6 (lower). Note: only a selected run of many runs for each catalyst is included; the k_{obs} values in the Hammett plots represent the average of at least 2 runs.

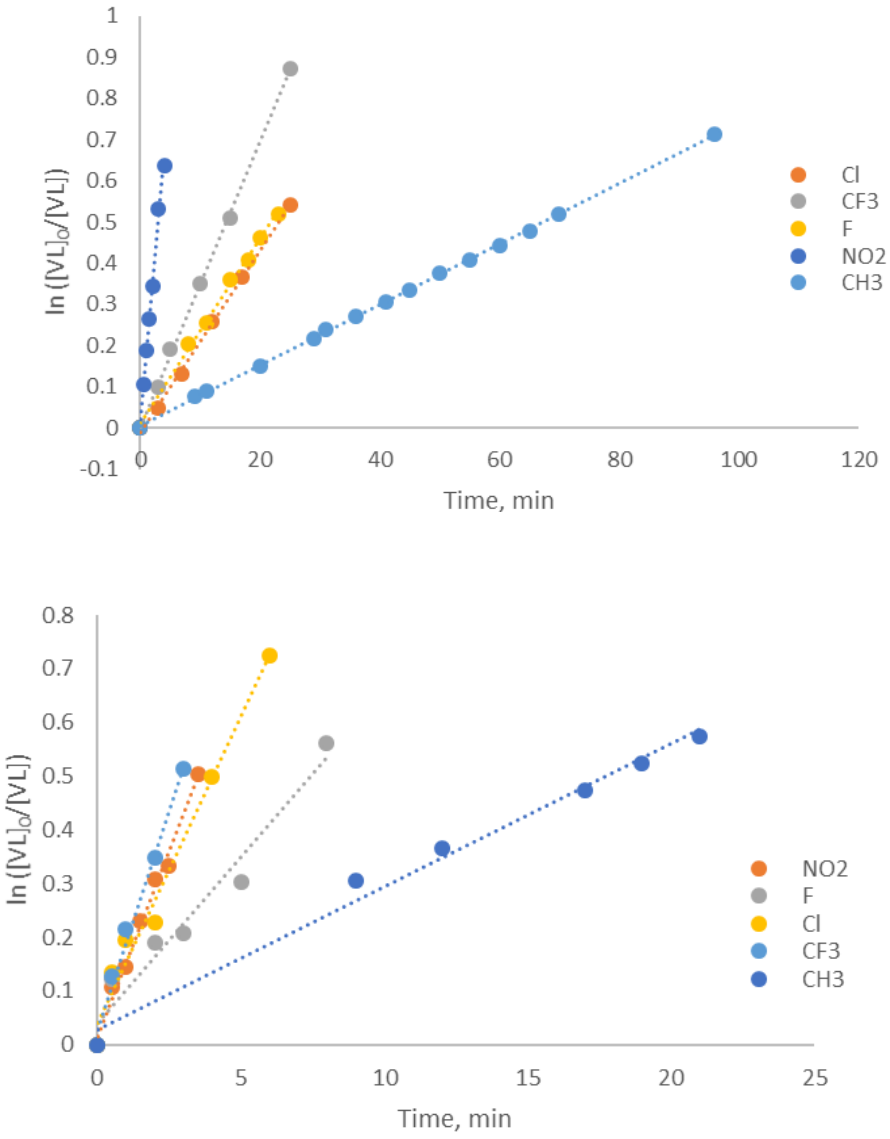

Figure 2.30. Plot of ln([VL]$_0$/[[VL]) Vs time for *p*-X-O in benzene-d_6 (upper) and acetone-d_6 (lower). Note: only a selected run of many runs for each catalyst is included; the k_{obs} values in the Hammett plots represent the average of at least 2 runs.

MANUSCRIPT III

Published in ACS Macromolecules

Bisurea and Bisthiourea H-Bonding Organocatalysts for Ring-Opening Polymerization: Cues for the Catalyst Design

Rukshika S. Hewawasam, U.L.D. Inush Kalana, Nayanthara U. Dharmaratne, Thomas J. Wright, Timothy M. Bannin, Elizabeth T. Kiesewetter and Matthew K. Kiesewetter

Chemistry, University of Rhode Island, Kingston, RI, USA

Corresponding Author: Matthew Kiesewetter, Ph.D.

Chemistry

University of Rhode Island

140 Flagg Road

Kingston, RI, 02881, USA

Email address: mkiesewetter@uri.edu

ABSTRACT

A series of conformationally flexible bis(thio)urea H-bond donors plus base cocatalyst were applied to the ring- opening polymerization (ROP) of lactones. The rate of the ROP displays a strong dependence on the length and identity of the tether, where a circa five methylene-unit long tether exhibits the fastest ROP. Any constriction to conformational freedom is deleterious to catalysis. For the ROP of δ-valerolactone (VL) and ε-caprolactone (CL), the bisurea H-bond donors are more effective, but for lactide, the bisthioureas are more active catalysts. The ROP reactions are rapid and controlled across a wide range of reaction conditions, including solvent-free conditions, exhibiting excellent weight control from low Mn to high polymers. The active mechanism is highly dependent on the identity of the base cocatalyst, and a mechanistic rationale for the observations is discussed. Implications for the design of future generation catalysts are discussed.

INTRODUCTION

H-bonding organocatalysts for ring-opening polymerization (ROP) are a facile means of generating precisely tailored macromolecules.[1–3] Among the larger class of H-bonding organocatalysts, (thio)urea H-bond donors stand out for the remarkable level of control they can rendered in polymer synthesis.[4,5] The thiourea plus base mediated ROP of lactone and carbonate monomers are thought to effect enchainment by H-bond activation of monomer by thiourea and initiating/propagating chain end by base; these catalysts are most active in non-polar solvent.[5] The urea plus base class of H-bonding catalysts offer no apology in terms of rate and are among the most active catalysts for the ROP of lactones.[6–8] Several mechanistic studies by our group and others have shown that (thio)urea/base mediated ROP can proceed by one of two mechanisms: *neutral H-bonding* or *(thio)imidate mediated* ROP (Scheme 3.1).[7–10] Which mechanism is operative depends largely on reaction conditions (high temperature,[11] polar solvent,[10,12,13] strong electron-withdrawing groups on H-bond donor,[10] early reaction time and strong bases favor imidate)[7,8] though generally ureas are more active than thioureas and imidate mediated ROP is far more active than neutral H-bonding.[3] Remarkably, these 'hyperactive' catalysts for ROP remain controlled.

The synthetic addition of one or more (thio)urea H-bond donating arms to the parent (thio)urea has been shown to substantially increase the activity of (thio)urea H-bond donors.[6,14] Our group first disclosed bis- and tris-(thio)urea H-bond donors for ROP,[6,14] and other intramolecular Lewis acid donors have been used.[15] In general, the bis-(thio)ureas (**2-O** and **2-S**, Figure 3.1) are more active than mono-(thio)urea (**1-O** and **1-**

S), and ureas are more active than thioureas for the bis-(thio)urea plus base mediated ROP of lactone and carbonate monomers.[3,6,13] However, this rule of thumb does not apply for the (thio)urea plus base mediated ROP of lactide (LA), where the higher rates are displayed by (bis)-thioureas (versus (bis)-ureas) of like substitution.[12] Again, the high rates exhibited by **2-O** and **2-S** plus base for ROP occur without the reduction of reaction control. Pan *et al.* synthesized bisurea H-bond donors featuring rigid linkers,[16] which were less active for ROP than the flexible 3-carbon tethered **2-O** and **2-S** reported by our group.[6,14] In the pantheon of conformationally flexible linkers that can be envisaged, only one has been reported.[6] In light of the recent interest in these catalysts, we disclose here several bisurea and bisthiourea H-bond donors for ROP with flexible linkers, most with higher activity and control than the parent **2-X** system. We extend previously proposed mechanisms to the (thio)urea plus alkylamine base mediated ROP of LA to explain why thioureas have been observed to be more effective (versus ureas).

EXPERIMENTAL SECTION

General Considerations. All chemicals were purchased from Fisher Scientific and used as received unless stated otherwise. Benzene-*d6* and chloroform-*d* were purchased from Cambridge Isotope Laboratories, distilled from calcium hydride and stored under N_2. Acetone-*d6* was purchased from Cambridge Isotope Laboratories, distilled from calcium sulfate and stored under N_2. δ-valerolactone (VL), ε-caprolactone (CL) and benzyl alcohol were distilled under high vacuum from calcium hydride prior to use. Dry CH_2Cl_2 was obtained from an Innovative Technology solvent purification system. All experiments were conducted in a stainless-steel glovebox under N_2 unless stated otherwise. NMR experiments were performed on a Bruker Avance III 300 or 400 MHz spectrometer. Urea and thiourea H-bond donors were prepared by established methods.[17,18]

Mass spectrometry experiments were performed using a Thermo Electron (San Jose, CA, USA) LTQ Orbitrap XL mass spectrometer affixed with electrospray ionization (ESI) interface in a positive ion mode. Collected mass spectra were averaged for at least 50 scans. Tune conditions for infusion experiments (10 μL/min flow, sample concentration 5 μg/mL in 50/50 v/v water/ methanol) were as follows: ion spray voltage, 5000 V; capillary temperature, 275^{O}C; sheath gas (N_2, arbitrary units), 11; auxiliary gas (N_2, arbitrary units), 2; capillary voltage, 21 V; and tube lens, 90 V; multipole 00 offset, -4.25 V; lens 0 voltage, - 5.00; multipole 1 offset, - 8.50 V; Multipole RF Amplitude, 400 V; Ion trap's AGC target settings for Full MS was 3.0e4 and FT's 2.0e5 (with 3 and

2 averaged microscans , respectively). Prior to analysis, the instrument was calibrated for positive ions using Pierce LTQ ESI positive ion calibration solution (lot #PC197784).

Example ROP of VL in benzene-d_6. To a 7 mL vial, **2-O5** (14.69 mg, 0.024 mmol), VL (100.00 mg, 0.998 mmol) and benzene-*d6* (250 μL) were added. The contents were stirred until the solution became homogenous. To a second 7 ml vial, benzyl alcohol (2.16 mg, 0.019 mmol), MTBD (3.67 mg, 0.024 mmol) and benzene-*d6* (250 μL) were added. The contents in the second vial were transferred to the first vial via Pasteur pipette, and the contents were agitated to mix. The reaction solution was then transferred to an NMR tube, and the progress of the reaction monitored by ^{1}H NMR. The reaction was quenched by the addition of benzoic acid (3.00 mg, 0.024 mmol). Polymer isolated by precipitation with hexanes, and the volatiles were removed under high vacuum before characterization via GPC.

Example solvent-free ROP of VL. A 1.5 mL vial was charged with **2-O5** (12.23 mg, 0.019 mmol), benzyl alcohol (2.15 mg, 0.019 mmol), VL (400.00 mg, 3.99 mmol), magnetic stir bar and stirred until homogeneous. A second vial was charged with MTBD (3.05 mg, 0.019 mmol). The contents of the first vial were transferred to the second vial using a Pasteur pipette, and the solution was stirred. Reaction progress was monitored by taking aliquots of the reaction mixture – either ~1.5 μL solution or a small amount of solid extracted via spatula – at different time intervals and quenched in a solution of benzoic acid in chloroform-*d*. Conversion was determined via ^{1}H NMR. The polymer

samples in the aliquots were isolated by precipitating with hexanes, and the volatiles were removed under high vacuum before characterization via GPC.

Synthesis of urea H-bond donors

1,1'-(propane-1,3-diyl)bis(3-(3,5-bis(trifluoromethyl)phenyl)urea) **(2-O3)-** A dried 10 mL Schlenk flask was charged with a stir bar, dichloromethane (7 mL), 3,5-bis(trifluoromethyl)phenyl isocyanate (0.21 g, 0.86 mmol), and 1,3-diaminopropane (0.03 mL, 0.43 mmol) was added dropwise to the Schlenk flask. After stirring overnight, the reaction mixture was filtered via suction filtration and rinsed with 3 portions of cold CH_2Cl_2 to provide a pure white powder that was freed of volatiles under high vacuum. Yield: 97%. Characterization matches literature.[6]

1,1'-(ethane-1,2-diyl)bis(3-(3,5-bis(trifluoromethyl)phenyl)urea) **(2-O2)-** A flame dried 25 ml Schlenk flask was charged with a stir bar, dichloromethane (25 mL), 3,5-bistrifluoromethylphenyl isocyanate (1 g, 3.91 mmol), and ethylenediamine (0.13 mL, 1.95 mmol) was added dropwise to the Schlenk flask. After stirring overnight, the reaction mixture was filtered via suction filtration and rinsed with 3 portions of cold CH_2Cl_2 to provide a pure white powder that was freed of volatiles under high vacuum. Yield: 65%. NMR spectra given below. HRMS: calc. $(C_{20}H_{15}F_{12}N_4O_2+H)^+ = 571.0998$; found $m/z = 571.0998$.

1,1'-(butane-1,4-diyl)bis(3-(3,5-bis(trifluoromethyl)phenyl)urea) **(2-O4)-** A flame dried 25 ml Schlenk flask was charged with a stir bar, dichloromethane (25 mL), 3,5-

bistrifluoromethylphenyl isocyanate (1 g, 3.91 mmol), and 1,4-diaminobutane (0.20 mL, 1.95 mmol) was added dropwise to the Schlenk flask. After stirring overnight, the reaction mixture was filtered via suction filtration and rinsed with 3 portions of cold CH_2Cl_2 to provide a pure white powder that was freed of volatiles under high vacuum. Yield: 70%. NMR spectra given below. HRMS: calc. ($C_{22}H_{19}F_{12}N_4O_2$+H)+= 599.1238; found *m/z* =599.1311.

1,1'-(pentane-1,5-diyl)bis(3-(3,5-bis(trifluoromethyl)phenyl)urea) **(2-O5)-** A flame dried 25 ml Schlenk flask was charged with a stir bar, dichloromethane (25 mL), 3,5-bistrifluoromethylphenyl isocyanate (1 g, 3.91 mmol), and 1,5-diaminopentane (0.22 mL, 1.95 mmol) was added dropwise to the Schlenk flask. After stirring overnight, the reaction mixture was filtered via suction filtration and rinsed with 3 portions of cold CH_2Cl_2 to provide a pure white powder that was freed of volatiles under high vacuum. Yield: 74%. NMR spectra given below. HRMS: calc. ($C_{23}H_{21}F_{12}N_4O_2$+H)+= 613.1467; found *m/z* = 613.1467.

1,1'-(hexane-1,6-diyl)bis(3-(3,5-bis(trifluoromethyl)phenyl)urea) **(2-O6)-** A flame dried 25 ml Schlenk flask was charged with a stir bar, dichloromethane (25 mL), 3,5-bistrifluoromethylphenyl isocyanate (1 g, 3.91 mmol), and hexamethylenediamine (0.25 mL, 1.95 mmol) was added dropwise to the Schlenk flask. After stirring overnight, the reaction mixture was filtered via suction filtration and rinsed with 3 portions of cold CH2Cl2 to provide a pure white powder that was freed of volatiles under high vacuum. Yield: 80%. NMR spectra given below. HRMS: calc. ($C_{24}H_{23}F_{12}N_4O_2$+H)+= 627.1624; found *m/z* = 627.1624.

1,1'-(dodecane-1,12-diyl)bis(3-(3,5-bis(trifluoromethyl)phenyl)urea) **(2-O12)-** A flame dried 100 ml Schlenk flask was charged with a stir bar, dichloromethane (20 mL), 3,5-bistrifluoromethylphenyl isocyanate (0.63 g, 2.5 mmol), and 1,12-diaminododecane (0.25 g, 1.25 mmol) was added dropwise to the Schlenk flask. After stirring overnight, the reaction mixture was filtered via suction filtration and rinsed with 3 portions of cold CH2Cl2 to provide a pure white powder that was freed of volatiles under high vacuum. Yield: 92%. NMR spectra given below. HRMS: calc. ($C_{30}H_{34}F_{12}N_4O_2$+H)+= 711.2382; found *m/z* = 711.2563.

1,1'-((methylazanediyl)bis(ethane-2,1-diyl))bis(3-(3,5-bis(trifluoromethyl)phenyl)urea) **(2-O5-N)-** A flame dried 50 ml Schlenk flask was charged with a stir bar, dichloromethane (20 mL), 3,5-bistrifluoromethylphenyl isocyanate (1.08 g, 4.26 mmol), and N1-(2-aminoethyl)-N1-methylethane-1,2-diamine (0.27 mL, 2.13 mmol) was added dropwise to the Schlenk flask. After stirring overnight, the reaction mixture was filtered and rinsed with 3 portions of cold CH_2Cl_2 to provide a pure white powder that was freed of volatiles under high vacuum. Yield: 47%. NMR spectra given below. HRMS: calc. ($C_{23}H_{21}F_{12}N_5O_2$+H)$^+$= 628.1564; found *m/z* = 628.1594.

1,1'-(oxybis(ethane-2,1-diyl))bis(3-(3,5-bis(trifluoromethyl)phenyl)urea) **(2-O5-O) -** A flame dried 50 ml Schlenk flask was charged with a stir bar, dichloromethane (20 mL), 3,5-bistrifluoromethylphenyl isocyanate (2.2 g, 8.14 mmol), and 2,2'-oxybis(ethan-1-amine) (0.44mL, 4.07 mmol) was added dropwise to the Schlenk flask. After stirring overnight, the reaction mixture was filtered and rinsed with 3 portions of cold CH_2Cl_2

to provide a pure white powder that was freed of volatiles under high vacuum. Yield: 90%. NMR spectra given below. HRMS: calc. $(C_{22}H_{19}F_{12}N_4O_3+H)^+$= 615.1260; found *m/z* = 615.1260.

1,1'-(2,2-dimethylpropane-1,3-diyl)bis(3-(3,5-bis(trifluoromethyl)phenyl)urea) **(2-O3-diMe)** - A flame dried 50 ml Schlenk flask was charged with a stir bar, dichloromethane (20 mL), 3,5-bistrifluoromethylphenyl isocyanate (0.63 g, 2.5 mmol) 2,2-Dimethyl-1,3-propanediamine and (0.15 mL, 1.25 mmol). After stirring overnight, the reaction mixture was filtered and rinsed with 3 portions of cold CH_2Cl_2 to provide a pure white powder that was freed of volatiles under high vacuum. Yield: 47%. NMR spectra given below. HRMS: calc. $(C_{23}H_{21}F_{12}N_4O_2)^+$ = 613.1467 found *m/z* =613.1467.

Synthesis of thiourea H-bond donors

1,1'-(ethane-1,2-diyl)bis(3-(3,5-bis(trifluoromethyl)phenyl)thiourea) **(2-S2)-** A flame dried 50 ml Schlenk flask was charged with a stir bar, dichloromethane (20 mL), 3,5-bis(trifluoromethyl)phenyl isothiocyanate (2.1 g, 7.7 mmol), and ethylenediamine (0.26 mL, 3.9 mmol) was added dropwise to the Schlenk flask. After stirring overnight, the reaction mixture was filtered and rinsed with 3 portions of cold CH_2Cl_2 to provide a pure white powder that was freed of volatiles under high vacuum. Yield: 64%. Characterization matches literature.[18]

1,1'-(propane-1,3-diyl)bis(3-(3,5-bis(trifluoromethyl)phenyl)thiourea) **(2-S3)-** A flame dried 50 ml Schlenk flask was charged with a stir bar, dichloromethane (20 mL), 3,5-bis(trifluoromethyl)phenyl isothiocyanate (2.0 g, 7.4 mmol), and 1,3-diaminopropane

(0.27 mL, 3.7 mmol) was added dropwise to the Schlenk flask. After stirring overnight, the reaction mixture was filtered via suction filtration and rinsed with 3 portions of cold CH_2Cl_2 to provide a pure white powder that was freed of volatiles under high vacuum. Yield: 58%. Characterization matches literature.[6]

1,1'-(butane-1,4-diyl)bis(trifluoromethyl)phenyl)thiourea) **(2-S4)-** A flame dried 50 ml Schlenk flask was charged with a stir bar, dichloromethane (20 mL), 3,5-bis(trifluoromethyl)phenyl isothiocyanate (1.49 g, 5.5 mmol), and 1,4-diaminobutane (0.27 mL, 2.7 mmol) was added dropwise to the Schlenk flask. After stirring overnight, the reaction mixture was filtered via suction filtration and rinsed with 3 portions of cold CH_2Cl_2 to provide a pure white powder that was freed of volatiles under high vacuum. Yield: 35%. NMR spectra given below. HRMS: calc. $(C_{22}H_{19}F_{12}N_4S_2+H)^+$= 631.0845; found *m/z* =631.0825.

1,1'-(pentane-1,5-diyl)bis(3-(3,5-bis(trifluoromethyl)phenyl)thiourea) **(2-S5)-** A flame dried 50 ml Schlenk flask was charged with a stir bar, dichloromethane (20 mL), 3,5-bis(trifluoromethyl)phenyl isothiocyanate (1.49 g, 5.5 mmol), and 1,5-diaminopentane (0.32 mL, 2.7 mmol) was added dropwise to the Schlenk flask. After stirring overnight, the reaction mixture was filtered via suction filtration and rinsed with 3 portions of cold CH_2Cl_2 to provide a pure white powder that was freed of volatiles under high vacuum. Yield: 57%. NMR spectra given below. HRMS: calc. $(C_{23}H_{21}F_{12}N_4S_2+H)^+$= 645.1011; found *m/z* = 645.1016.

1,1'-(hexane-1,6-diyl)bis(3-(3,5-bis(trifluoromethyl)phenyl)thiourea) **(2-S6)**- A flame dried 50 ml Schlenk flask was charged with a stir bar, dichloromethane (20 mL), 3,5-bis(trifluoromethyl)phenyl isothiocyanate (1.87 g, 6.88 mmol), and hexamethylenediamine (0.44 mL, 3.44 mmol) was added dropwise to the Schlenk flask. After stirring overnight, the reaction mixture was filtered via suction filtration and rinsed with 3 portions of cold CH_2Cl_2 to provide a pure white powder that was freed of volatiles under high vacuum. Yield: 76%. NMR spectra given below. HRMS: calc. $(C_{24}H_{23}F_{12}N_4S_2+H)^+$= 659.1167; found *m/z* =659.1148.

1,1'-(dodecane-1,12-diyl)bis(3-(3,5-bis(trifluoromethyl)phenyl)thiourea) **(2-S12)** - A flame dried 50 ml Schlenk flask was charged with a stir bar, dichloromethane (20 mL), 3,5-bis(trifluoromethyl)phenyl isothiocyanate (0.68 g, 2.52 mmol), and 1,12-diaminododecane (0.25 g, 1.25 mmol) was added dropwise to the Schlenk flask. After stirring overnight, the reaction mixture was filtered via suction filtration and rinsed with 3 portions of cold CH_2Cl_2 to provide a pure white powder that was freed of volatiles under high vacuum. Yield: 91%. NMR spectra given below. HRMS: calc. $(C_{30}H_{35}F_{12}N_4S_2+H)^+$= 743.2033; found *m/z* = 743.2086.

1,1'-((methylazanediyl)bis(ethane-2,1-diyl))bis(3-(3,5-bis(trifluoromethyl)phenyl)thiourea) **(2-S5-N)-** A flame dried 50 ml Schlenk flask was charged with a stir bar, dichloromethane (20 mL), 3,5-bistrifluoromethylphenyl isothiocyanate (1.48 g, 4.26 mmol), and N1-(2-aminoethyl)-N1-methylethane-1,2-diamine (0.27 mL, 2.13 mmol). After stirring overnight, the reaction mixture was filtered via suction filtration and rinsed with 3 portions of cold CH_2Cl_2 to provide a pure

white powder that was freed of volatiles under high vacuum. Yield: 67%. NMR spectra given below. HRMS: calc. $(C_{23}H_{21}F_{12}N_5S_2+H)^+$= 660.1120; found *m/z* = 660.1120.

*1,1'-(oxybis(ethane-2,1-diyl))bis(3-(3,5-bis(trifluoromethyl)phenyl)thiourea)***(2-S5-O)-** A flame dried 50 ml Schlenk flask was charged with a stir bar, dichloromethane (25 mL), 3,5-bistrifluoromethylphenyl isothiocyanate (2.21 g, 8.14 mmol), and 2,2'-oxybis(ethan-1-amine) (0.44 mL, 4.07 mmol). After stirring overnight, the reaction mixture was filtered via suction filtration and rinsed with 3 portions of cold CH_2Cl_2 to provide a pure white powder that was freed of volatiles under high vacuum. Yield: 86%. NMR spectra given below. HRMS: calc. $(C_{22}H_{19}F_{12}N_4OS_2+H)^+$= 647.0803; found *m/z* = 647.0803.

RESULTS AND DISCUSSION

In the bis(thio)urea plus MTBD cocatalyzed (0.024 mmol) ROP of VL (1.0 mmol, 2 M) from benzyl alcohol (0.02 mmol) in C_6D_6, the bis(thio)ureas featuring a 5-carbon (methylene) tether were most active. Using established procedures,[6] electron deficient bis(thio)ureas were synthesized featuring linear aliphatic tethers ranging from two to twelve methylene units, bisthioureas (**2-Sn**) and bisureas (**2-On**) in Figure 3.1 (n = 2, 3, 4, 5, 6, 12), see Supplemental Information, SI. The **2-O2** H-bond donor was insoluble in solvents relevant for ROP. Especially versus the rigid (thio)urea tethers,[16] our results here suggest that the most effective catalysis arises when the (thio)urea moieties are allowed to interact with one another, lending credence to the originally proposed mechanism whereby bis(thio)urea moieties bring about ROP through an *activated-(thio)urea* mechanism characterized by one (thio)urea stabilizing through internal H-bond activation the (thio)urea which activates the lactone for enchainment, Figure 3.1.[6,14] We propose that the increased efficacy of **2-S5** and **2-O5** plus MTBD (versus other linker lengths) arises from the stability of the pseudo-7-membered cycle formed by intramolecular H-bonding – the (thio)urea moiety being largely rigid. The enhanced rates displayed by **2-O5** and **2-S5** are enhanced by a factor of two versus their respective 'parent' **2-X3** H-bond donor, and this enhanced rate does not result in increased M_w/M_n. The ROP are living in behavior, both **2-S5** and **2-O5** plus MTBD produce linear evolution of M_n versus conversion (Figure 3.2) and M_n that is predictable by $[M]_o/[I]_o$ (Table 3.7). In C_6D_6 (and other non-polar solvents), a H-bond mediated

mechanism of enchainment has been proposed;[3,6,9] urea plus base mediated ROP have repeatedly been shown to display faster rates than the analogous thiourea.[6,9]

Bisurea catalysts plus MTBD remain highly active for the ROP of VL in polar solvent and solvent-free conditions. In polar solvent (including solvent-free), the imidate mechanism of enchainment has been shown to be favored.[7,10,13] This mechanism is characterized by proton transfer from urea to MTBD, forming a highly active urea anion (imidate).[9] In the bisurea system, the incipient anion would be stabilized via intramolecular hydrogen bonding by the 'extra' urea moiety; hence, an *activated-(thio)urea anion mechanism* analogous to the neutral *activated (thio)urea* H-bonding mechanism can be envisaged, Figure 3.3.[14] This mechanism is corroborated by the observation that the five-methylene tether in the **2-O5**/MTBD cocatalyzed ROP of VL produces the most active ROP, just as in the H-bonded system. Reproducing an established experiment,[13] when **2-O5** is treated with 1 equivalent of MTBD in acetone-d_6, an upfield chemical shift is observed, consistent with anion formation and an imidate mechanism (Figure 3.4). The individual urea moieties are indistinguishable, which suggests that the anion/neutral urea exchange is rapid on the NMR timescale (400 MHz). Treatment with an additional equivalent of MTBD (0.096 M MTBD, 0.048 M **2-O5**) does not further shift the bisurea resonances, which suggest that bisimidate is not formed and corroborates previous observations of bis-(thio)ureas operating as a single H-bond donating species. Further, the rate of the **2-O5**/MTBD (0.048 M **2-O5**; 0.096 M MTBD) cocatalyzed ROP of VL under the respective conditions are identical (Figure 3.5), suggesting that the ideal stoichiometry for bisurea/base mediated ROP in an imidate

mechanism is 1:1. Similar relative rates (for the bisureas) are observed under solvent free conditions (Table 3.2) as in acetone-d_6.

Two bisurea H-bond donors featuring heteroatom-containing tethers were synthesized and indicate a sensitive relationship between cocatalyst geometry and reaction rate. Both of the **2-O5-N** or **2-O5-O** (Figure 3.1) plus MTBD cocatalyzed ROP of VL showed slightly reduced reaction times versus the 'parent' **2-O5** under all conditions: benzene-d_6, acetone-d_6 and solvent-free (Table 3.3). The reactions remained well-controlled, especially solvent-free where $M_w/M_n < 1.03$. The relative reaction times in each of C_6D_6, acetone-d_6 and solvent-free fall in the order **2-O5-O** (fastest) < **2-O5-N** < **2-O5** (slowest). We attribute the subtle changes in reaction time to minute changes in the tether length, where the normal both lengths are C-O < C-N < C-C. This suggests that the most active bis-(thio)urea tether length is somewhere between four and five methylene units long, which may be a useful parameter in the design of advanced H-bond donating catalyst systems. However, these relative rates may be coincidence and could be easily attributed to increased conformational flexibility due to the heteroatom, but these results suggest that there is no stark change in mechanism due to the presence of the heteroatom. As opposed to ROP in solution, bisurea plus MTBD cocatalyzed ROP under solvent-free conditions provide the best weight control (by $[M]_o/[I]_o \leq 500$), narrowest distributions ($M_w/M_n \leq 1.05$) and access to the highest molecular weights (Table 3.8), consistent with previous observations;[12] the **2-O5-O** H-bond donor is especially active and well controlled. The ROP of CL with these cocatalysts (plus MTBD) exhibit the same relative reaction times and display good control, Table 3.3.

Additionally, we synthesized a symmetric derivative of bisurea **2-O5** featuring a 3,3-dimethyl substitution, **2-O5-diMe**, which is less active as a cocatalyst (with MTBD) for the ROP of VL (C_6D_6, 90 % conv in 1 hour). This suggests that any steric compression or hindered bond rotation arising from the geminal dimethyl substitution (i.e. Thorpe-Ingold effect)[19] is deleterious to ROP. The bisthiourea analogues of these bisurea H-bond donors were also synthesized, but they displayed reduced rates and control versus the bisureas (see Table 3.9). These modified bis-(thio)urea H-bond donors emphasize the sensitive interplay of catalyst structure towards ROP activity.

ROP of Lactide

The most active bis(thio)urea H-bond donors from the VL studies were applied for the ROP of lactide in CH_2Cl_2 and solvent-free with Me_6TREN cocatalyst.[20] Low solubility of bisureas under reaction conditions limited all direct comparisons, but this and previous studies[12] show that the bisthioureas are more effective than the corresponding bisureas for the ROP of LA (Table 3.4). In the case of lactide, weak alkylamine base cocatalysts are used because stronger imine bases (e.g. MTBD) will polymerize lactide in the absence of H-bond donor in a less-controlled ROP.[5,20,21] We speculated that the increased rate observed for bisthiourea (versus bisurea) plus Me_6TREN mediated ROP of lactide was due to a change in mechanism between the two species. Indeed, the ^{1}H NMR of **2-S5-O** (acetone-d_6) shows an upfield shift for the aromatic resonances in **2-S5-O** in the presence (versus absence) of Me_6TREN, suggesting the formation of an imidate species, whereas the chemical shifts for **2-O5-O** with and without Me_6TREN are negligibly different, suggesting H-bonding (see Figure 3.9). The same experiment

when conducted with **1-S** or TCC shows downfield chemical shifts consistent with H-bonding.[22] Similar to the acetone-d_6 experiment, the ROP results in CH_2Cl_2 (Table 3.4) suggest that the **2-S5-O** plus Me_6TREN mediated ROP of lactide proceeds via an imidate mechanism while **2-O5-O** is an H-bond mediated enchainment.

For identically substituted ureas and thioureas in the ROP of LA, the thiourea is the more active catalyst, and this is attributed to the pK_a of the H-bond donor. The difference in mechanism for the two H-bond donating catalysts presumably arises because any thiourea will be more acidic than its identically substituted (e.g. 3,5-bistrifluoromethyl phenyl) urea.[23,24] When a pair of mono-H-bond donors (urea or thiourea) of the same pK_a are used as cocatalysts with Me_6TREN for the ROP of lactide, the urea is the more active catalyst, Table 3.5. Having identical pK_a, such a pair of urea and thiourea will effect enchainment by the same mechanism, and hence, the more polar urea (or imidate) is the more active H-bond donor. When a highly acidic H-bond donor is employed (Table 3.5, last entry), the incipient (thio)imidate displays reduced activity arising from its low basicity, as previously observed.[10,23] These observations are seemingly contrary to the (thio)urea plus strong base mediated ROP of other lactones (e.g. valerolactone or caprolactone).[7,9,11,23] However, in this latter scenario, the stronger base cocatalyst (versus Me_6TREN) can deprotonate either the urea or thiourea.[13] In that event, the urea (or resulting imidate) will always be more active than the thiourea (or thioimidate).[7]

CONCLUSION

A series of conformationally flexible bis(thio)urea H-bond donors were applied with the appropriate base cocatalysts for the ROP of lactones. Conformational flexibility is essential for catalyst activity, and the (thio)urea moieties separated by circa five methylene units displays the most rapid ROP. As a summary of our work here and previously, Table 3.6 collects the catalyst systems of this type which we find to be optimal for a given monomer and solvent. Synthetic polymer chemists should hew towards **2-S5-O** for the ROP of lactide; it is readily soluble, easily accessible and is among the most active organocatalysts for the synthesis of polylactide. That bisthioureas (versus bisureas) are more active for the ROP of LA is contrary to what is observed for VL and CL, and the higher activity of the thioureas is rendered by the alkylamine cocatalyst, which is unable to deprotonate the (bis)urea catalyst and enter the highly active imidate mediated ROP. For VL and CL, the bisurea **2-O5-O** plus MTBD cocatalyst system is the most active bis(thio)urea examined, and the reaction is well controlled, especially under the easily employable solvent-free conditions. We trust that the results of this study will be informative for the synthesis of advanced H-bond donating catalysts for ROP, and such work is ongoing in our lab.

REFERENCES

1. Kamber, N. E. *et al.* Organocatalytic ring-opening polymerization. *Chem. Rev.* **107**, 5813–5840 (2007).

2. Kiesewetter, M. K., Shin, E. J., Hedrick, J. L. & Waymouth, R. M. Organocatalysis: Opportunities and challenges for polymer synthesis. *Macromolecules* **43**, 2093–2107 (2010).

3. Fastnacht, K. V., Datta, P. P. & Kiesewetter, M. K. Bifunctional and Supramolecular Organocatalysts for Polymerization. in *Organic Catalysis for Polymerization* (eds. Dove, A. P., Sardon, H. & Naumann, S.) 87–120 (Royal Society of Chemistry, 2019).

4. Bas G. G. Lohmeijer Frank Leibfarth, John W. Logan, R. C. P. *et al.* Guanidine and Amidine Organocatalysts for Ring-Opening Polymerization of Cyclic Esters. *Macromolecules* **39**, 8574–8583 (2006).

5. Pratt, R. C. *et al.* Exploration, optimization, and application of supramolecular thiourea-amine catalysts for the synthesis of lactide (co)polymers. *Macromolecules* **39**, 7863–7871 (2006).

6. Fastnacht, K. V. *et al.* Bis- and Tris-Urea H-Bond Donors for Ring-Opening Polymerization: Unprecedented Activity and Control from an Organocatalyst. *ACS Macro Lett.* **5**, 982–986 (2016).

7. Lin, B. & Waymouth, R. M. Urea anions: Simple, fast, and selective catalysts for ring-opening polymerizations. *J. Am. Chem. Soc.* **139**, 1645–1652 (2017).

8. Zhang, X., Jones, G. O., Hedrick, J. L. & Waymouth, R. M. Fast and selective ring-opening polymerizations by alkoxides and thioureas. *Nat. Chem.* **8**, 1047–1053 (2016).

9. Dharmaratne, N. U., Pothupitiya, J. U. & Kiesewetter, M. K. The mechanistic duality of (thio)urea organocatalysts for ring-opening polymerization. *Org. Biomol. Chem.* **17**, 3305–3313 (2019).

10. Pothupitiya, J. U., Hewawasam, R. S. & Kiesewetter, M. K. Urea and Thiourea H-Bond Donating Catalysts for Ring-Opening Polymerization: Mechanistic Insights via (Non)linear Free Energy Relationships. *Macromolecules* **51**, 3203–3211 (2018).

11. Coderre, D. N., Fastnacht, K. V., Wright, T. J., Dharmaratne, N. U. & Kiesewetter, M. K. H-Bonding Organocatalysts for Ring-Opening Polymerization at Elevated Temperatures. *Macromolecules* **51**, 10121–10126 (2018).

12. Pothupitiya, J. U. *et al.* H-Bonding Organocatalysts for the Living, Solvent-Free Ring-Opening Polymerization of Lactones: Toward an All-Lactones, All-Conditions Approach. *Macromolecules* **50**, 8948–8954 (2017).

13. Dharmaratne, N. U., Pothupitiya, J. U., Bannin, T. J., Kazakov, O. I. & Kiesewetter, M. K. Triclocarban: Commercial Antibacterial and Highly Effective H-Bond Donating Catalyst for Ring-Opening Polymerization. *ACS Macro Lett.* **6**, 421–

425 (2017).

14. Spink, S. S., Kazakov, O. I., Kiesewetter, E. T. & Kiesewetter, M. K. Rate Accelerated Organocatalytic Ring-Opening Polymerization of l-Lactide via the Application of a Bis(thiourea) H-bond Donating Cocatalyst. *Macromolecules* **48**, 6127–6131 (2015).

15. Xu, S. *et al.* Internal Lewis pair enhanced H-bond donor: boronate-urea and tertiary amine co-catalysis in ring-opening polymerization. *Polym. Chem.* **7**, 6843–6853 (2016).

16. Du, F. *et al.* Solvent-free ring-opening polymerization of lactones with hydrogen-bonding bisurea catalyst. *J. Polym. Sci. Part A Polym. Chem.* **57**, 90–100 (2019).

17. Lohmeijer, B. G. G. *et al.* Guanidine and amidine organocatalysts for ring-opening polymerization of cyclic esters. *Macromolecules* **39**, 8574–8583 (2006).

18. Bertucci, M. A., Lee, S. J. & Gagné, M. R. Selective transamidation of 3-oxo-N-acyl homoserine lactones by hydrazine derivatives. *Org. Biomol. Chem.* **12**, 7197–7200 (2014).

19. Ansyln, E. V. & Dougherty, D. A. Catalysis. in *Modern Physical Organic Chemistry* 490–530 (2006).

20. Kazakov, O. I. I. & Kiesewetter, M. K. K. Cocatalyst Binding Effects in

Organocatalytic Ring-Opening Polymerization of l -Lactide. *Macromolecules* **48**, 6121–6126 (2015).

21. Coady, D. J. *et al.* Catalyst Chelation Effects in Organocatalyzed Ring-Opening Polymerization of Lactide. *ACS Macro Lett.* **1**, 19–22 (2012).

22. Kazakov, O. I., Datta, P. P., Isajani, M., Kiesewetter, E. T. & Kiesewetter, M. K. Cooperative Hydrogen-Bond Pairing in Organocatalytic Ring- Opening Polymerization. (2014).

23. Lin, B. & Waymouth, R. M. Organic Ring-Opening Polymerization Catalysts: Reactivity Control by Balancing Acidity. *Macromolecules* **51**, 2932–2938 (2018).

24. Jakab, G., Tancon, C., Zhang, Z., Lippert, K. M. & Schreiner, P. R. (Thio)urea organocatalyst equilibrium acidities in DMSO. *Org. Lett.* **14**, 1724–1727 (2012).

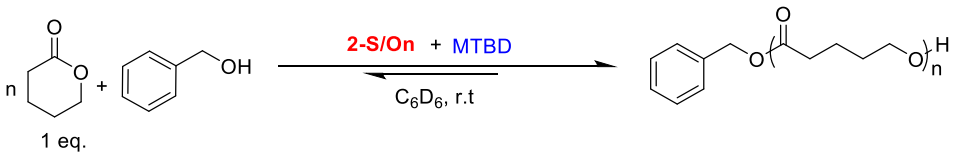

H-bond donor (**2-Xn**)	time (min)	conv.[b] (%)	M_n[c] (g/mol)	M_w/M_n[c]
2-S2	92	88	8 300	1.06
2-S3	80	89	9 000	1.06
2-S4	53	90	8 200	1.06
2-S5	50	91	9 500	1.05
2-S6	69	89	9 200	1.04
2-S12	250	87	8 200	1.04
2-O3	20	89	8 900	1.07
2-O4	20	92	9 600	1.06
2-O5	12	89	9 500	1.05
2-O6	15	90	9 900	1.06
2-O12	35	90	9 900	1.07

Table 3.1. Bis(thio)Urea and MTBD cocatalyzed ROP of VL in C_6D_6.[a]

a. Reaction conditions: VL (1.0 mmol, 1 equiv, 2 M), benzyl alcohol (0.019 mmol), bis(thio)urea/MTBD (0.024 mmol each) in C_6D_6. b. Monomer conversion was monitored via ^{1}H NMR. c. M_n and M_w/M_n were determined by GPC (CH_2Cl_2) versus polystyrene standards.

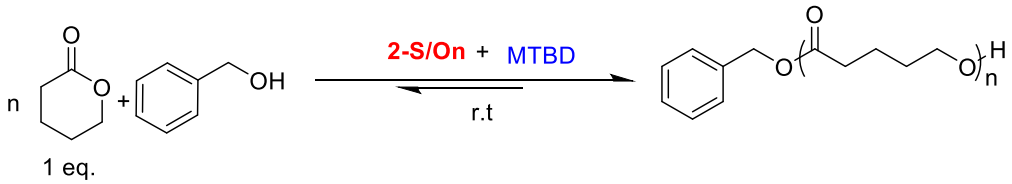

solvent	H-bond donor (**2-Xn**)	time (min)	conv.[a] (%)	M_n[b] (g/mol)	M_w/M_n[b]
acetone-d_6[c]	**2-S5**	180	90	8 900	1.08
	2-O5	12	84	8 200	1.05
	2-O12	40	84	8 200	1.10
solvent-free[d]	**2-O3**	20	99	42 300	1.05
	2-O4	22	99	49 600	1.04
	2-O5	12	99	42 300	1.03
	2-O6	19	99	39 400	1.02
	2-O12	29	99	39 200	1.02

Table 3.2. Bis(thio)urea plus MTBD cocatalyzed ROP of VL in acetone-d_6 and solvent-free conditions.

a) Monomer conversion was monitored via ^{1}H NMR. b) M_n and M_w/M_n were determined by GPC (CH_2Cl_2) versus polystyrene standards c) Reaction conditions: VL (1.0 mmol, 1 equiv, 2 M), benzyl alcohol (0.019 mmol), bis(thio)urea/MTBD (0.024 mmol each) inacetone-d_6. b) Reaction conditions: VL (3.99 mmol, 1 equiv), benzyl alcohol (0.019 mmol), cocatalyst (0.019 mmol each).

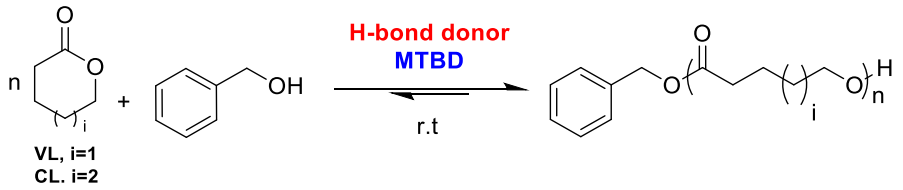

VL or CL	Solvent	H-bond donor (**2-O5-N/O**)	Time (min)	conv.[a] (%)	M_n[b](g/mol)	M_w/M_n[b]
VL	benzene-d_6[c]	**2-O5-N**	10	88	8 000	1.05
		2-O5-O	5	90	8 000	1.06
	acetone-d_6[c]	**2-O5-N**	8	86	7 800	1.10
		2-O5-O	5	86	7 700	1.11
	solvent-free	**2-O5-N**[d]	5	91	37 500	1.02
		2-O5-O[e]	4	99	110 500	1.03
CL	solvent-free[d]	**2-O5**	30	99	50 500	1.14
		2-O5-N	18	99	51 100	1.20
		2-O5-O	8	99	47 000	1.13

Table 3.3. ROP of VL or CL cocatalyzed by MTBD plus bis-ureas with heteroatom-containing tethers

a) Monomer conversion was monitored via ^{1}H NMR. b) M_n and M_w/M_n were determined by GPC (CH_2Cl_2) versus polystyrene standards. c) Reaction conditions: VL (1.0 mmol, 1 equiv, 2 M), benzyl alcohol (0.019 mmol), cocatalyst (0.024 mmol each) in C_6D_6 or acetone-d_6. d) Solvent-free reaction conditions: VL or CL (3.99 mmol, 1 equiv), benzyl alcohol (0.019 mmol), cocatalyst (0.019 mmol each). e) Solvent-free reaction conditions: VL (3.99 mmol, 1 equiv), benzyl alcohol (0.008 mmol), cocatalyst (0.019 mmol each).

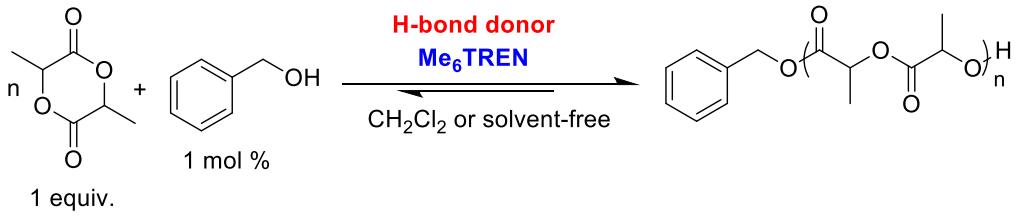

solvent	H-bond donor (**2-X5-N/O**)	Time (min)	conv.[a](%)	M_n[b] (g/mol)	M_w/M_n[b]
CH_2Cl_2 [c]	**2-S5**	12	90	17 400	1.05
	2-S5-N	20	90	17 600	1.04
	2-S5-O	5	90	18 800	1.04
solvent-free [d]	**2-O5-O**	105	90	15 800	1.13
	2-S5-O	15	90	18 500	1.06

Table 3.4. Bis(thio)Urea and Me_6TREN cocatalyzed ROP of L-LA

a) Monomer conversion was monitored via ^{1}H NMR. b) M_n and M_w/M_n were determined by GPC (CH_2Cl_2) versus polystyrene standards. c) Reaction conditions: L-LA (0.693 mmol, 1 equiv, 1 M), benzyl alcohol (0.0069 mmol,), cocatalyst (0.017 mmol each) in CH_2Cl_2. d) Solvent-free reaction conditions: L-LA (1.38 mmol, 1 equiv), benzyl alcohol (0.0138 mmol), cocatalyst (0.007 mmol each) at 100 °C

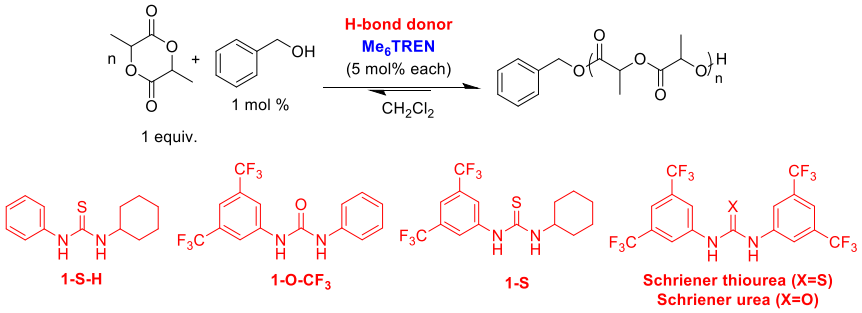

H-bond donor	pK_a[b]	Time (min)	conv.[c] (%)	M_n[d] (g/mol)	M_w/M_n[d]
1	16.8	1440	-	-	-
2	16.1	35	90	17900	1.04
1-S	13.2	48	90	18900	1.07
3	13.8	1	92	19300	1.07
4	8.5	600	90	18100	1.04

Table 3.5. Mono(thio)Urea and Me_6TREN cocatalyzed ROP of L-LA.[a]

a) Reaction conditions: L-LA (0.50 mmol, 1 equiv, 1 M), benzyl alcohol (0.005 mmol,), cocatalyst (0.025 mmol each) in CH_2Cl_2. b) pK_a values in DMSO[23] c) Monomer conversion was monitored via ^1H NMR. d) M_n and M_w/M_n were determined by GPC (CH_2Cl_2) versus polystyrene standards.

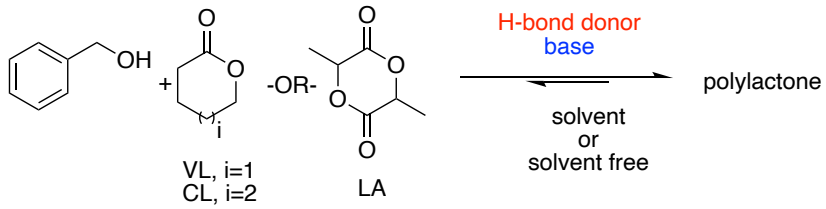

Monomer	Solvent	cocatalyst	Proposed mechanism	refs
VL	C_6D_6 [a]	Trisurea/MTBD (16 µmol each)	Neutral H-bonding	6
	acetone-d_6 [a]	2-O5-O/MTBD (24 µmol each)	Imidate mediated	herein
	solvent-free[b]	2-O5-O/MTBD (19 µmol each)	Imidate mediated	herein
CL	C_6D_6 [a]	Trisurea/MTBD (16 µmol each)	Neutral H-bonding	6
	solvent-free[b]	2-O5-O/MTBD (19 µmol each)	Imidate mediated	herein
LA	CH_2Cl_2[c]	2-S5-O /ME_6TREN (17 µmol each)	Imidate mediated	herein
	solvent-free[b]	2-S5-O/ ME_6TREN (7 µmol each)	Imidate mediated	herein

Table 3.6. Optimal (Thio)urea H-Bond Donor Plus Organic Base Cocatalysts for ROP

a) Reaction conditions: Monomer (1.0 mmol, 1 eq. 2 M), benzyl alcohol (0.019 mmol), cocatalyst in C_6D_6 or in acetone-d_6. b) Solvent-free reaction conditions: VL or CL (3.99 mmol, 1 equiv), benzyl alcohol (0.019 mmol), cocatalyst (0.019 mmol each) c) Reaction conditions: LA (0.693 mmol, 1 equiv, 1 M), benzyl alcohol (0.0069 mmol), cocatalyst (0.017 mmol each) in CH_2Cl_2. d) Solvent-free reaction conditions: L-LA (1.38 mmol, 1 equiv), benzyl alcohol (0.0138 mmol), cocatalyst (0.007 mmol each) at 100 °

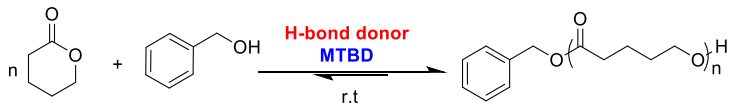

Entry	Solvent	$[M]_o/[I]_o$	M_n[b] (g/mol)	M_w/M_n[b]
		2-O5		
1	benzene	50	9500	1.05
2		100	19600	1.05
3		200	30900	1.07
4	acetone	50	9100	1.05
5		100	12000	1.05
6		200	16900	1.15
7	solvent-free[c]	50	10500	1.10
8		100	21500	1.07
9		200	42300	1.03
10		500	96200	1.16
		2-O5-O		
11	benzene	50	8000	1.06
12		100	20000	1.07
13		200	38700	1.10
14	acetone	50	7700	1.10
15		100	19700	1.04
16		200	35700	1.03
17	solvent-free[c]	50	10500	1.10
18		100	23600	1.10
19		200	43500	1.02
20		500	110500	1.03

Table 3.7. Bis(thio)urea plus MTBD cocatalyzed ROP of VL.[a]

a) Reaction conditions: VL (1.0 mmol, 1 equiv, 2 M), cocatalyst (0.024 mmol each) b) M_n and M_w/M_n were determined by GPC (CH_2Cl_2) versus polystyrene standards. c) Reaction conditions: VL (3.99 mmol) cocatalyst (0.019 mmol each).

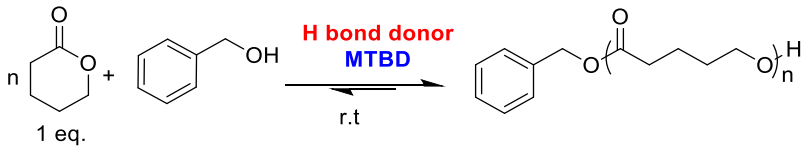

Entry	Solvent	H bond donor (**2-Xn**)	Time (min)	Conv.[a] (%)	M_n[b] (g/mol)	M_w/M_n[b]
1	acetone-d_6[c]	**2-S2**	635	88	9500	1.08
2		**2-S3**	685	85	8700	1.11
3		**2-S4**	644	89	9100	1.10
4		**2-S6**	636	88	8900	1.09
5		**2-S12**	1090	87	6800	1.10
6		**2-O3**	20	84	7200	1.07
7		**2-O4**	20	85	7600	1.09
8		**2-O6**	20	86	7900	1.10
9	solvent-free[d]	**2-S2**	240	99	35400	1.09
10		**2-S3**	210	99	40600	1.10
11		**2-S4**	150	99	41900	1.08
12		**2-S5**	60	99	45500	1.06
13		**2-S6**	120	99	42100	1.13
14		**2-S12**	330	99	39700	1.15

Table 3.8. Different tethered bis(thio)urea and MTBD cocatalyzed ROP of VL.

a) Monomer conversion was monitored via ^{1}H NMR. b) M_n and M_w/M_n were determined by GPC (CH_2Cl_2) versus polystyrene standards. c) Reaction conditions: VL (1.0 mmol, 1 equiv, 2 M), benzyl alcohol (0.019 mmol,), cocatalyst (0.024 mmol each) in acetone-d_6. d) Solvent free-reaction conditions: VL (3.99 mmol, 1 equiv), benzyl alcohol (0.019 mmol), cocatalyst (0.019 mmol each).

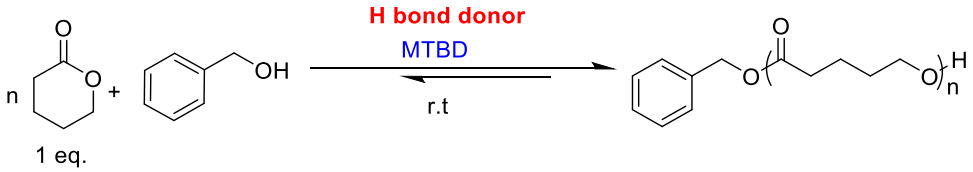

Solvent	H-bond donor (**2-S5-N/O**)	Time (min)	conv. [a] (%)	M_n[b] (g/mol)	M_w/M_n[b]
benzene-d_6 [c]	**2-S5-N**	100	89	8 600	1.05
	2-S5-O	50	90	10 600	1.03
acetone-d_6 [c]	**2-S5-N**	240	84	7 700	1.07
	2-S5-O	210	83	10 500	1.04
solvent-free[d]	**2-S5-N**	90	97	42 600	1.06
	2-S5-O	60	99	43 600	1.06

Table 3.9. ROP of VL cocatalyzed by MTBD plus Bisthioureas with Heteroatom-containing Tethers

a) Monomer conversion was monitored via ^{1}H NMR. e) M_n and M_w/M_n were determined by GPC (CH_2Cl_2) versus polystyrene standards. c) Reaction conditions: VL (1.0 mmol, 1 equiv, 2 M), benzyl alcohol (0.019 mmol), cocatalyst (0.024 mmol each) in C_6D_6 or acetone-d_6, d) Solvent free-reaction conditions: VL (3.99 mmol, 1 equiv), benzyl alcohol (0.019 mmol), cocatalyst (0.019 mmol each).

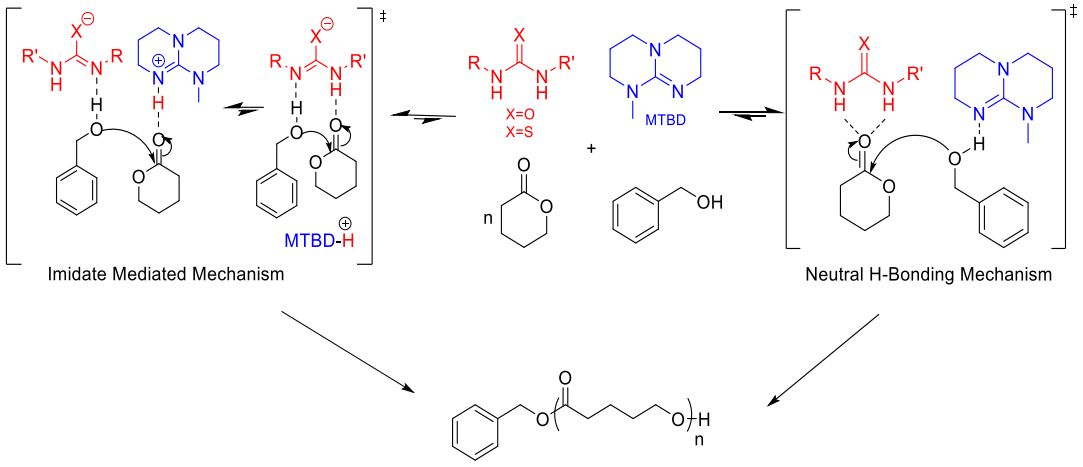

Scheme 3.1. Neutral H-bond versus imidate mediated ROP of VL.

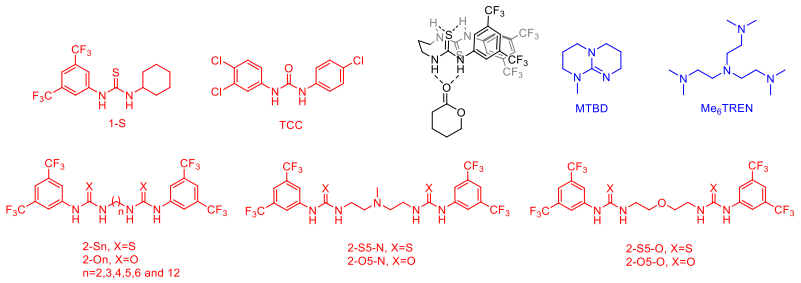

Figure 3.1**.** Mono(thio)urea, bis(thio)urea donors evaluated for the 1-X/2-X plus MTBD and Me_6TREN mediated ROP of VL, CL, L-LA and proposed *activated-thiourea* mode activation for bis-donors.

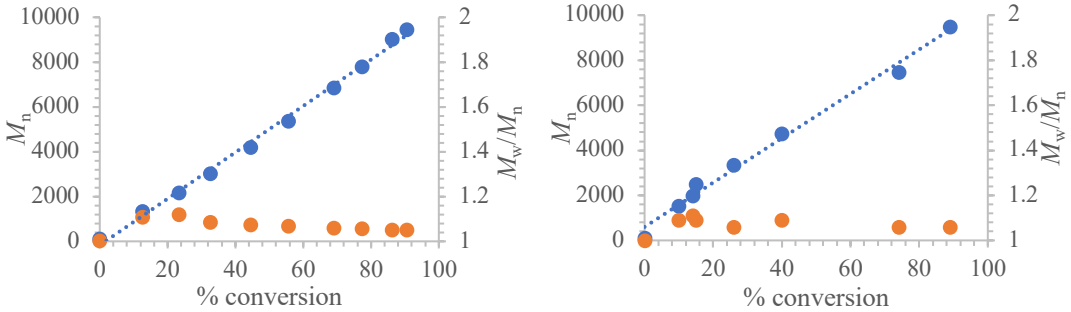

Figure 3.2**.** M_n and M_w/M_n versus conversion for the H-bond donor plus MTBD cocatalyzed ROP of VL using (left) **2-S5**and (right) **2-O5**. Reaction conditions: VL (1.0 mmol, 1 equiv, 2 M), benzyl alcohol (0.019 mmol), **2-X5**/MTBD (0.024 mmol each) in C_6D_6.

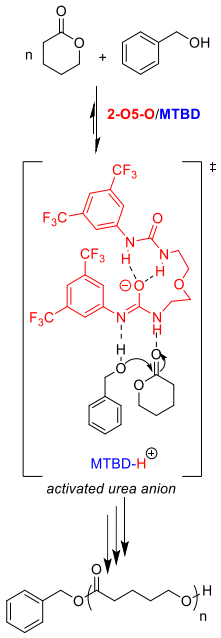

Figure 3.3. Proposed activated (thio)urea anion mechanism for the bisurea plus MTBD mediated ROP of VL.

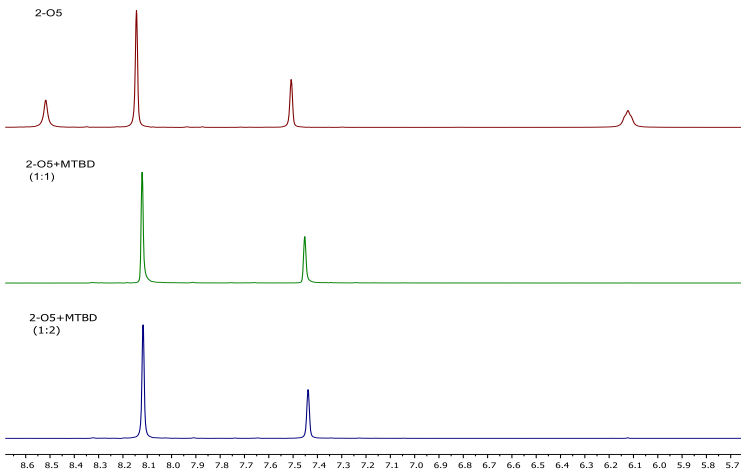

Figure 3.4. Downfield portion of ^{1}H NMR spectra (400 MHz, ppm) of **2-O5** plus MTBD in acetone-d_6.

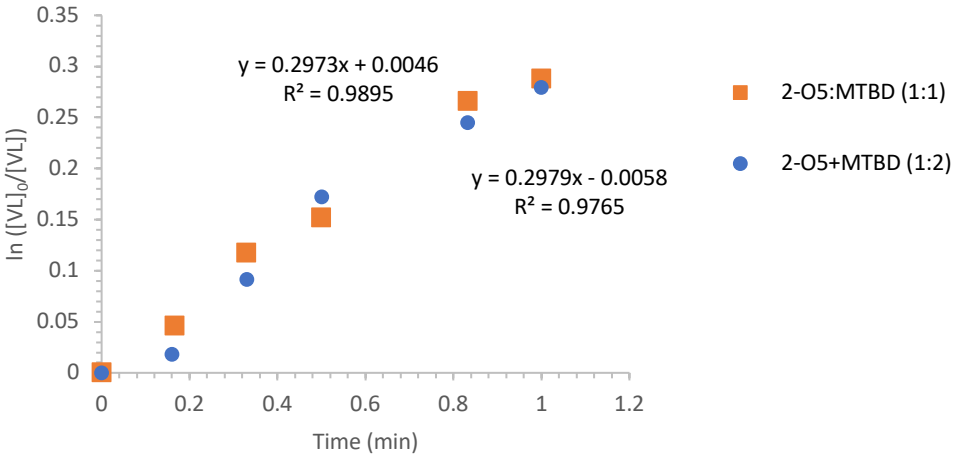

Figure 3.5. First order evolution of VL versus time for the **2-O5**/MTBD catalyzed ring-opening polymerization of VL. Conditions: VL (2 M, 1 mmol), benzyl alcohol (2 mol%, 0.019 mmol), 2-O5 (0.024 mmol), MTBD orange - 0.024 mmol, blue- 0.048 mmol) in acetone-d_6.

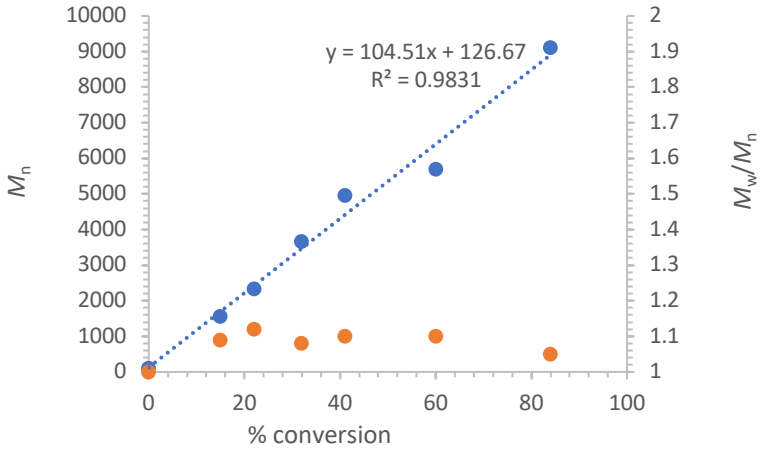

Figure 3.6 M_n and M_w/M_n versus conversion for **2-O5** catalyst. Reaction conditions: VL (1.0 mmol, 1 equiv, 2 M), benzyl alcohol (0.019 mmol), cocatalyst (0.024 mmol each) in acetone-d_6.

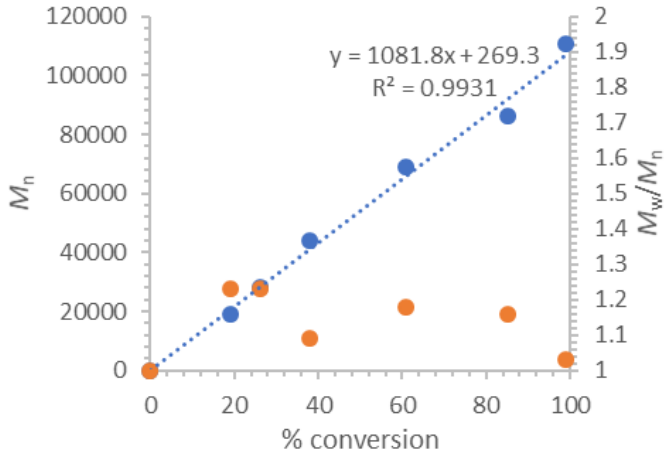

Figure 3.7. M_n and M_w/M_n versus conversion for **2-O5-O** catalyst. Reaction conditions: VL (3.99 mmol, 1 equiv), benzyl alcohol (0.008 mmol), cocatalyst (0.024 mmol each) under solvent free conditions.

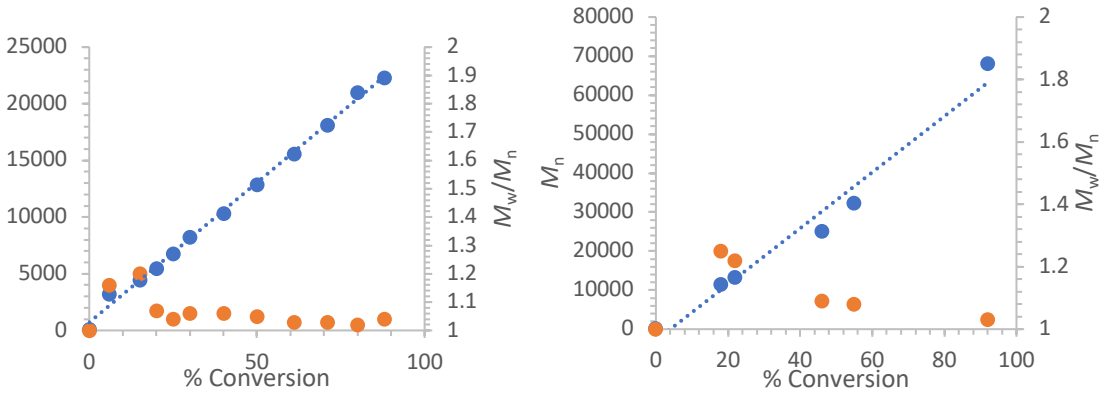

Figure 3.8. (left) M_n and M_w/M_n versus conversion for **2-S5**, (right) M_n versus conversion for **2-O5** catalyst. Reaction conditions: VL (3.99 mmol, 1 equiv.), benzyl alcohol (0.019 mmol,), cocatalyst (0.019 mmol each) under solvent free conditions.

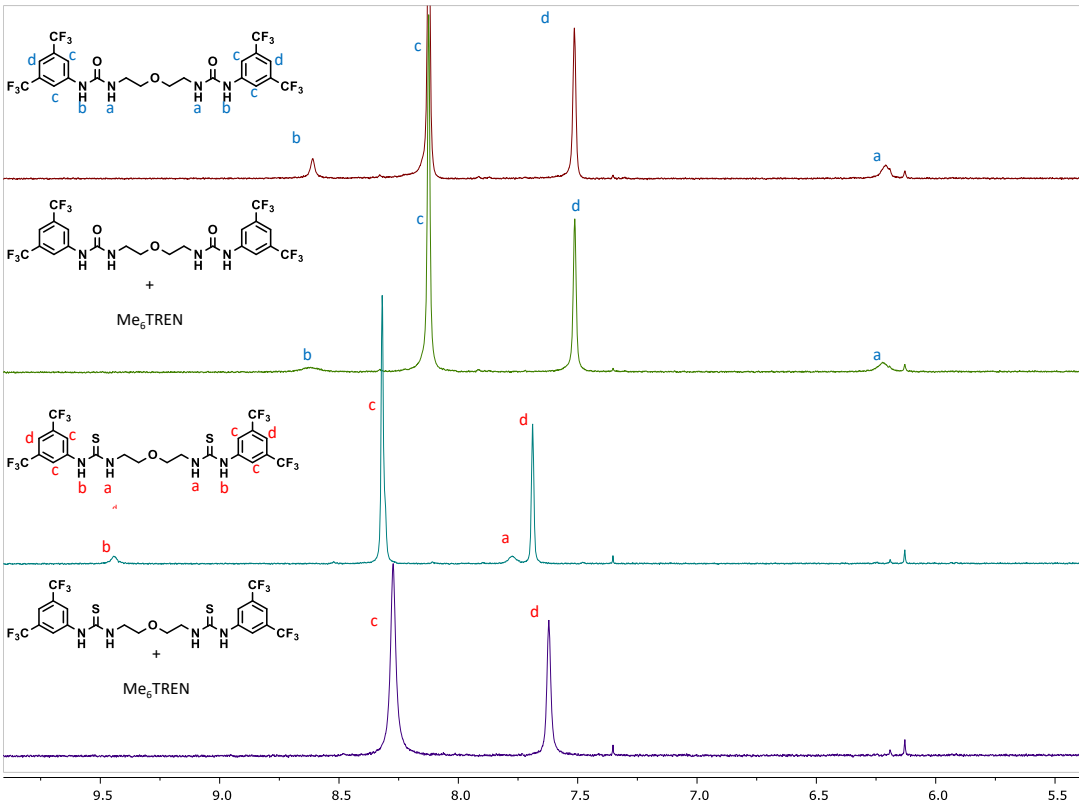

Figure 3.9. Downfield portion of ^{1} H NMR spectra (400 MHz, ppm) of **2-O5-O** and **2-S5-O** with and without Me_6TREN in acetone- d_6.

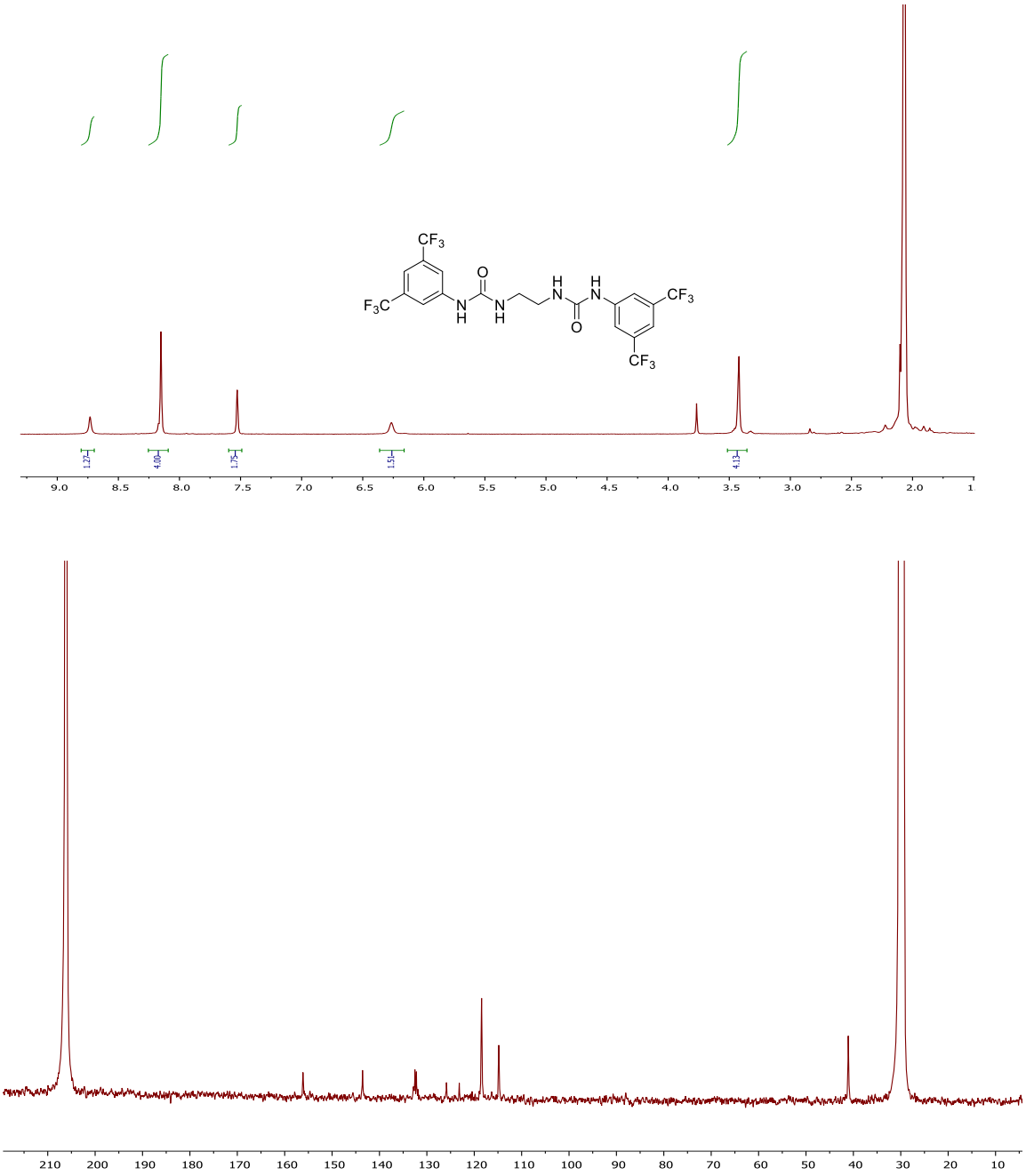

Figure 3.10. (Upper) ^{1}H NMR (acetone-d_6, 400 MHz, ppm) spectrum of 1,1'-(ethane-1,2-diyl)bis(3-(3,5-bis(trifluoromethyl)phenyl)urea) **(2-O2)**, (Lower) ^{13}C NMR (acetone-d_6, 100 MHz, ppm) spectrum of 1,1'-(ethane-1,2-diyl)bis(3-(3,5-bis(trifluoromethyl)phenyl)urea).

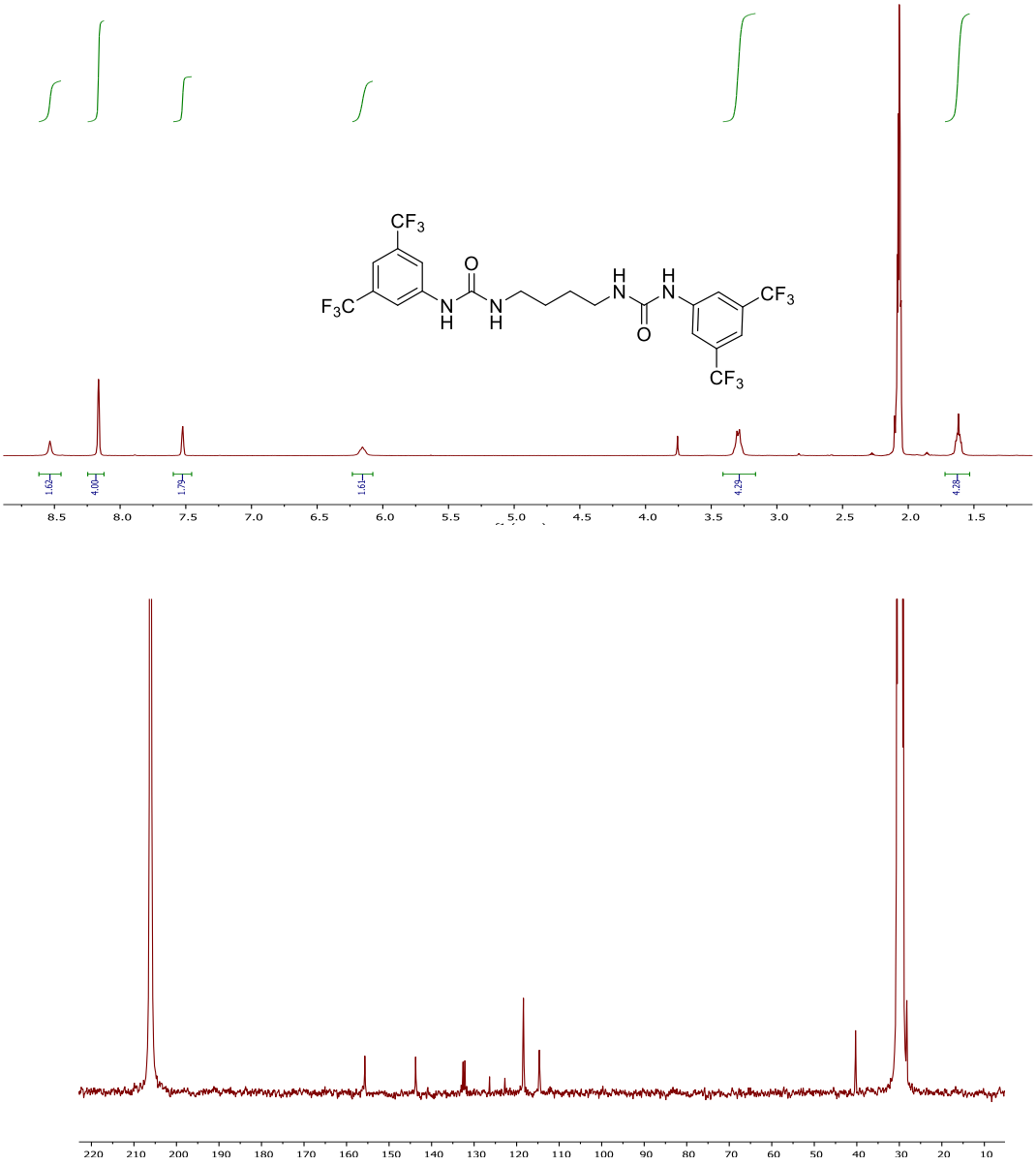

Figure 3.11. (Upper) ^{1}H NMR (acetone-*d6*, 400 MHz, ppm) spectrum of 1,1'-(butane-1,4-diyl)bis(3-(3,5- bis(trifluoromethyl)phenyl)urea) **(2-O4)**, (Lower) ^{13}C NMR (acetone-*d6*, 100 MHz, ppm) spectrum of 1,1'- (butane-1,4-diyl)bis(3-(3,5-bis(trifluoromethyl)phenyl)urea).

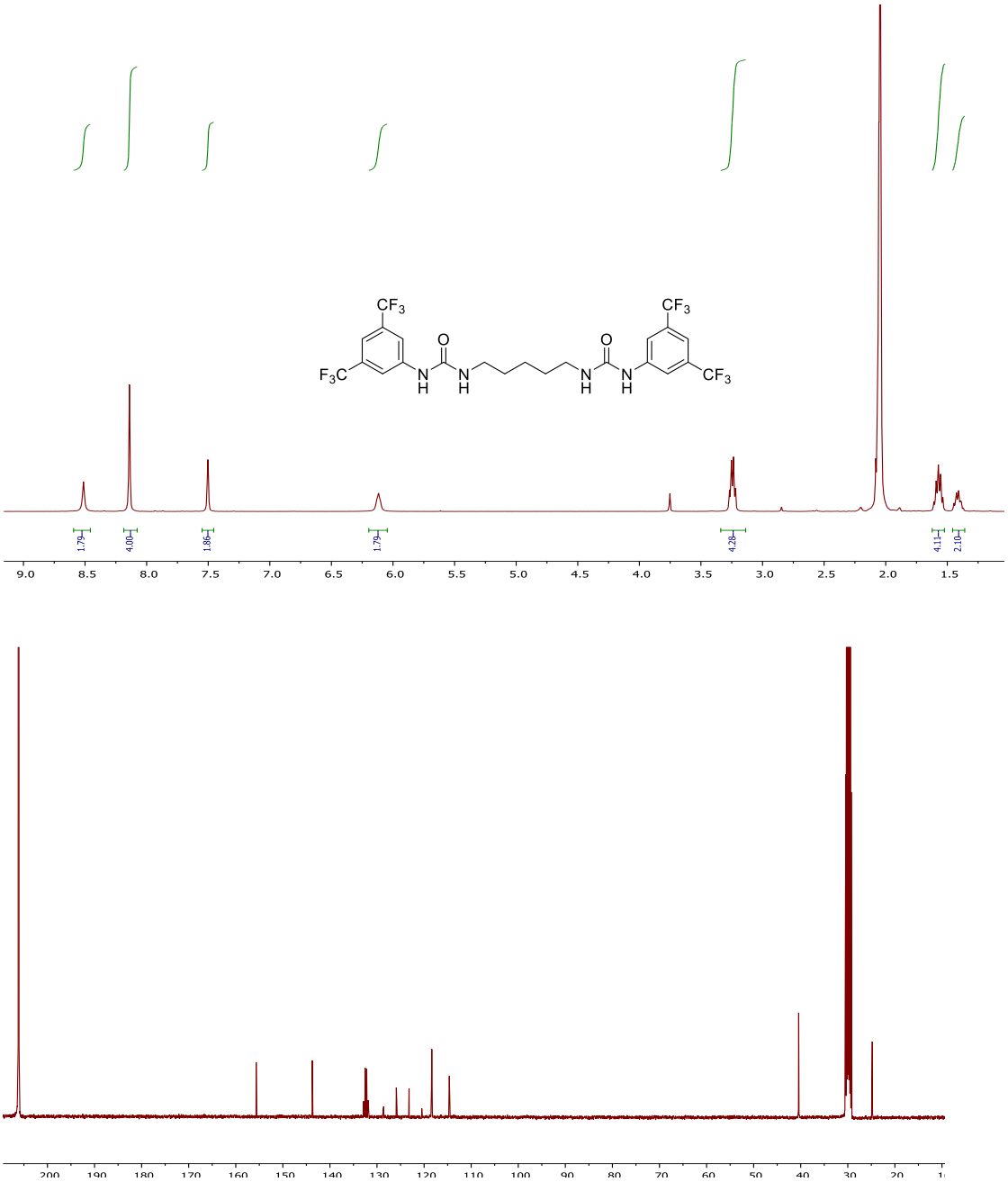

Figure 3.12. (Upper) ^{1}H NMR (acetone-*d6*, 400 MHz, ppm) spectrum of 1,1'-(pentane-1,5-diyl)bis(3-(3,5- bis(trifluoromethyl)phenyl)urea)**(2-O5)**, (Lower) ^{13}C NMR (acetone-*d6*, 100 MHz, ppm) spectrum of 1,1'- (pentane-1,5-diyl)bis(3-(3,5-bis(trifluoromethyl)phenyl)urea).

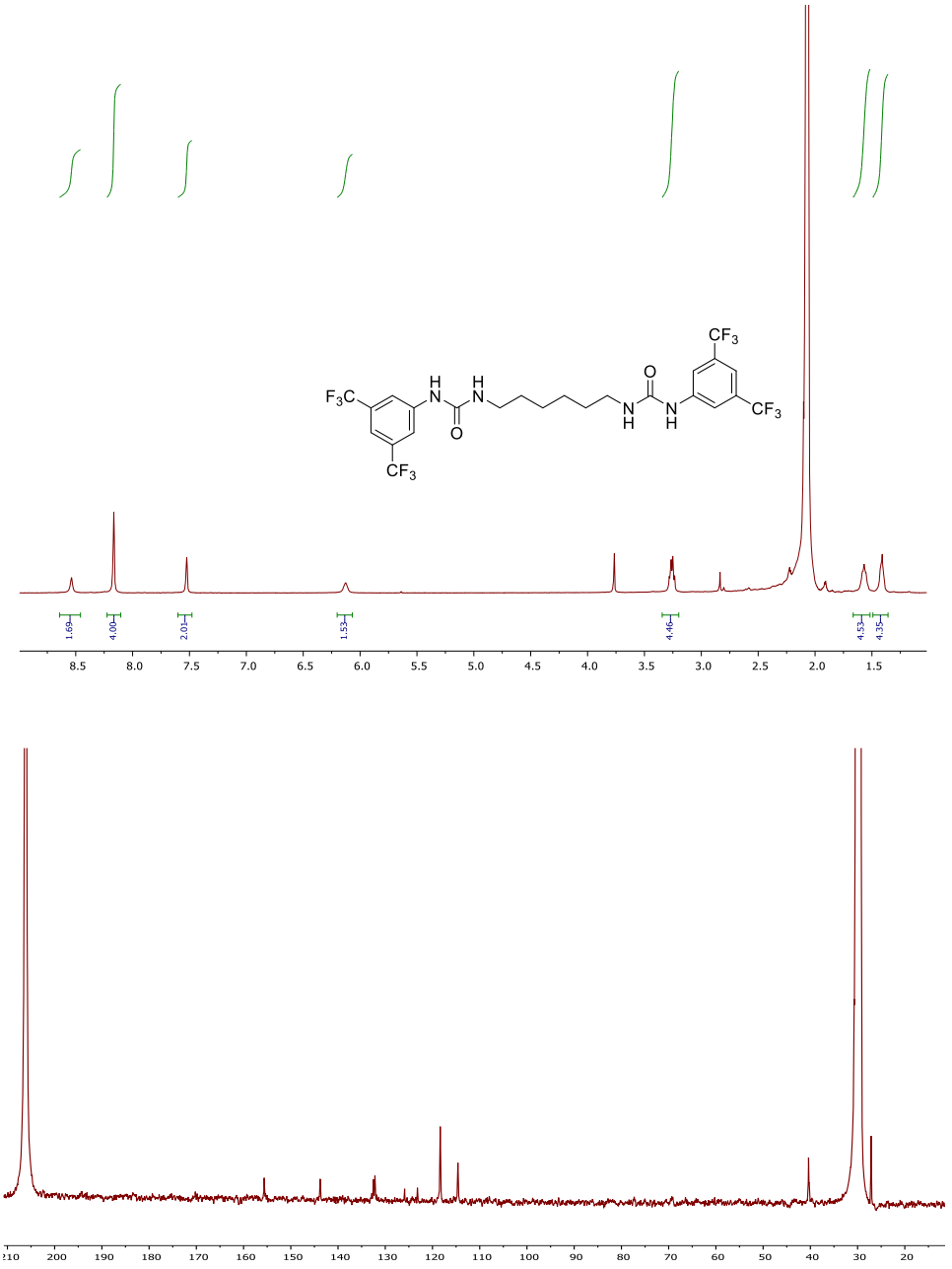

Figure 3.13. (Upper) ^{1}H NMR (acetone-d_6, 400 MHz, ppm) spectrum of 1,1'-(hexane-1,6-diyl)bis(3-(3,5- bis(trifluoromethyl)phenyl)urea) **(2-O6)**, (Lower) ^{13}C NMR (acetone-d_6, 100 MHz, ppm) spectrum of 1,1'- (hexane-1,6-diyl)bis(3-(3,5-bis(trifluoromethyl)phenyl)urea).

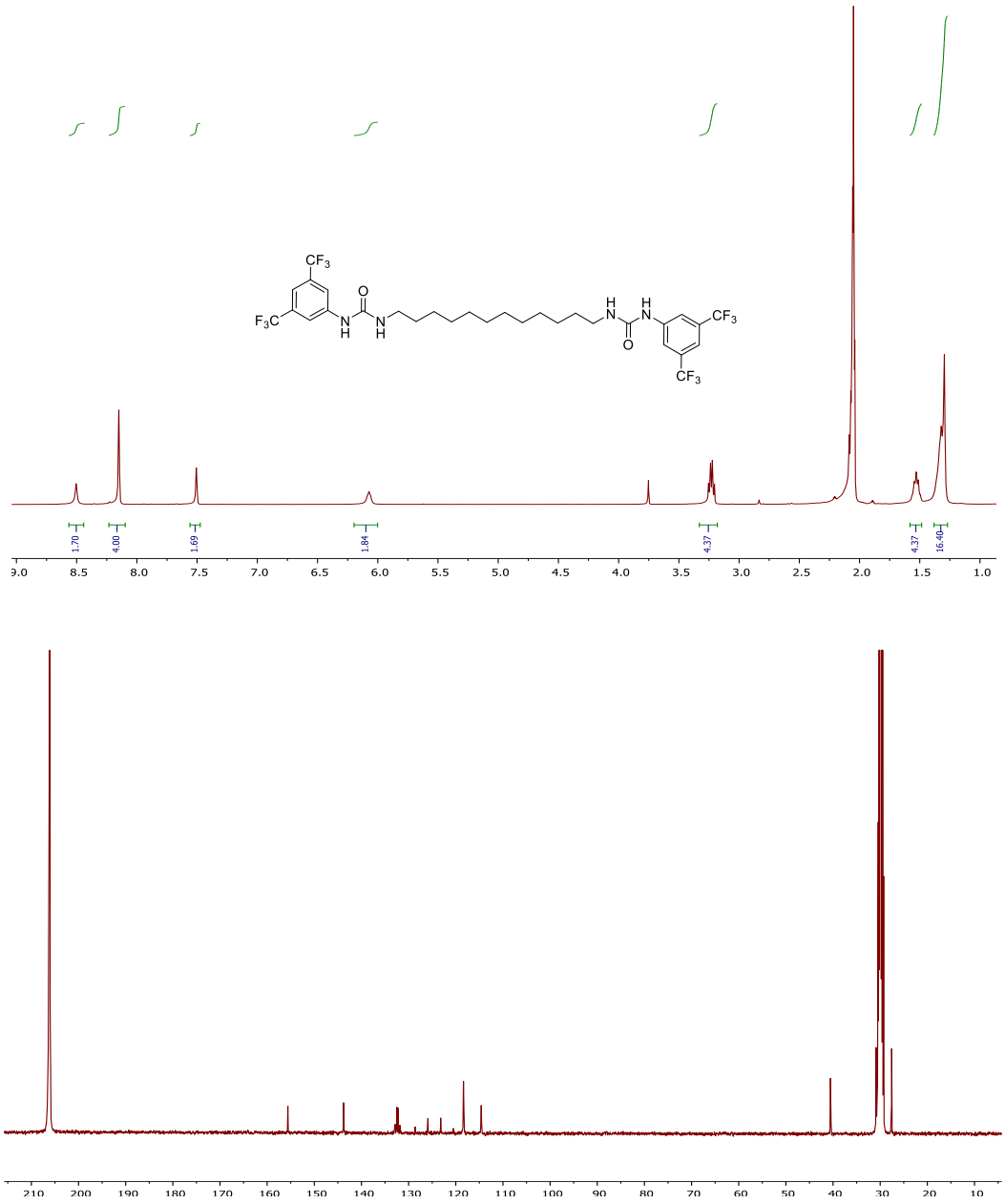

Figure 3.14. (Upper) ^{1}H NMR (acetone-*d6*, 400 MHz, ppm) spectrum of 1,1'-(dodecane-1,12-diyl)bis(3-(3,5- bis(trifluoromethyl)phenyl)urea) **(2-O12)**, (Lower) ^{13}C NMR (acetone-*d6*, 100 MHz, ppm) spectrum of 1,1'- (dodecane-1,12-diyl)bis(3-(3,5-bis(trifluoromethyl)phenyl)urea).

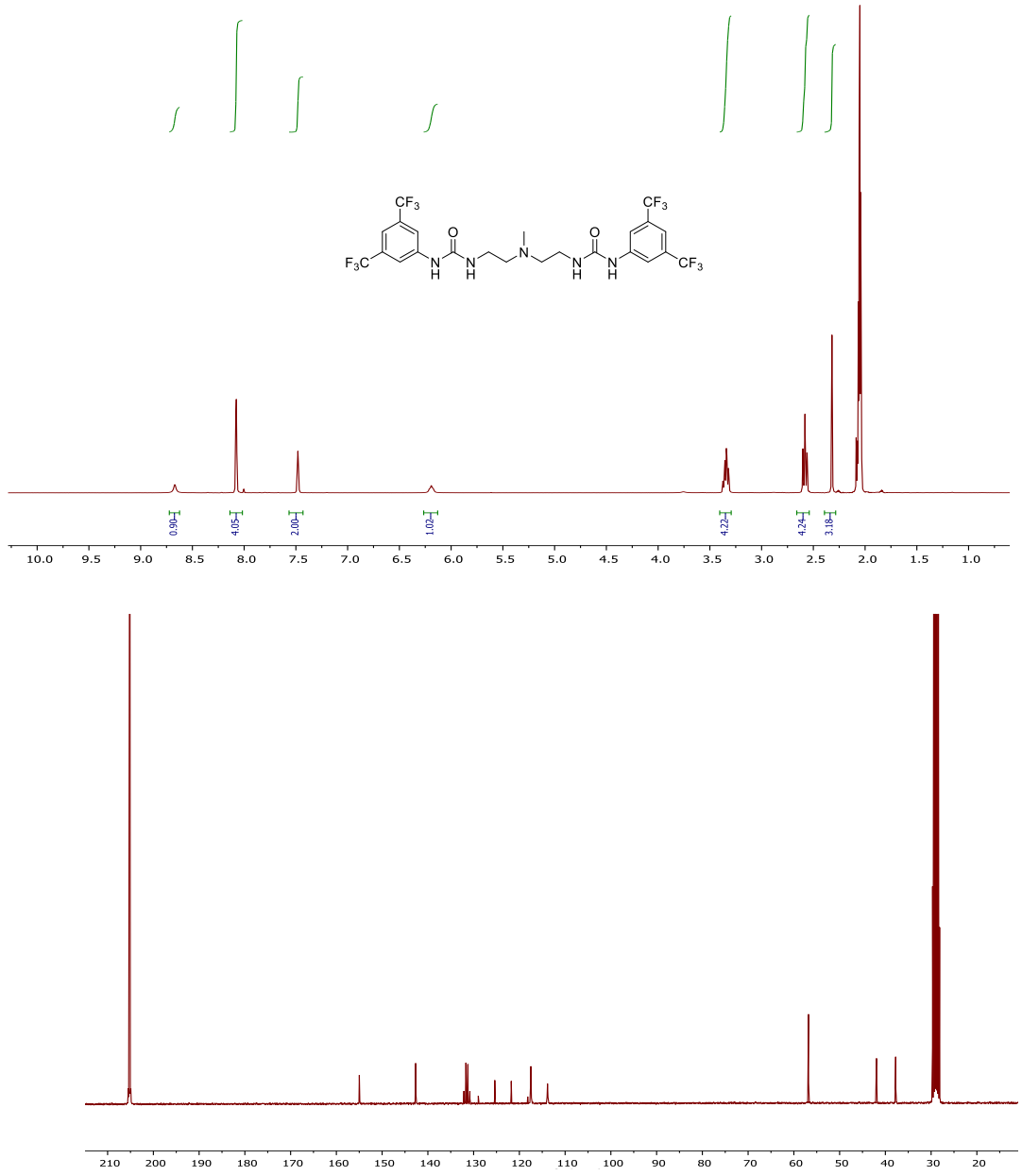

Figure 3.15. (Upper) ^{1}H NMR (acetone-d_6, 400 MHz, ppm) spectrum of 1,1'-((methylazanediyl)bis(ethane-2,1-diyl))bis(3-(3,5-bis(trifluoromethyl)phenyl)urea) **(2-O5-N)**, (Lower) ^{13}C NMR (acetone-d_6, 100 MHz, ppm) spectrum of 1,1'-((methylazanediyl)bis(ethane-2,1-diyl))bis(3-(3,5-bis(trifluoromethyl)phenyl)urea).

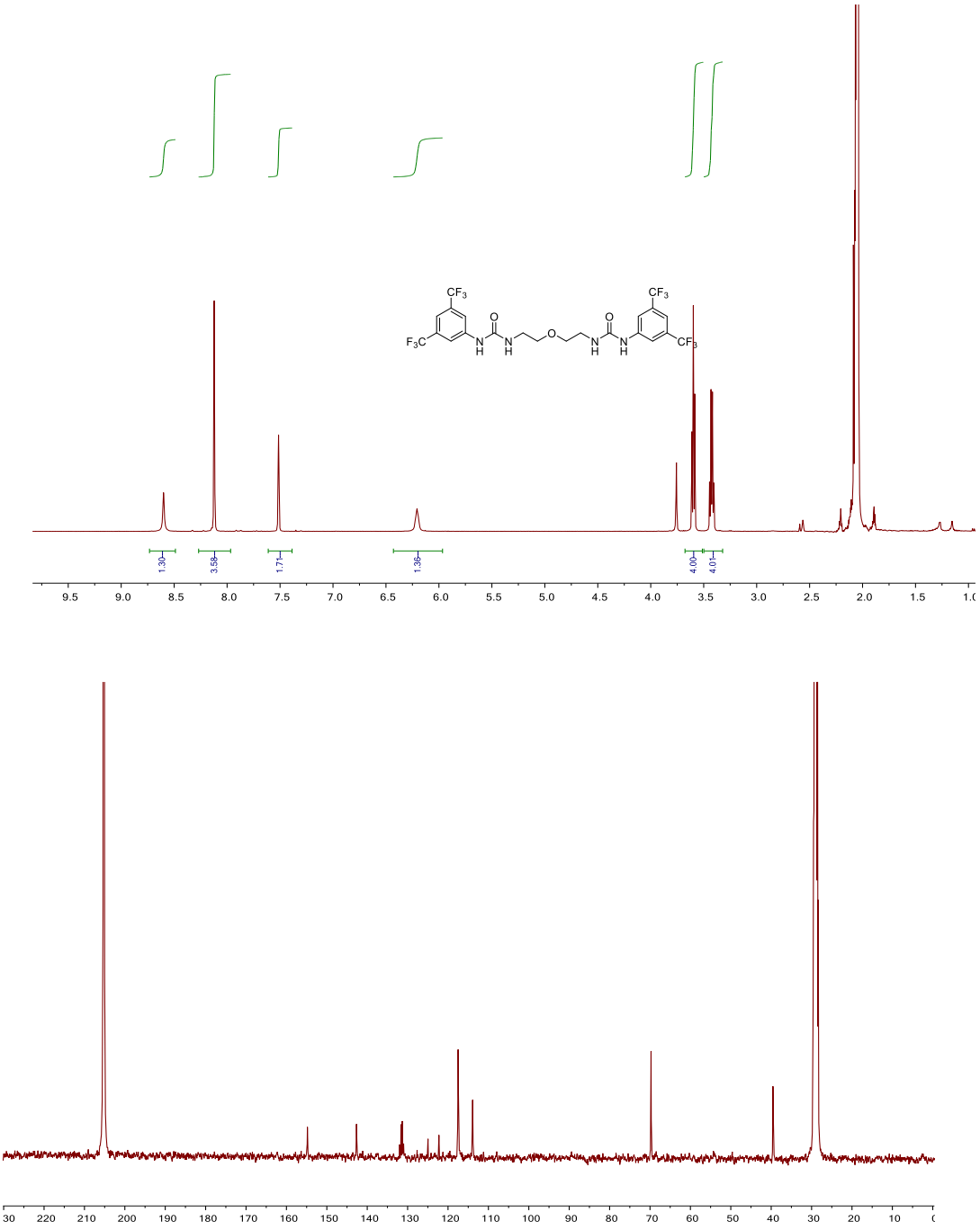

Figure 3.16. (Upper) ^{1}H NMR (acetone-d_6, 400 MHz, ppm) spectrum of 1,1'-(oxybis(ethane-2,1-diyl))bis(3-(3,5-bis(trifluoromethyl)phenyl)urea) **(2-O5-O)**, (Lower) ^{13}C NMR (acetone-d_6, 100 MHz, ppm) spectrum of 1,1'-(oxybis(ethane-2,1-diyl))bis(3-(3,5-bis(trifluoromethyl)phenyl)urea).

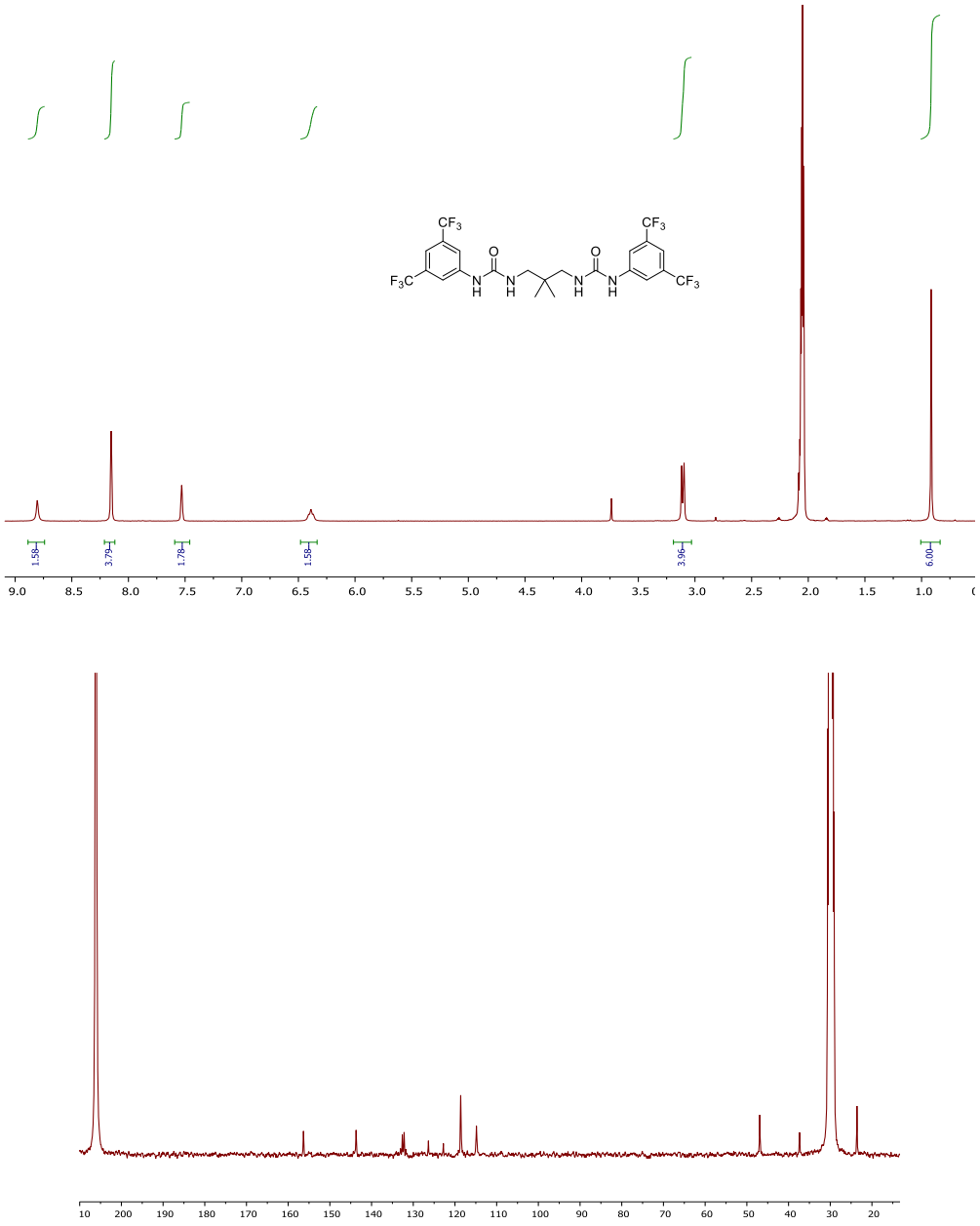

Figure 3.17. (Upper) ^{1}H NMR (acetone-d_6, 400 MHz, ppm) spectrum of 1,1'-(2,2-dimethylpropane-1,3-diyl)bis(3-(3,5-bis(trifluoromethyl)phenyl)urea) **(2-O3-diMe)** , (Lower) ^{13}C NMR (acetone-d_6, 100 MHz, ppm) spectrum of 1,1'-(2,2-dimethylpropane-1,3-diyl)bis(3-(3,5-bis(trifluoromethyl)phenyl)urea).

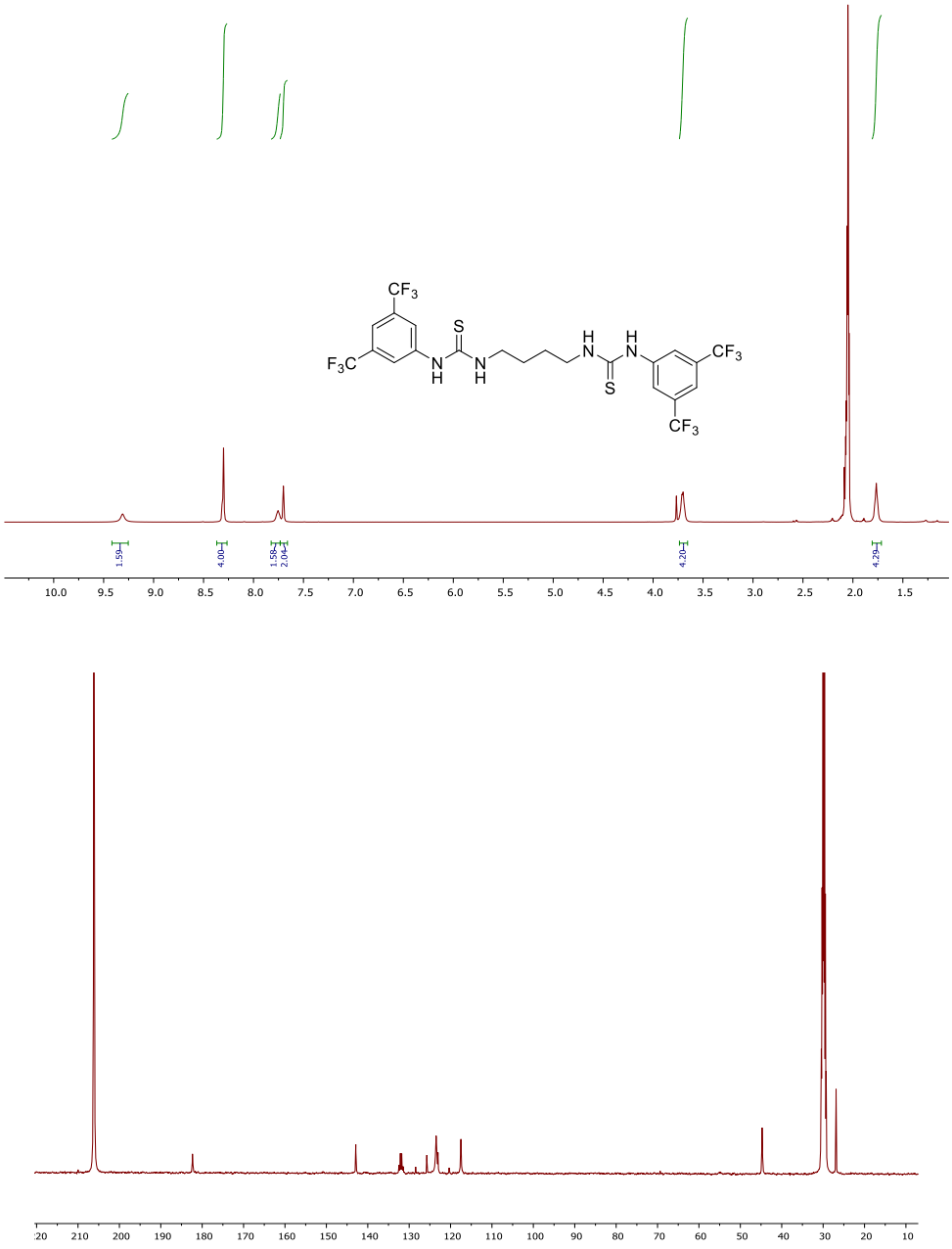

Figure 3.18. (Upper) ^{1}H NMR (acetone-d_6, 400 MHz, ppm) spectrum of 1,1'-(butane-1,4-diyl)bis(3-(3,5-bis(trifluoromethyl)phenyl)thiourea) **(2-S4)**, (Lower) ^{13}C NMR (acetone-d_6, 100 MHz, ppm) spectrum of 1,1'-(butane-1,4-diyl)bis(3-(3,5-bis(trifluoromethyl)phenyl)thiourea).

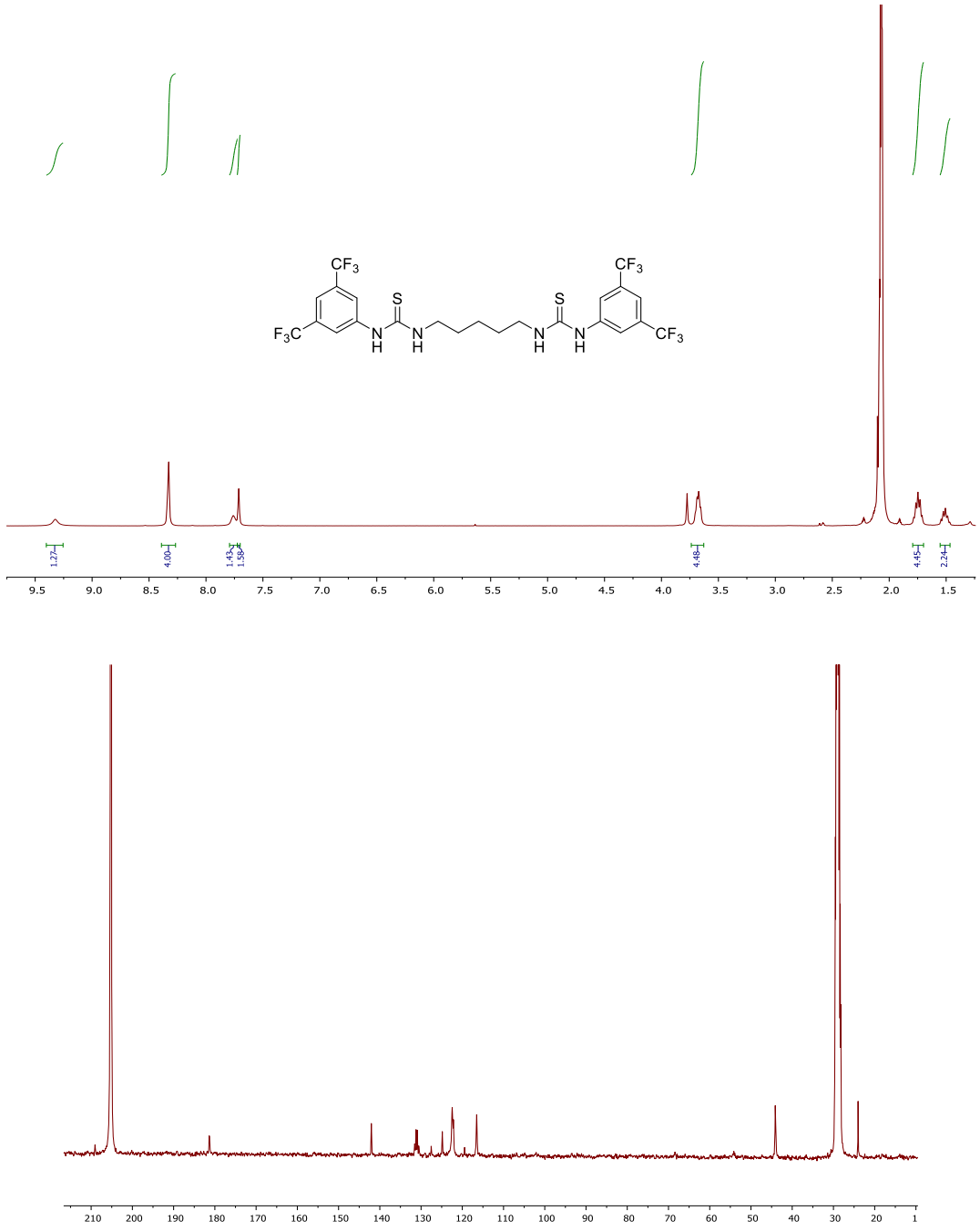

Figure 3.19. (Upper) ^{1}H NMR (acetone-d_6, 400 MHz, ppm) spectrum of 1,1'-(pentane-1,5-diyl)bis(3-(3,5-bis(trifluoromethyl)phenyl)thiourea) **(2-S5)**, (Lower) ^{13}C NMR (acetone-d_6, 100 MHz, ppm) spectrum of 1,1'-(pentane-1,5-diyl)bis(3-(3,5-bis(trifluoromethyl)phenyl)thiourea).

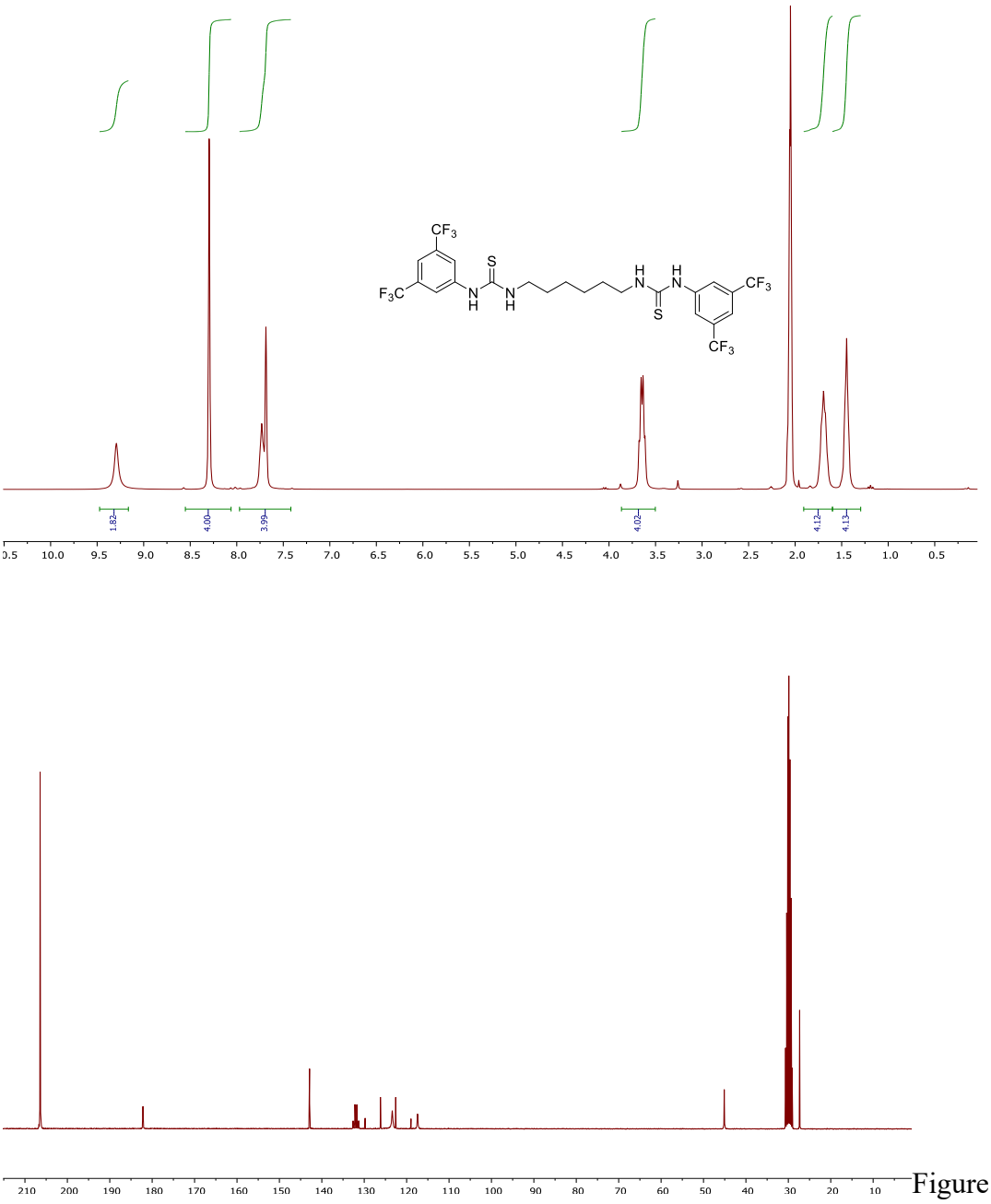

Figure 3.20. (Upper) ^{1}H NMR (acetone-d_6, 400 MHz, ppm) spectrum of 1,1'-(hexane-1,6-diyl)bis(3-(3,5-bis(trifluoromethyl)phenyl)thiourea) **(2-S6)**, (Lower) ^{13}C NMR (acetone-d_6, 100 MHz, ppm) spectrum of 1,1'-(hexane-1,6-diyl)bis(3-(3,5-bis(trifluoromethyl)phenyl)thiourea).

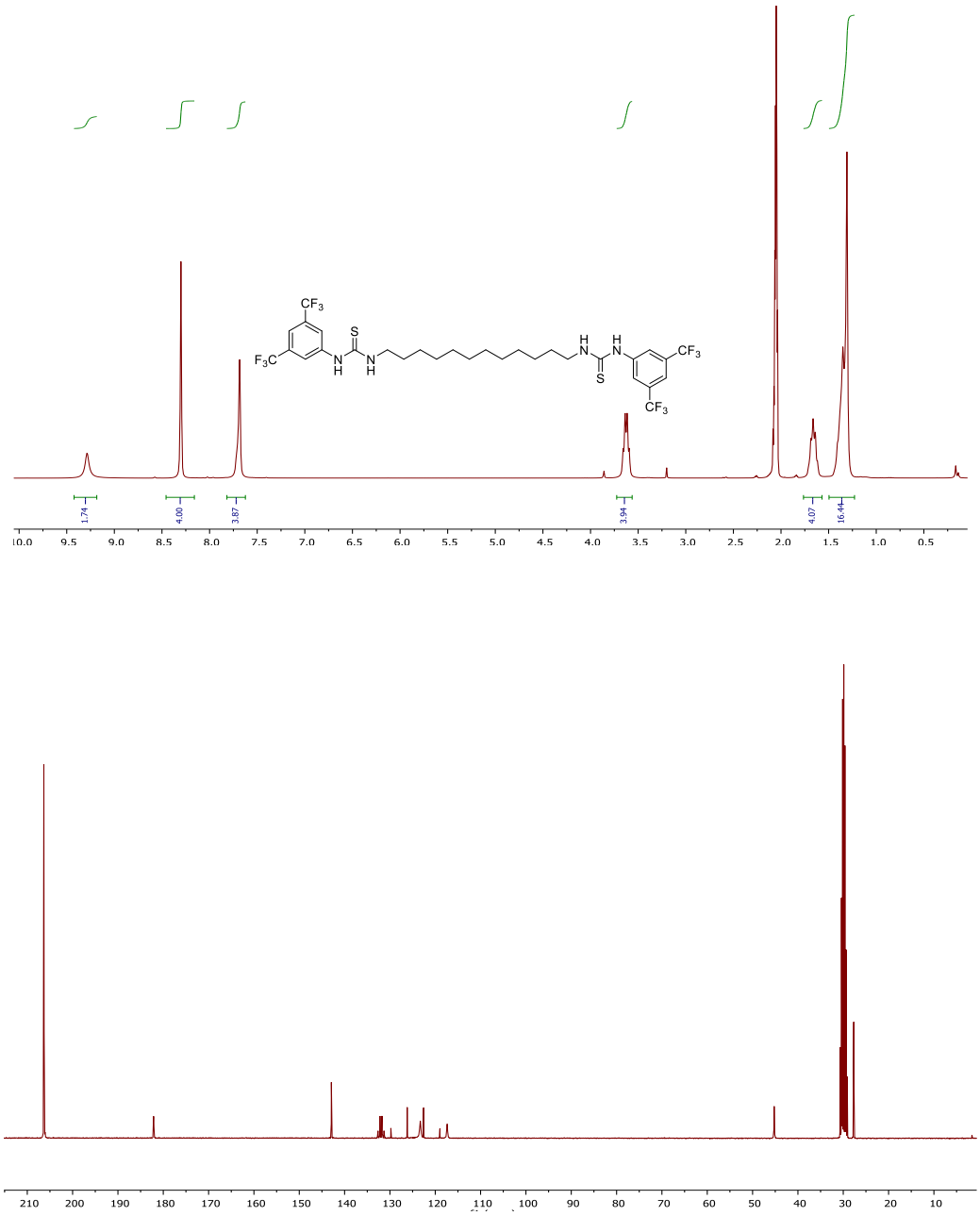

Figure 3.21. (Upper) ^{1}H NMR (acetone-d_6, 400 MHz, ppm) spectrum of 1,1'-(dodecane-1,12-diyl)bis(3-(3,5-bis(trifluoromethyl)phenyl)thiourea) **(2-S12)**, (Lower) ^{13}C NMR (acetone-d_6, 100 MHz, ppm) spectrum of 1,1'-(dodecane-1,12-diyl)bis(3-(3,5-bis(trifluoromethyl)phenyl)thiourea).

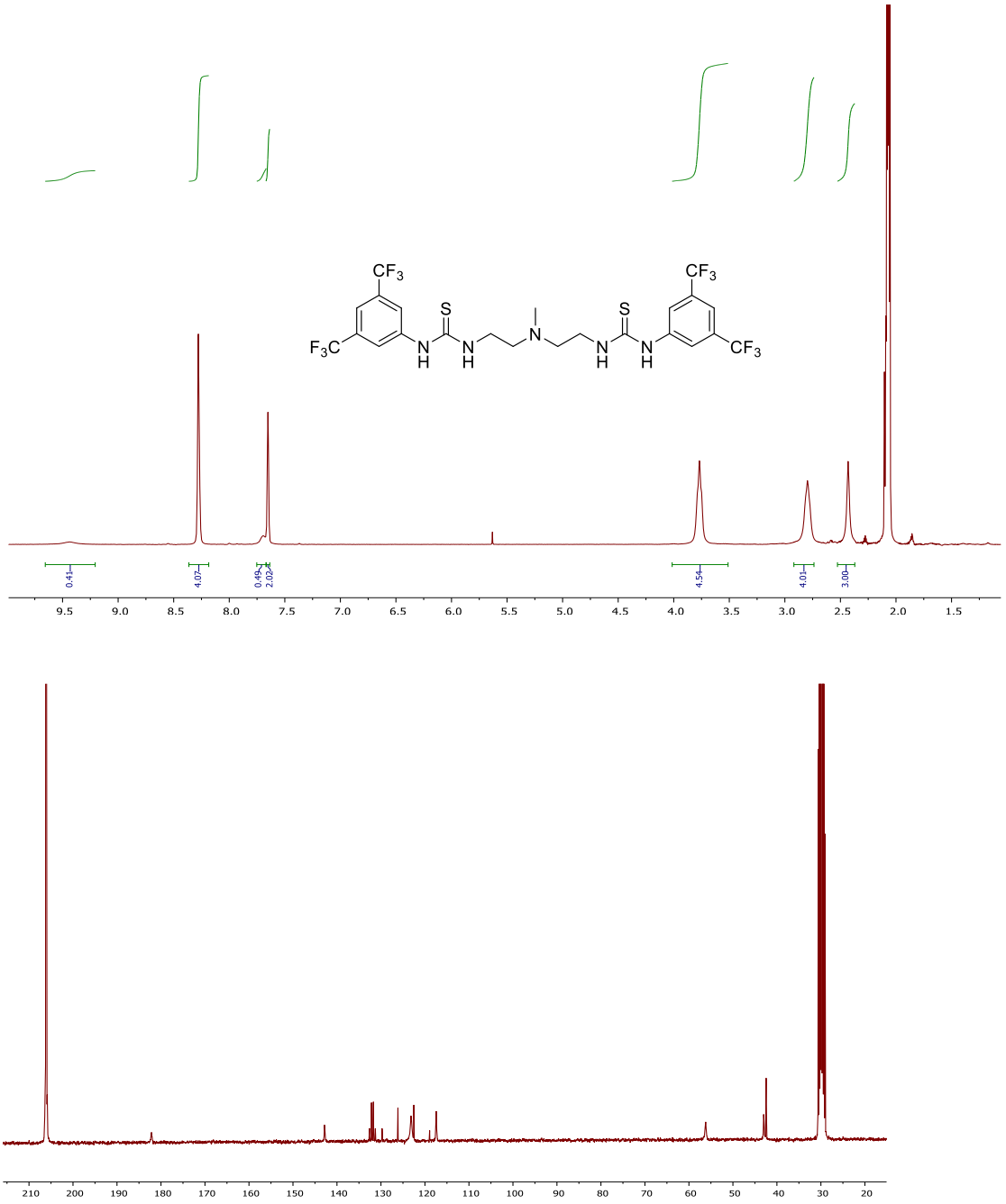

Figure 3.22. (Upper) ^{1}H NMR (acetone-d_6, 400 MHz, ppm) spectrum 1,1'-((methylazanediyl)bis(ethane-2,1-diyl))bis(3-(3,5-bis(trifluoromethyl)phenyl)thiourea) **(2-S5-N)**, (Lower) ^{13}C NMR (acetone- d_6, 100 MHz, ppm) spectrum of 1,1'-((methylazanediyl)bis(ethane-2,1-diyl))bis(3-(3,5-bis(trifluoromethyl)phenyl)thiourea)

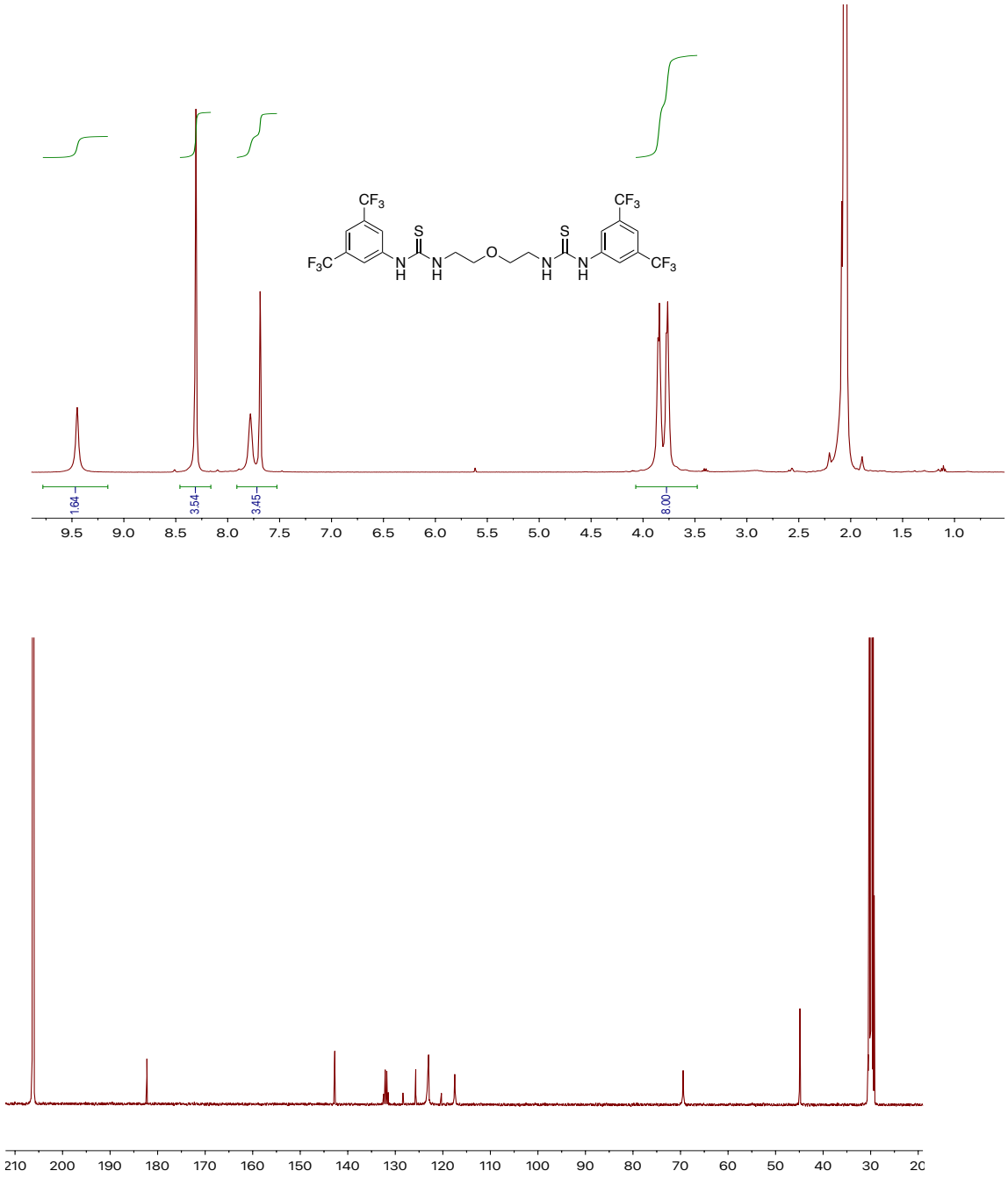

Figure 3.23. (Upper) ^{1}H NMR (acetone- d_6, 400 MHz, ppm) spectrum 1,1'-(oxybis(ethane-2,1-diyl))bis(3-(3,5-bis(trifluoromethyl)phenyl)thiourea) **(2-S5-O)**, (Lower) ^{13}C NMR (acetone- d_6, 100 MHz, ppm) spectrum of 1,1'-(oxybis(ethane-2,1-diyl))bis(3-(3,5-bis(trifluoromethyl)phenyl)thiourea).

MANUSCRIPT IV

Formatted for publication in ACS macromolecules

Higher-Order Kinetics in δ-Valerolactone (VL) for Ring-Opening Polymerization

Rukshika S. Hewawasam, and Matthew K. Kiesewetter

Chemistry, University of Rhode Island, Kingston, RI, USA

Corresponding Author: Matthew Kiesewetter, Ph.D.

Chemistry

University of Rhode Island

140 Flagg Road

Kingston, RI, 02881, USA

Email address: mkiesewetter@uri.edu

ABSTRACT

(Thio)urea/ amine base cocatalysts are commonly employed for well-controlled, highly active "living" organocatalytic ring-opening polymerizations (ROPs) of cyclic esters in nonpolar and in polar solvents. An extensive kinetic study was carried out with ROP of VL employing 2-O and 3-O/amine base in polar solvents. It revealed that multiple urea moieties in 2-O and 3-O facilitate activation of several monomers, which resulted in higher-order kinetics in monomer and high initial rates in ROP reactions. H-bond donor/alkyl amine base cocatalyzed ROP of LA was conducted by varying initial LA concentrations ($[LA]_0$) while holding other parameters constant. The rate acceleration was exhibited in the presence of low [LA]0, and kinetic order in H-bond donor depends on $[LA]_0$. Copolymers of VL with IPP and N-BOC are synthesized, and it was revealed the polymer architecture could be modified due to higher-order kinetics of VL with 3-O/MTBD in polar solvents.

INTRODUCTION

Ring-opening polymerization (ROP) is a versatile technique to attain well-controlled and well-defined polymers.[1–5] H-bonding organocatalysts have become an irreplaceable tool in gaining selectivity in the ROP of cyclic lactones.[6,7] The (thio)urea plus base cocatalyst system has drawn our attention due to its remarkable selectivity towards the monomer and tunability. This thio(urea) plus base cocatalyst has bifunctional activation of the monomer and the initiator through H-bonding[3,8]. Over the past decade, this catalyst system was tuned to increase the selectivity and the rate by several research groups. As a result, several mechanistic insights were investigated. Indeed, among those strategies, H-bond mediated pathway and (thio)imidate mediated pathway standout[1,9–12]. Mechanistic pathway of the ROP of lactones mainly depends on solvent polarity, temperature, the acidity of the H- bond donor, and the basicity of the base. Remarkably, (thio)imidate mediated pathway shows higher rates and selectivity, which preferred in reaction conditions such as polar solvents[9,10,13,14], high temperatures[15,16], strong electron-withdrawing functional groups on H-bond donor[10,17]and strong bases.[9,17.] (Scheme 4.1)

We previously reported that electron-deficient aryl ureas have proved to be particularly efficacious compared to thioureas for ROP of δ-valerolactone (VL) and ε-caprolactone (CL) despite the solvent polarity.[10,13] Additionally, we disclosed that a synthetic addition of one or more (thio)urea H-bond donating moieties to **1-O/S**, could give an exquisite combination of higher rates and higher selectivity in ROP of lactones.[13,18,19] The activity of **2-O/S** catalyst in (non)polar solvents and the effect of confirmation

flexibility in between (thio)urea moieties have been well explained.[13] It is proved that **3-O**/MTBD cocatalyzed ROP occurs through an activated-urea mechanism where single urea moiety activates the lactone and that urea is powered by intramolecular H-bonding network by other two urea moieties in nonpolar solvents.[18] However, there is still no proven evidence about mechanistic details on **3-O** catalyzed ROP in polar solvents. Herein, a detailed thermodynamic and kinetic analysis has presented for **3-O**/MTBD cocatalyzed ROP of VL to provide a comprehensive mechanistic picture. We believe that elucidation of the nascent mechanistic insights of ROP would enhance the development of the organocatalysts field.

EXPERIMENTAL SECTION

General Considerations. All chemicals were purchased from Fisher Scientific and used as received unless stated otherwise. Benzene-d_6 and chloroform-*d* were purchased from Cambridge Isotope Laboratories, distilled from calcium hydride and stored under N_2. Acetone-d_6 was purchased from Cambridge Isotope Laboratories, distilled from calcium sulfate and stored under N_2. δ-valerolactone (VL), ε-caprolactone (CL), and benzyl alcohol were distilled under high vacuum from calcium hydride prior to use. Dry CH_2Cl_2 was obtained from an Innovative Technology solvent purification system. All experiments were conducted in a stainless-steel glovebox under N_2 unless stated otherwise. NMR experiments were performed on a Bruker Avance III 300 or 400 MHz spectrometer. Urea and thiourea H-bond donors were prepared by established methods.[3,20] N-Boc monomer and IPP monomer was prepared according to literature.[21,22]

Mass spectrometry experiments were performed using a Thermo Electron (San Jose, CA, USA) LTQ Orbitrap XL mass spectrometer affixed with electrospray ionization (ESI) interface in a positive ion mode. Collected mass spectra were averaged for at least 50 scans. Tune conditions for infusion experiments (10 μL/min flow, sample concentration 5 μg/mL in 50/50 v/v water/ methanol) were as follows: ion spray voltage, 5000 V; capillary temperature, 275oC; sheath gas (N2, arbitrary units), 11; auxiliary gas (N2, arbitrary units), 2; capillary voltage, 21 V; and tube lens, 90 V; multipole 00 offset,

-4.25 V; lens 0 voltage, - 5.00; multipole 1 offset, - 8.50 V; Multipole RF Amplitude, 400 V; Ion trap's AGC target settings for Full MS was 3.0e4 and FT's 2.0e5 (with 3 and 2 averaged microscans , respectively). Prior to analysis, the instrument was calibrated for positive ions using Pierce LTQ ESI positive ion calibration solution (lot #PC197784).

Example ROP of VL in benzene-d_6. To a 7 mL vial, **2-O** (14.69 mg, 0.024 mmol), VL (100.00 mg, 0.1 mmol) and benzene-d_6 (250 μL) were added. The contents were stirred until the solution became homogenous. To a second 7 ml vial, benzyl alcohol (2.16 mg, 0.02 mmol), MTBD (3.67 mg, 0.024 mmol) and benzene-d_6 (250 μL) were added. The contents in the second vial were transferred to the first vial via Pasteur pipette, and the contents were agitated to mix. The reaction solution was then transferred to an NMR tube, and the progress of the reaction monitored by ^{1}H NMR. The reaction was quenched by the addition of benzoic acid (3.00 mg, 0.024 mmol). Polymer isolated by precipitation with hexanes, and the volatiles were removed under high vacuum before characterization via GPC.

Example binding study of a urea to VL- Stock solutions were prepared in acetone-d_6 of VL (2 M) and 1,1',1''-(nitrilotris(propane-3,1-diyl))tris(3-(3,5-bis(trifluoromethyl)phenyl)urea (**3-O**) (1 mM). To an NMR tube, 100 μL of the urea stock solution and different amounts of VL stock solution were added, and the final volume of solution was taken up to 500 μL with acetone-d_6. The final concentrations of VL in the NMR tubes were varied between 1.6 M $\geq [VL]_o \geq$ 0 mM, and the concentration of the urea was 0.2 mM. ^{1}H NMR spectra (referenced to residual acetone-H) were

acquired for each solution at 300 K, and the chemical shift of the ortho-protons of phenyl urea was determined. The binding was determined by a line fitting method, and the values match those obtained by Lineweaver-Bruker method.[23–25]

Example Kinetic Isotopic Effect study- To a 7 mL vial, **2-O** (14.7 mg, 0.024 mmol), VL (100 mg, 0.998 mmol) and acetone-d_6 (200.0 µL) were added. The contents were stirred until the solution became homogenous. To a second 7 mL vial, benzyl alcohol (1.08 mg, 0.009 mmol), MTBD (3.6 mg, 0.024 mmol) and $CDCl_3$ (300.0 µL) were added. The contents in the second vial were transferred to the first vial via Pasteur pipette, and the contents were agitated to mix. Several aliquots were taken in different time intervals. Aliquots were quenched using benzoic acid solution. The conversion of reaction was monitored by ^{1}H NMR. This was repeated with varying portions of $CHCl_3$ in the chloroform portion of the solvent: 75 %, 50 %, and 25%. The k_{obs} of each reaction were plot against the percentage of $CDCl_3$, and the line was extrapolated to obtain rate at 100 % $CHCl_3$ with which the k_H/k_D value was calculated.

Determination of Thermodynamic Parameters- To a 7 mL vial, (3-O) (3.96 mg, 0.004 mmol), VL (50 mg, 0.449 mmol) and acetone-d_6 (250.0 µL) were added. The contents were stirred until the solution became homogenous. To a second 7 mL vial benzyl alcohol (0.539 mg, 0.004 mmol), MTBD (0.63 mg, 0.004 mmol) and acetone-d_6 (250.0 µL) were added. The contents in the second vial were transferred to the first vial via Pasteur pipette, and the contents were agitated to mix. Polymerization was conducted at different temperatures; 25 ˚C, 30 ˚C, 35 ˚C, 40 ˚C, and 45 ˚C. Several aliquots were taken in different time intervals. Aliquots were quenched using benzoic acid solution.

The conversion of reaction was monitored by ^{1}H NMR. The thermodynamic values of ROP activation were determined from Arrhenius plot and Eyring plot.

Example of determining observed rate constant (k_{obs}) for ROP of VL- To a 7 mL vial, **2-O** (14.69 mg, 0.024 mmol), VL (100.00 mg, 0.998 mmol) and acetone-d_6 (250 μL) were added. The contents were stirred until the solution became homogenous. To a second 7 ml vial, benzyl alcohol (2.16 mg, 0.019 mmol), MTBD (3.67 mg, 0.024 mmol) and acetone-d_6 (250 μL) were added. The contents in the second vial were transferred to the first vial via Pasteur pipette, and the contents were agitated to mix. Several aliquots were taken in different time intervals and those were quenched using benzoic acid solution. The reaction solution was then transferred to an NMR tube, and the progress of the reaction monitored by ^{1}H NMR. The reaction was quenched by the addition of benzoic acid (3.00 mg, 0.024 mmol). Reaction conversions were monitored using ^{1}H NMR. Observed rate constants (k_{obs})/min were extracted from a second order evolution of [VL] versus time, where k_{obs} is:

$$\text{Rate} = -d[VL]/dt = k_{obs}[VL]^2$$

$$k_{obs} = k_p[\text{cocats}][\text{alcohol}] \text{ and}$$

$$(1/[VL]_o)-(1/[VL]) = k_{obs}\, t$$

The (thio)urea plus base cocatalyzed ROP was previously shown to be first order in [(thio)urea + base]$_0$ as opposed to [(thio)urea]$_0$[base]$_0$.[26]

Determination of kinetic order in monomer - The kinetic order of monomer (n) was determined from a series of experiments varying the concentration of monomer. All the other reagent concentrations were kept constant throughout the experiments. Initial rates (R_i) were obtained in polymerization reactions. R_i versus concentration of monomer was plotted where R_i is,

$$R_i = k_{obs} [M]^n$$

Kinetic Order Determination- The kinetic order in each species was determined from a series of experiments varying the concentration of species of interest. All the other reagents concentrations were kept constant throughout each series of experiments. Rate constants (k_{obs}) were obtained in polymerization reactions. k_{obs} versus concentration of interest species was plotted in order to obtain order of the interested species.

Determination of thermal properties- Melting temperatures (T_m) of PLA synthesized in this study were determined by differential scanning calorimetry (DSC) using a Shimadzu differential scanning calorimeter 60 plus that has been calibrated using high purity indium at a heating rate of 5 °C/min. Polymer sample (5 mg) was first heated to 180 ºC at 5 ºC/min, held at this temperature for 1 h to anneal the sample. The sample was cooled to 25 ºC at 5 ºC/min, held for 10 min, and reheated to 250 ºC at 5 ºC/min. All thermal data was obtained from the second cycle.

Determination of percent isotacticity- The ^1H decoupled NMR spectra of the isolated polymer were acquired on a Varian 500 MHz at 50ºC. The samples for ^1H NMR were prepared 1mg/ml in $CDCl_3$. The ^1H NMR spectrum of the polymer was obtained by

selective decoupling by irradiating the methyl region, and tacticity was determined from the methine region according to published procedures.[7,27,28]

RESULTS AND DISCUSSION

The ROP of VL (1.0mmol, 2 M) cocatalyzed by **3-O** plus MTBD (0.0165 mmol each) initiated from benzyl alcohol (0.01 mmol) in acetone-d_6 shows rate acceleration similar as in C_6D_6 where the monomer conversion reached to 90% in 5 minutes at room temperature. The ROP of VL using **3-O**/MTBD in acetone-d_6 is highly controlled, and exhibits living characteristics by linear evolution of M_n versus conversion and M_n predictable from $[M]_0/[I]_0$ (Table 4.6 and Figure 4.6). However, the linear first-order behavior of the monomer concentration was truncated that may be associated with higher-order kinetics of the monomer concentration in the rate-determining step. Based on this observation, we believe that a higher number of monomers could be activated by **3-O** in the transition state of the reaction. This is further verified by kinetic studies. As we believe, this is the first study that shows the living polymerization behavior of ROP with higher-order evolution of monomer.

Chemical kinetics of ROP of VL cocatalyzed by 3-O/MTBD in acetone-d_6

A kinetic study was conducted in order to establish the reaction order of the monomer in the ROP of VL. A set of ROPs was carried out with different monomer concentrations ([VL]= 2 M to 0.2 M) while holding the concentration of cocatalyst (0.033 M, 0.0165 mmol each), and benzyl alcohol (0.02 M, 0.01 mmol) constant in acetone-d_6. The resulting plot (Figure 4.2) of observed initial rates (R_i) versus $[VL]_0^3$, is linear, which describes the third-order behavior of the [VL] in the ROP of VL. $R_i = k_{obs}[VL]^3$, where $k_{obs} = k_P([\mathbf{3\text{-}O}] + [MTBD])[\text{benzyl alcohol}]$, and k_P is the polymerization rate constant.

Experimental results suggest that three monomers could be activated by **3-O,** which facilitated in polar solvents. Higher-order kinetics of lactone monomers have been seen previously with metal catalysts, as mentioned in literature.[29] Kinetic studies were also undertaken to elucidate the role of benzyl alcohol and **3-O**/MTBD in the ROP of VL. We observe first-order kinetics in the initiator and also, first-order kinetics in cocatalyst, which is typical behavior for ROP of lactones.[3,19,26] (Figure 4.7) Comparatively, we observe first-order kinetics in monomer concentration for ROP of VL cocatalyzed by **3-O**/MTBD in C_6D_6. (Figure 4.8) NMR binding studies of **3-O**/VL and **1-O**/VL have been carried out in acetone-*d*$_6$. As expected, no significant chemical shifts have been observed of the H-bond donor up to ~ 1000 equivalents of VL, which suggests weak binding (K_{eq} ~2) between the monomer and catalysts. Also, the poor solubility of **3-O** in C_6D_6 limits the measuring of the binding constant between VL and **3-O** in C_6D_6. Hence, the binding constant rationale cannot be used in explaining the activity of **3-O** catalyzed ROP in polar solvents. Our group first disclosed the intramolecular H-bond network system in the **3-O** catalyst in nonpolar solvents.[18] However, we believe that intramolecular H-bonding of **3-O** can be disrupted in polar solvents, which facilitates the activation of multiple monomers.

Bisurea catalysts plus base remain highly active for the ROP of lactones in both nonpolar and polar solvents.[13] However, the deviation of the latter portion of the first order plot indicates higher order kinetics of monomer in the ROP of VL cocatalyzed by bisurea/MTBD in polar solvents (Figure 4.9). The ROP of VL cocatalyzed by **2-O**/MTBD in acetone-*d*$_6$ shows second-order kinetics of monomer, which is supported

by kinetic studies. (Figure 4.3) Yet, it exhibits living characteristics, and the reaction is highly controlled ($M_w/M_n \sim 1.06$).

Kinetic isotope effect (KIE) studies for ROP were conducted to understand the effect of propagating alcohol H/D substitution on the ROP rates. It implies that ground-state binding is an adequate model for understanding the transition state of the mechanism, and due to the binding events among some reagents prior to chain enchainment can be affected for ROP rates. The k_H/k_D of ROP were measured for the **1-O**, **2-O**, **3-O** /MTBD cocatalyzed (0.1 M each, 0.05 M each, 0.033 M each, respectively) ROP of VL (1 mmol, 2 M) from benzyl alcohol (0.02 M) in a mixture of acetone-d_6/$CDCl_3$/$CHCl_3$ (50% acetone-d_6, 50% chloroform), where the H/D ratio in the chloroform blends is adopted by the benzyl alcohol. Kinetic isotope studies on observed rate constant for the **3-O**/MTBD and **2-O**/MTBD cocatalyzed ROP of VL show a later transition state versus the **1-O**/MTBD cocatalyzed ROPs (Table 4.1). The KIEs range from $k_H/k_D = 2.17$ for **1-O** in chloroform to $k_H/k_D = 6.11$ for **3-O** in the blend of acetone-d_6 and chloroform. Also, we observe that larger KIE values in acetone-d_6/$CDCl_3$/$CHCl_3$ versus in C_6D_6/$CDCl_3$/$CHCl_3$ which suggest a later transition state in acetone is characterized by an extensive H/D jump between alcohol to monomer in chain enchainment. Hence, we believe that several monomers can be attached to the **2-O** and **3-O** in its transition state. The later transition state also characterized by more equal sharing of the H/D in the imidate mediated mechanism.

The thermal behavior of various H-bond donors plus MTBD was determined under ROP conditions in acetone-d_6. The observed rate constant (k_{obs}) for the first order evolution

of [VL] ($[VL]_o$ = 1 M, 0.5 mmol) were measured for the **1-O**/MTBD cocatalyzed ROP from benzyl alcohol (0.01 mmol) in acetone-d_6 and the observed rate constants for the second or third evolution of [VL] were measured for **2-O** and **3-O** plus MTBD cocatalyzed ROP respectively, at several temperatures from 25 to 40 °C, (Table 4.1), and an Eyring plot was constructed for each cocatalyst system(Figure 4.10). The concentration of H-bond donating moiety was held constant between runs. The 1 M $[VL]_o$ was chosen for the ROP because the slower reaction kinetics facilitates monitoring by aliquot or ^{1}H NMR. For all the cocatalyst systems, the Eyring plots are linear over the entire temperature window, where it shows the thermal stability of cocatalysts system in acetone-d_6 at elevated temperatures.[15] Further, thermodynamic parameters such as entropy of activation ($\Delta S^{\ddagger}$) and enthalpy of activation ($\Delta H^{\ddagger}$) of the ROP provides stability of the transition state. The **3-O**/MTBD cocatalyzed ROP has highest $\Delta H^{\ddagger}$ (17.10 ± 0.08 kcal/mol) and **1-O**/MTBD cocatalyzed ROP has lowest $\Delta H^{\ddagger}$ (4.92 ± 0.01 kcal/mol) which suggests that there can be a correlataion of three monomers with **3-O** in the tranition state . This trend was observed earlier for monourea to multiurea plus MTBD cocatalyzed ROP.[15] Here, we propose that low activation of enthalpy gained by the simultaneous activation of a higher number of monomers by **3-O** in acetone-d_6. (Scheme 4.2) It is also proven that bisimidate is not formed even with an additional equivalent of base treatment which can support our proposed mechanism.[13]

It is known that more imidate characteristics can be formed using strong bases or/and in polar solvents also, ROP via imidate mediate mechanism could provide faster rates and

highly controlled reactions. In this study, it is also observed that more imidate characteristics in reaction conditions preferred in higher-order kinetics (Table 4.2), which explains faster rates for ROP via imidate mediated mechanism. Less imidate characteristics in reaction conditions prefer the first-order evolution of the monomer. For example, **2-O**/MTBD cocatalysed ROP of VL follows first-order kinetics in monomer in C_6D_6 and **2-O**/BEMP cocatalyzed ROP of VL in C_6D_6 exhibits second-order kinetics in [VL].

It is also observed that in **3-O**/MTBD cocatalyzed ROP of VL in acetone-d_6 has higher initial rates than in C_6D_6. However, in acetone-d_6 latter portion of the reaction is sluggish compared in C_6D_6. Here we reasoned that order kinetics in monomer depends on the initial monomer concentration, and when reaction proceeds, monomer concentration decreases resulted in attenuation of order kinetics in the monomer. Similar results were noticed with **2-O**/MTBD cocatalyzed ROP of VL. The ROP of CL with **3-O** plus MTBD/BEMP cocatalyst in acetone-d_6 exhibits the slow relative reaction times than VL and displays good control, which is similar to previously reported.[3] However, higher-order kinetics in monomer concentration was not observed with CL even with more imidate characteristics formed by a combination of a strong base: BEMP with **3-O**. (Figure 4.11)

ROP of L-Lactide

ROP of L-Lactide (LA) with **3-O**/Me_6TREN was conducted in acetone-d_6. Contrary to ROP of VL, when increasing the $[LA]_o$, initial rates were decreased. Since it is already proven that thiourea catalysts are more active than their urea analogs in solvent and under solvent-free conditions.[13] Further studies in ROP of L-Lactide were carried out with **1-S** and **2-S** plus Me_6TREN in CH_2Cl_2. When **1-S** and **2-S** plus Me_6TREN cocatalysts (0.024 mmol each, 0.012 mmol respectively) are applied for the ROP of LA (1 M, 0.5 mmol) initiated from benzyl alcohol (0.005 mmol) in CH_2Cl_2, the ROP reactions exhibit "living" behavior with first-order evolution of monomer and predictable M_n from $[M]_0/[I]_0$. (Table 4.3, 4.7 and Figure 4.12) In contrast to the ROP of VL, CL, or carbonate monomers, mild base cocatalysts are required for the ROP of lactide.[19,26,30] However, we observe that the rate acceleration with low initial LA concentrations regardless of the type of H-bond donor, type of base, and the polarity of the solvent. (Table 4.3 and Figure 4.13 and 4.14) Kinetic studies were also undertaken to help in elucidating the role of initial LA concentration in the ROP of LA. While holding the benzyl alcohol concentration (0.05 mmol, 0.01 M), and cocatalyst concentration (0.024 mmol, 0.05 M) constant in CH_2Cl_2, $[LA]_0$ was varied from 2 M to 0.1 M. The plot of initial rate (R_i) versus $[LA]_0$ is an exponential decay where its shows attenuation of rates with high initial monomer concentrations. Yet, ROP reactions remain highly controlled. Albeit, with extremely low initial monomer concentration, loss of control can be observed. (Figure 4.4) For the ROP of LA, the effects of reaction conditions on polymer tacticity must also be considered. The poly(lactide) was isolated

and analyzed by selectively decoupled ^{1}H NMR revealing the polylactide (PLA) isotacticity decreases with low initial monomer concentrations, which suggests epimerization is high when it has high catalyst loading %. Isotactic PLA is highly crystalline, where it can be measured by melting temperature (T_m). When isotacticity decreases, T_m decreases where it shows the loss of crystallinity due to the epimerization. We observe, loss of crystallinity with low initial monomer concentration where epimerization takes place.

A study by our group has shown that ROP of LA displays second-order kinetics in [**1-S**] with $[LA]_0$ = 0.5 mmol, 1 M.[8] Herein, we disclose that order kinetics in [**1-S**] get altered along with the $[LA]_0$. We observe that second-order kinetics in **1-S** in the ROP of LA with high $[LA]_0$ ($[LA]_0$ =2 M) and first-order kinetics in **1-S** with low $[LA]_0$ ($[LA]_0$ = 0.4 M). (Figure 4.5) We posited that observed differing kinetic order in **1-S** might account for the different activities and rates in the ROP of lactide with various $[LA]_0$. This suggests a mechanism that may involve one **1-S** moiety in the transition state of the ring-opening in low LA concentration, which kinetically resulted in high rates, maybe due to less steric hindrance of the transition state. When in high LA concentration, two **1-S** moieties coming together are facilitated, which kinetically resulted in low rates in the ROP of LA. Further studies have been carried out with DBU catalyzed ROP of LA to determine the involvement of H-bond donor for this kinetic evolution. ROP of LA catalyzed by DBU initiated from benzyl alcohol in CH_2Cl_2 exhibits living characteristics and rate accelerated with high monomer concentrations. (Table 4.4) However, with low initial monomer concentrations, M_w/M_n was slightly

broadened, and epimerization was facilitated, which is indicated by low T_m values. Hence, these observations reinforce the conclusion that the magnitude and the nature of cocatalyst interactions have a dramatic effect on the kinetics of the ROP reaction.

Copolymerization

The observation of higher-order kinetics of VL with **3-O** suggests that copolymerization of VL and other monomers could change polymer architecture resulted in different polymer materials. In the one-pot ROP of VL (0.5 mmol) and IPP (0.5 mmol) from benzyl alcohol (0.01 mmol) with **1-S**/MTBD (0.05 mmol) in CH_2Cl_2 cocatalyst system fully converts IPP to polymer in 20 hr, which resulted in gradient-block copolymer where it has first-order kinetics for both monomers. (Table 4.5) However, **3-O**/MTBD cocatalyzed ROP of VL and IPP (1:1) resulted in a random copolymer of VL and IPP in 60 mins, where it observed second-order behavior in VL and first-order behavior in IPP. Copolymerization of VL and N-BOC monomer was also performed employing the **1-S**/MTBD and **3-O**/MTBD, where it is observed faster rates with **3-O**/MTBD, and it changed the polymer architecture from block copolymer to random copolymer.

CONCLUSION

We propose that **3-O**/MTBD cocatalyzed ROP of VL undergoes via an activated imidate mechanism, where it can activate three monomers through H-bonding in polar solvents. Hence, it can follow higher-order kinetics in monomer resulted in higher initial rates. Yet, these ROPs exhibit living characteristics and remain highly selective. It is noted that higher-order kinetics in monomer with remaining living characteristics in the ROP of lactones for organocatalysts is first reported to our knowledge. Higher kinetics in VL with **3-O** would be useful in altering polymer architectures of copolymers.

REFERENCES

1. Kiesewetter, M. K., Shin, E. J., Hedrick, J. L. & Waymouth, R. M. Organocatalysis: Opportunities and challenges for polymer synthesis. *Macromolecules* **43**, 2093–2107 (2010).

2. Dove, A. P. Organic catalysis for ring-opening polymerization. *ACS Macro Lett.* **1**, 1409–1412 (2012).

3. Lohmeijer, B. G. G. *et al.* Guanidine and amidine organocatalysts for ring-opening polymerization of cyclic esters. *Macromolecules* **39**, 8574–8583 (2006).

4. Kamber, N. E. *et al.* Organocatalytic ring-opening polymerization. *Chem. Rev.* **107**, 5813–5840 (2007).

5. Dove, A. P., Pratt, R. C., Lohmeijer, B. G. G., Waymouth, R. M. & Hedrick, J. L. Thiourea-based bifunctional organocatalysis: Supramolecular recognition for living polymerization. *J. Am. Chem. Soc.* **127**, 13798–13799 (2005).

6. Dharmaratne, N. U., Pothupitiya, J. U. & Kiesewetter, M. K. The mechanistic duality of (thio)urea organocatalysts for ring-opening polymerization. *Org. Biomol. Chem.* **17**, 3305–3313 (2019).

7. Pratt, R. C. *et al.* Exploration, optimization, and application of supramolecular thiourea-amine catalysts for the synthesis of lactide (co)polymers. *Macromolecules* **39**, 7863–7871 (2006).

8. Kazakov, O. I. & Kiesewetter, M. K. Cocatalyst Binding Effects in Organocatalytic Ring-Opening Polymerization of l -Lactide. *Macromolecules* **48**, 6121–6126 (2015).

9. Dharmaratne, N. U., Pothupitiya, J. U., Bannin, T. J., Kazakov, O. I. & Kiesewetter, M. K. Triclocarban: Commercial Antibacterial and Highly Effective H-Bond Donating Catalyst for Ring-Opening Polymerization. *ACS Macro Lett.* **6**, 421–425 (2017).

10. Pothupitiya, J. U., Hewawasam, R. S. & Kiesewetter, M. K. Urea and Thiourea H-Bond Donating Catalysts for Ring-Opening Polymerization: Mechanistic Insights via (Non)linear Free Energy Relationships. *Macromolecules* **51**, 3203–3211 (2018).

11. Lin, B. & Waymouth, R. M. Urea anions: Simple, fast, and selective catalysts for ring-opening polymerizations. *J. Am. Chem. Soc.* **139**, 1645–1652 (2017).

12. Zhang, X., Jones, G. O., Hedrick, J. L. & Waymouth, R. M. Fast and selective ring-opening polymerizations by alkoxides and thioureas. *Nat. Chem.* **8**, 1047–1053 (2016).

13. Hewawasam, R. S. *et al.* Bisurea and Bisthiourea H-Bonding Organocatalysts for Ring-Opening Polymerization: Cues for the Catalyst Design. *Macromolecules* **52**, 9232–9237 (2019).

14. Pothupitiya, J. U. *et al.* H-Bonding Organocatalysts for the Living, Solvent-Free Ring-Opening Polymerization of Lactones: Toward an All-Lactones, All-Conditions

Approach. *Macromolecules* **50**, 8948–8954 (2017).

15. Coderre, D. N., Fastnacht, K. V., Wright, T. J., Dharmaratne, N. U. & Kiesewetter, M. K. H-Bonding Organocatalysts for Ring-Opening Polymerization at Elevated Temperatures. *Macromolecules* **51**, 10121–10126 (2018).

16. Basterretxea, A., Jehanno, C., Mecerreyes, D. & Sardon, H. Dual Organocatalysts Based on Ionic Mixtures of Acids and Bases: A Step Toward High Temperature Polymerizations. *ACS Macro Lett.* **8**, 1055–1062 (2019).

17. Lin, B. & Waymouth, R. M. Organic Ring-Opening Polymerization Catalysts: Reactivity Control by Balancing Acidity. *Macromolecules* **51**, 2932–2938 (2018).

18. Fastnacht, K. V. *et al.* Bis- and Tris-Urea H-Bond Donors for Ring-Opening Polymerization: Unprecedented Activity and Control from an Organocatalyst. *ACS Macro Lett.* **5**, 982–986 (2016).

19. Spink, S. S., Kazakov, O. I., Kiesewetter, E. T. & Kiesewetter, M. K. Rate Accelerated Organocatalytic Ring-Opening Polymerization of l -Lactide via the Application of a Bis(thiourea) H-bond Donating Cocatalyst. *Macromolecules* **48**, 6127–6131 (2015).

20. Bertucci, M. A., Lee, S. J. & Gagné, M. R. Selective transamidation of 3-oxo-N-acyl homoserine lactones by hydrazine derivatives. *Org. Biomol. Chem.* **12**, 7197–7200 (2014).

21. Venkataraman, S. *et al.* A Simple and Facile Approach to Aliphatic N-Substituted Functional Eight-Membered Cyclic Carbonates and Their Organocatalytic Polymerization. *J. Am. Chem. Soc.* **137**, 13851–13860 (2015).

22. Stukenbroeker, T. S., Solis-Ibarra, D. & Waymouth, R. M. Synthesis and topological trapping of cyclic poly(alkylene phosphates). *Macromolecules* **47**, 8224–8230 (2014).

23. Deranleau, D. A. Theory of the Measurement of Weak Molecular Complexes. I. General Considerations. *J. Am. Chem. Soc.* **91**, 4044–4049 (1969).

24. Horman, I. & Dreux, B. Estimation of Association Constants of Bimolecular Organic Complexes. *Anal. Chem.* **55**, 1219–1221 (1983).

25. Peters, S. J. & Stevenson, C. D. The complexation of the Na+ by 18-crown-6 studied via nuclear magnetic resonance. *J. Chem. Educ.* **81**, 715–717 (2004).

26. Kazakov, O. I., Datta, P. P., Isajani, M., Kiesewetter, E. T. & Kiesewetter, M. K. Cooperative hydrogen-bond pairing in organocatalytic ring-opening polymerization. *Macromolecules* **47**, 7463–7468 (2014).

27. Thakur, K. A. M. *et al.* High-resolution 13C and 1H solution NMR study of poly(lactide). *Macromolecules* **30**, 2422–2428 (1997).

28. Ovitt, T. M. & Coates, G. W. Stereochemistry of lactide polymerization with chiral catalysts: New opportunities for stereocontrol using polymer exchange

mechanisms. *J. Am. Chem. Soc.* **124**, 1316–1326 (2002).

29. Chen, H. Y., Huang, B. H. & Lin, C. C. A highly efficient initiator for the ring-opening polymerization of lactides and ε-caprolactone: A kinetic study. *Macromolecules* **38**, 5400–5405 (2005).

30. Doyle, A. G. & Jacobsen, E. N. Small-molecule H-bond donors in asymmetric catalysis. *Chem. Rev.* **107**, 5713–5743 (2007).

Urea	$\Delta H^{\ddagger}$ [a] (kcal/mol)	$\Delta S^{\ddagger}$ [a] (cal/(mol K))	KIE
1-O	4.92 ± 0.01	-45.03±46	2.17[b]
2-O	12.81± 0.02	-22.80 ± 17	3.65[c], 2.7[d]
3-O	17.10 ± 0.08	-4.70 ± 19	6.11[e], 3.68[f]

Table 4.1. $\Delta H^{\ddagger}$, $\Delta S^{\ddagger}$, and KIE values for the 3-O/MTBD cocatalyzed ROP of VL

(a) Reaction conditions: VL (0.5 mmol, 1 equiv, 1.00 M), benzyl alcohol (0.005 mmol), **1-O**, **2-O**, **3-O** (0.024 mmol, 0.012 mmol, 0.008 mmol respectively) and MTBD (matched to H-bond donor mmol) in acetone-d_6. (b) VL (1 mmol, 2.00 M); **1-O**/MTBD (0.1 M each); benzyl alcohol (0.02 M) in $CDCl_3/CHCl_3$. The k_H and k_D were extracted from plots of k_{obs} vs %D in the chloroform feed. (c) VL (1 mmol, 2.00 M); **2-O**/MTBD (0.05 M each); benzyl alcohol (0.02 M) in acetone-d_6/$CDCl_3/CHCl_3$ (50% C_6D_6: 50% $CDCl_3/CHCl_3$), (d) $C_6D_6/CDCl_3/CHCl_3$ (50% C_6D_6: 50% $CDCl_3/CHCl_3$) (e) VL (1 mmol, 2.00 M); **3-O**/MTBD (0.033 M each); benzyl alcohol (0.02 M) in acetone-d_6/$CDCl_3/CHCl_3$ (50% C_6D_6: 50% $CDCl_3/CHCl_3$), (f) $C_6D_6/CDCl_3/CHCl_3$ (50% C_6D_6: 50% $CDCl_3/CHCl_3$)

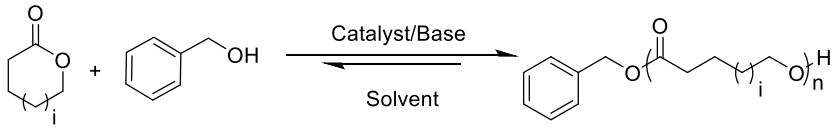

VL, i=1
CL, i=2

Entry	Solvent	Initial rate[b]	Time (min)	Conversion [c]%	Order of the monomer
1	acetone [d]	1.352	5	86	3rd
2	benzene [d]	0.833	5	90	1st
3	benzene [e]	0.217	25	91	1st
4	acetone [e]	0.819	26	88	2nd
5	benzene [f]	0.026	141	90	1st
6	acetone [f]	0.038	131	85	2nd
7	benzene [g]	0.864	4	90	2nd
8	acetone [g]	0. 862	4	90	2nd
9	acetone [h]	0.3179	20	90	1st
10	benzene [h]	0.2257	45	90	1st
11	acetone [i]	0.044	955	87	1st
12	acetone [j]	0.1538	20	88	1st

Table 4.2. Urea catalyst plus base co-catalyzed ROP of VL and CL in different solvents [a]

(a) Reaction conditions: VL (1.0 mmol, 1 equiv, 2 M), benzyl alcohol (0.02 mmol) b) R_i was determined by [M] versus time plot. c) Monomer conversion was monitored via ^{1}H NMR d) **3-O** /MTBD (0.0165 mmol each) , e) **2-O**/MTBD (0.024 mmol each), f) **2-O**/DBU (0.024 mmol each), g) VL (0.5 mmol, 1 equiv, 1 M) **2-O**/BEMP (0.024 mmol each), h) VL (1.0 mmol, 1 equiv, 2 M), benzyl alcohol (0.02 mmol) **1-O**/MTBD

(0.05 mmol) (i) CL (1.3 mmol, 1 equiv, 2.25 M) **3-O**/MTBD (0.014 mmol each), (j) CL (0.85 mmol, 1 equiv, 1.1 M) **3-O**/BEMP (0.01 mmol each)

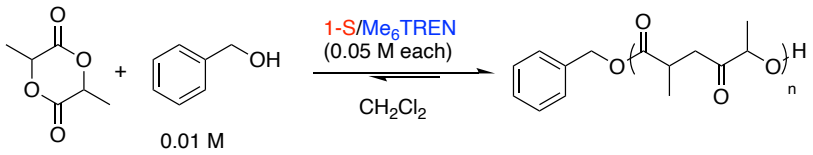

Entry	[L-LA]$_0$ (M)	Time (min)	Conv. %[b]	[M]$_o$/[I]$_o$	M_n[c] (g/mol)	M_w/M_n[c]	% iso[d]	T_m[e]
1	2.0	605	78	200	25330	1.05	0.98	168
2	1.0	248	90	100	18600	1.06	0.95	162
3	0.5	138	90	50	8400	1.08	0.92	158
4	0.4	130	90	38	6200	1.12	0.80	152
5	0.1	30	90	10	1200	1.14	-	-

Table 4.3. 1-S plus Me_6TREN cocatalyzed ROP of L-LA in CH_2Cl_2[a]

a) Reaction conditions: [LA]$_0$ =2 M to 0.1 M, benzyl alcohol (0.05 mmol, 0.010 M), **1-S**/ME$_6$TREN (0.024 mmol, 0.05 M each) in CH_2Cl_2. b) Monomer conversion was monitored via ^{1}H NMR. C) M_n and M_w/M_n were determined by GPC (CH_2Cl_2) versus polystyrene standards. d) % iso= fractional percent isotactic e) T_m obtained by DSC.

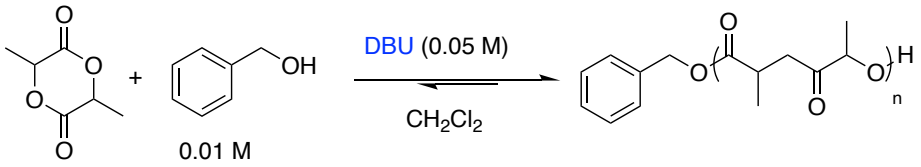

Entry	[L-LA] (M)	Time (min)	Conv. %[b]	$[M]_o/[I]_o$	M_n[c] (g/mol)	M_w/M_n[c]	T_m[d]
1	2	3	92	200	36100	1.08	152
2	1	5	92	100	22300	1.13	145
3	0.5	15	94	50	14000	1.10	139
4	0.25	30	95	25	6200	1.14	126

Table 4.4. DBU catayzed ROP of L-LA in CH_2Cl_2[a]

a. Reaction conditions: benzyl alcohol (0.010 M), DBU (0.05 M) in CH_2Cl_2. b) Monomer conversion was monitored via ^1H NMR. C) M_n and M_w/M_n were determined by GPC (CH_2Cl_2) versus polystyrene standards d) T_m obtained by DSC

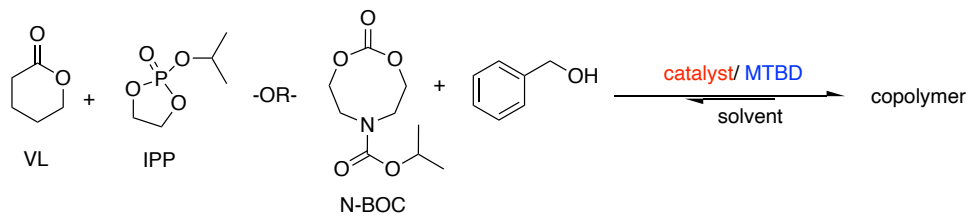

Entry	monomers	catalyst	Time (min)	Conv% (VL: IPP)	Order-VL	Order-IPP	M_n[b]	M_w/M_n[b]
1[c]	VL: IPP (1:1)	**1-S**	1215	62:100	1st	1st	25300	1.40
2[d]		**3-O**	60	82:83	2nd	1st	27300	1.52
3[c]	VL: N-BOC (1:1)	**1-S**	45	20:90	1st	1st	3900	1.14
4[d]		**3-O**	5	77:85	2nd	1st	4600	1.23

Table 4.5: One-pot copolymerization of IPP/N-BOC and VL[a]

a) Reaction conditions: 3 M ([VL] + [IPP]) 1 mmol total and 3 M ([VL] + [N-Boc]) 1 mmol total (b) M_n and M_w/M_n were determined by GPC (CH_2Cl_2) vs polystyrene standards. (c) **1-S**/MTBD (0.05 mmol each), benzyl alcohol (0.01 mmol) in CH_2Cl_2. (d) **3-O**/ MTBD (0.016 mmol)), benzyl alcohol (0.01 mmol) in acetone-d_6. c) **1-O**/MTBD (0.05 mmol each), benzyl alcohol (0.04 mmol) in CH_2Cl_2. (d) **3-O**/ MTBD (0.016 mmol), benzyl alcohol (0.04 mmol) in acetone-d_6.

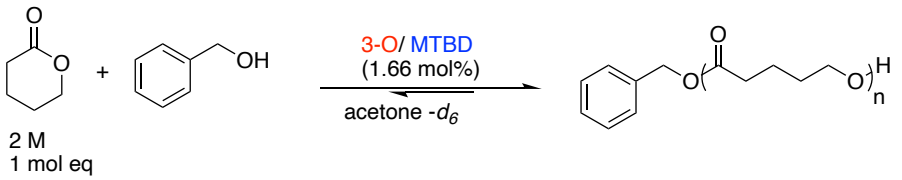

Entry	$[M]_0/[I]_0$	Conv. %[b]	M_n[c]	M_w/M_n[c]
1	50	90	7000	1.03
2	100	90	14170	1.04
3	200	89	28300	1.05
4	500	88	39900	1.12

Table 4.6. 3-O plus MTBD cocatalyzed ROP of VL[a]

a) Reaction conditions: VL (1.0 mmol, 1 equiv, 2 M), **3-O** /MTBD (0.0165 mmol) b) Monomer conversion was monitored via ^{1}H NMR c) M_n and M_w/M_n were determined by GPC (CH_2Cl_2) versus polystyrene standard)

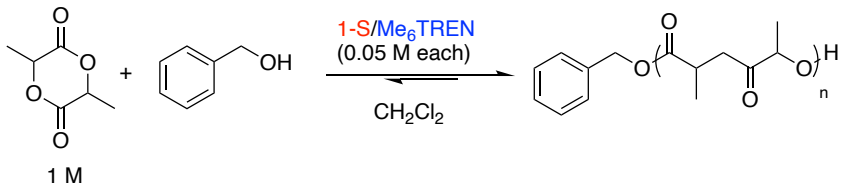

Entry	$[M]_0/[I]_0$	Conv. %[b]	M_n[c] (g/mol)	M_w/M_n[c]
1	200	90	34500	1.06
2	100	88	19400	1.07
3	50	94	11400	1.06

Table 4.7. 1-S plus ME_6TREN cocatalyzed ROP of L-LA[a]

a) Reaction conditions: LA (0.5 mmol, 1 equiv, 1 M), **1-S** / ME_6TREN (0.024 mmol) b) Monomer conversion was monitored via ^{1}H NMR c) M_n and M_w/M_n were determined by GPC (CH_2Cl_2) versus polystyrene standard.

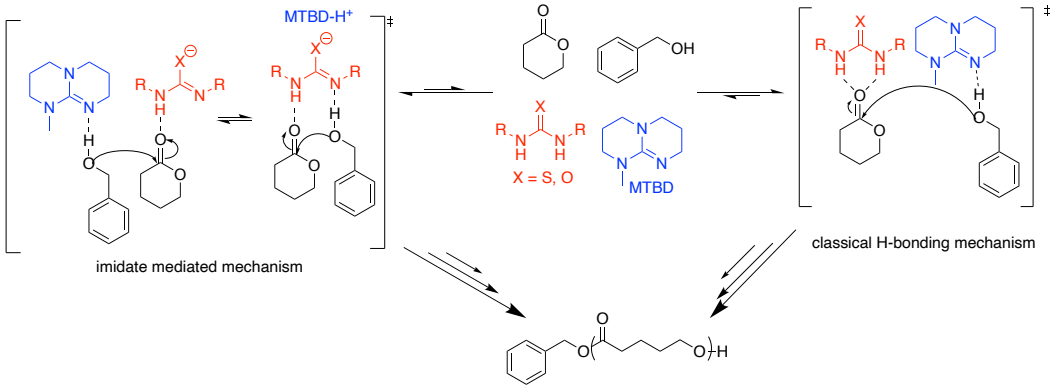

Scheme 4.1. Equilibrium between classical H-bonding mechanism and imidate mediated mechanism

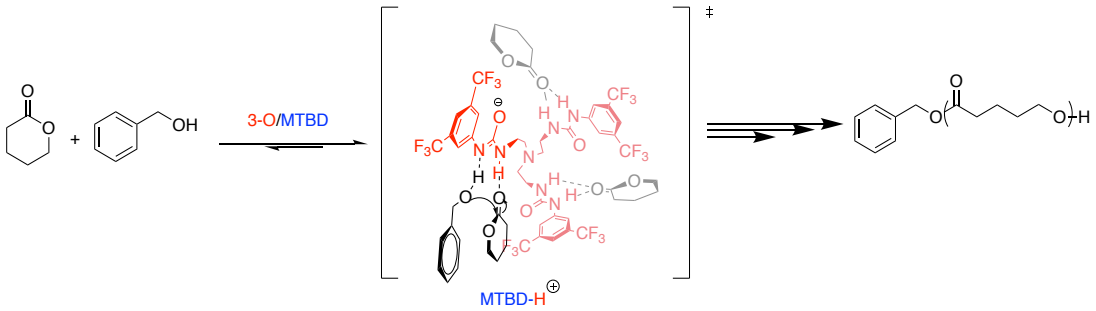

Scheme 4.2. Proposed Mechanism for the 3-O/MTBD cocatalyzed ROP of VL

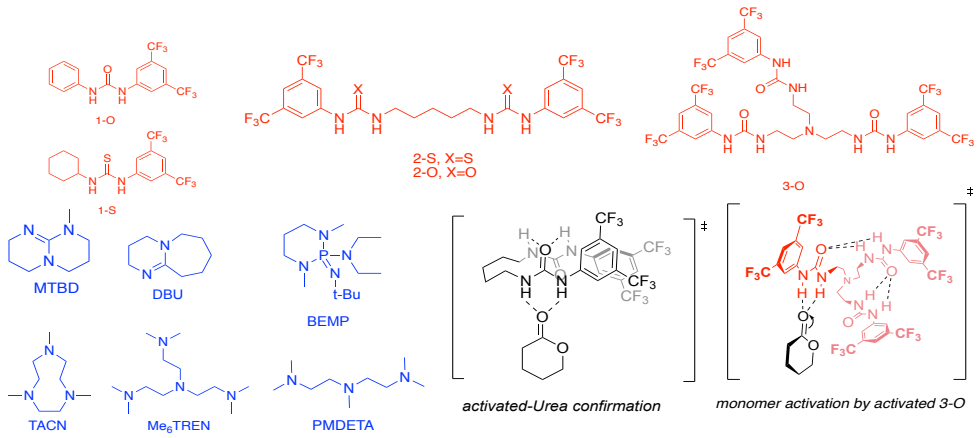

Figure 4.1. Base and Urea cocatalysts gaged for ROP

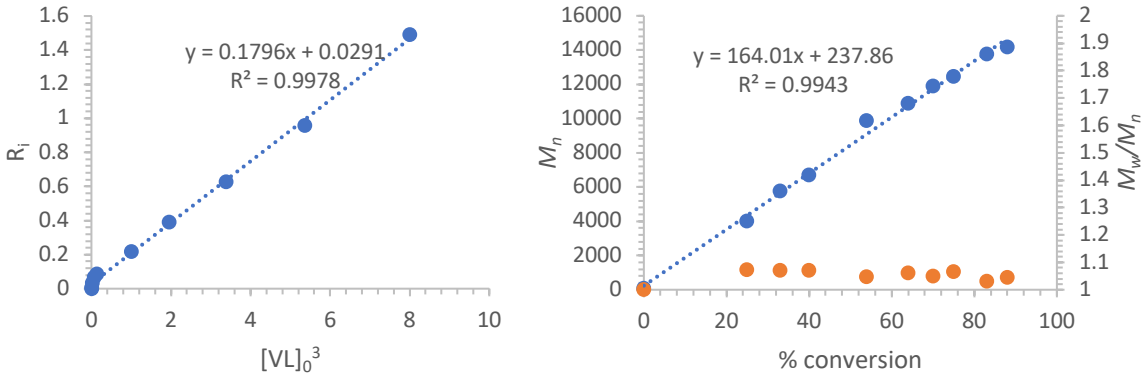

Figure 4.2. (left) For the ROP of VL , R_i versus $[VL]_0^3$. Reaction conditions: $[VL]_0$ (2 M to 0.2 M), benzyl alcohol (0.02 M), **3-O**/MTBD (0.033 M) in acetone-d_6. (right) M_n and M_w/M_n versus conversion for the **3-O** plus MTBD-cocatalyzed ROP of VL. Reaction conditions: VL (1.00 mmol, 2 M), benzyl alcohol (0.01 mmol, 0.02 M), **3-O**/MTBD (0.016 mmol, 0.033 M) in acetone-d_6.

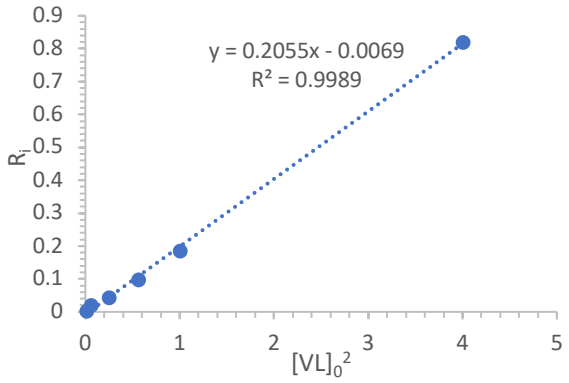

Figure 4.3. For the ROP of VL , R_i versus $[VL]_0^2$. Reaction conditions: $[VL]_0$ (2 M to 0.1 M), benzyl alcohol (0.02 M), **2-O**/MTBD (0.05 M) in acetone-d_6.

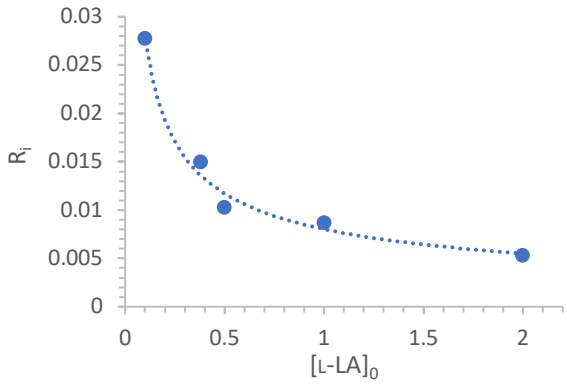

Figure 4.4. For the ROP of LA , R_i versus $[LA]_0$. Reaction conditions: $[LA]_0$ (2 M to 0.1 M), benzyl alcohol (0.01 M), **1-S**/ ME_6TREN (0.05 M) in CH_2Cl_2.

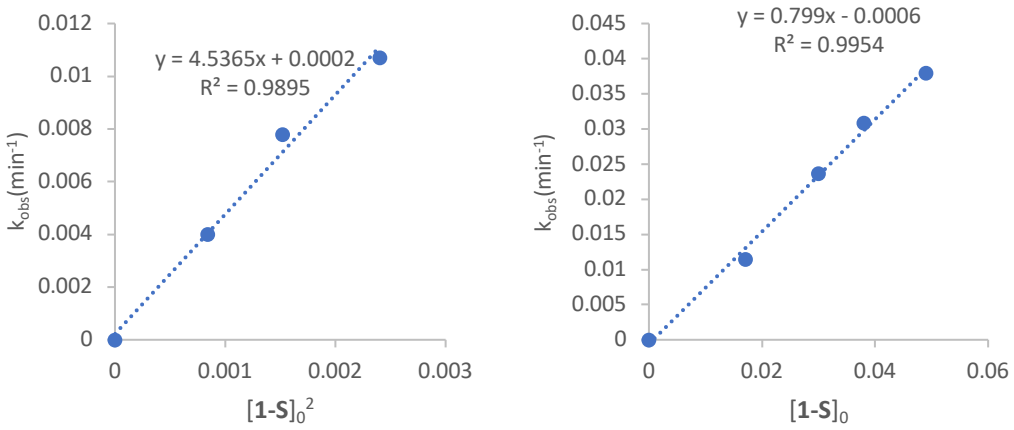

Figure 4.5. Observed rate constant, k_{obs}, versus initial concentration of the **1-S** (left) Second order kinetics in **1-S** :Reaction conditions: L-LA (2 M, 1.0 mmol) , benzyl alcohol (0.01 M), Me_6TREN (0.05 M) , $[\mathbf{1\text{-}S}]_0$ = (0.05 M to 0.029 M), (right) first order kinetics in **1-S**: Reaction conditions: L-LA (0.4 M, 0.2 mmol) , benzyl alcohol (0.01 M), Me_6TREN (0.05 M) , $[\mathbf{1\text{-}S}]_0$ = (0.05 M to 0.029 M). k_{obs} were obtained by first order evolution plots.

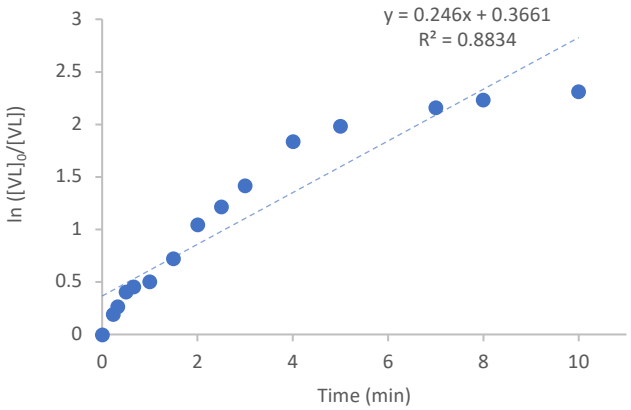

Figure 4.6. First order evolution of VL versus time for the **3-O** /MTBD cocatalyzed ring-opening polymerization of VL. Reaction conditions: VL (2 M, 1 mmol), benzyl alcohol (0.02 mmol), **3-O**/MTBD (0.016 mmol each) in acetone-d_6.

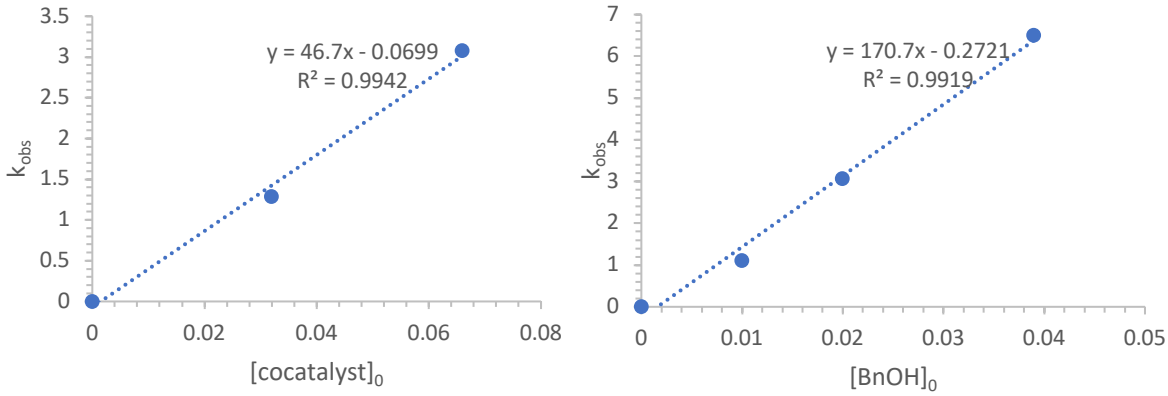

Figure 4.7. (left) For the ROP of VL , k_{obs} versus [[**3-O**] + [MTBD]]$_0$. Reaction conditions: [VL]$_0$ (1 mmol, 2 M), benzyl alcohol (0.01 mmol, 0.02 M), **3-O**/MTBD (0.016-0.033 M each) in acetone-d_6. (right) For the ROP of VL , k_{obs} versus [benzyl alcohol]$_0$ Reaction conditions: VL (1.00 mmol, 2 M), benzyl alcohol (0.01-0.04 M), **3-O**/MTBD (0.016 mmol, 0.033 M each) in acetone-d_6. k_{obs} were obtained by third order evolution plots.

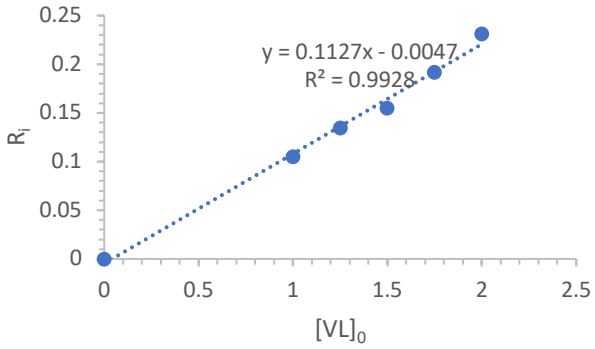

Figure 4.8. For the ROP of VL , R_i versus [VL]$_0$. Reaction conditions: [VL]$_0$ (2 M to 1 M), benzyl alcohol (0.02 M), **3-O**/MTBD (0.033 M) in C_6D_6

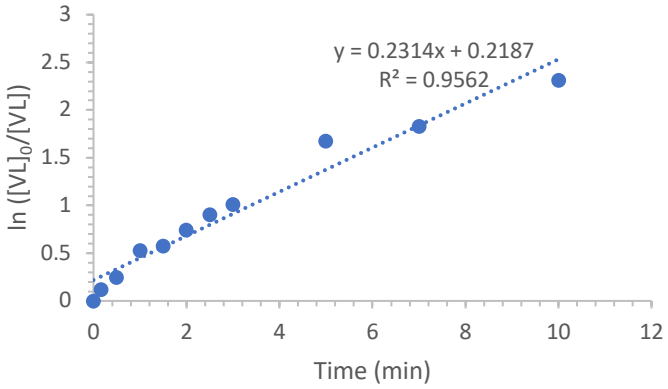

Figure 4.9. First order evolution of VL versus time for the **2-O** /MTBD cocatalyzed ring-opening polymerization of VL. Reaction conditions: VL (2 M, 1 mmol), benzyl alcohol (0.02 mmol), **2-O**/MTBD (0.024 mmol each) in acetone-d_6

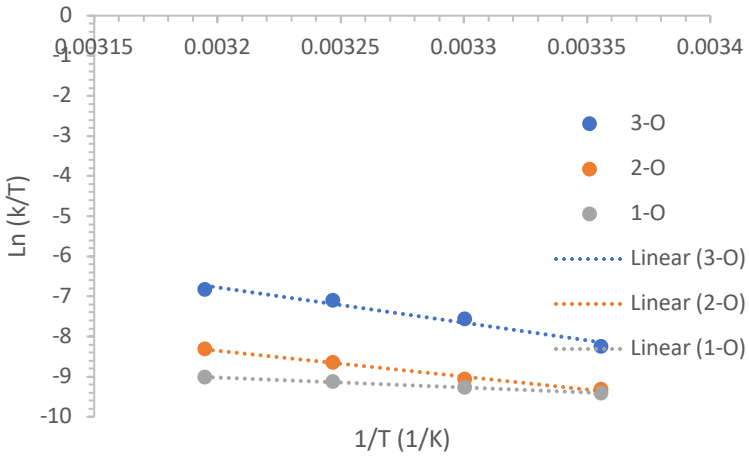

Figure 4.10. Eyring Plots for the ROP of VL co-catalyzed by **1-O**/MTBD (blue), **2-O**/MTBD (orange) and **3-O**/MTBD (gray). Reaction conditions: VL (0.5 mmol, 1 equiv, 1.00 M), benzyl alcohol (0.005 mmol), **1-O**, **2-O**, **3-O** (0.024 mmol, 0.012 mmol, 0.008 mmol respectively) and MTBD (matched to H-bond donor mmol) in acetone-d_6.

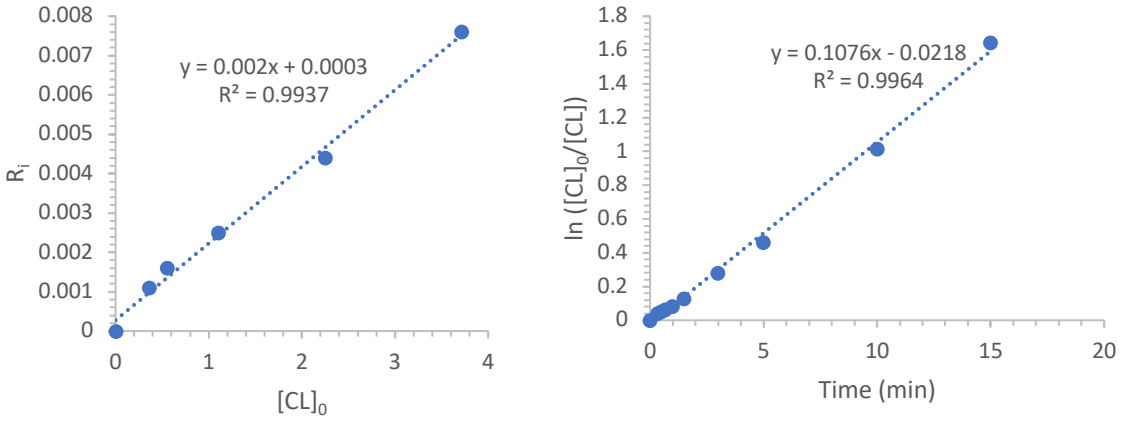

Figure 4.11. (left) For the ROP of CL , R_i versus $[CL]_0$. Reaction conditions: $[CL]_0$ (3.7 M to 0.4 M), benzyl alcohol (0.02 M), **3-O**/MTBD (0.033 M) in acetone-d_6. (right) First order evolution of CL versus time for the **3-O** /MTBD cocatalyzed ring-opening polymerization of CL. Reaction conditions: CL (1.75 M, 0.88 mmol), benzyl alcohol (0.008 mmol), **3-O**/BEMP (0.014 mmol each) in acetone-d_6

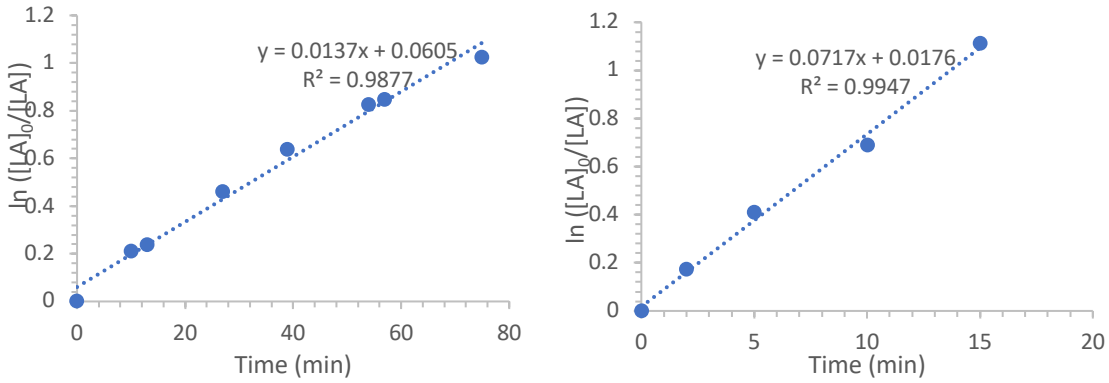

Figure 4.12. (left) First order evolution of LA versus time for the **1-S** / ME_6TREN cocatalyzed ring-opening polymerization of LA. Reaction conditions: L-LA (1 M, 0.50 mmol), benzyl alcohol (0.005 mmol), **1-S**/ME_6TREN (0.024 mmol each) in CH_2Cl_2. (right) First order evolution of LA versus time for the **2-S** / ME_6TREN cocatalyzed ring-opening polymerization of LA. Reaction conditions: L-LA (1 M, 0.50 mmol), benzyl alcohol (0.005 mmol), **2-S**/ME_6TREN (0.012 mmol each) in CH_2Cl_2.

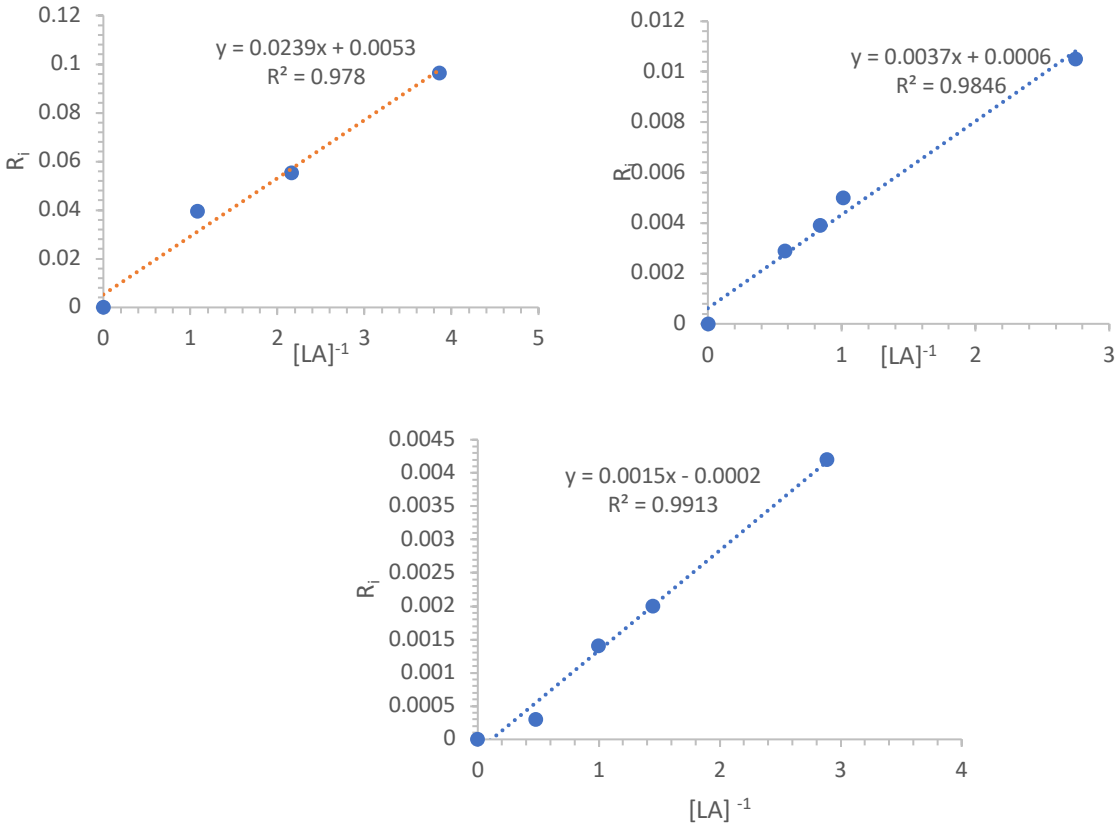

Figure 4.13. For the ROP of LA , R_i versus $[LA]^{-1}{}_0$. (left) Reaction conditions: $[LA]_0$ (2 M to 0.25 M), benzyl alcohol (0.01 M), **2-S**/ME_6TREN (0.024M each) in CH_2Cl_2. (right) Reaction conditions: $[LA]_0$ (1.75 M to 0.36 M), benzyl alcohol (0.01 M), **2-O**/ME_6TREN (0.024M each) in acetone-d_6. (bottom) Reaction conditions: $[LA]_0$ (1.5 M to 0.35 M), benzyl alcohol (0.01 M), **3-O**/ME_6TREN (0.015M each) in acetone-d_6.

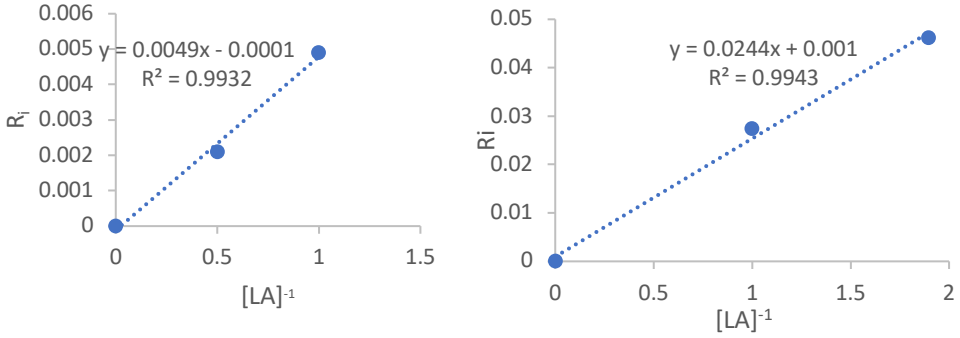

Figure 4.14. For the ROP of LA , R_i versus $[LA]^{-1}{}_0$. (left) Reaction conditions: $[LA]_0$ (2 M to 1 M), benzyl alcohol (0.01 M), **1-S**/PMDTA (0.05 M each) in CH_2Cl_2. (right) Reaction conditions: $[LA]_0$ (1 M to 0.5 M), benzyl alcohol (0.01 M), **1-S**/TACN (0.05 M each) in CH_2Cl_2.

MANUSCRIPT V

Formatted for publication in ACS macromolecules

Organocatalytic Synthesis of Poly-(thiono)esters from (thiono)macrolactones: New Materials from Sulfur-Containing Lactones

U. L. D. Inush Kalana, Rukshika S. Hewawasam, Partha P. Datta, and Matthew K. Kiesewetter

Chemistry, University of Rhode Island, Kingston, RI, USA

Corresponding Author: Matthew Kiesewetter, Ph.D.

Chemistry

University of Rhode Island

140 Flagg Road

Kingston, RI, 02881, USA

Email address: mkiesewetter@uri.edu

ABSTRACT

Synthesis of polymers with

sulfur on the polymer backbone is challenging, yet we synthesized poly(thiono)esters from (thiono)macrolactones. For the first time, organocatalytic ring-opening polymerization (ROP) of thiono-macrolactones was conducted. The ROP of less strained (thiono)macrolactones retains the characteristics of living polymerization even at elevated temperatures. The copolymerization of tnPDL and PDL showed altered material properties compared to its homopoly(thiono)lactone. The poly(thionolactones) were oxidized under mild conditions to synthesize solid, flexible, and porous crosslinked polymers with remarkable material properties yet undergoing hydrolytic degradation. These crosslinked polymers can be applied in gold recovery, which could extract Au^{3+} from an aqueous solution, which could be used as a polymeric water filter.

INTRODUCTION

Ring-opening polymerization (ROP) of cyclic lactones has come a long way from 2001 with the aid of organocatalysts.[1] Since then a wide a range of monomers have been used for ROP in the presence of H-bond mediated cocatalyst systems which have produced polymers with an excellent rate, selectivity, and control. [2–5] As the world's demand for the polyesters increases, polymers like poly (ω- petadecalactone) (PPDL) have attracted much interest as they resemble the material properties of low-density polyethylene (LDPE) as a consequence of its long aliphatic polymer backbones.[6] In previous studies, ROP of macrolactones like ω-Pentadecalactone (ω-PDL) has been carried out via enzymatic ring-opening polymerization (eROP) using enzymatic catalysts like Lipase B with broad molecular weight distribution (M_w/M_n).[7–10] Many reports promote metal-catalysts for the ROP of macrolactones.[6,11–15] Recently, N-heterocyclic molecules and phosphazene bases catalyzed ROPs have been carried out for macrolactones.[3,16,17] Recent studies in our lab have shown the ROP of ω-PDL, and Ethylene Brassylate (EB) can be easily executed to get controlled, well-defined polymers, in the presence of H-bond mediated cocatalyst system under solvent-free conditions at elevated temperatures.[18]

Sulfur-containing polymers have an increasing interest as modern materials due to their properties such as biodegradability, biocompatibility,[19] metal coordination ability, high refractive index, self-healing ability,[20] etc. However, the chemistry and the material

properties of sulfur-containing polymers are mostly unexplored. In 2016, our group disclosed H-bond mediated ROP of thiono-caprolactone (tnCL) in a controlled manner.[21] It was also revealed that replacing the O- atom in the carbonyl group (C=O) of the monomer by an S-atom is a unique and convenient method for tuning material properties.

Due to the unique chemical reactivity of sulfur, polymers with sulfur on their backbone can undergo a wide range of post-polymerization reactions such as; disulfide crosslinking. Recent studies have exemplified that disulfide crosslinked polymers hold promise for diverse applications including drug delivery, gene delivery, synthesis of self-healing materials, and molecular imprinting.[22–25] Thus, the unique properties of disulfide bonds should be taken as an advantage in designing and synthesizing novel polymer materials.

In this work, the organocatalytic ROP of a series of strained and less strained (thiono)lactones namely, ζ-heptalactone (HL), ζ-thionoheptalactone (tnHL), η-nonalactone (NL), η thiononononalactone (tnNL), ω-pentadecalactone (PDL), ω-thionopentadecalactone (tnPDL), ethylene brassylate (EB) and thiono-ethylene brassylate (tnEB) (Figure 5.1) was done with the use of H-bond mediated cocatalyst systems. This report demonstrates the formation of crosslinked polymers under mild reaction conditions to synthesize novel polymer materials with the potential of using as metal filters.

EXPERIMENTAL SECTION

General Considerations. All chemicals were used as received unless stated otherwise. Hexamethyldisiloxane (HMDO), P_4S_{10}, cycloheptanone, cyclooctanone, 3-chloroperbenzoic acid (*m*-CPBA) and 2-tert-butylimino-2-diethylamino-1,3-dimethylperhydro-1,3,2-diazaphosphorine (BEMP) were supplied by Acros Organics. Sodium thiosulfate ($Na_2S_2O_3$•$5H_2O$) was purchased from Allied Chemical. Sigma-Aldrich provided ω-pentadecalactone (PDL). Acetonitrile, potassium carbonate, sodium carbonate, sodium bicarbonate, sodium sulfate, magnesium sulfate, benzyl alcohol, benzoic acid, ethyl acetate, dichloromethane, toluene and hexane were purchased from Fisher Scientific. Acetone-d_6, chloroform-*d* and benzene-d_6 were supplied by Cambridge Isotope Laboratories and distilled from CaH_2 under a nitrogen atmosphere.O-dichlorobenzene was supplied by Fisher Scientific and distilled from CaH2 under nitrogen atmosphere. Benzyl alcohol was distilled from CaH_2 under high vacuum. Toluene was dried on an Innovated Technologies solvent purification system with alumina columns and nitrogen working gas. **1** [3,5-bis(trifluoromethyl)phenyl]-3-cyclohexyl-thiourea (CyTU), and **2** 1,1',1"-(nitrilotris(ethane-2,1-diyl))tris(3-(3,5-bis(trifluromethyl)phenyl)urea (Tris-U2C) were synthesized and purified according to literature procedures.[5,26] Triclocarban (TCC), 1,8-Diazabicyclo[5.4.0]undec-7-ene (DBU), 7-methyl-1,5,7-triazabicyclo[4.4.0]dec-5-ene (MTBD), and 1,5,7-triazabicyclo[4.4.0]dec-5-ene (TBD) were purchased from Tokyo Chemical Industry (TCI). All polymerization reactions were performed in an MBRAUN or INERT stainless-steel glovebox equipped with a gas purification system under a nitrogen

atmosphere using glass vials and magnetic stir bars which were baked overnight at 140 °C. NMR experiments were performed on a Bruker Avance III 300 MHz or 400 MHz spectrometer. The chemical shifts for proton (^{1}H) and carbon (^{13}C) NMR were recorded in parts per million (ppm) relative to a residual solvent. Size exclusion chromatography (SEC) was performed at 30°C in dichloromethane (DCM) using an Agilent Infinity GPC system equipped with three Agilent PLGel columns 7.5 mm × 300 mm (5 μm pore sizes: 103, 104, and 105 Å). M_n and M_w/M_n were determined versus polystyrene standards (500 g/mol − 3150 kg/mol; Polymer Laboratories). Mass spectrometry experiments were performed using a Thermo Electron (San Jose, CA, USA) LTQ Orbitrap XL mass spectrometer affixed with electrospray ionization (ESI) interface in a positive ion mode. Collected mass spectra was averaged for at least 50 scans. Tune conditions for infusion experiments (10 μL/min flow, sample concentration 2 μg/mL in 50/50 v/v water/methanol) were as follows: ion spray voltage, 4000 V; capillary temperature, 275°C; sheath gas (N_2, arbitrary units), 15; auxiliary gas (N_2, arbitrary units), 2; capillary voltage, 21 V; and tube lens, 90 V; multipole 00 offset, -4.25 V; lens 0 voltage, - 5.00; multipole 1 offset, - 8.50 V; Multipole RF Amplitude, 400 V; Ion trap's AGC target settings for Full MS was 3.0e4 and FT's 2.0e5 (with 3 and 2 averaged microscans , respectively). Prior to analysis, the instrument was calibrated for positive ions using Pierce LTQ ESI positive ion calibration solution (lot #PC197784). Differential scanning calorimetry (DSC) curves were obtained on a Shimadzu DSC-60A instruments under N_2 calibrated with an indium standard. The heating and cooling curves of DSC were run under a nitrogen atmosphere at a heating rate of ±10°C/min in a 40 μL aluminum pans. Thermogravimetric analysis (TGA) was performed using a TGA Q500 from TA

Instruments under a N_2 atmosphere at a heating rate of 10 °C/min from 25 to 600 °C. The surface analysis of the crosslinked polymer was carried out using the Thermo Scientific Photoelectron Spectrometer (XPS) equipped with 180^o double-focusing hemispherical analyzer and a monocromatized Al Kα radiation source. The rheology study for PtnPDL-CLP was done using an ARES-G2 rheometer with 25 mm parallel plates with 2.0 N axial force at room temperature.

Synthesis of ζ-Heptalactone (HL). The procedure to synthesize ζ-heptalactone (HL) was adopted from previous literatures with some modifications.[27] Initially, appropriate amount of *m*-CPBA (4.6 g, 18 mmol) was subjected to a round bottom flask, followed by the addition of dichloromethane (50 mL) and cycloheptanone (2.10 mL, 27 mmol). The reaction mixture was stirred at moderate speed for 5 days after which the reaction was quenched with 10% (w/v) sodium thiosulfate. The mixture was then washed with sodium bicarbonate followed by extraction with dichloromethane thrice. After drying with sodium sulfate, rotary evaporation was performed to yield a colorless oil. This oil was then purified by silica-gel column chromatography with 1:1 mixture of ethyl acetate and hexane. Yield: 2.17 g, 95%. Product matched previous literature characterization.[27]

Synthesis of η-Nonalactone (NL). The procedure to synthesize η-Nonalactone (NL) was adopted from previous literatures with some modifications.[11] Initially, cyclooctanone (10.0 g, 0.0792 mol) was subjected to a round bottom flask followed by the addition of dichloromethane (150 ml). The solution was cooled in an ice bath and an appropriate amount of *m*-CPBA (40.98 g, 0.2376 mol) was slowly added to the solution. The reaction mixture was then refluxed at 70 ºC for 7 days. After 7 days the solution was

cooled back to 0 ºC before removal of the salts through the vacuum filtration. The filtered solution was then washed with 10% (w/v) sodium thiosulfate (2 x 150 ml), saturated sodium carbonate (3 x 150 ml) and saturated sodium chloride (3 x 150 ml). After drying with magnesium sulfate, rotary evaporation was performed to yield a colorless oil. This oil was then purified by a Kugelrohr distillation at 40 ºC for 1 hour under 100 m Torr. Yield: 5.32 g, 53%. Product matched previous literature characterization.[11]

Synthesis of ζ-thionoheptalactone (tnHL). This procedure for the synthesis of ζ-thionoheptalactone (tnHL) was also adapted from a previous literature study with some modifications.[28] Similar to tnCL synthesis, HL (4.04 g, 31.50 mmol), HMDO (11.20 mL, 52.49 mmol), P_4S_{10} (3.04 g, 7.87 mmol) and acetonitrile (35 mL) were refluxed for 2 hours at moderate stirring. The reaction was cooled in an ice-water bath for 30 mins during which quenching with distilled water (2 mL/mmol of P_4S_{10}) and sodium phosphate dibasic (8 mmol/mmol of P_4S_{10}) was performed. Extraction with ethyl acetate followed thrice. After solvent removal, the yellow-orange oil was purified through a silica-gel column chromatography with 3:7 ethyl acetate-to-hexane solvent mixture to give a light-yellow solid powder in 42% yield, 1.89 g. The product was verified with previous literature characterization.[28]

Synthesis of η-thiononononalactone (tnNL. The procedure for the synthesis of η-thiononononalactone (tnNL) was also adapted from a previous literature study with some modifications.[28] NL (3.00 g, 21.11 mmol), HMDO (8.20 ml, 35.25 mmol), P_4S_{10} (2.51 g, 5.27 mmol) and acetonitrile (23 ml) were refluxed for 4 hours at 80 ºC and moderate

stirring. The reaction was cooled in an ice-water bath for 30 mins during which quenching with distilled water (2 ml/mmol of P_4S_{10}) and sodium carbonate (8 mmol/mmol of P_4S_{10}) was performed. The reaction mixture was then vigorously stirred at 0 ºC for 30 mins. The extraction was done with ethyl acetate (3 x 50 ml). After solvent removal, the yellow-orange oil was purified through a silica-gel column chromatography with 1:10 ethyl acetate-to-hexane solvent mixture to give a light-yellow oil. The product was further purified by a Kugelrohr distillation at 60 ºC for 2-3 hours under 200 m Torr. The product yield was 22%, 0.67 g.

Synthesis of ω-thionopentadecalactone (tnPDL). The synthesis of ω-thionopentadecalactone (tnPDL) was carried out according to the previous literature study.[28] PDL (5.00 g, 20.80 mmol), HMDO (7.38 ml, 34.72 mmol), P_4S_{10} (2.31 g, 5.19 mmol) and Xylene 20.80 ml was refluxed for 5 hours at moderate stirring. The reaction was then cooled in an ice-water bath for 30 mins during which quenching with distilled water (1 ml/mmol of P_4S_{10}) and sodium carbonate (4 mmol/mmol of P_4S_{10}) was performed. The reaction mixture was then vigorously stirred at 0 ºC for 30 mins. The extraction was done with hexane (3 x 50 ml). After solvent removal, the yellow-orange oil was purified through a silica-gel column chromatography with 1% ethyl acetate in hexane solvent mixture to give a light-yellow oil. The product was further purified by a Kugelrohr distillation at 120 ºC for 2-3 hours under 100 m Torr. The product yield was 42%, 2.1 g. The product was verified with previous literature characterization.[28]

Synthesis of thiono-ethylene brassylate (tnEB). Curphey's method was followed for the synthesis of thiono-ethylene brassylate (tnEB)[21].[29] The necessary reagents (ethylene brassylate (13 mL, 50 mmol), HMDO (17 mL, 80 mmol), P_4S_{10} (11.11 g, 25 mmol) and *o*-xylene (50 mL)) were refluxed for about 9 hours after which the reaction mixture was cooled in an ice-water bath for almost an hour after quenching the reaction with aqueous sodium carbonate solution and distilled water. Extraction was then executed with dichloromethane thrice. The yellow oil that was obtained after solvent removal was then subjected to silica gel column chromatography with 5:95 ethyl acetate-to-hexane mixture. Then removal of solvent gave the pure form of product in yellow oil with 50% yield, 7.54 g. HRMS m/z calcd ($C_{15}H_{27}O_2S_2^+$) 303.1447, found 303.1436. ^{1}H NMR (400 MHz, $CDCl_3$) δ 4.72 (s, 4H), 2.75 (t, *J*=7.2, 4H), 1.70 (p, *J*=7.1, 4H), 1.37 – 1.11 (m, 12 H). ^{13}C NMR (100 MHz, $CDCl_3$) δ 25.9, 25.9, 26.0, 26.2, 26.9, 45.9, 68.3, 223.4.

Example Ring opening polymerization of tnPDL. tnPDL (0.250 g, 0.975 mmol) was added to a 20 mL scintillation vial with a stir bar along with TCC (0.015 g, 0.048 mmol), BEMP (0.013 g, 0.048 mmol) and benzyl alcohol (1.0×10^{-3} g, 9.74×10^{-3} mmol) in the glovebox. The vial was then placed in a pre-heated hot plate within the glovebox set at 100 °C. The reaction mixture was then stirred until all the catalysts dissolved in the monomer solution. A quench solution of benzoic acid (2 mol eq. to base) in dichloromethane was made. Aliquots (~20 μL) were then taken from the reaction vial at various time intervals and quenched with a solution (~100 μL) from the benzoic acid solution. ^{1}H NMR was taken of the aliquot solution to determine conversion in $CDCl_3$. The polymer was then precipitated out of hexane and high vacuum was applied to

remove volatiles to subsequently obtain molecular weights by GPC.Yield 62%; Mw/M_n = 1.8; $M_{n\ (GPC)}$= 35800; $M_{n\ (NMR)}$ = 21000. ^{1}H and ^{13}C NMR spectra display characteristic resonances of the polymer with thionoester repeat unit and thiocarbonyl peak at 224 ppm in the ^{13}C spectrum (see Figure 5.25).

Example of co-polymerization of tnPDL and PDL. PDL (125 mg, 0.52 mmol) and tnPDL (125 mg, 0.48 mmol) were added to a 20 mL scintillation vial with a stir bar along with TCC (0.015 g, 0.050 mmol), BEMP (0.013 g, 0.050 mmol) and benzyl alcohol (1.0×10^{-3} g, 0.01 mmol) in the glovebox. The vial was then placed in a pre-heated hot plate within the glovebox set at 100 °C. The reaction mixture was then stirred until all the catalysts dissolved in the monomer solution. A quench solution of benzoic acid (2 mol eq. to base) in dichloromethane was made. Aliquots (~20 μL) were then taken from the reaction vial at various time intervals and quenched with a solution (~100 μL) from the benzoic acid solution. ^{1}H NMR was taken of the aliquot solution to determine conversion in $CDCl_3$. The polymer was then precipitated out of hexane and high vacuum was applied to remove volatiles to subsequently obtain molecular weights by GPC. Yield 80%; Mw/M_n = 1.6; $M_{n\ (GPC)}$= 33800; and ^{13}C NMR spectra display characteristic resonances of the polymer with thionoester repeat unit and peaks at 224 ppm and 174 ppm for thiocarbonyl and carbonyl respectively in the ^{13}C spectrum (see Figure 5.26).

Synthesis of P(tnPDL-b-CL) polymer- The synthesis of block co-polymer was started with the ROP of tnPDL. The ROP of tnPDL was carried out same as above. The homopolymer was washed with methanol to use for the next step of the polymerization

process. The ROP of CL (0.5 M, 0.781 mmol) was then carried out with TCC/BEMP (5 mol%,0.0478 mmol) at room temperature in dichloromethane, using the purified PtnPDL as a macro-initiator. A quench solution of benzoic acid (2 mol eq. to base) in dichloromethane was made. Aliquots (~20 μL) were then taken from the reaction vial at various time intervals and quenched with a solution (~100 μL) from the benzoic acid solution. ^{1}H NMR was taken of the aliquot solution to determine conversion in $CDCl_3$. The polymer was then precipitated out of hexane and high vacuum was applied to remove volatiles to subsequently obtain molecular weights by GPC. Yield 75%; Mw/M_n = 2.0; $M_{n\ (GPC)}$= 31000; and ^{13}C NMR spectra display characteristic resonances of the polymer with thionoester repeat unit and peaks at 224 ppm and 174 ppm for thiocarbonyl and carbonyl respectively in the ^{13}C spectrum (Figure 5.27).

Determination of Thermodynamic Parameters for tnHL . A polymerization reaction was run with tnHL (0.100 g, 0.693 mmol), TBD (4.83×10^{-3} g, 0.035 mmol) initiated from benzyl alcohol (7.50×10^{-4} g, 6.93×10^{-3} mmol) in C_6D_6 (1 M in monomer) inside an NMR tube. After determining equilibrium for the reaction at room temperature, ^{1}H NMR was acquired from 298 K to 333 K by heating the sample in a variable temperature NMR probe. Data points were taken twice, during heating and cooling. Since both the heating and cooling $[M]_{eq}$ values are within error of each other, only the heating values were considered. Then the thermodynamic values for the ROP of tnHL were determined from a Van't Hoff plot of the data where the error was calculated from linear regression at 95% confidence interval.

Example of Synthesis of cross-linked polymer. The polyhomo(thionolactone) or co-polymer was dissolved in CH_2Cl_2 and transferred in to a 6-8 kDa dialysis bag and stirred in methanol for an overnight. The purified homo-polymer was then dried under reduced pressure. The cleaned homo- polymer was then weighed (~200 mg), transferred to a 100 ml beaker and was dissolved in 4 ml of CH_2Cl_2. To the beaker with the dissolved polymer, 20 ml of excess aqueous NaOCl was added. The reaction mixture was then vigorously stirred for18 hours to obtain a white color solid polymer. The solid polymer was then blotted on paper towels to remove excess solvent and dried under reduced pressure. The dried polymer was then washed with water to remove excess NaOCl. The polymer was then dried again under reduced pressure. The product recovery was >99.99% (~200 mg).

Procedure for hydrolytic degradation study of PtnPDL-CLP. Polymer samples (approximately 25 mg of the cross-linked polymer) were transferred into empty 20 mL scintillation vials. Each vial was charged with 10 mL of aqueous 0.25 M HCl, aqueous 0.25 M NaOH solution, or distilled water. All vials were vigorously stirred for the duration of the study. To take a data point the polymer pieces were taken out from the solution and blotted to remove the aqueous solution form the surface. Then the polymer samples were dried under high vacuumed for an overnight and weighed. The percent mass loss is given $[mass]_o - [mass]_i / [mass]_o$.[21] The same steps were repeated over a ten days period daily.

Procedure for gold extraction with different amounts of PtnPDL-CLP. A 100 ppm Au^{3+} solution was prepared by dissolving 10 mg of $NaAuCl_4.2H_2O$ salt in 50 ml of DI water. The absorbance was measured for a diluted series of the Au^{3+} solution with different concentrations (5 ppm, 25 ppm, 50 ppm and 75 ppm) using UV-vis spectrophotometer to construct the calibration curve. Into a 10 ml of 100 ppm Au^{3+} solution, was added 25 mg, 50 mg and 100 mg of small PtnPDL-CLP pieces. The solution was stirred for three days and the remaining concentration of Au^{3+} was measured at different time periods using UV-vis spectrophotometer to calculate the extraction efficiency.

Procedure for gold recovery from pyrolysis. Into a 10 ml of 100 ppm Au^{3+} solution, 50 mg of small PtnPDL-CLP pieces was added and stirred for 3 days. The supernatant was removed, and the polymer was dried under high vacuum at room temperature to afford 53.20 mg gray colored solid polymer. The polymer was then pyrolyzed in air at 1000 ˚C for 30 minutes with the heating rate of 10 °C/min to afford 0.45 mg of gold metal. The recovery of extracted Au^{3+} as gold metal after the pyrolysis was 99%.

RESULTS AND DISCUSSION

Organocatalytic ROP of (thiono)macrolactones

The efficacy of cocatalyst systems for the ROP of newly synthesized (thiono)macrolactones was evaluated. The TCC/BEMP cocatalyzed ROP of macro(thiono)lactones in non-polar solvents proved to be the optimized conditions (Table 5.1). Though, NL showed better rates and controlled polymerization with **2**/BEMP in benzene. The ROP of (thiono)macrolactones initiated from benzyl alcohol exhibited the characteristics of a living polymerization, which is typical for organocatalyzed ROP of strained lactones (Figure 5.2). Initiation of a tnNL (2.0 M) ROP cocatalyzed by TCC/BEMP (0.031 mmol each) from 1-pyrenebutanol (0.012 mmol) exhibits overlapping UV, and refractive index traces in the gel permeation chromatogram (GPC) of the resulting polymer indicates the high-end group fidelity (Figure 5.7). In general, the polymerization rates of the (thiono)macrolactones are faster than their corresponding oxygenated lactones, which were also observed in previously published reports.[21] It was proposed that the increase in electrostatic charges and the polarity of the C=X (X=O/S) bond of the monomer in the binding of TCC could affect the reaction rates. However, the ROP of tnHL showed lower reaction rates than expected (Table 5.1), which contrasts the behavior of CL versus tnCL in the presence of **1**.[21]

Larger ring size monomers, (tn)PDL and (tn)EB need to be polymerized at an elevated temperature due to the low ring strain and to enhance the entropic driving force for the reaction.[11] Thus, the ROP of (tn)PDL was done at high monomer concentration (5 M,

0.974 mmol) using TCC/base (5 mol%,0.0478 mmol) at 100 ˚C in toluene and was able to generate high monomer conversions (Table 5.1), while, no conversion was observed for the same ROP at room temperature. The ROP of tnPDL showed a linear evolution plot of molecular weight versus conversion and the linear first-order kinetics, exhibiting the living characteristics of this system with a comparatively narrow M_w/M_n (Figure 5.10). Though the organic catalysts are susceptible to decomposition at high temperatures,[30] neither decomposition nor deactivation was observed for TCC/base cocatalyzed system at high temperatures, which proves the thermal stability of the H-bonding catalysts. TBD catalyzed ROP of (thiono)macrolactones shows relative low rates (Table 5.6) compared to TCC/base cocatalyzed ROP at elevated temperatures, which is consistent with published data.[18]

High conversions for the ROP of (tn)EB were restricted even with the optimized conditions where only 64% conversion was obtained (Table 5.1). This is consistent with previous ROP results of EB in solvent where 44% conversion was reached while neat conditions produced almost full conversion.[18] This is also in correlation with what can be expected for macrolactones of this ring size, where the entropic driving force for the reaction with minimal or negligible contribution from enthalpy for ROP.[31] Though, tnEB showed a 1st order linear evolution, the linearity of the molecular weight versus conversion curve has deviated as it approaches higher conversions (Figure 5.11).

With the increment of the ring size, it is more prone to higher transesterification reactions, which can interrupt the controlled and living behavior of polymerization of (thiono)macrolactones. As illustrated in Table 5.1, the M_w/M_n of the ROP of the eight-

membered ring (tn)HL and M_w/M_n of the ROP of seventeen membered ring (tn)EB are 1.04 and 1.90 respectively. This is generally expected for macrolactone, and to mitigate this issue copolymerization has been performed for this monomer's oxygenated derivative with other lactones.[5,9,18,32,33] Additionally, high molecular weights were not obtained ($[M]_0/[I]_0 \geq 100$) for ROP of (thiono)macrolactones, consistent with the previous observations[3,18] which indicates the importance of the emergence of efficient organocatalysts.

Previous studies have reported the homopolymerization of NL using Mg $(BHT)_2(THF)_2$, which took longer and required heating at 80˚C.[11] However, we performed the ROP of NL (2M, 0.703 mmol) using organic cocatalysts **2** /BEMP (1.67 mol%, 0.0117 mmol) at room temperature in a living and controlled manner (Table 1, Figure 5.12). At elevated temperatures, the ROP of NL with **2**/BEMP (1.67 mol%, 0.0117 mmol) in toluene showed rapid reaction rates, yet the polymerization is living and controlled (Table 5.7). The ROP of tnNL (2 M, 0.632 mmol) was carried out with TCC/BEMP (5 mol%, 0.0315 mmol) cocatalyst system to form PtnNL and much faster rates (99% conversion in 4 hrs) were observed compared to PNL with relatively good control in M_n and M_w/M_n (Figure 5.2). The scale of the ring size, starting from 9 membered cyclic lactone ((tn)NL) indicates macrolactone behavior in terms of a more extended period to reach the equilibrium and broader M_w/M_n.

To identify the driving force for the ROP of the (thiono)macrolactones, monomer equilibrium concentration $[M_{eq}]_o$ was measured as a function of the temperature to construct the Van't Hoff plots (Figure 5.13 and 5.14). All (thiono)macrolactones

(tn(NL),tn(PDL),tn(EB)) showed zero to almost negligible enthalpic contribution while entropy values were substantial when compared to smaller lactones, like (tn)HL (See SI). The thermodynamic data suggest the ROP of larger lactones is mainly governed by entropy as expected.[16]

Mechanistic aspects of ROP

Mechanistic studies by our group and others have shown that ROP can proceed by one of two mechanisms; neutral H-bonding or imidate (Scheme 5.1).[26,34–36] It is proven that in polar solvents and at high temperatures, it is more favored via imidate mechanism. We observed that decreasing rates for the ROP of (thiono)macrolactones (tnNL,tnPDL and tnEB) in polar solvents. Thus, we believe that the bulkiness of monomers could minimize the dual functionality of the imidate structure, which resulted in low rates. Herein, we propose, classical H-bond mediated mechanism for the ROP of (thiono)macrolactones in non-polar solvents. (Scheme 5.2)

Co-Polymerization of macrolactones

The copolymerization of tnPDL and PDL was also carried out in one pot. TCC/BEMP (5 mol%, 0.0478 mmol each) were added to the mixture of PDL (2.5 M, 1.0 equiv), tnPDL (2.5 M, 1.0 equiv) and benzyl alcohol (1 mol%, 0.0097 mmol) in toluene at 100 ˚C. The polymerization achieved full conversion in 5 hrs resulting in a high polymer with comparatively narrow molecular weight distribution (M_n = 34100, M_w/M_n = 1.66). Both monomers were observed to undergo ROP at similar rates with a rate constant ratio of 1.40 (k_{tnPDL}/k_{PDL} = 1.40), suggesting it forms a random copolymer (Figure 5.15).

Furthermore, the ^{13}C NMR confirms the random monomer incorporation in copolymerization with equal intensities of the tnPDL-tnPDL versus tnPDL-PDL resonances (both at 72.52 ppm) (Figure 5.26). The material properties of the P(tnPDL-*co*-PDL) were analyzed by differential scanning calorimetry (DSC). The T_m of PPDL and PtnPDL showed as 93 ˚C and 54 ˚C respectively, whereas P(tnPDL-*co*-PDL) showed 63 ˚C which demonstrate the alteration of material properties in the presence of S on the polymer backbone.

The poly-thionolactones showed different material properties compared to their corresponding poly-lactones. In previous studies reported by our group disclosed that the homopoly(ε-thionocaprolactone) (PtnCL) is a liquid polymer,[21] correspondingly PtnHL, and PtnNL are liquid polymers, whereas PtnPDL and PtnEB are amorphous polymers. Due to the size of the S atom on the polymer backbone, the inter and intramolecular polymer chain interaction may get restricted ensuing liquid/amorphous polymer materials.

Crosslinked polymers (CLPs) from poly(thiono)lactones

The poly(thionolactones) synthesized in this study contain thiocarbonyl groups on their polymer backbone. The ability of sulfur to reach higher oxidation states facilitate the inter/intramolecular crosslinking of these polymers. The homopolymer of tnPDL (PtnPDL) was firstly treated with an excess amount of commercially available NaOCl at room temperature to synthesize the PtnPDL crosslinked polymer (PtnPDL-CPL) (See **SI**). The resulting product turned out to be a white-colored(opaque), insoluble, and

flexible solid polymer (Figure 5.3. (a)). The opaqueness of the polymers is due to the light scattering by the highly crosslinked polymer network.[37,38]

Characterization of crosslinked porous polymer

Surface characterization was done for the PtnPDL-CLP, using X-ray photoelectron spectroscopy (XPS). The experiment was carried out in a Thermo Scientific XPS instrument equipped with 180° double-focusing hemispherical analyzer and a monocromatized Al Kα radiation source. As the polymer is a non-conductive material, the surface was hit by the electrons using a flood gun. Binding energy (BE) corrections were done taking the position of C-H/C-C at 284.7 eV as a reference. The sample was dried under reduced pressure for overnight before the experiment, and the pressure of the analysis chamber was in the range of 10^{-9} – 10^{-10} mbar to assure a low level of surface contamination during the experiment. The sampling spot size of the experiment was 200 μm.

The basic surface analysis was carried out for the carbon (C) and sulfur (S) elements to discover the functional groups involved in crosslinking. As shown in Figure 5.4 (a). the experiment was carried out for C 1s core and S 2p core. The C 1s region always shows significant, intense, and well-separated peak shifts as C changes its oxidation states.[39] In Figure 5.4 (a), the 286.1 eV represents the ester linkage on the polymer backbone. The peak at 287.0 eV signifies the polymer's carbon-sulfur functional group, which is involved in the formation of the inter/intramolecular crosslinking. The peak with the

highest BE (288.9 eV) illustrates the unoxidized/unreacted thiocarbonyl groups on the polymer backbone.

Figure 5.4 (b) shows the BEs of S 2p, and the two peaks represent the different oxidation states of the sulfur atom.[40] The peak at 163.9 eV embodies the disulfide (S-S) groups, whereas the peak at 168.3 eV signifies the sulfone (R`R-SO_2) groups in the polymer network. However, the peak intensities of the two peaks illustrate that the polymer contains more sulfone groups over disulfide groups, which is also proven by the area under the curve ratio (sulfone groups: disulfide groups is 8:1). The XPS data of S 2p demonstrate sulfone and disulfide groups as the possible functional groups involved in the inter/intra-polymer chain crosslinking process.

A dynamic rheology study was carried out on an ARES G2 rheometer (TA Instruments, USA) to characterize the viscoelastic properties of the PtnPDL-CLP. The mechanical response of the crosslinked polymer was measured as it is deformed under shear stress (or strain), which illustrates the relationship between mechanical behavior and the molecular motion of the polymer. The rheology study was done by measuring shear storage modulus (or storage modulus) (G′) and shear loss modulus (or loss modulus) (G″) as a function of angular frequency (ω) using parallel plates at room temperature. The experimental results showed a decrement of G′ and an increment of G″ with the increasing angular frequency (See Figure 5.16), which demonstrates a reduced elastic behavior and an increased viscous behavior of the material; when applying a workforce. The crossover point of G′ and G″ suggests the formation of a three-dimensional network of the CLP.[41]

With the inspiration of the synthesis of PtnPDL-CLP, the oxidation of the homopolymers of tnCL (PtnCL), tnHL (PtnHL), and the di-block copolymer of P(tnPDL-*b*-CL) was carried out to synthesize their corresponding CLPs (PtnCL-CLP, PtnHL-CLP, and P(tnPDL-*b*-CL)-CLP). As shown in Figure 5.3(b), the morphology of all CLPs turned out to be opaque, solid, and flexible. Besides, the cross-sectional images of the CLPs taken by the optical microscope showed that all CLPs have a porous polymer network (Figure 5.3(c)), which occurred due to the crosslinking. Thus, porosity% of each polymer was obtained via the swelling test.

Each of the CLP disk was pre-weighed (W_d) before the test and was immersed in THF for a total of 20 minutes at room temperature (23 ˚C). At 2 minutes intervals, the polymer disk was removed from the solvent, and the excess surface THF was removed by blotting on a filter paper to get the swollen disk weight (Ws). The swelling ratio was determined using equation (1).[40]

$$Swelling\ ratio\ = \frac{(Ws - Wd)g}{(Wd)\ g} \qquad (1)$$

The final swollen weights (Ws) of the CLP disks were used to calculate the porosity of the polymer material using equation (2), where V is the volume of the CLP disk, and ρ is the density of THF(0.8892 g cm^{-3}).[42] Results were averaged on three independent runs.

$$Porosity\ \% = \frac{(Ws - Wd)}{V\rho} \times 100 \qquad (2)$$

The order of increasing swelling ratios for the polymer disks was P(tnPDL-*b*-CL) > PtnPDL-CLP > PtnHL-CLP > PtnCL-CLP, indicating that the extent of crosslinking has a profound influence on the solvent absorption capability of the CLPs (See Figure 5.17). Similarly, the calculated porosity% values are proportional to the swelling ratios (Table 5.2), which illustrates that the polymer chain length may affect the porosity of the CLPs. This observation led us to investigate the crosslinked densities of the CLPs.

Before the calculation of crosslinked densities, the Flory-Huggins polymer-solvent interaction parameter (χ) was calculated by using equation (3). δ_1 and δ_2 stand for the solubility parameters of the solvent (THF = 18.30 $J^{1/2}$ $cm^{-3/2}$) and the polymer respectively, where *Vs* is the molar volume of the solvent, *R* is the universal gas constant, and *T* is the absolute temperature.[43] Here, we use the Hansen solubility parameters of PPDL (17.5 $J^{1/2}$ $cm^{-3/2}$) and PCL (19.5 $J^{1/2}$ $cm^{-3/2}$) to estimate the interaction parameter (χ) of the CLPs.[44,45] As the solubility parameter is independent on the molar volume of the solvent (*Vs*), it is a convenient metric when comparing structurally dissimilar polymer networks.[46] Thus, we assumed the solubility parameter values of PtnCL-CLP and PtnHL-CLP are same as PCL, where PtnPDL-CLP and P(tnPDL-*b*-CL)-CLP are same as PPDL.

$$\chi = \frac{(\delta 1 - \delta 2)^2 \, Vs}{RT} \qquad (3)$$

The crosslinked densities were calculated based on Flory-Rehner equation (4) using the data obtained from the swelling test.[43]

$$-[\ln(1-Vp)+Vp+\chi Vp = Vs\boldsymbol{n}[Vp^{\frac{1}{3}}+\frac{Vp}{2}] \qquad (4)$$

Vp is the volume fraction of polymer in the swollen weight, and ***n*** stands for the crosslinked density of the polymer. The results in Table 5.2 give a better understanding of the relationship between the porosity% and the crosslinked density, where a gradual decrement of the porosity was shown with the increment of the crosslinked density (Figure 5.18). The crosslinked di-block copolymer (P(tnPDL-*b*-CL)-CLP) showed the highest porosity% (~ 82 %), and the lowest crosslinked density **(**0.45 mmol.cm^{-3}) as only a half of the polymer backbone can get crosslinked. Furthermore, the P(tnPDL-*b*-CL)-CLP becomes a transparent polymer once it is immersed in the solvent (Figure 5.19). The high porosity and the rearrangement of the crosslinked polymer network could result in a transparent polymer in the presence of a solvent.

Thermal stability and degradation of CLP

The crosslinked homopolymer of PtnPDL exhibited remarkable thermal stability, yet the polymer is degradable. Thermal Gravimetry Analysis (TGA) was conducted under nitrogen to examine the thermal stability of the PtnPDL-CLP. The TGA data revealed an onset temperature of decomposition (T_d) of 421 ˚C with less than 10% mass loss up to T_d. Furthermore, the hydrolytic degradation study was carried out for the PtnPDL-CLP. In this experiment, a 20 ml scintillation vial was charged with a 25 mg piece of PtnPDL-CLP, deionized water, 0.25 M solution of HCl, or 0.25 M solution of NaOH. The weight of the insoluble CLP piece was monitored over time (Figure 5.5). Under basic conditions, the polymer showed a rapid degradation compared to acidic and

neutral conditions, as observed in previous studies.[21] The CLP degraded to approximately more than half of its original mass after 10 days.

Gold recovery application of CLP

Besides the currency value, gold is a metal with outstanding properties such as good ductility, high thermal/electrical conductivity, and chemical stability.[47] The annual demand for gold is around 4000 t/year and 1500 t of it produced by recycling industrial products, including electronic wastes (e-waste), which have a much higher gold content (300-350 g/t) compared to an economical grade ore (0.3-17 g/t).[48,20] Alkyl cyanides and other alternative leachants, including thiourea, thiosulfate, bromide, iodide, and sodium hypochlorite, have been used to recover gold. Yet, they have their own drawbacks such as toxicity and low efficiency.[20,47,49] Thus; greener approaches have a high demand for gold recovery. In recent studies, high sulfur content polymers and polythioamides have been used to recover gold because of their strong metal coordination properties.[20,50] As it is shown in the XPS data in Figure 5.4, the PtnPDL-CLP has unoxidized C=S on the polymer backbone in addition to crosslinked S-S. Thus, a hypothesis was built up that the CLP might be able to extract gold ions from an aqueous solution.

The PtnPDL-CLP was used to investigate the ability of its metal complexation. In this study, different amount of PtnPDL-CLP was added into the aqueous solution of Au^{3+}. The polymer was stirred in the Au^{3+} solution for three days, and it was observed that the solution was fading with time (Figure 5.6.a). The remaining Au^{3+} concentration of the supernatant was measured at different time intervals by UV-vis spectrophotometer to

calculate the extraction efficiency (Figure 5.20). It was disclosed that the extraction capacity depends on the amount of CLP added, whereas 52%, 77%, and 88% extraction efficiencies were shown by the samples with 25 mg, 50 mg, and 100 mg of CLPs, respectively. Hence it proves that the newly synthesized CLPs are capable of extracting gold from aqueous solutions.

Subsequently, the extracted gold was recovered from the CLP by pyrolysis of the (PtnPDL-CLP)-Au^{3+} complex. The complex was heated at 1000 ˚C in the air for 30 minutes to recover 99% of the extracted gold (Figure 5.6.b). Recent studies have shown the sulfur-containing polymers are also capable of extracting toxic heavy metals.[20,50] Thus, we believe these newly synthesized crosslinked porous polymers have a high potential of using as a polymeric filter in the application of water purification.

CONCLUSION

The organocatalytic ROP of (thiono)macrolactones exhibit characteristics of "living" polymerization in the presence of an H-bond donor. Fast reaction rates were observed for (thiono)macrolactones with TCC/base cocatalyst system in non-polar solvents at elevated temperatures, and it was proven the polymerizations are entropically driven. The copolymer synthesized from tnPDL and PDL showed altered material properties. The S-atom's unique reactivity was taken as an advantage to synthesize novel crosslinked polymer materials from homopoly(thiono)lactones and block copolymers via oxidation reaction under mild conditions. The resultant material turned out to be a porous, solid, and flexible polymer. Polymer characterization and material property analysis revealed that the polymer is degradable and has higher thermal stability. Further, the extent of the porosity and the degree of crosslinking were studied. It was disclosed these polymers could be utilized in gold recovery due to the binary coordination between S and Au^{3+}. Thus, we believe those polymers have a high potential of absorbing other heavy metals and can be used for water purification.

REFERENCES

1. Lohmeijer, B. G. G. *et al.* Guanidine and amidine organocatalysts for ring-opening polymerization of cyclic esters. *Macromolecules* **39**, 8574–8583 (2006).

2. Kiesewetter, M. K., Shin, E. J., Hedrick, J. L. & Waymouth, R. M. Organocatalysis: Opportunities and challenges for polymer synthesis. *Macromolecules* **43**, 2093–2107 (2010).

3. Bouyahyi, M., Pepels, M. P. F., Heise, A. & Duchateau, R. ω-Pentandecalactone Polymerization and ω-Pentadecalactone/ε-Caprolactone Copolymerization Reactions Using Organic Catalysts. *Macromolecules* **45**, 3356–3366 (2012).

4. Dove, A. P. Controlled ring-opening polymerisation of cyclic esters: Polymer blocks in self-assembled nanostructures. *Chem. Commun.* 6446–6470 (2008) doi:10.1039/b813059k.

5. Pratt, R. C. *et al.* Exploration, optimization, and application of supramolecular thiourea-amine catalysts for the synthesis of lactide (co)polymers. *Macromolecules* **39**, 7863–7871 (2006).

6. Wilson, J. A., Hopkins, S. A., Wright, P. M. & Dove, A. P. Synthesis and Postpolymerization Modification of One-Pot Pentadecalactone Block-like Copolymers. *Biomacromolecules* **16**, 3191–3200 (2015).

7. Van Der Meulen, I. *et al.* Polymers from functional macrolactones as potential

biomaterials: Enzymatic ring opening polymerization, biodegradation, and biocompatibility. *Biomacromolecules* **9**, 3404–3410 (2008).

8. Van Der Mee, L. *et al.* Investigation of lipase-catalyzed ring-opening polymerizations of lactones with various ring sizes: Kinetic evaluation. *Macromolecules* **39**, 5021–5027 (2006).

9. De Geus, M. *et al.* Performance polymers from renewable monomers: High molecular weight poly(pentadecalactone) for fiber applications. *Polym. Chem.* **1**, 525–533 (2010).

10. Focarete, M. L., Scandola, M., Kumar, A. & Gross, R. a. Physical Characterization of Poly (pentadecalactone) Synthesized by Lipase-Catalyzed Ring-Opening Polymerization. *J. Polym. Sci. Part B Polym. Phys.* **39**, 1721–1729 (2001).

11. Wilson, J. A., Hopkins, S. A., Wright, P. M. & Dove, A. P. Synthesis of ω-pentadecalactone copolymers with independently tunable thermal and degradation behavior. *Macromolecules* **48**, 950–958 (2015).

12. Wilson, J. A., Hopkins, S. A., Wright, P. M. & Dove, A. P. 'Immortal' ring-opening polymerization of ω-pentadecalactone by Mg(BHT)2(THF)2. *Polym. Chem.* **5**, 2691–2694 (2014).

13. Zhong, Z., Dijkstra, P. J. & Feijen, J. Controlled ring-opening polymerization of ω-pentadecalactone with yttrium isopropoxide as an initiator. *Macromol. Chem. Phys.* **201**, 1329–1333 (2000).

14. Myers, D. *et al.* Ring opening polymerization of macrolactones: High conversions and activities using an yttrium catalyst. *Polym. Chem.* **8**, 5780–5785 (2017).

15. Bouyahyi, M. & Duchateau, R. Metal-based catalysts for controlled ring-opening polymerization of macrolactones: High molecular weight and well-defined copolymer architectures. *Macromolecules* **47**, 517–524 (2014).

16. Ladelta, V., Bilalis, P., Gnanou, Y. & Hadjichristidis, N. Ring-opening polymerization of ω-pentadecalactone catalyzed by phosphazene superbases. *Polym. Chem.* **8**, 511–515 (2017).

17. Walther, P. & Naumann, S. N-Heterocyclic Olefin-Based (Co)polymerization of a Challenging Monomer: Homopolymerization of ω-Pentadecalactone and Its Copolymers with γ-Butyrolactone, δ;-Valerolactone, and ϵ-Caprolactone. *Macromolecules* **50**, 8406–8416 (2017).

18. Pothupitiya, J. U. *et al.* H-Bonding Organocatalysts for the Living, Solvent-Free Ring-Opening Polymerization of Lactones: Toward an All-Lactones, All-Conditions Approach. *Macromolecules* **50**, 8948–8954 (2017).

19. Kricheldorf, H. R. & Schwarz, G. Poly(thioester)s. *J. Macromol. Sci. Part A Pure Appl. Chem.* **44**, 625–649 (2007).

20. Cao, W., Dai, F., Hu, R. & Tang, B. Z. Economic Sulfur Conversion to Functional Polythioamides through Catalyst-Free Multicomponent Polymerizations of

Sulfur, Acids, and Amines. *J. Am. Chem. Soc.* **142**, 978–986 (2020).

21. Datta, P. P. & Kiesewetter, M. K. Controlled Organocatalytic Ring-Opening Polymerization of ε-Thionocaprolactone. *Macromolecules* **49**, 774–780 (2016).

22. Peng, Q., Zhong, Z. & Zhuo, R. Disulfide cross-linked polyethylenimines (PEI) prepared via thiolation of low molecular weight PEI as highly efficient gene vectors. *Bioconjug. Chem.* **19**, 499–506 (2008).

23. Zelikin, A. N., Quinn, J. F. & Caruso, F. Disulfide cross-linked polymer capsules: En route to biodeconstructible systems. *Biomacromolecules* **7**, 27–30 (2006).

24. Yoon, J. A. *et al.* Self-healing polymer films based on thiol-disulfide exchange reactions and self-healing kinetics measured using atomic force microscopy. *Macromolecules* **45**, 142–149 (2012).

25. Gyarmati, B., Némethy, Á. & Szilágyi, A. Reversible disulphide formation in polymer networks: A versatile functional group from synthesis to applications. *Eur. Polym. J.* **49**, 1268–1286 (2013).

26. Fastnacht, K. V. *et al.* Bis- and Tris-Urea H-Bond Donors for Ring-Opening Polymerization: Unprecedented Activity and Control from an Organocatalyst. *ACS Macro Lett.* **5**, 982–986 (2016).

27. Rajabi, M., Lanfranchi, M., Campo, F. & Panza, L. Synthesis of a series of hydroxycarboxylic acids as standards for oxidation of nonanoic acid. *Synth. Commun.*

44, 1149–1154 (2014).

28. Curphey, T. J. Thionation with the reagent combination of phosphorus pentasulfide and hexamethyldisiloxane. *J. Org. Chem.* **67**, 6461–6473 (2002).

29. Cherkasov, R. a. *et al.* Thionation with the reagent combination of phosphorus pentasulfide and hexamethyldisiloxane. *Tetrahedron* **41**, 5061–5087 (1985).

30. Mezzasalma, L., Dove, A. P. & Coulembier, O. Organocatalytic ring-opening polymerization of L-lactide in bulk: A long standing challenge. *Eur. Polym. J.* **95**, 628–634 (2017).

31. Pascual, A., Sardon, H., Veloso, A., Ruipérez, F. & Mecerreyes, D. Organocatalyzed synthesis of aliphatic polyesters from ethylene brassylate: A cheap and renewable macrolactone. *ACS Macro Lett.* **3**, 849–853 (2014).

32. Hedrick, J. L. *et al.* Application of complex macromolecular architectures for advanced microelectronic materials. *Chem. - A Eur. J.* **8**, 3308–3319 (2002).

33. Pratt, R. C., Nederberg, F., Waymouth, R. M. & Hedrick, J. L. Tagging alcohols with cyclic carbonate: A versatile equivalent of (meth)acrylate for ring-opening polymerization. *Chem. Commun.* **2**, 114–116 (2008).

34. Dharmaratne, N. U., Pothupitiya, J. U., Bannin, T. J., Kazakov, O. I. & Kiesewetter, M. K. Triclocarban: Commercial Antibacterial and Highly Effective H-Bond Donating Catalyst for Ring-Opening Polymerization. *ACS Macro Lett.* **6**, 421–

425 (2017).

35. Coderre, D. N., Fastnacht, K. V., Wright, T. J., Dharmaratne, N. U. & Kiesewetter, M. K. H-Bonding Organocatalysts for Ring-Opening Polymerization at Elevated Temperatures. *Macromolecules* **51**, 10121–10126 (2018).

36. Hewawasam, R. S. *et al.* Bisurea and Bisthiourea H-Bonding Organocatalysts for Ring-Opening Polymerization: Cues for the Catalyst Design. *Macromolecules* **52**, 9232–9237 (2019).

37. Fu, J. Strong and tough hydrogels crosslinked by multi-functional polymer colloids. *J. Polym. Sci. Part B Polym. Phys.* **56**, 1336–1350 (2018).

38. Tokita, M. Structure and frictional properties of colloid gel. *Polymers (Basel).* **6**, 651–666 (2014).

39. Sherwood, P. M. A. Surface analysis of carbon and carbon fibers for composites. *J. Electron Spectros. Relat. Phenomena* **81**, 319–342 (1996).

40. Lindberg, B. J. *et al.* Molecular Spectroscopy by Means of ESCA II. Sulfur compounds. Correlation of electron binding energy with structure . *Phys. Scr.* **1**, 286–298 (1970).

41. Weng, L., Chen, X. & Chen, W. Rheological characterization of in situ crosslinkable hydrogels formulated from oxidized dextran and N-carboxyethyl chitosan. *Biomacromolecules* **8**, 1109–1115 (2007).

42. Lai, J. Y. & Li, Y. T. Functional assessment of cross-linked porous gelatin hydrogels for bioengineered cell sheet carriers. *Biomacromolecules* **11**, 1387–1397 (2010).

43. Yang, Z., Peng, H., Wang, W. & Liu, T. Crystallization behavior of poly(ε-caprolactone)/layered double hydroxide nanocomposites. *J. Appl. Polym. Sci.* **116**, 2658–2667 (2010).

44. Bordes, C. *et al.* Determination of poly(ε-caprolactone) solubility parameters: Application to solvent substitution in a microencapsulation process. *Int. J. Pharm.* **383**, 236–243 (2010).

45. Delgove, M. A. F. *et al.* Increasing the solubility range of polyesters by tuning their microstructure with comonomers. *Polym. Chem.* **8**, 4696–4706 (2017).

46. Schneiderman, D. K. & Hillmyer, M. A. Aliphatic Polyester Block Polymer Design. *Macromolecules* **49**, 2419–2428 (2016).

47. Kakumazaki, J., Kato, T. & Sugawara, K. Recovery of gold from incinerated sewage sludge ash by chlorination. *ACS Sustain. Chem. Eng.* **2**, 2297–2300 (2014).

48. Sun, D. T., Gasilova, N., Yang, S., Oveisi, E. & Queen, W. L. Rapid, Selective Extraction of Trace Amounts of Gold from Complex Water Mixtures with a Metal-Organic Framework (MOF)/Polymer Composite. *J. Am. Chem. Soc.* **140**, 16697–16703 (2018).

49. Yue, C. *et al.* Environmentally Benign, Rapid, and Selective Extraction of Gold from Ores and Waste Electronic Materials. *Angew. Chemie - Int. Ed.* **56**, 9331–9335 (2017).

50. Parker, D. J., Chong, S. T. & Hasell, T. Sustainable inverse-vulcanised sulfur polymers. *RSC Adv.* **8**, 27892–27899 (2018).

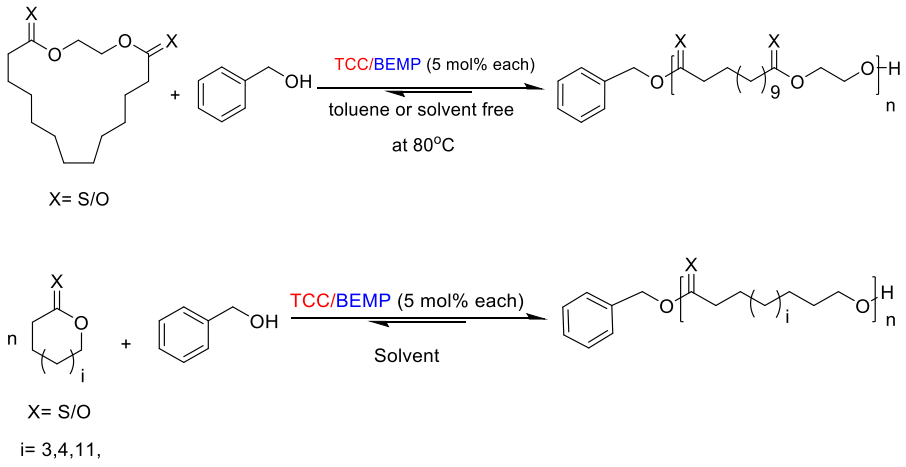

Entry	Monomer	Time	%conversion[b]	M_n [c](g/mol)	M_w/M_n[c]
1	HL	4 mins	88	12600	1.04
2	tnHL	38 mins	92	14700	1.19
3[d]	NL	10 hrs	90	25500	1.48
4	tnNL	4 hrs	99	24200	1.70
5[e]	PDL	8 hrs	87	32100	1.46
6[e]	tnPDL	5 hrs	90	35800	1.80
7[f]	EB	2 hrs	92	44800	1.60
8[g]	tnEB	1 hr	64	10600	1.90

Table 5.1. Optimized conditions for the ROP of (thiono)macrolactone[a].

(a) Reaction conditions: HL, tnHL, NL and tnNL ([2 M], 0.78 mmol, 1.04 mmol, 0.703 mmol, and 0.632 mmol respectively, 1 equiv), benzyl alcohol (1 mol%) TCC/BEMP (5 mol% each) in C_6D_6 at room temperature. b. Monomer conversion was monitored via ^{1}H NMR. c. M_n and M_w/M_n were determined by GPC (CH_2Cl_2) versus polystyrene standards. d. **2**/BEMP (1.67 mol%, 0.0117 mmol). e. PDL and tnPDL ([5 M] 1.050 mmol and 0.974 mmol respectively, 1 equiv), in toluene at 100˚C. f. Solvent-free conditions: EB (2.95 mmol, 1 equiv), benzyl alcohol (0.014 mmol), cocatalyst (0.07 mmol) at 80 ˚C. g. ([2 M], 1.32 mmol, 1 equiv,) in toluene at 80 ˚C.

polymer	Swelling ratio	Porosity%	Crosslinked density(***n***) (mmol.cm^{-3})
PtnCL-CLP	4.60 ± 0.01	38.86 ± 0.12	6.47 ± 0.01
PtnHL-CLP	5.16 ± 0.02	47.43 ± 0.22	3.95 ± 0.02
PtnPDL-CLP	9.40 ± 0.03	54.62 ± 0.22	3.00 ± 0.01
P(tnPDL-*b*-CL)-CLP	9.72 ± 0.25	82.31 ± 0.85	0.45 ± 0.00

Table 5.2. Calculated crosslinked densities and the porosity% of the CLPs from swelling test data[a]

(a) Swelling tests were carried out in THF at room temperature. Swelling ratios, porosity%, and the crosslinked densities (***n***) were calculated using equation (1), (2), and (4), respectively.

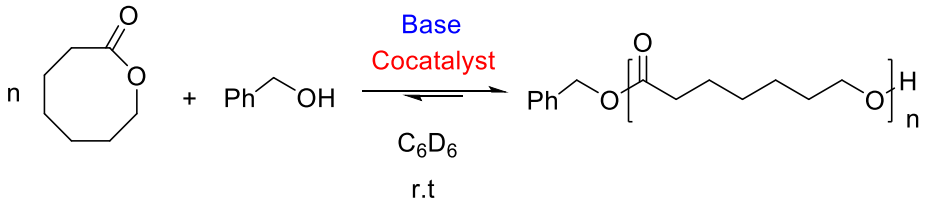

Entry	Base	Cocatalyst	Conv.[b] (%)	Time(min)	M_n[c] (g/mol)	M_w/M_n[c]
1[d]	TBD	-	93	120	24600	1.59
2	BEMP	TCC	88	4	12600	1.04
3	MTBD	TCC	94	360	23800	1.02
4	DBU	TCC	89	1260	18200	1.03
5[e]	BEMP	**2**	98	50	23800	1.13
6[e]	MTBD	**2**	89	120	24300	1.03
7[e]	DBU	**2**	89	1080	17800	1.03

Table 5.3. ROP of HL with urea/base cocatalyst system [a]

(a) Reaction conditions: HL (2 M, 0.78 mmol, 1 equiv), benzyl alcohol (1 mol%, 0.0078 mmol), TCC/base (5 mol%, 0.039 mmol each) in C_6D_6. (b) Monomer conversion were monitored via ^{1}H NMR. (c) M_n and M_w/M_n were determined by GPC (CH_2Cl_2) versus polystyrene standards. (d) TBD (1 mol%, 0.0078 mmol). e. **2**/base (1.67 mol%, 0.013 mmol each).

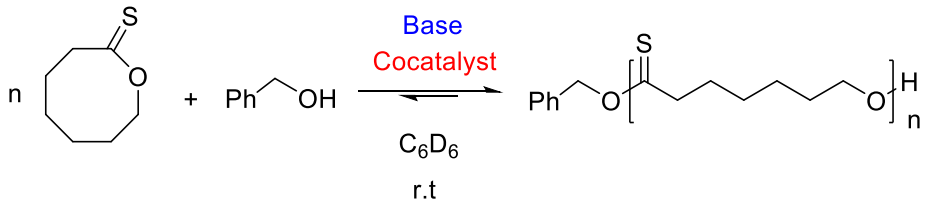

Entry	Base	Cocatalyst	Conv.[b] (%)	Time(min)	M_n[c] (g/mol)	M_w/M_n[c]
1	BEMP	TCC	92	38	14700	1.19
2	MTBD	TCC	92	220	14900	1.20
4[d]	MTBD	**2**	85	720	11700	1.19
5[e]	TBD	-	89	21	19400	1.13

Table 5.4. ROP of tnHL with urea/base cocatalyst system[a]

(a)Reaction conditions: tnHL (2 M, 1.04 mmol, 1 eq), benzyl alcohol (1 mol%, 0.010 mmol), TCC/base (5 mol%, 0.034 mmol each) in C_6D_6. (b) Monomer conversion were monitored via ^{1}H NMR. (c) M_n and M_w/M_n were determined by GPC (CH_2Cl_2) versus polystyrene standards. (d) **2**/base (1.67 mol%, 0.0115 mmol each). e. TBD (1 mol%, 0.0104 mmol).

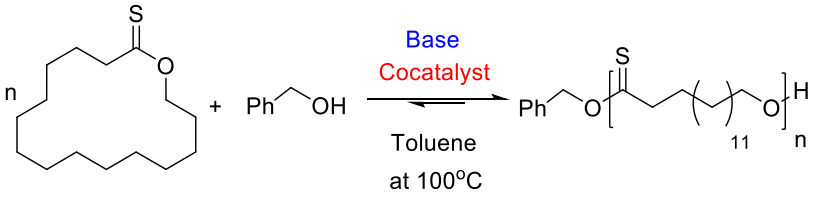

Entry	Base	Cocatalyst	Conv.[b] (%)	Time(min)	M_n[c] (g/mol)	M_w/M_n[c]
1[d]	TBD	-	85	360	35000	1.93
2	BEMP	TCC	90	300	35800	1.80
3	MTBD	TCC	93	270	31400	1.82

Table 5.5**.** ROP of tnPDL with urea/base cocatalyst system [a]

(a) Reaction conditions: tnPDL (5 M, 0.974 mmol, 1 eq), benzyl alcohol (1 mol%, 0.0097 mmol) TCC/base (5 mol%, 0.0478 mmol each) in toluene at 100 ˚C. (b) Monomer conversion were monitored via ^{1}H NMR. (c) M_n and M_w/M_n were determined by GPC (CH_2Cl_2) versus polystyrene standards. d. TBD (2 mol%, 0.0194 mmol).

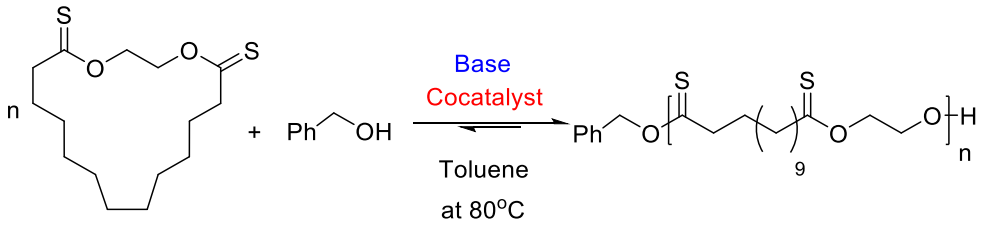

Entry	Base	Cocatalyst	Conv.[b] (%)	Time(hrs)	M_n[c] (g/mol)	M_w/M_n[c]
1	BEMP	TCC	64	1	10600	1.90
2	MTBD	TCC	67	8	8900	1.80
3[d]	BEMP	**2**	6	77	-	-
4[d]	MTBD	**2**	29	77	-	-

Table 5.6. ROP of tnEB with urea/base cocatalyst system [a]

(a)Reaction conditions: tnEB (2 M, 1.32 mmol, 1 eq), benzyl alcohol (1mol%, 0.0132 mmol), TCC/base (5 mol%, 0.0661 mmol each) in toluene at 80 ˚C. (b) Monomer conversion were monitored via ^{1}H NMR. (c) M_n and M_w/M_n were determined by GPC (CH_2Cl_2) versus polystyrene standards. (d) **2**/base (1.67 mol%, 0.022 mmol each).

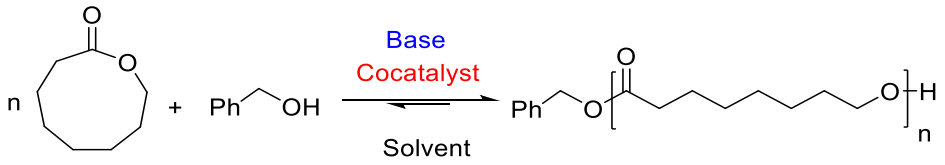

Entry	Base	Cocatalyst	Solvent	Temperature	Conv.[b] (%)	Time(hrs)	M_n[c] (g/mol)	M_w/M_n[c]
1[d]	TBD	-	toluene	RT	85	76	12100	1.68
2	BEMP	TCC	acetone-d_6	RT	96	25	18000	1.80
3	MTBD	TCC	acetone-d_6	RT	27	24	9200	1.31
4	DBU	TCC	acetone-d_6	-	-	-	-	-
5	BEMP	TCC	benzene-d_6	RT	80	48	22000	1.57
6[e]	BEMP	**2**	benzene-d_6	RT	90	10	25500	1.48
7[f]	BEMP	**2**	toluene	80˚C	97	3	29000	1.55

Table 5.7. ROP of NL with urea/base cocatalyst system [a]

(a) Reaction conditions: NL (2 M, 0.703 mmol, 1 eq), benzyl alcohol (1 mol%, 0.0070 mmol) TCC/base (5 mol%, 0.0351 mmol each), (b) Monomer conversion were monitored via ^{1}H NMR. (c) M_n and M_w/M_n were determined by GPC (CH_2Cl_2) versus polystyrene standards (d) TBD (5 mol%, 0.0351 mmol), (e) **2**/base (1.67 mol%, 0.0117 mmol each), (f) **2**/base (1.67 mol%, 0.0117 mmol each) in toluene at 80˚C.

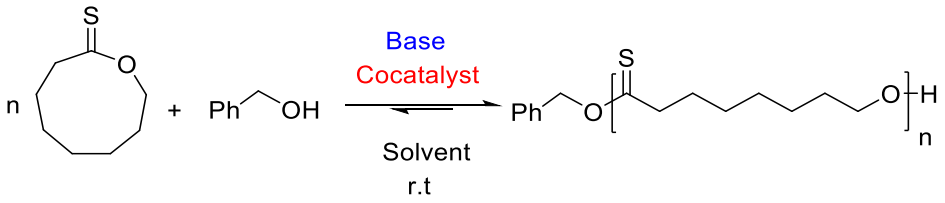

Entry	Base	Cocatalyst	Solvent	Conv.[b] (%)	Time(hrs)	M_n[c] (g/mol)	M_w/M_n[c]
1	BEMP	TCC	acetone-d_6	95	4	23500	1.81
2	MTBD	TCC	acetone-d_6	75	48	14800	1.73
3	BEMP	TCC	benzene- d_6	99	4	24200	1.70
4[d]	BEMP	**2**	benzene- d_6	-	-	-	-

Table 5.8. ROP of tnNL with urea/base cocatalyst system [a]

(a)Reaction conditions: tnNL (2 M,0.632 mmol, 1 eq), benzyl alcohol (1 mol%,0.0063 mmol) TCC/base (5 mol%, 0.0315 mmol each), (b) Monomer conversion were monitored via ^{1}H NMR. (c) M_n and M_w/M_n were determined by GPC (CH_2Cl_2) versus polystyrene standards. (d) **2**/base (1.67 mol% ,0.0105 mmol each)

Thermodynamic Parameters	$\Delta H°_p$ [kcal/mol]	$\Delta S°_p$ [cal/mol K]	$T_{ceiling}$ °(C)
HL[a]	-4.60435	-8.98852	239.098
tnHL[a]	-5.35373	-11.6812	185.170
NL[b]	0	5.5908	-273.15
tnNL[b]	0	7.7739	-273.15
tnPDL[c]	0	6.8870	-273.15
EB[d]	0	7.7898	-273.15
tnEB[d]	0	6.3789	-273.15

Table 5.9. Thermodynamic properties of macrolactones

(a)Reaction conditions: tnHL and HL (0.5 M, 1 equiv), benzyl alcohol (1 mol%,), TBD (5 mol%,) in C_6D_6. (b)tnNL (0.5 M, , 1 equiv,), benzyl alcohol (1 mol%,) TCC/BEMP (5 mol%, each) in C_6D_6. (c) TnPDL (2.5 M, 1 equiv), benzyl alcohol (2 mol%,) TCC/BEMP (2.5 mol%,) in C_6D_6.(d) EB and tnEB (2.5 M, 1 equiv), benzyl alcohol (2 mol%,) TCC/BEMP (2.5 mol%,) in C_6D_6

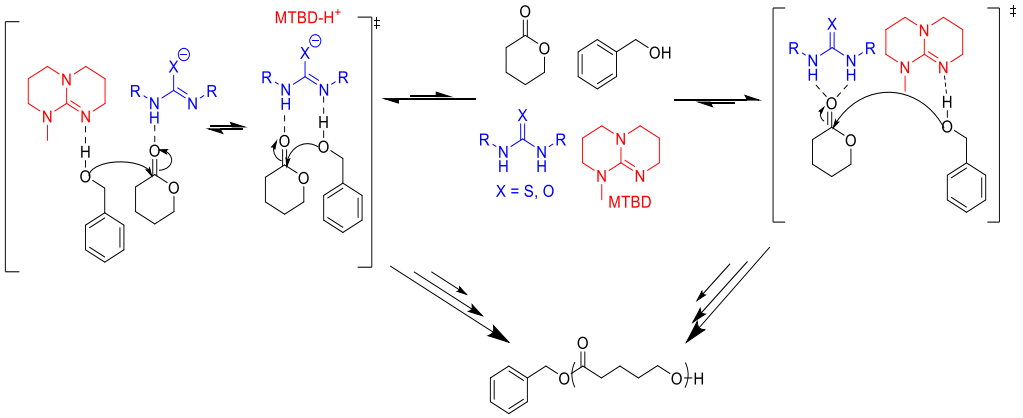

Scheme 5.1. Imidate-mediated and H-bond mediated mechanism for the ROP of cyclic esters

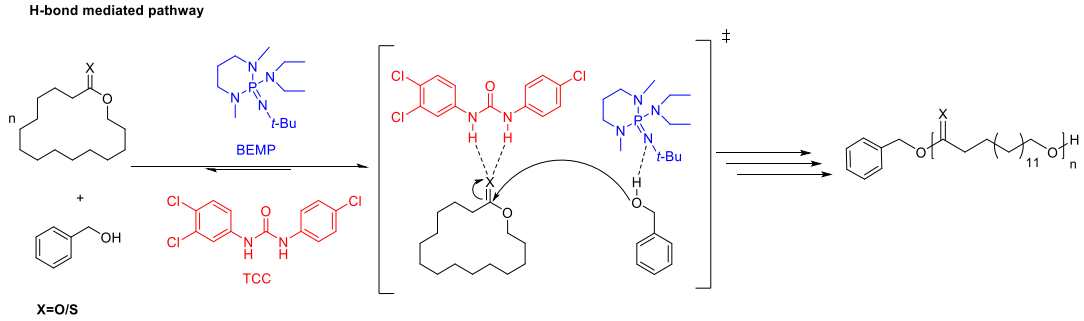

Scheme 5.2. Proposed mechanism for macro(thiono)lactone

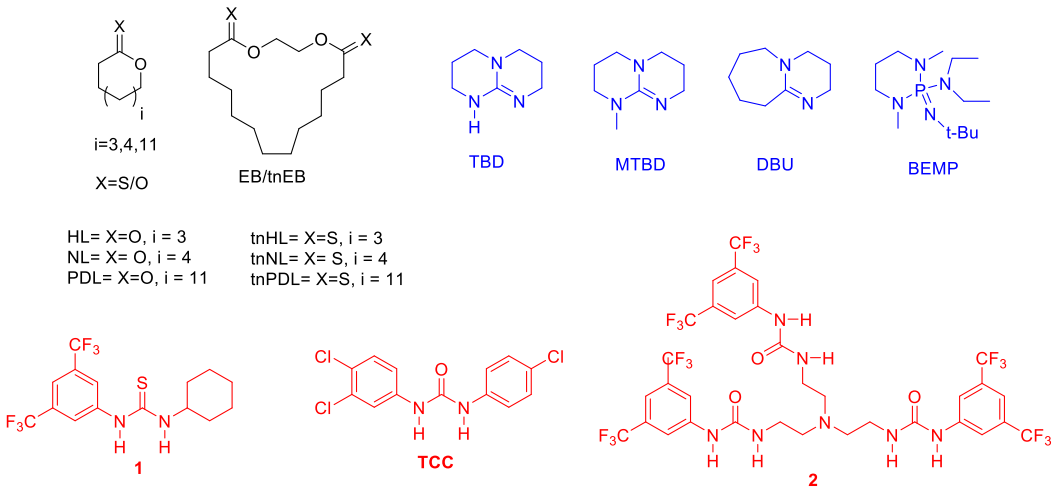

Figure 5.1. monomers, bases and (thio)urea cocatalysts screened in this study

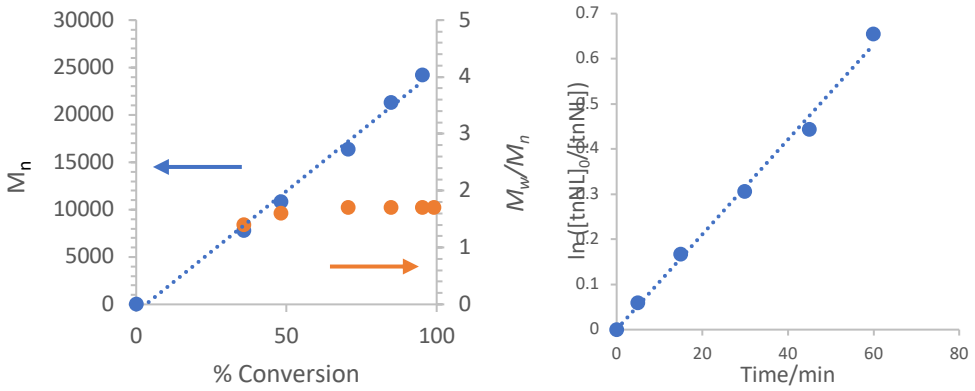

Figure 5.2. (Left) M_n versus conversion (Right) First order evolution of [tnNL] versus time

Reaction conditions: tnNL (2 M, 0.632 mmol, 1 equiv), benzyl alcohol (1 mol%, 0.0063 mmol) catalyzed by TCC/BEMP (5 mol%, 0.0315 mmol each) in C_6D_6.

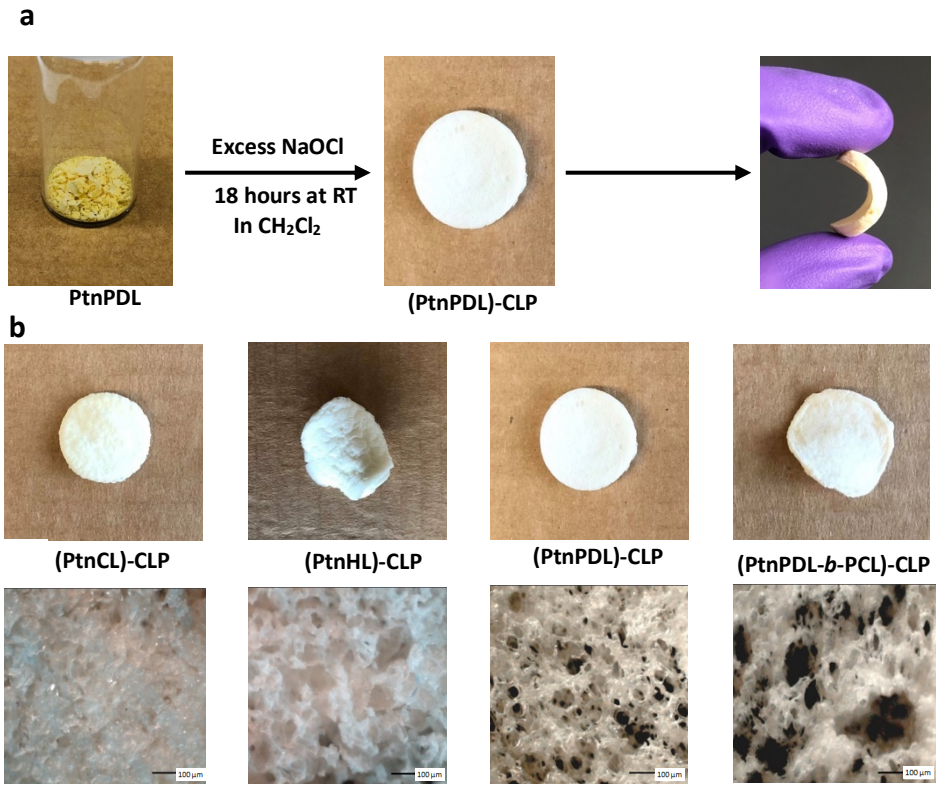

Figure 5.3. (a) Image of PtnPDL-CLP flexible polymer. (b) Images of PtnCL, PtnHL, and P(tnPDL-*b*-CL) CLPs (c) cross sectional morphology of crosslinked polymers with optical microscopic; magnification X 10.

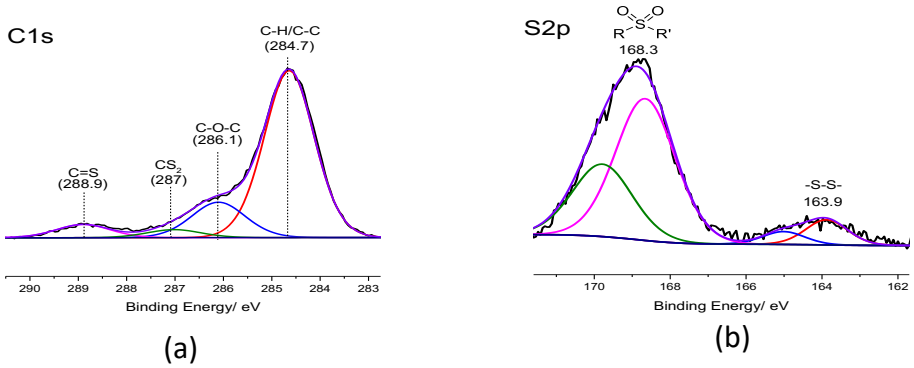

Figure 5.4. (a) XPS spectrum for the C 1s (b) XPS spectrum for the S 2p

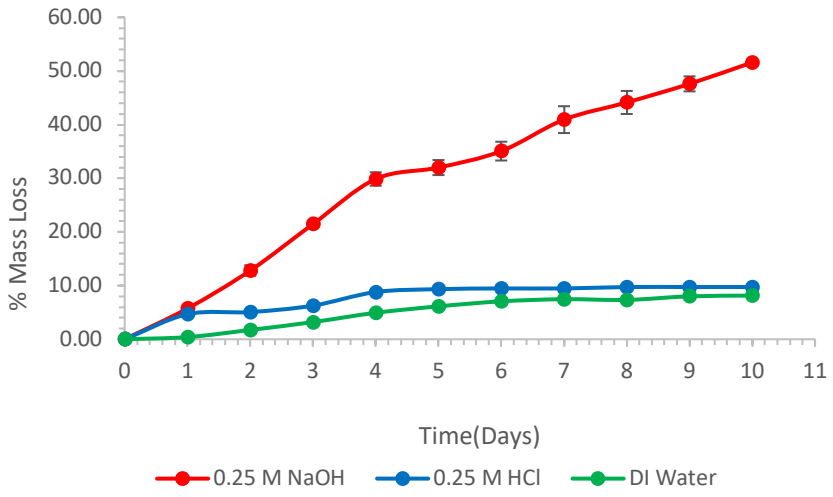

Figure 5.5. Percent mass loss for PtnPDL-CLP in acidic (0.25 M HCl), basic (0.25 M NaOH), and neutral (distilled water) conditions versus time. The results shown are an average of three replicates.

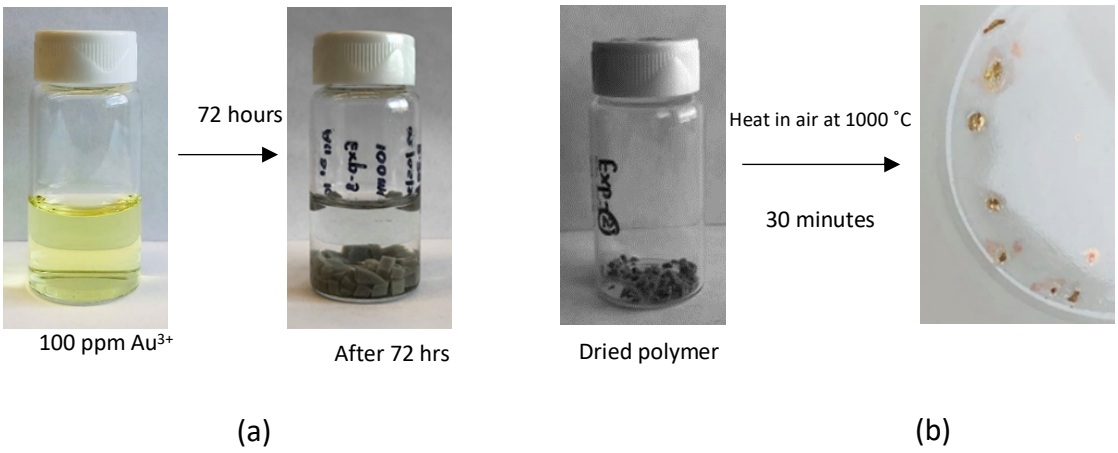

Figure 5.6. a. Time-dependent extraction of Au^{3+} with 100 mg of PtnPDL-CLP. Inset: The gold extraction process with PtnPDL-CLP. $[Au^{3+}]_o$ = 100 ppm, Au^{3+} volume = 10 ml. b. The gold recovery process with PtnPDL-CLP.

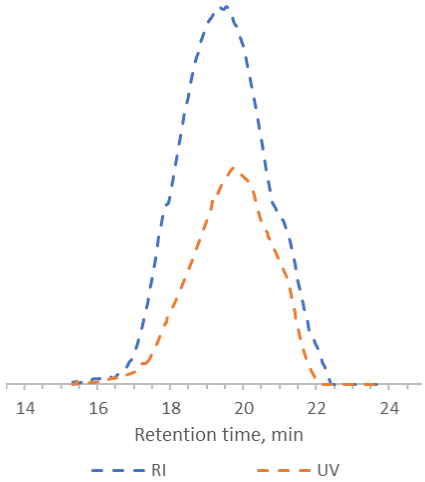

Figure 5.7. RI and UV GPC traces of the ROP initiated from pyrenebutanol for tnNL. Conditions: tnNL (2 M, 0.631 mmol), 1-pyrenebutanol (2mol%, 0.012 mmol), TCC/BEMP (5mol%, 0.0315 mmol each) in acetone-d_6.

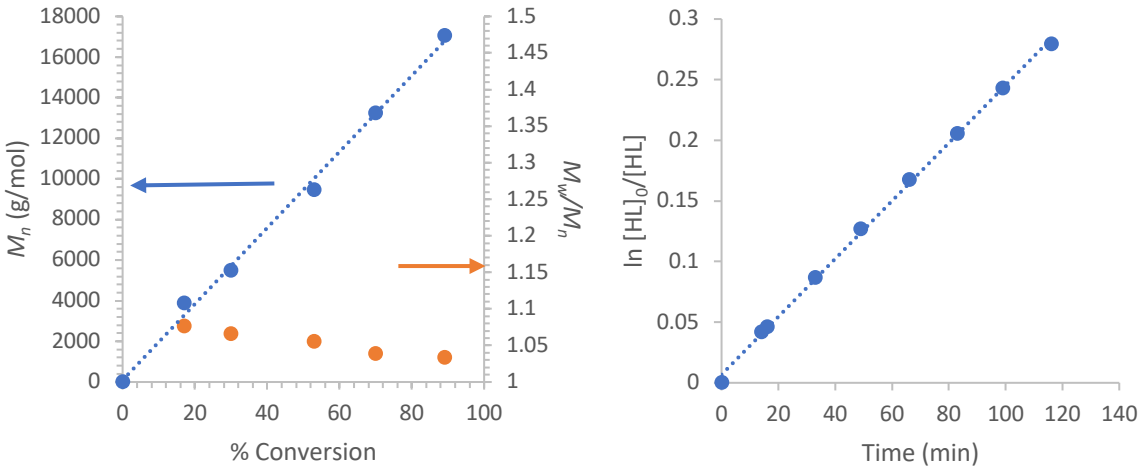

Figure 5.8. (Left) M_n versus conversion. (Right) First order evolution of [HL] versus time.Reaction conditions: HL (2 M, 0.78 mmol), benzyl alcohol (1 mol%, 0.0078 mmol) catalyzed by TCC/MTBD (5 mol%, 0.039 mmol each) in C_6D_6.

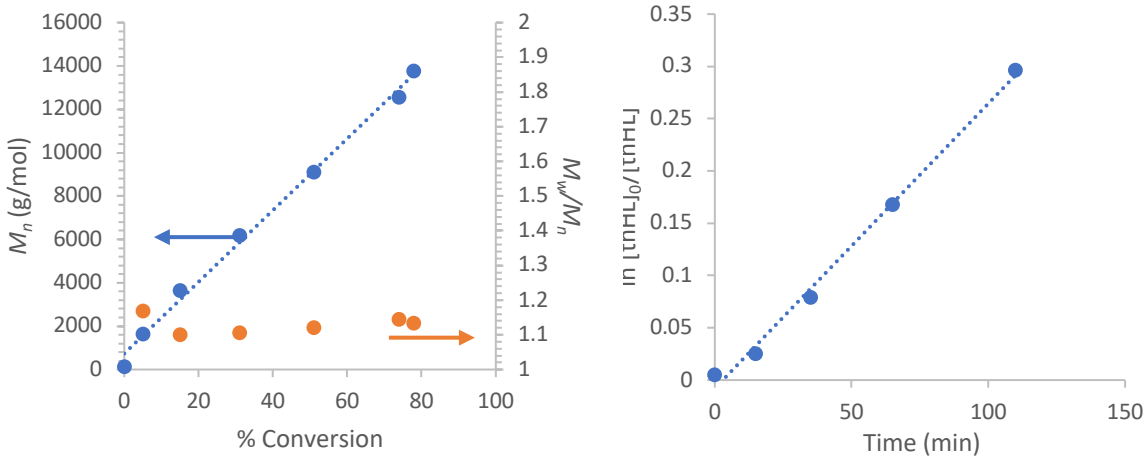

Figure 5.9. (Left) M_n versus conversion. (Right) First order evolution of [tnHL] versus time. Reaction conditions: tnHL (2 M, 1.04 mmol, 1 eq), benzyl alcohol (1 mol%, 0.010 mmol), TCC/MTBD (5 mol%, 0.034 mmol each) in C_6D_6

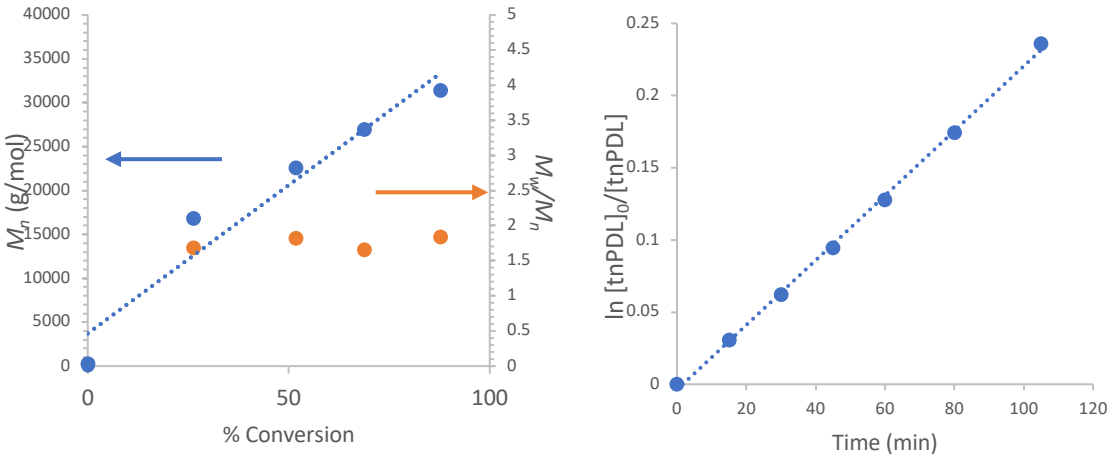

Figure 5.10. (Left) M_n versus conversion. (Right) First order evolution of [tnPDL] versus time. Reaction conditions: tnPDL (5 M, 0.974 mmol), benzyl alcohol (1 mol%, 0.0097 mmol) catalyzed by TCC/MTBD (5 mol%, 0.0478 mmol each) in toluene at 100 ˚C.

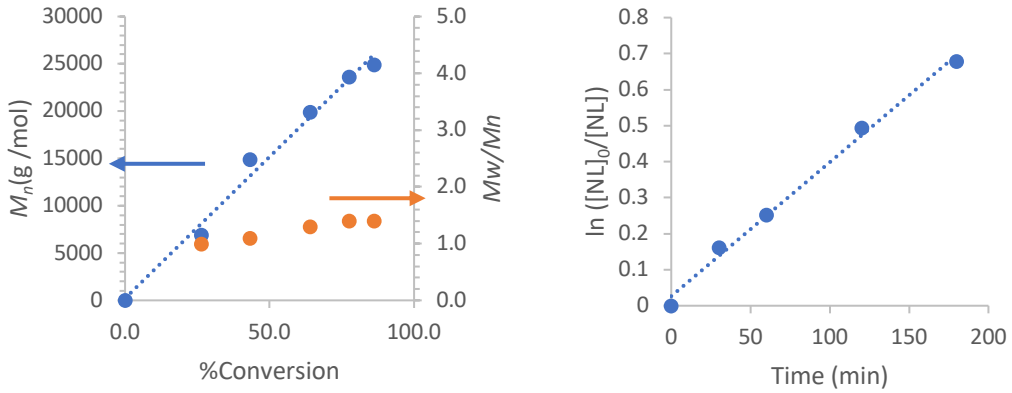

Figure 5.11. (Left) M_n versus conversion. (Right) First order evolution of [tnEB] versus time Reaction conditions: tnEB (2 M, 1.32 mmol), benzyl alcohol (1 mol%, 0.0132 mmol) catalyzed by TCC/MTBD (5 mol%, 0.0661 mmol each) in toluene at 80 ˚C.

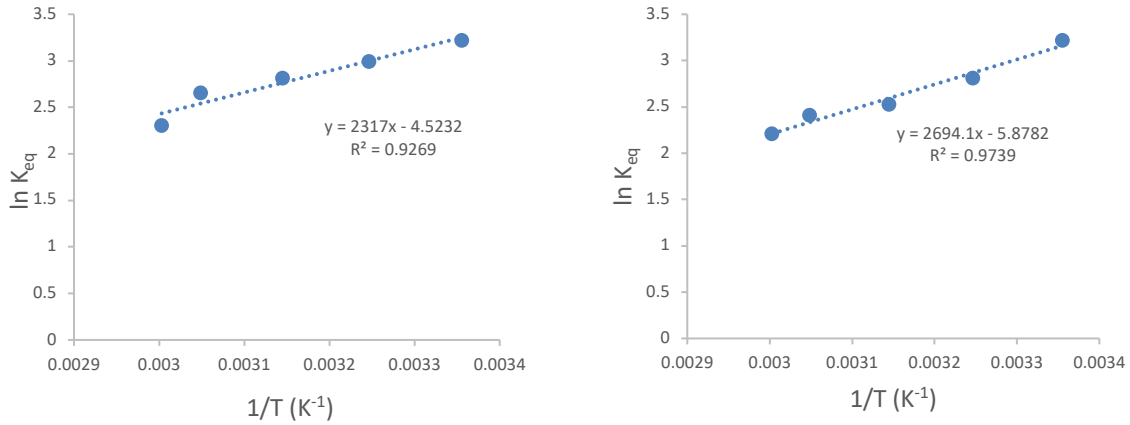

Figure 5.12 (Left) M_n versus conversion. (Right) First order evolution of [NL] versus time. Reaction conditions: NL (2 M, 0.703 mmol), benzyl alcohol (1 mol%, 0.0070 mmol) catalyzed by **2**/BEMP (1.67 mol%, 0.0117 mmol each) in C_6D_6.

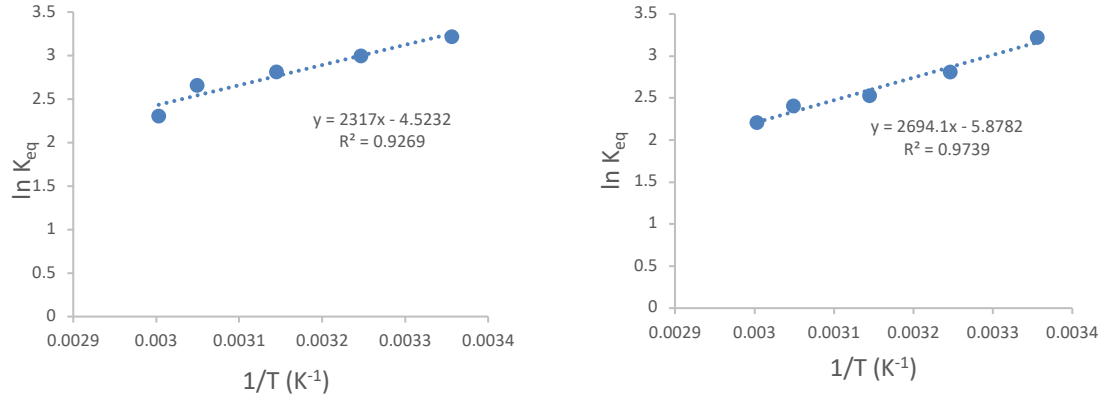

Figure 5.13. (Left) Van't Hoff plot for the TBD (5 mol%, 0.3465 mmol) catalyzed ROP of HL (0.5 M, 0.780 mmol, 1 eq) from benzyl alcohol (1 mol% 0.0078 mmol) in C_6D_6. (Right) Van't Hoff plot for the TBD (5 mol%, 0.3465 mmol) catalyzed ROP of tnHL (1 M, 0.694 mmol, 1 eq) from benzyl alcohol (1 mol%, 0.0069 mmol) in C_6D_6.

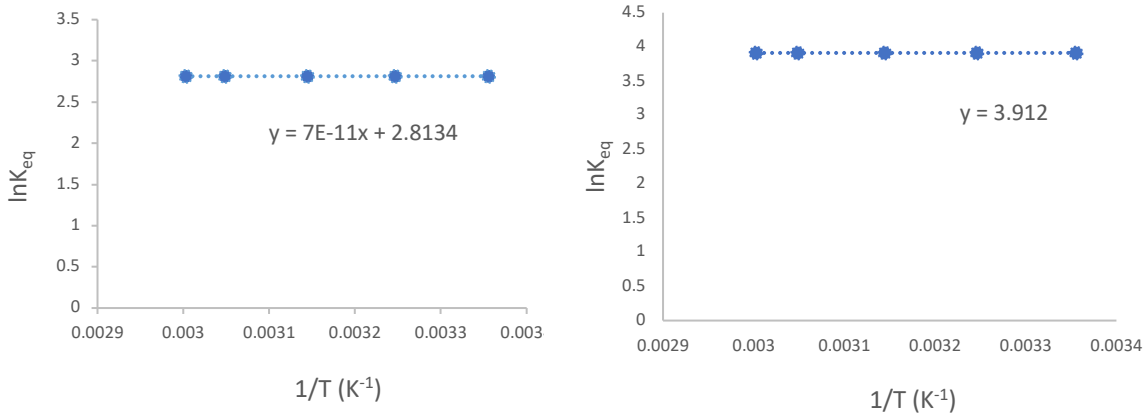

Figure 5.14. (Left) Van't Hoff plot for the TCC/BEMP (5 mol%, 0.0117 mmol each) catalyzed ROP of NL (0.5 M, 0.703 mmol, 1 equiv,) from benzyl alcohol (1 mol%, 0.0070 mmol) in C_6D_6. (Right) Van't Hoff plot for the TCC/BEMP (5 mol%, 0.0315 mmol mmol each) catalyzed ROP of tnNL (0.5 M, 0.632 mmol, 1 equiv,) from benzyl alcohol (1 mol%,0.0063 mmol) in C_6D_6.

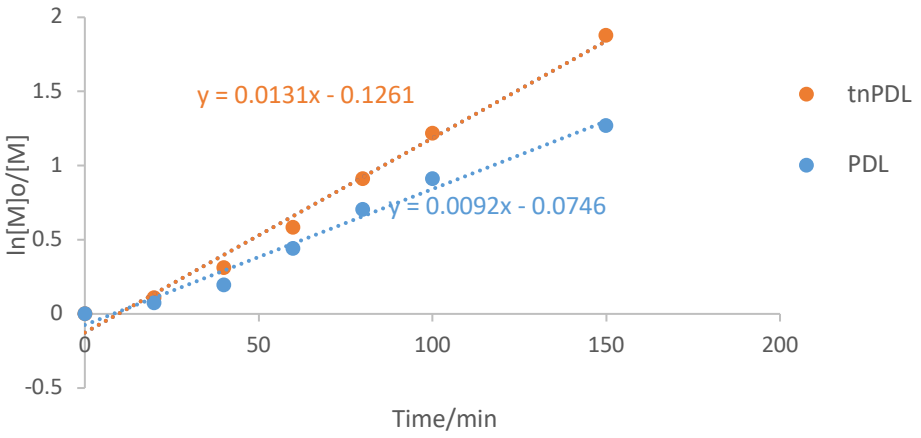

Figure 5.15**.** First order evolution curve of [Monomer] versus Time for the TCC/BEMP catalyzed P(tnPDL-*co*-PDL) co-polymer. Reaction conditions: tnPDL and PDL (2.5 M, 125 mg each), benzyl alcohol (1 mol%, 0.0097 mmol) catalyzed by TCC/BEMP (5 mol%, 0.0478 mmol each) in toluene at 100 ˚C.

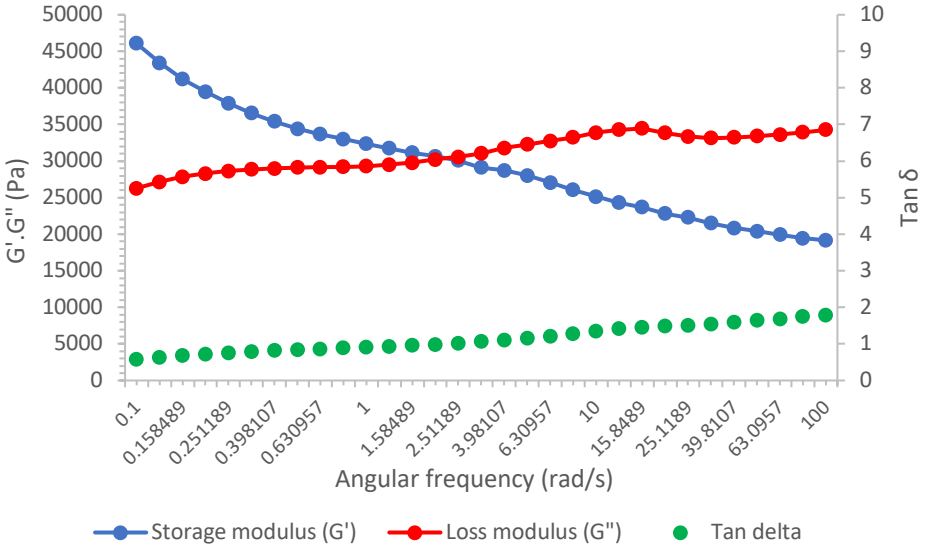

Figure 5.16. Storage (G´) and loss modulus (G˝) as a function of angular frequency (ω) for the PtnPDL-CLP at 25 ˚C

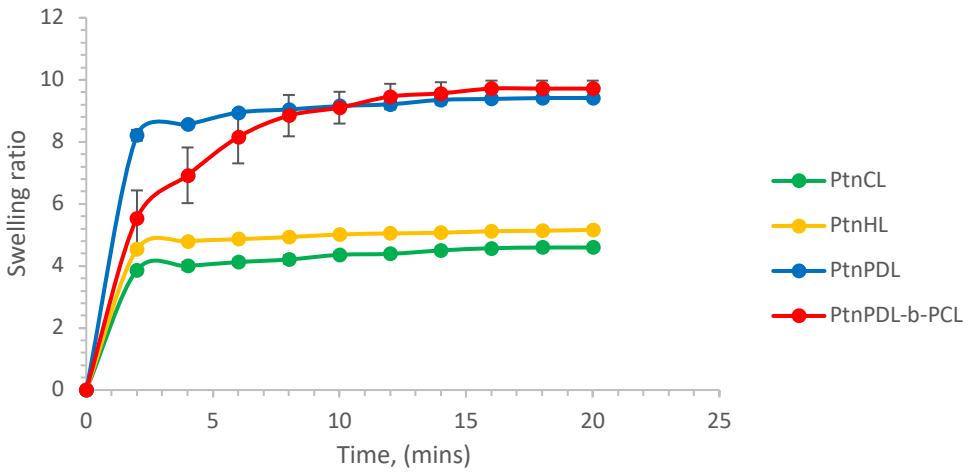

Figure 5.17. Swelling ratios of crosslinked polymers in THF

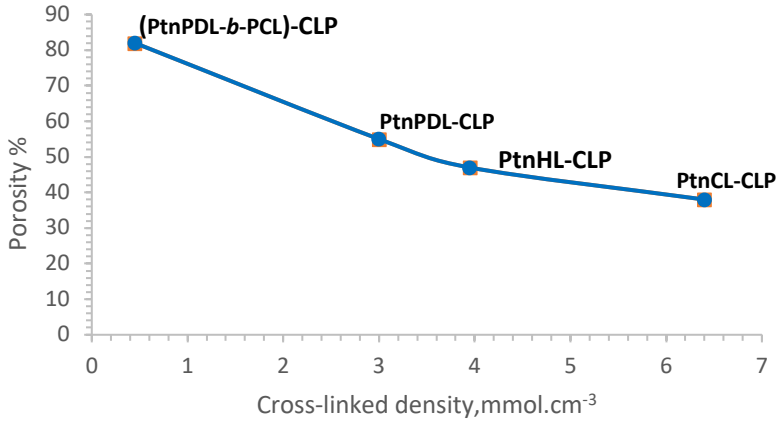

Figure 5.18. Dependence of porosity on cross-linked density of CLPs

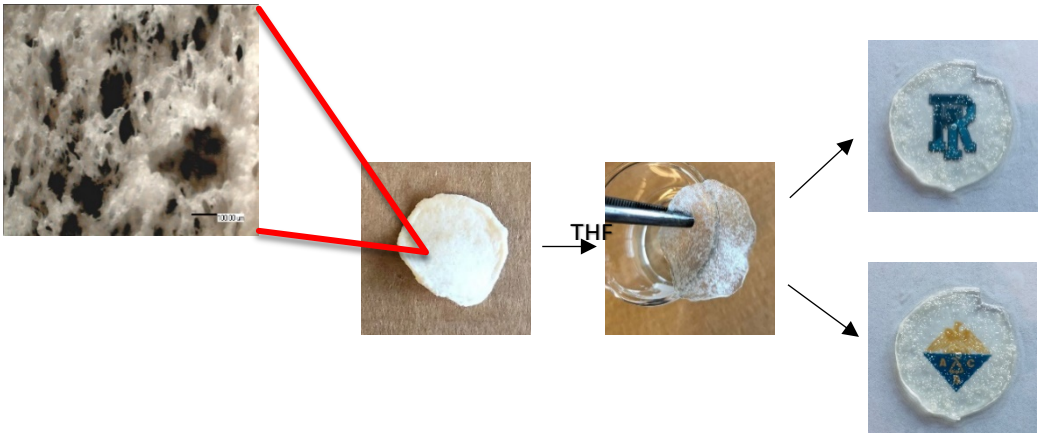

Figure 5.19. Images of the transparent P(tnPDL-*b*-CL)-CLP after immersed in THF

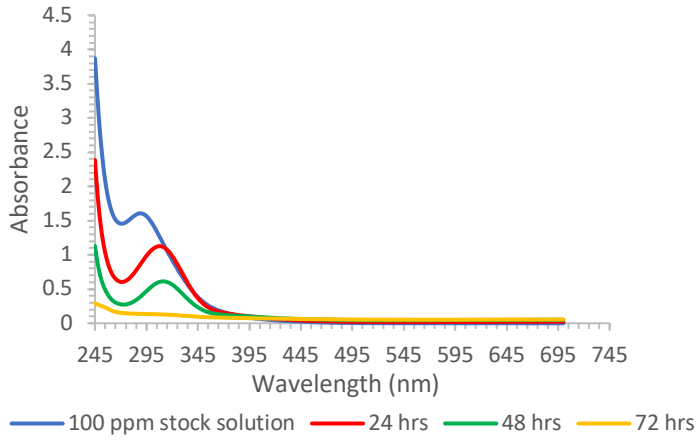

Figure 5.20. UV-vis spectrum for the Au^{3+} (100 ppm aqueous solution) extraction with PtnPDL CLP (100 mg)

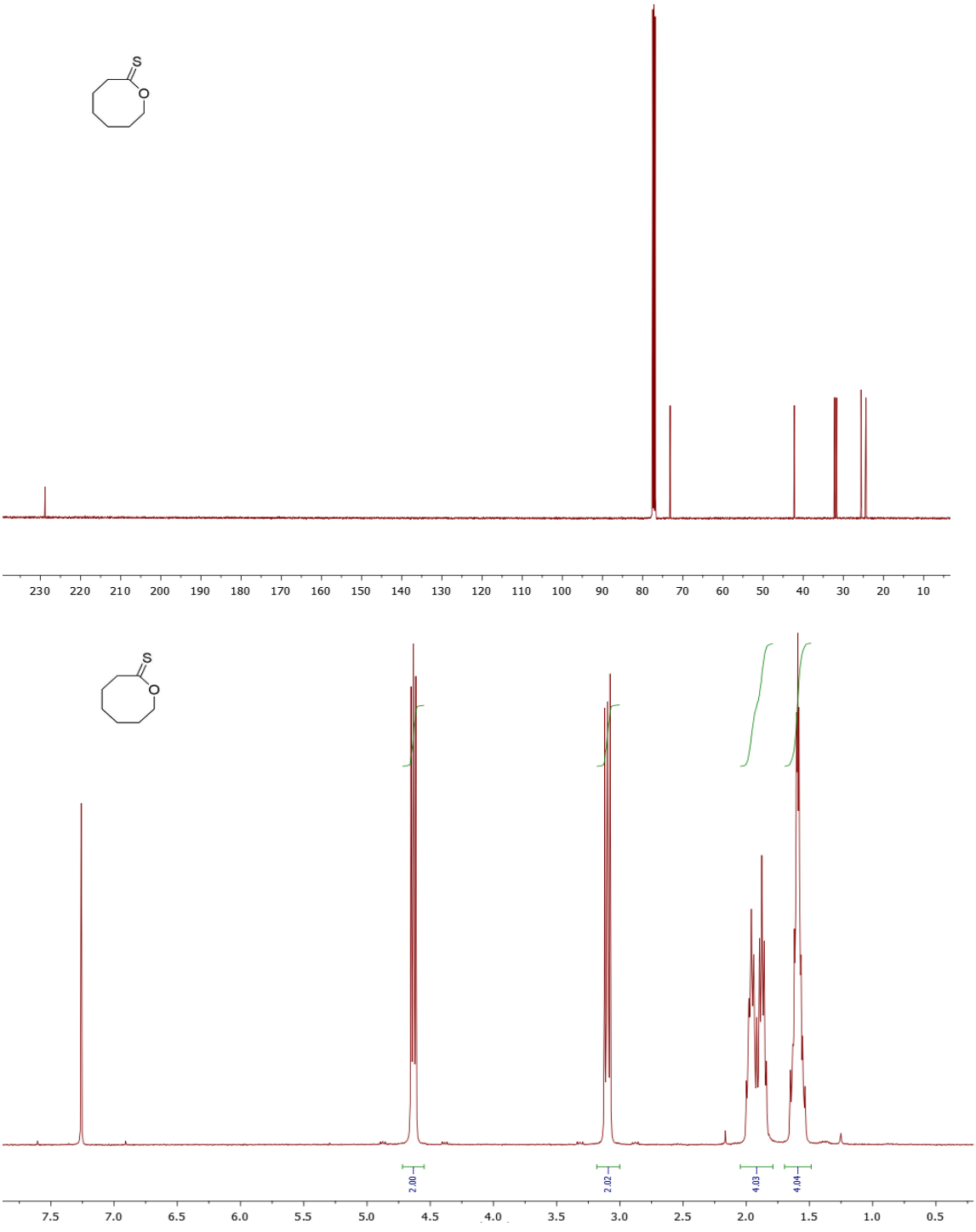

Figure 5.21. (Upper) ^{1}H NMR ($CDCl_3$, 300 MHz, ppm) spectrum of tnHL (Lower) ^{13}C NMR ($CDCl_3$, 100 MHz, ppm) spectrum of tnHL.

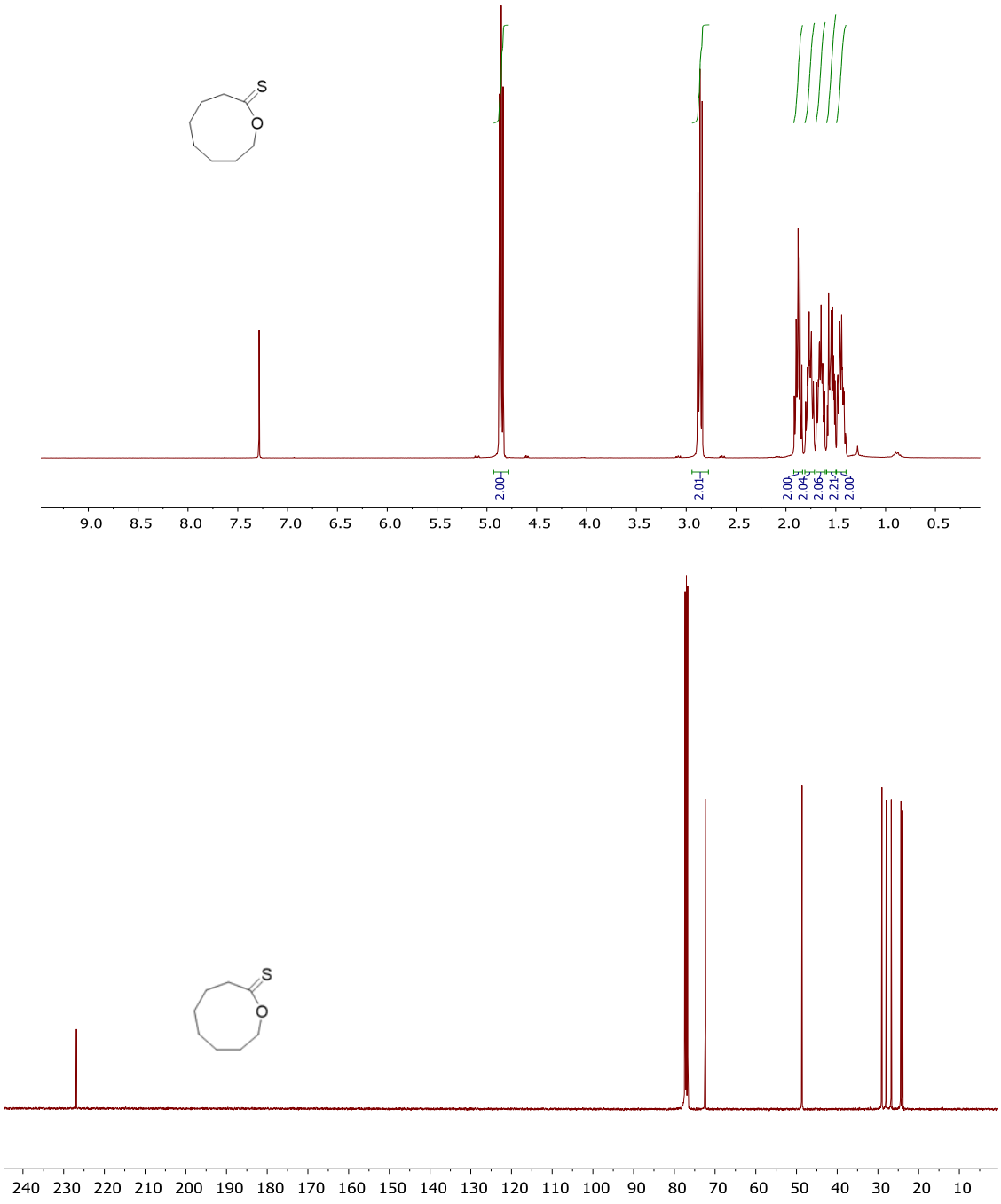

Figure 5.22**.** (Upper) ^{1}H NMR ($CDCl_3$, 300 MHz, ppm) spectrum of tnNL (Lower) ^{13}C NMR ($CDCl_3$, 100 MHz, ppm) spectrum of tnNL

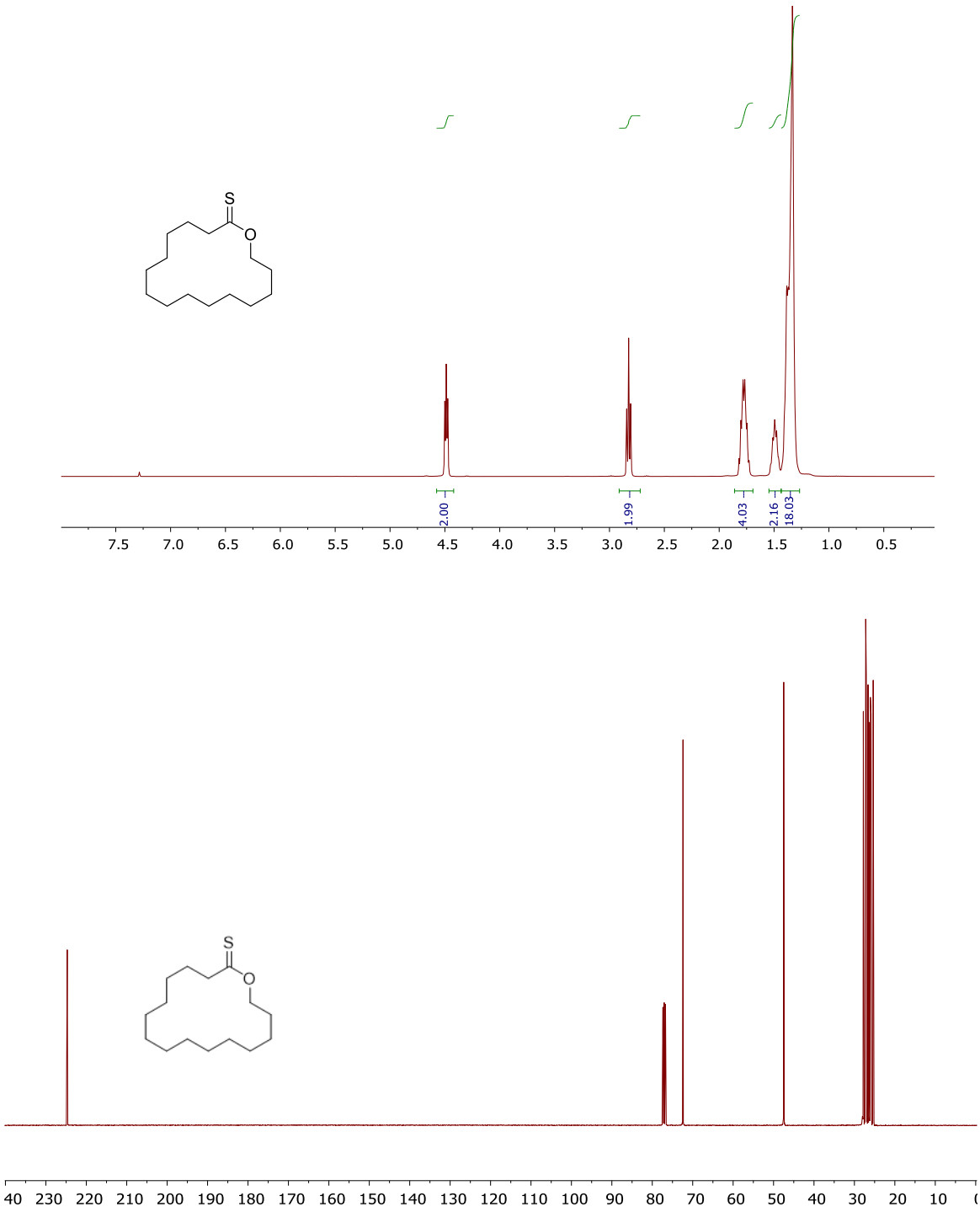

Figure 5.23. (Upper) ^{1}H NMR ($CDCl_3$, 300 MHz, ppm) spectrum of tnPDL (Lower) ^{13}C NMR ($CDCl_3$, 100 MHz, ppm) spectrum of tnPDL.

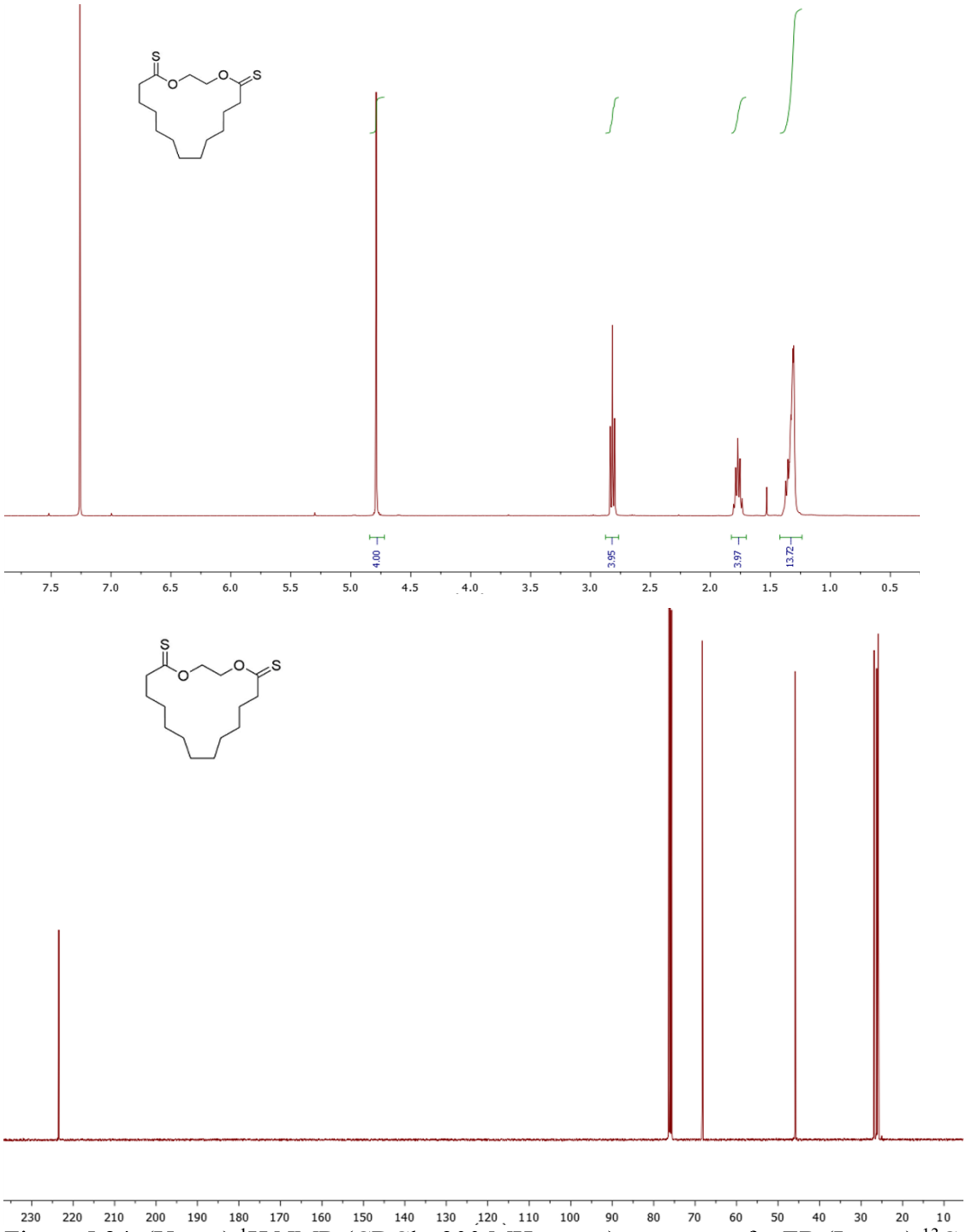

Figure 5.24. (Upper) ^{1}H NMR ($CDCl_3$, 300 MHz, ppm) spectrum of tnEB (Lower) ^{13}C NMR ($CDCl_3$, 100 MHz, ppm) spectrum of tnEB.

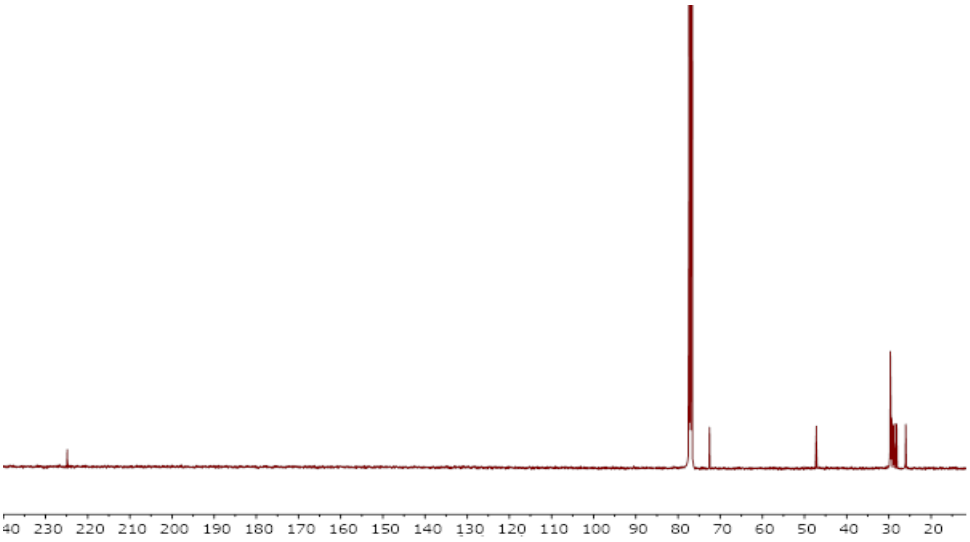

Figure 5.25. ^{13}C (100 MHz, $CDCl_3$) spectrum of homopolymer of PtnPDL (5 M, toluene) initiated from benzyl alcohol (1 mol%) catalyzed by TCC/BEMP (5 mol% each), displaying no carbonyl peak but thiocarbonyl resonance at 224 ppm.

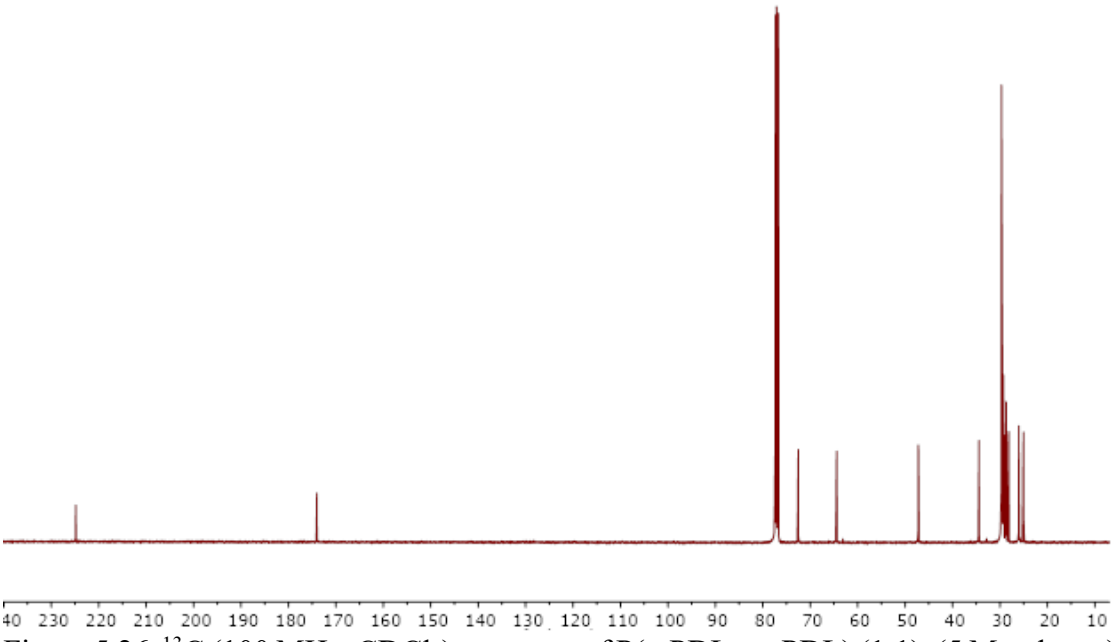

Figure 5.26. ^{13}C (100 MHz, $CDCl_3$) spectrum of P(tnPDL-*co*-PDL) (1:1), (5 M, toluene) initiated from benzyl alcohol (1 mol%) catalyzed by TCC/BEMP (5 mol% each), displaying thiocarbonyl resonance at 224 ppm and carbonyl resonance at 174 ppm.

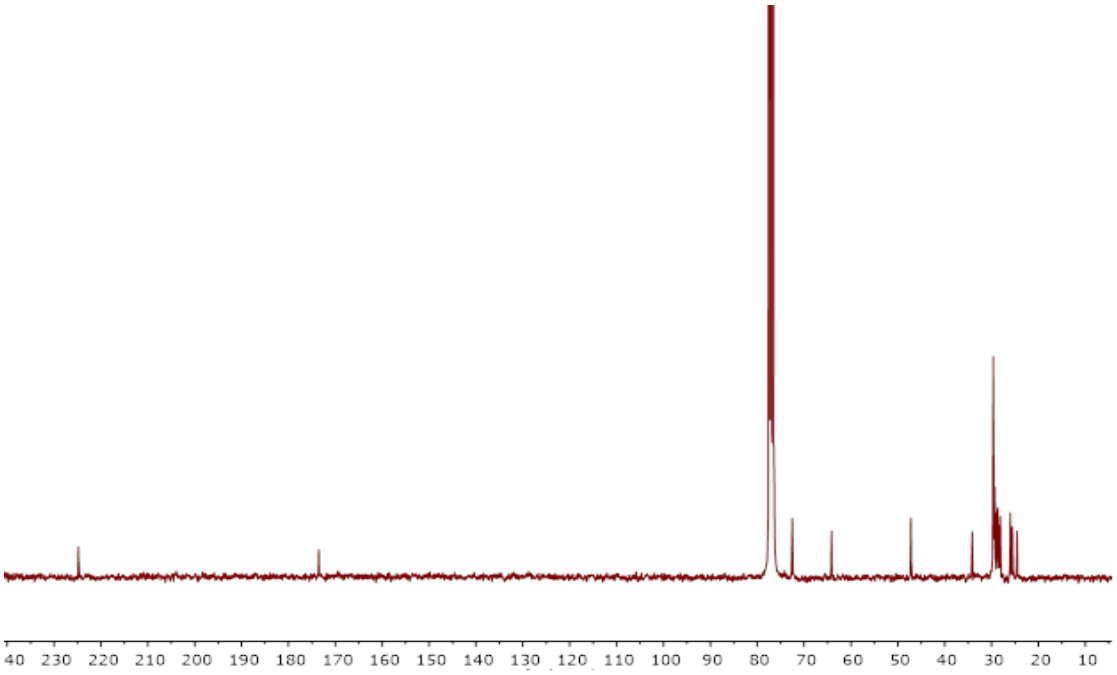

Figure 5.27. ^{13}C (100 MHz, $CDCl_3$) spectrum of P(tnPDL-*b*-CL) (1:1), (0.5 M, CH_2Cl_2) initiated from PtnPDL as a macroinitiator, catalyzed by TCC/BEMP (5 mol% each), displaying thiocarbonyl resonance at 224 ppm and carbonyl resonance at 174 ppm.